N-Amino Heterocycles – Applications in Flash Vacuum Pyrolysis

Emma Jayne Rozgowska, MChem

Thesis presented for the degree of

Doctor of Philosophy

The University of Edinburgh

February 2011

Declaration

I declare that the work presented in this thesis was carried out by myself, unless otherwise stated by reference, and that it has not been previously submitted for any higher degree.

This thesis describes the results of research carried out in the research labs of Professor Hamish McNab in the department of Chemistry at the University of Edinburgh.

Emma Jayne Rozgowska

University of Edinburgh

February 2011

For Hamish,

Wherever you are, I hope I have made you proud

Acknowledgements

I would like to thank the McNabbers past and present for the help, advice and cake over the years; Karen, Mary, Rich, Will, Ran, Patrick, Martha and Craig especially, you have all made my PhD years ones I will treasure.

I would like to say a very special thank you to Professor Hamish McNab, whose guidance has been invaluable and who has always been there whenever advice, help or a motivational chat has been needed. He has been an amazing supervisor and his support has been very much appreciated.

Many thanks to J. Millar, J. Bella and M. De Cremoux for NMR spectroscopy help, A. Taylor for mass spectrometry services and P. Richardson for DFT calculation advice.

Last but by no means least I want to thank Michael who has kept me going, picked me up and never lost faith in me. Your love and encouragement has gotten me through and for that, I can never thank you enough.

Abstract

Routes to *N*-amino heterocycles were reviewed and findings applied to generate flash vacuum pyrolysis (FVP) precursors of two types – ketene generators and azol-1-yl radical generators.

N-Amino heterocycles can be used as nitrogen radical generators, the N-N bond being homolytically cleaved at furnace temperatures of approximately 850 °C. A number of 2-substituted benzimidazoles were synthesised and subsequently *N*-aminated. The 2-arylbenzimidazole precursors 1-amino-2-(2-methylphenyl)-1*H*-benzimidazole and 1-amino-2-(2-ethylphenyl)-1*H*-benzimidazole were synthesised and subjected to FVP. The hydrogen transfer processes of the resulting azol-1-yl radicals were investigated. Pyrolysis of 1-amino-2-(2-methylphenyl)-1*H*-benzimidazole resulted in three products; 2-(2-methylphenyl)-1*H*-benzimdazole, 11*H*-benzo[4,5]imidazo[1,2-*a*]isoindole and 1-(2-methylphenyl)-1*H*-benzo[*d*]imidazol-2-amine. Pyrolysis of 1-amino-2-(2-ethylphenyl)-1*H*-benzimidazole resulted in five products, four of which have been successfully isolated and identified as 2-(2-ethylphenyl)-1*H*-benzimidazole, 5,6-dihydrobenzo[4,5]imidazo[2,1-*a*]isoquinoline, 1-(2-ethylphenyl)-1*H*-benzo[*d*]imidazol-2-amine and 11-methyl-11*H*-benzo[4,5]imidazo[2,1-*a*]isoindole. The mechanism of formation of most products is initiated by hydrogen atom transfer to the azol-1-yl radical position.

N-Aminopyrazole was reacted with 5-methoxymethylene-2,2-dimethyl-1,3-dioxane-4,6-dione to form the corresponding 5-(*N*-aminopyrazolyl)methylene derivative, which, when subjected to FVP, eliminates acetone and carbon dioxide to form a methyleneketene. This subsequently undergoes a [1,3]-hydrogen shift giving an imidoylketene which can collapse onto the neighbouring nitrogen atom forming pyrazolo[1,2-*a*][1,2,3]triazin-5-ium-4-olate (a novel heterocyclic mesomeric betaine system) or cyclise onto the adjacent carbon atom to yield a pyrazolopyridazinone. On variation of the furnace temperature it was apparent the former forms at relatively

moderate temperatures (~500 °C) whereas the latter begins to predominate as the furnace temperature increases (~700 °C). The relationship between these kinetic and thermodynamic products was modelled using DFT calculations. By using substituted pyrazole precursors, substituents could be incorporated into all three available positions around the pyrazole ring. Using substituted acrylic esters as alternative imidoylketene generators, substituents could also be incorporated into both available positions in the pyridazinone ring. All corresponding betaine and pyrazolopyridazinone products were isolated and characterised.

Contents

Abbreviations

δ_H, δ_C	chemical Shift
DMSO	dimethyl sulfoxide
DCM	dichloromethane
THF	tetrahydrofuran
DMF	*N,N*-dimethylformamide
$MgSO_4$	anhydrous magnesium sulfate
$NaHCO_3$	sodium hydrogen carbonate
DIB	(diacetoxy)iodobenzene
MMMA	methoxymethylene Meldrum's acid
MSH	*O*-mesitylsulfonylhydroxylamine
PPh_3	triphenylphosphine
Pd/C	palladium on carbon
mol	moles
NMR	nuclear magnetic resonance
s	singlet
d	doublet
t	triplet
m	multiplet
br	broad
d d	doublet of doublets
d t	doublet of triplets
J	coupling constant
quat	quaternary carbon

MHz	megaHertz
°C	degrees Celsius
mp	melting point
bp	boiling point
lit.	literature
m/z	mass to charge ratio
EI	electron impact ionisation
FAB	fast atom bombardment
h	hours
min	minutes
cm^3	cubic centimetres
g	grams
conc.	concentrated
aq.	aqueous
sat.	saturated
w	weight
T_f	furnace temperature
T_i	inlet temperature
P	pressure
t	time
B3LYP	Becke 3-parameter, Lee Yang Parr
Ha	Hartrees
MP2	Møller-Plesset
cc-pVDZ	Correlation-consistent polarized valence double-zeta basis set

DFT	density functional theory
NBS	*N*-bromosuccinimide
TFA	Trifluoroacetic acid

1. Introduction

1.1 *N*-Amino-azoles

Azole is a term that generally covers any 5-membered heterocycle that contains two heteroatoms, one of which is nitrogen. Some typical azoles are shown in Figure 1. They are an important class of compounds being found abundantly in nature, for example in nucleic acids and alkaloids, and are also widely synthesised finding uses as dyes, insecticides, in organic electronics and of course in pharmaceuticals. Their syntheses are well documented and their reactions have been extensively investigated.

However, one reaction that has not been particularly exploited is their *N*-amination, and it is this reaction that is the key step in the synthesis of starting materials used for the generation of the essentially unknown azol-1-yl radicals **1** by flash vacuum pyrolysis (FVP) and a major point of interest in the context of this work (Figure 1).

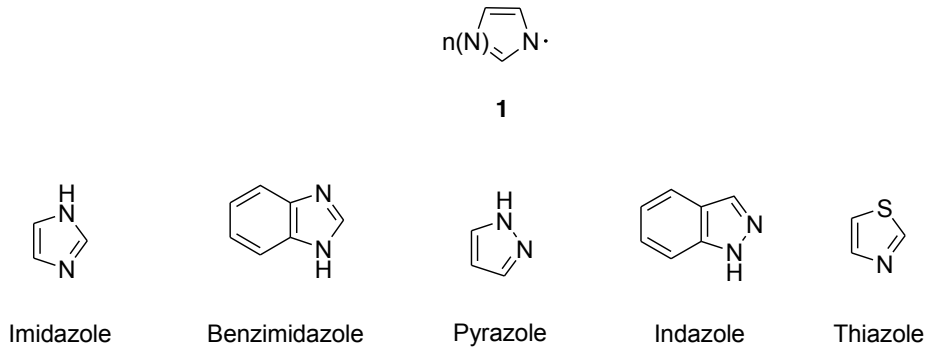

Figure 1: Example of an azol-1-yl radical and some common azole and diazole ring systems

When subjected to FVP conditions, *N*-amino groups undergo homolysis of the N-N bond producing a nitrogen centred radical, in the case of *N*-amino heterocycles this

would lead to the generation on an azol-1-yl radical (Scheme 1). *N*-Amino heterocycles can also be used to generate another class of precursor for FVP which exploit pericyclic rather than radical-type chemistry. Condensation of *N*-amino heterocycles with methoxymethylene Meldrum's acid (MMMA) **2** results in a starting material **3** which upon pyrolysis decomposes to form an imidoylketene moiety **4** which can then undergo cyclisation onto adjacent atoms. An example of this is also shown in Scheme 1.

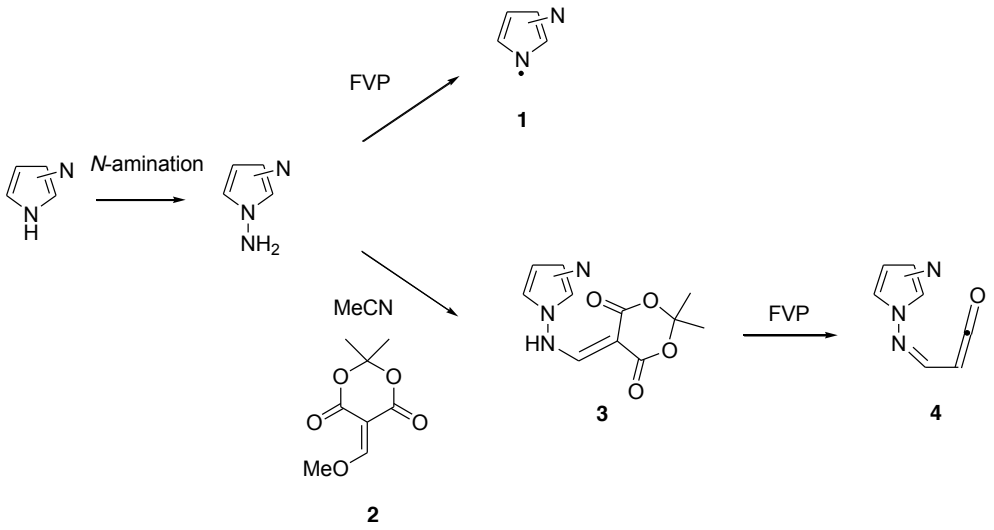

Scheme 1: Schematic showing how *N*-amino heterocycles can be exploited in both radical and pericyclic reactions by FVP

It is therefore possible to see how powerful the *N*-amination reaction can be in this context, *N*-Amino-azoles could be used in two very different ways with regards to FVP; the generation of azol-1-yl radicals and investigation of their reactions and in the synthesis of methylene Meldrums's acid derivatives and the pericyclic reactions of the imidoylketenes generated from these *via* FVP.

1.2 *N*-Amination of Azoles

There are three general methods that can be used to generate *N*-amino-azoles;

- Cyclisation of appropriate acyclic compounds (usually hydrazine derivatives)
- Transformation (or recyclisation) of heterocycles
- Direct electrophilic amination of azoles

The cyclisation of acyclic compounds and recyclisation of existing heterocycles are methods that although in principle can be of use in the generation of many *N*-amino-azoles, the application of these methods are more suited to the synthesis of more complex multi-substituted molecules as will be discussed later. By far the most appealing method in the context of this work is direct amination of the existing azole.

The electrophilic *N*-amination reaction can be carried out using a number of reagents (Figure 2), which vary in their electrophilicity and hence relative amination strength. The most common of these are hydroxylamine derivatives that are proficient electrophilic NH_2^+ equivalents that have been shown to transfer the amino group to nitrogen nucleophiles. Of these hydroxylamine-*O*-sulfonic acid **4** (HOSA) is the the most used, and it has been shown to be successful in *N*-aminating a number of azoles. Others include chloramines [1] **5**, *O*-(diphenylphosphinyl)hydroxylamine [2] **6** (DPPH), *O*-(*p*-nitrobenzoyl)hydroxylamine [1] **7** (NbzH), *O*-mesitylsulfonylhydroxylamine [3] **8** (MSH), *O*-dinitrophenylhydroxylamine [4] **9** (DNPH) and *O*-*p*-tolylsulfonylhydroxylamine [5] **10** (TSH).

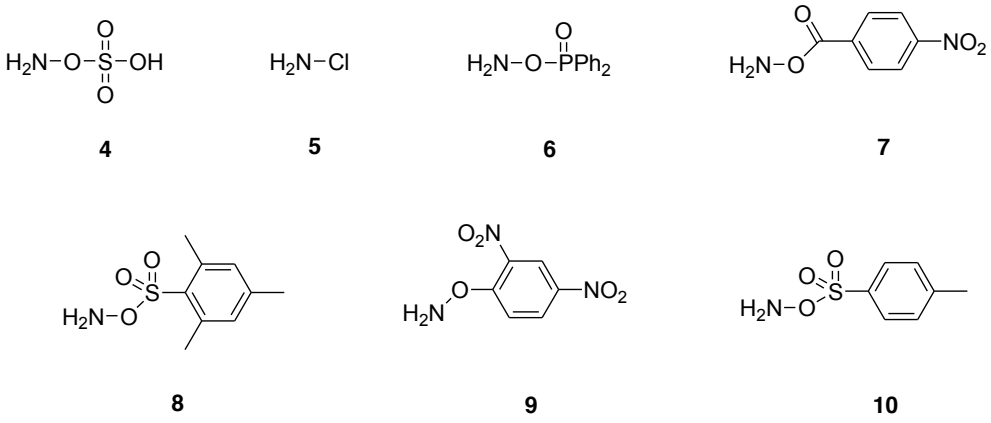

Figure 2: Common available *N*-aminating reagents

HOSA **4** is generally the most used as it is the most readily available, however it has drawbacks; it can be used in aqueous media but is only occasionally successful in non-aqueous solvents (for example DMF) and its use in non-aqueous solvents decreases the yield of *N*-aminated product. HOSA decomposes in alkali; the resulting anion of which is the reactive species which supplies the electrophilic source of NH_2 for amination. The mechanism of HOSA amination is shown in scheme 2. The electrophilicity of the NH_2 group of these reagents is dependent upon the strength of the electron-withdrawing moiety attached to the hydroxylamine group (NH_2-O-), hence many equivalents of the aminating agent may be needed to push the reaction to completion. Base is used to deprotonate the azole nitrogen atom, which then acts as a nucleophile attacking the electrophilic NH_2. Because of these drawbacks HOSA has not been found to be efficient for the amination of sterically hindered or poorly nucleophilic *N*-anions. When the azole to be aminated has a low NH-acidity, one of the other agents with greater electrophilicity (for example MSH) must be used for successful reaction.

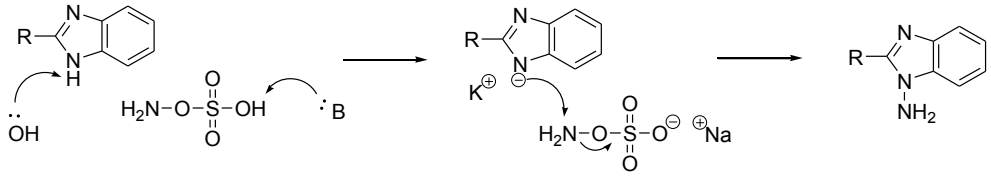

Scheme 2: Mechanism of *N*-amination using HOSA

The direct *N*-amination of azoles was reviewed in 1992 by Kuzmenko and Pozharskii, [6] a summary of which is outlined here.

Virtually all of the recorded *N*-aminopyrazoles synthesised have been achieved *via* direct amination using HOSA or occasionally MSH. Pyrazole **11** itself is *N*-aminated in a 52% yield (**12**) using HOSA in aqueous alkali (Scheme 3). [7] There is also one example of the *N*-amination of 3,5-dimethylpyrazole **13** using chloramine in a ^{15}N labelling experiment. [8] This was done to determine the position of the nitrogen atom on oxidation of the *N*-aminopyrazole **14** which generates 4,6-dimethyl-1,2,3-benzotriazine **15** on oxidation using lead tetraacetate (Scheme 3). This example illustrates the versatility of these *N*-amination reagents. Generally the yields obtained are high (> 70%) but this tends to diminish as the number and steric bulk of substituents on the ring increases.

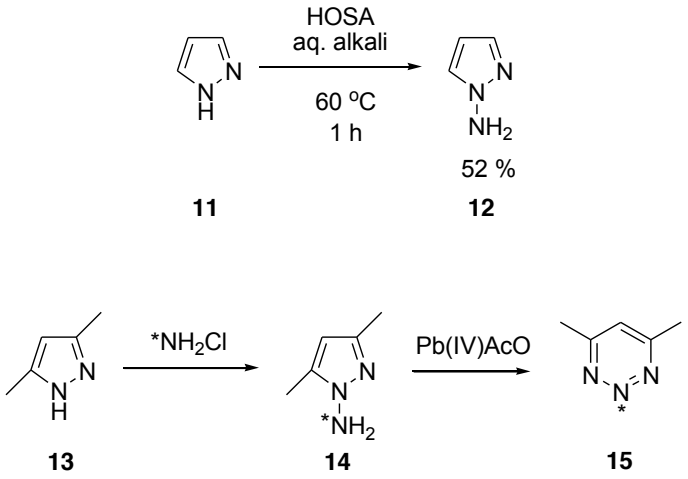

Scheme 3: *N*-amination of pyrazole using HOSA and *N*-aminaion of 3,5-dimethylpyrazole using labelled chloramine to investigate oxidation using lead tetraacetate to produce benzotriazines

Indazoles 16 can also be *N*-aminated using HOSA in aqueous alkali with ethanol to produce a mixture of 1-amino 17 and 2-amino 18 isomers, usually the 1-amino derivate predominates, with the 2-amino never usually exceeding 30% of the total reaction mixture (Scheme 4). These isomers can easily be separated using column chromatography. [9]

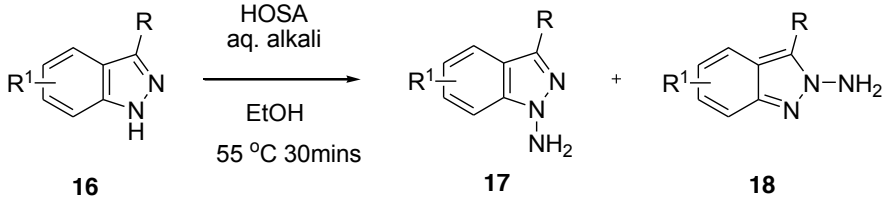

Scheme 4: *N*-amination of indazole using HOSA to form both isomers

N-Amino Heterocycles – Applications in Flash Vacuum Pyrolysis

There are not many examples of direct *N*-amination of imidazoles by comparison with those of other azoles. In 1982 Klotzer *et al*[2] reported the amination of 2-nitro and 2-methyl-4(5)-nitroimidazoles using DPPH **6** and the corresponding sodium or lithium salt of the imidazole **19** in *N*-methylpyrrolidone (NMP) as solvent and *in situ* reaction with benzaldehyde (Scheme 5). [2] This afforded the *N*-benzylideneamino derivative **20** which was subsequently hydrolysed to the respective substituted 1-aminoimidazoles **21**.

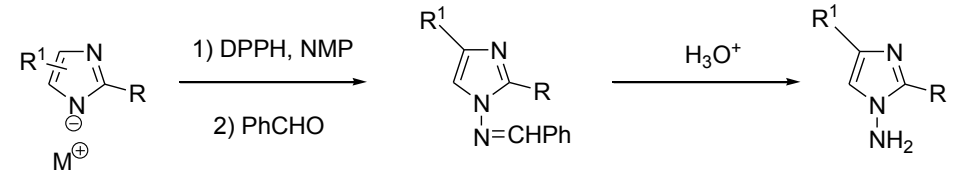

19 **20** **21**

$M^{\oplus}$ = Li^+, Na^+

Scheme 5: *N*-amination of imidazole salts using DPPH

In addition to the above, the *N*-aminoimidazolium salts **22** were synthesised in reasonable yields by heating 1-substituted imidazoles and MSH in dichloromethane.

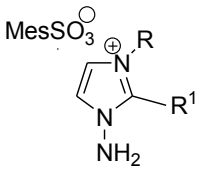

22

The key method for the synthesis of *N*-aminobenzimidazoles **23** is direct amination and HOSA dominates as the most effective reagent. The reaction is undertaken again in aqueous alkali using a large excess of HOSA to push the reaction to completion. Using this method yields of up to 86% are reported for various 2-substituted

benzimidazoles **24** (Scheme 6). [6] If a particularly bulky substituent is present at the 2-position then the yield of the *N*-aminated product achieved with HOSA decreases and a more electrophilic reagent such as MSH can be more effective.

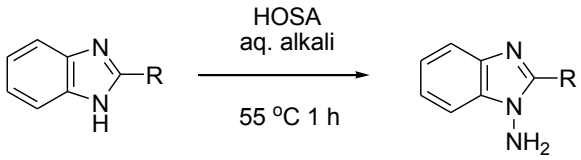

23 **24**

Scheme 6: *N*-amination of benzimidazole using HOSA

1- And 2-isomers of *N*-amino-1,2,3-triazoles can also be achieved *via* direct amination methods. For example it has been shown the 4,5-diphenyl-1,2,3-triazole **25** can be aminated using either HOSA (again in aqueous alkali) or with chloramine. In the former case (Scheme 7), a mixture of the 1- **26** and 2-aminotriazoles **27** was obtained in 94% yield. [10] On separation using column chromatography the ratio of these isomers was found to be approximately 1 : 1.

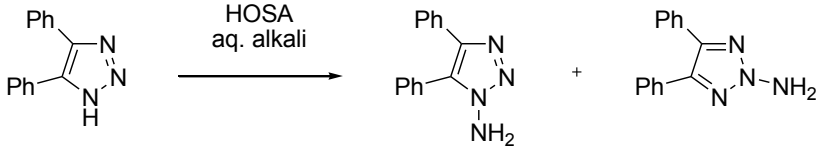

25 **26** **27**

Scheme 7: *N*-amination of 1,2,3-triazoles using HOSA

1.3 Advances in the *N*-amination of Azoles

Since the Kuzmenko review of 1992, many other papers detailing *N*-amination reactions of azoles with improved experimental methods and yields have been published. A selection of these has been chosen to outline current work, particularly in the area of benzimidazoles, pyrazoles and indazoles as these are the azoles of most importance to this work.

As was eluded to previously, HOSA does have limitations to its effectiveness as an *N*-aminating reagent, especially with substrates that contain base-sensitive functionalities and hence the resulting *N*-amino-azoles usually require some purification *via* chromatography. Hynes *et al.* [11] reported that for pyrrole and indole type azoles, chloramine is as effective a reagent for electrophilic amination as *O*-(2,4-dinitrophenyl)-hydroxylamine (DNPH) **9**. Chloramine was a preferred reagent to DNPH as the latter is not readily available and has the potential for detonation; additionally the waste generated contains 2,4-nitrophenol which is highly toxic. The chloramine method was adapted from that used to aminate amides in the synthesis of acylhydrazines. This method was modified and it was found that treatment of **28** with sodium hydride followed by chloramine in diethyl ether produced **29** in 89% isolated yield (Scheme 8).

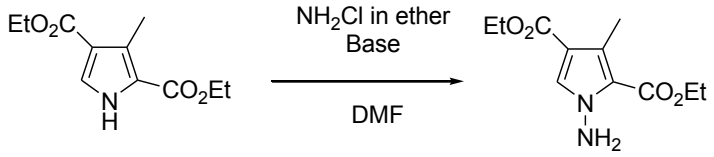

28 **29**

Scheme 8: *N*-amination of substituted pyrroles using chloramine

Two years after this initial chloramine method was published, an improved one-pot two-phase method was developed, [12] removing the need for the chloramine to be generated separately and dried before its further use, as it was generated in *situ*. The chloramine is highly soluble in water and sparingly so in methyl*tert*-butyl ether (MTBE) and it is this characteristic which is exploited in the two-phase method (Scheme 9). The chloramine is generated through the oxidation of ammonia by NaOCl in the aqueous layer and at the same time the substrate **30** is deprotonated by an excess of sodium hydroxide in the organic phase helped by a slight amount of Aliquat-336, (methyltrioctylammonium chloride) as a phase transfer reagent. The deprotonated substrate **31** then reacts with the small amount of chloramine present in the organic layer affording the desired *N*-amino derivative **32** in high yield. Once the reaction is complete the organic layer is easily separated and can be taken on to further reactions without the need for additional purification.

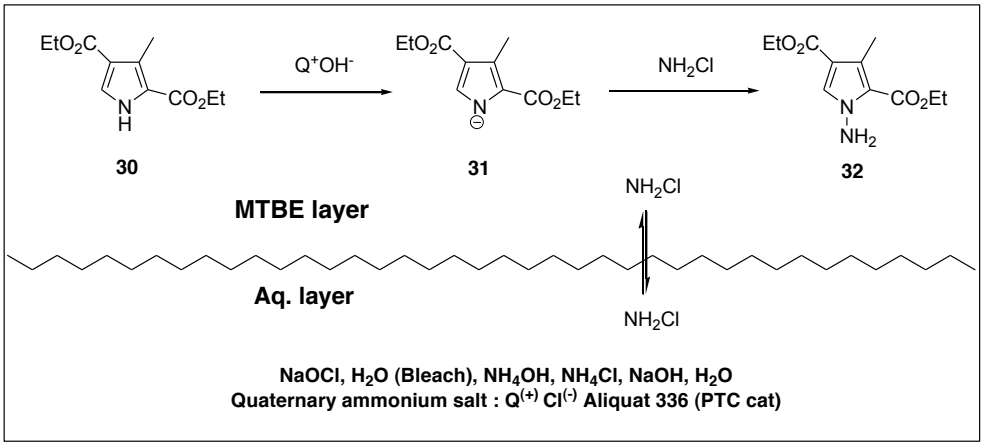

Scheme 9: Schematic showing concept behind 2-phase *N*-amination of pyrroles

Of the known *N*-aminating agents, some of the more versitile ones are (nitrophenyl)hydroxylamine derivatives. An investigation into the effectiveness of various substituted (nitrophenyl)hydroxylamines as aminating agents for quinazoline-2,4-diones was undertaken by Boyles *et al.* [13] This investigation was again prompted by safety concerns over the use of DNPH **9**, whose use, as

described above, creates detonation and waste stream concerns. The synthetic route to these (nitrophenyl)hydroxylamines (35a-d) is outlined in Scheme 10.

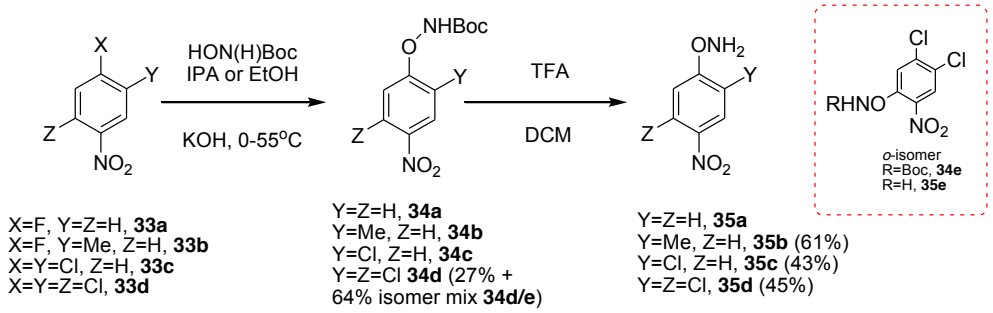

X=F, Y=Z=H, **33a**
X=F, Y=Me, Z=H, **33b**
X=Y=Cl, Z=H, **33c**
X=Y=Z=Cl, **33d**

Y=Z=H, **34a**
Y=Me, Z=H, **34b**
Y=Cl, Z=H, **34c**
Y=Z=Cl **34d** (27% +
64% isomer mix **34d/e**)

Y=Z=H, **35a**
Y=Me, Z=H, **35b** (61%)
Y=Cl, Z=H, **35c** (43%)
Y=Z=Cl, **35d** (45%)

Scheme 10: Synthesis of new (nitrophenyl)hydroxylamine aminating reagents

The first step in their synthesis is an aromatic nucleophilic substitution of *N*-Boc hydroxylamine on the halo arenes 33a-d to form the Boc protected (nitrophenyl)hydroxylamines 34a-d (34d also forms an *ortho* isomer 34e which can subsequently form the hydroxylamine 35e). Different acids were tried for the Boc cleavage step (formic acid, methanesulfonic acid and HCl in ethanol) but these gave poorer yields than TFA. The subsequent *N*-aminations of the quinazoline-2,4-diones 36 and 37, were carried out using sodium hydride as base in a 1 : 1 mixture of DMF and dioxane, but it was later found that potassium carbonate was a strong enough base for the reaction. Scheme 11 shows the final *N*-amination reaction conditions used. In the case of (nitrophenyl)hydroxyl amine 35d, this was used as a mixture of isomers 35d/35e in the *N*-amination, but was found on the separation of reaction products that only 35d was active in the *N*-amination as 35e was recovered unchanged.

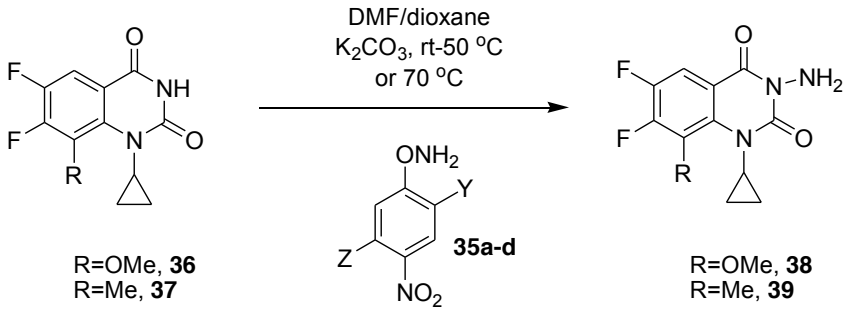

Scheme 11: *N*-amination of quinazolinediones using the previously synthesised (nitrophenyl)hydroxylamine reagents

The *N*-amination reactions were carried out using (nitrophenyl)hydroxylamines 35a-d on quinazoline-2,4-diones 36 and 37 at 50 or 70 °C, and the products were isolated by chromatography. It was found that *O*-(4-nitrophenyl)hydroxylamine 35a gave the best yields of *N*-aminated diones 38 and 39, and that it also had a much higher onset of decomposition temperature than the other (nitrophenyl)hydroxylamines (120 °C for 35a versus 90 °C for DNPH 9) so reactions could be safely carried out at 70 °C without risk of detonation. Although these *N*-aminations do not relate specifically to azoles, this method may be applicable to them.

A comparison of the effectiveness of electrophilic *N*-aminating reagents in the context of 2-oxazolidinones was carried out by Shen and Friestad [(1)] and was a thorough investigation into the efficiency of hydroxylamine based aminating reagents. These reagents were reacted with oxazolidinone 40 in the presence of a base (Scheme 12) either ^{n}BuLi or sodium hydride, which afforded the *N*-aminated product 41 and a small amount of starting material. As the product could not be separated from the starting oxazolidinone with ease, the *N*-aminated product 41 was then subject to condensation with benzaldehyde and purified by chromatography to produce the hydrazone 42. As the yields for this condensation step are reliably in excess of 90%, the yield of hydrazone was taken to be indicative of the effectiveness

of the amination reaction. This investigation showed that the most effective reagent in the case of oxazolidinones was *O*-(*p*-nitrobenzoyl)-hydroxylamine (NbzH, 7) with sodium hydride as base in dioxane at 60 °C. These conditions were then successfully applied to the amination of a variety of chiral 2-oxazolidinones.

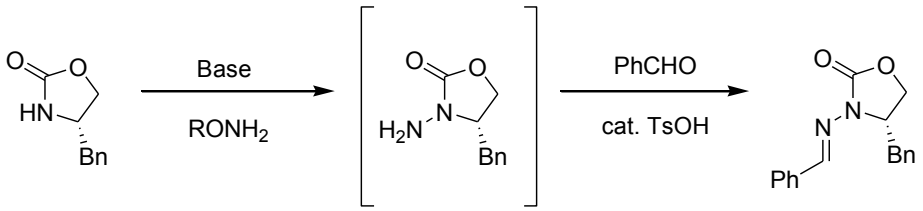

40 **41** **42**

Scheme 12: Reaction to gauge effectiveness of *N*-aminating reagents using 2-oxazolidinones

Imidazo[5,1-*f*][1,2,4]triazinones 43 are of major interest in pharmaceutical research, and the key step in their synthesis is the *N*-amination of 3*H*-imidazoles containing a 4-carbonyl group 44. Scheme 13 shows the general reaction conditions for this *N*-amination. [14]

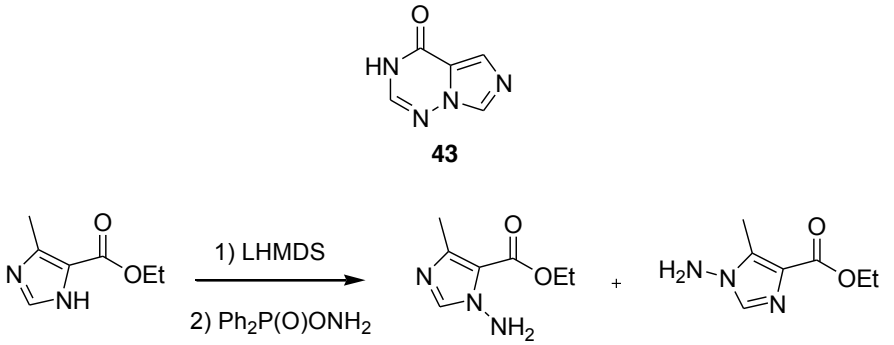

43

44 **45** **46**

Scheme 13: Synthesis of *N*-amino-3*H*-imidazoles en route to Imidazo[5,1-*f*][1,2,4]triazinones

The amination of imidazole 44 was first attempted using HOSA in anhydrous DMF, and 20% conversion to the *N*-aminoimidazole 46 was observed no matter what reaction variables were changed, even with a very large excess of HOSA. By switching to *O*-(diphenylphosphinyl)hydroxylamine (DPPH, 6) and using LHMDS as base in NMP solvent, 45 was consistently formed as the major isomer in greater than 70% yields. The minor isomer 46 cannot be carried through to imidazo[5,1-*f*][1,2,4]triazinones 43 and so separated from 45 by chromatography.

Vinogradova *et al.* [15] used *O*-picrylhydroxylamine to *N*-aminate 1-methoxymethyl and 1-acetyl derivatives of some substituted and some unsubstituted azoles. These included benzimidazole and imidazole which are of particular importance to this research. The limitations on HOSA amination seem to extend further than first thought; the reaction proceeds *via* the azole *N*-anion and if the parent azole has low NH-acidity and cannot readily be deprotonated or if the *N*-anion formed has a low nucleophilicity or low stability, the use of non-aqueous solvents and bases that are stronger than sodium hydroxide should make help facilitate the reaction. However there is some conflicting evidence over HOSA's ability to aminate in non-aqueous solvents. To combat these problems it was thought that if *N*-aminoazolium salts containing labile *N*-substituents could be made, then these could undergo amination and the labile groups removed afterwards to afford aminoazoles that may not be so readily directly aminated. The 1-methoxymethylbenzimidazole 47 and 1-methoxymethylimidazole 48 formed the expected 1-amino-3-methoxymethylimidazolium salts 49 and 50 which were then hydrolysed to 1-aminoazoles 51 and 52 with concentrated hydrochloric acid (Scheme 14).

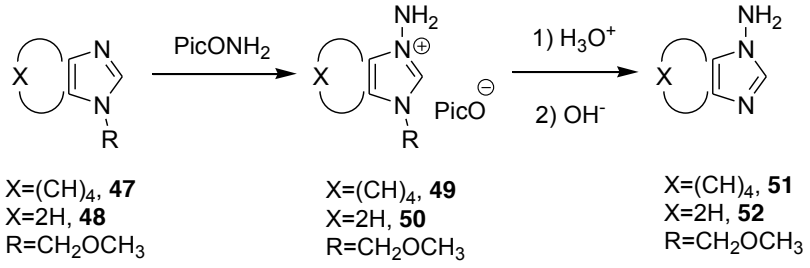

Scheme 14: Using *O*-picrylhydroxylamine to *N*-aminate imidazoles and benzimidazoles

This route was also successful for the *N*-amination of 2-cyanomethylbenzimidazole, and hence could most probably be adapted to most substituted benzimidazoles and imidazoles.

A different method using *O*-picrylhydroxylamine 53 was also used to *N*-aminate some more complex imidazole derivatives 54-57 (Scheme 15). [16] This method was employed because of their poor solubility in aqueous alkali.

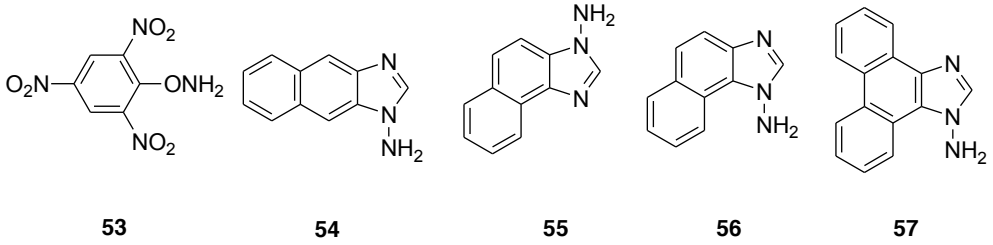

53 **54** **55** **56** **57**

Scheme 15: *O*-picrylhydroxylamine and some more complex ring systems successfully *N*-aminated *via* the method shown in scheme 14

Itoh *et al*[17] synthesised a wide variety of *N*-aminoazoles to investigate their radical scavenging properties. These were reacted with nitric oxide and with potassium

superoxide, both of which were found to de-aminate the azoles in very good yields. This result shows that the N-N bond is relatively weak and in the presence of free radicals can easily undergo homolysis. The *N*-aminoazoles were synthesised by either the standard reaction with HOSA in aqueous alkali at 50 °C or by using MSH with sodium hydride in tetrahydrofuran at 0 °C. This seems to suggest that amination of most azoles can be achieved by either one of these two methods.

Some 1,2,4,5-substituted imidazole derivatives have been found by Lagoja *et al* [18] to inhibit retroviral replication in HIV-1 strains that are resistant to other known non-nucleoside reverse transcriptase inhibitors (NNRTIs). Capravirine **58** is one such derivative and others of type **59** have been synthesised and tested for their antiviral activity (Scheme 16).

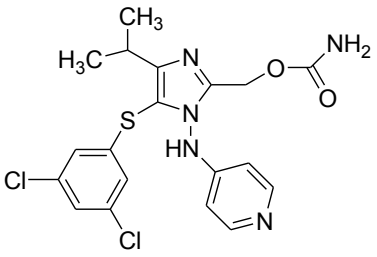

58

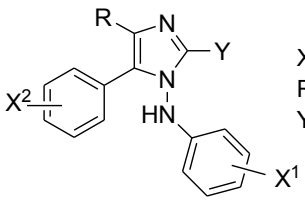

59

X1, X2: Hal, Alkyl
R: Alkyl, Aryl
Y: SH, H

Scheme 16: 1,2,4,5-substituted imidazoles showing properties of inhibiting HIV-1 replication

Preparation of these derivatives is an example of a direct ring-synthesis method for forming *N*-amino heterocycles. The corresponding *N*-aminoimidazoline-2-thiones **62** were made from substituted hydrazines **60**, α-bromoketones **61** and potassium thiocyanate, these then underwent desulfurisation with hydrogen peroxide in acetic acid to yield the associated *N*-aminoimidazole **63** (Scheme 17).

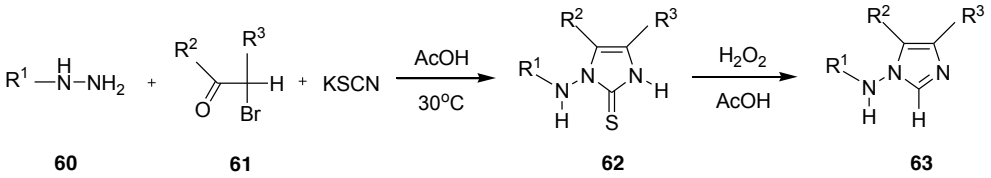

Scheme 17: Direct ring-synthesis of *N*-amino-2,4,5-substituted imidazoles

1-Aminobenzotriazole can also be produced by a direct-ring synthesis method (Scheme 18) starting from *o*-nitroaniline 64. [19] The *o*-nitroaniline was converted to its hydrochloride then reacted with sodium nitrite and diethyl malonate to form the hydrazone 65, which was subsequently hydrogenated to the corresponding amine 66. Further reaction with sodium nitrite forms the triazole ring 67 and concentrated hydrochloric acid produces the free 1-aminobenzotriazole 68.

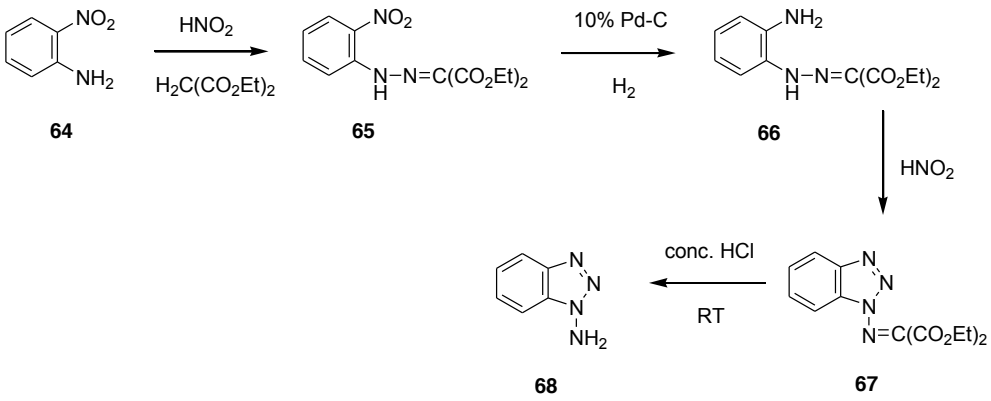

Scheme 18: Direct ring-synthesis of 1-aminobenzotriazole

1-Aminobenzotriazole 68 is an important compound to highlight, as it is an important precursor in the synthesis of benzyne. It can also be synthesised *via* direct amination of benzotriazole, but this also affords the 2-aminobenzotriazole, which is of no use in the production of benzyne and must be first removed by chromatography.

Substituted *N*-aminobenzimidazoles can also be obtained *via* a direct-ring synthesis method, which involves the acid-catalysed cyclisation of various substituted *o*-nitrophenylhydrazines under relatively mild conditions to yield the respective substituted *N*-aminobenzimidazoles. [20] Scheme 19 shows the general reaction conditions and a selection of some of the substituents successfully used to create the *N*-aminobenzimidazoles.

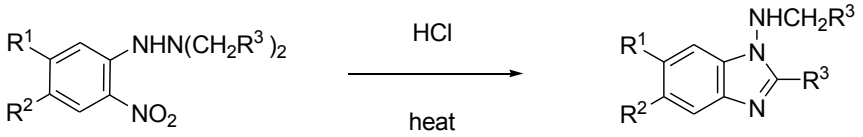

69 **70**

	R^1	R^2	R^3	$R^3 – R^3$	Yield (%)
a	H	H	H	-	60
b	Cl	H	H	-	68
c	H	NO_2	H	-	42
d	H	CF_3	H	-	50
e	H	CO_2 Et	H	-	79
f	H	H	-	$[CH_2]_3$	63
g	Cl	H	-	$[CH_2]_3$	23
h	H	NO_2	-	$[CH_2]_3$	50

Scheme 19 : General reaction for direct-ring synthesis of substituted *N*-amino benzimidazoles and table to illustrate various substituents used

It is known that structures of the type 69 can undergo cyclisation to benzotriazines 71 under base-catalysed conditions, [21] so how can the formation of substitued *N*-

aminobenzimidazoles **70** be confirmed to occur under acid-catalysed conditions? There is spectral data to back up the formation of the benzimidazoles; a clear coupling can be observed in the ^{1}H NMR spectrum between the NH and the adjacent CH_2 (or CH_3) group which on addition of deuterium oxide disappears. These data would eliminate the possibility of the product being a benzotriazine **71**.

The mechanism for the formation of the substituted benimidazoles **70** is shown in scheme 20. These reactions were also successfully carried out in polyphosphoric acid at 78 °C.

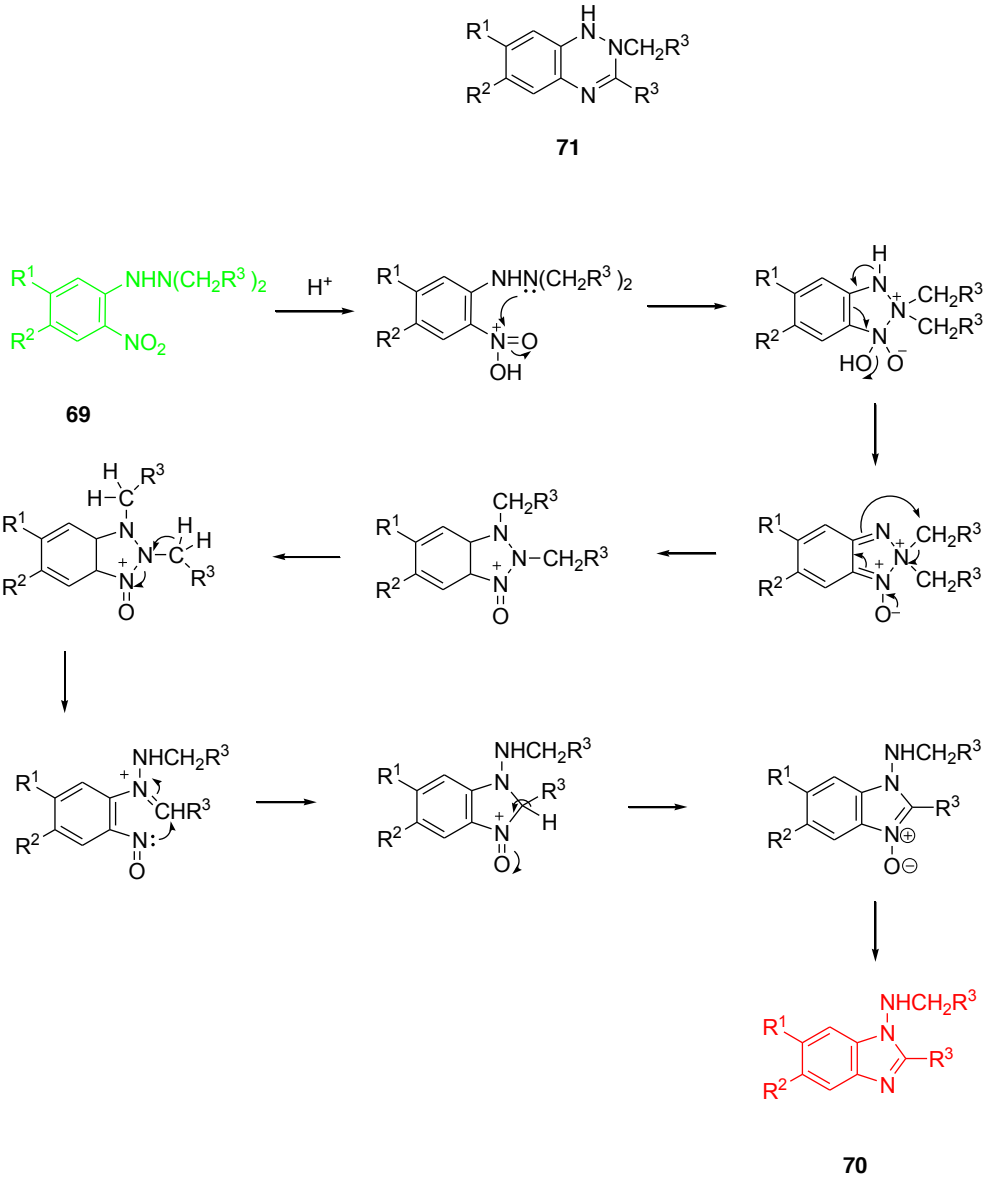

Scheme 20 : Mechanism of formation of substituted *N*-aminobenzimidazoles *via* direct-ring synthesis

2-Aminoindazole can be synthesised exculsively *via* a direct-ring synthesis also, which mean that there is no chromatography step required to remove the 1-aminoindazole isomer that would also be produced from a direct amination reaction using HOSA (scheme 21). [22]

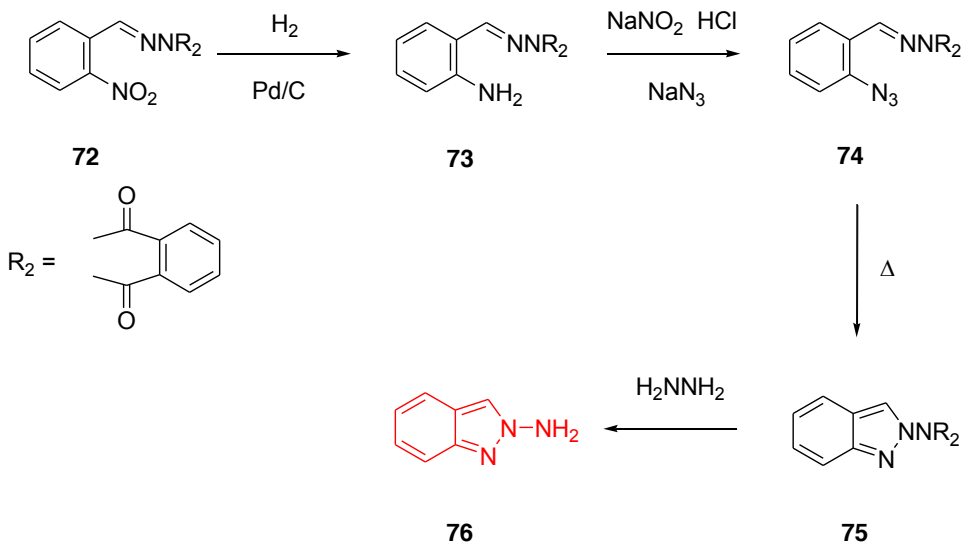

Scheme 21 : Direct synthesis of 2-aminoindazole from *N*-(*o*-nitrobenzal)aminophthalimide

The *N*-(*o*-nitrobenzal)aminophthalimide 72 is first reduced to the corresponding amine 73, which is then subjected to diazotization and reaction with sodium azide to produce the azide 74. When the azide 74 is heated the nitrene is generated which then cyclises onto the adjacent amine group to create the indazole 75. Reaction with hydrazine displaces the phthalimide groups producing the 2-aminoindazole 76 as a pure isomer.

1.4 Applications of *N*-aminoazoles

N-Amino heterocycles are usually found as substituted amines in commercially used compounds and pharmaceuticals or it many cases *N*-amino heterocycles are important intermediates in the synthesis of commercially used substances. Here we shall look at a few examples to highlight the importance of *N*-amino heterocycles and hence the *N*-amination reaction.

N-Amino Heterocycles – Applications in Flash Vacuum Pyrolysis

1,2-Diaminobenzimidazoles are prevalent *N*-amino heterocycles in the literature, as they are capable of undergoing condensation and cyclisation reactions with a range of reactants. As well as being ring systems with interesting electronic properties, they also have been shown to possess potent anti-fungal activity and hence may have pharmaceutical significance in the future.

When 2-alkylamino-1-aminobenzimidazoles 77a-e are refluxed in glacial acid with α-ketoglutaric acid (2-oxopentanedioic acid) cyclisation readily occurs to form the 4-alkyl-2-(2-carboxyethyl)triazino[2,3-*c*]benzimidazol-5*H*-3-ones 79a-e (Scheme 22). (23)

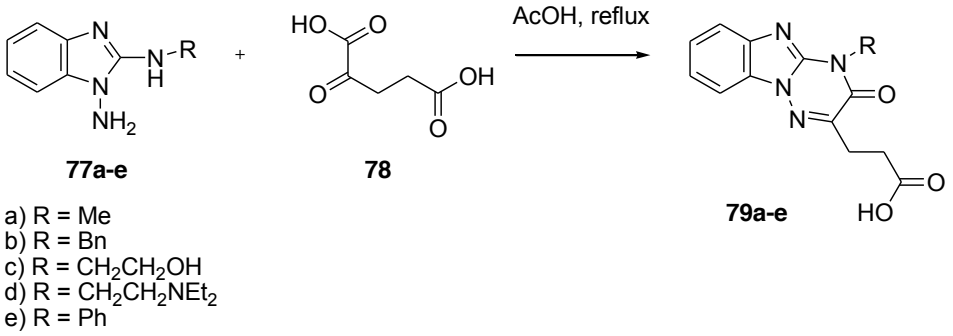

Scheme 22 : Reaction scheme for formation of 4-alkyl-2-(2-carboxyethyl)triazino[2,3-*c*]benzimidazol-5*H*-3-ones

This reaction works extremely well (75-80% yield), even for the substrate 77e, where the nucleophillicity of the secondary amino group is reduced by the electron-withdrawing nature of the phenyl group.

1,2-Diaminobenzimidazoles can also form *N*-substituted-triazinobenzimidazoles 82 and 83 by reaction of their quarternary 1,2-diamino-3-alkyl-benzimidazole salts 83 with α-ketoglutaric acid 78 and ethyl pyruvate 84 (scheme 23). (23) The quarternary

salts are formed from 1,2-diaminobenzimidazole and the corresponding alkylating agent (e.g MeI, BzBr etc).

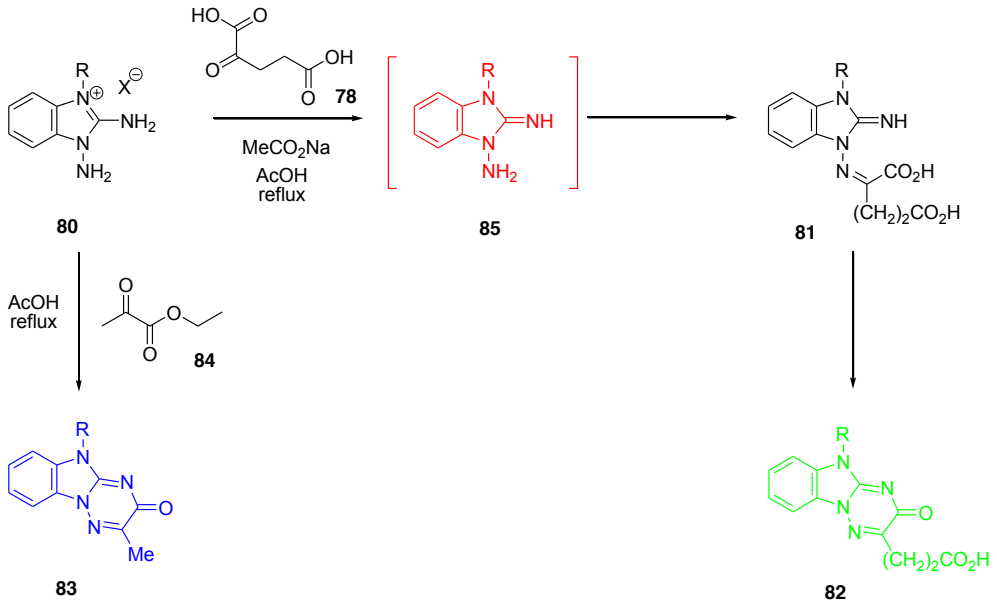

Scheme 23 : Formation of *N*-substituted-triazinobenzimidazoles from quarternary 1,2-diamino-3-R-benzimidazole salts

These reactions are preparatively very interesting since a wide range of salts of type 80 can be formed, with R groups ranging from methyl to CH_2CH_2OPh to β-piperidinoethyl. The cyclisation of these salts 80 with α-ketoglutaric acid 78 in acetic acid at reflux is much more difficult to achieve than cyclisation with ethyl pyruvate under the same conditions, however in the presence of sodium acetate the yields of the product 82 are increased significantly. It is believed that the sodium acetate facilitates the formation of the intermediate 85 which acitvates the nucleophilicity of both nitrogens atoms, so formation of intermediate 81 is easier leading to cyclisation to triazinones 82.

In the examples shown above, 1,2-diaminobenzimidazoles have been used in cyclisation reactions to form new 6-membered rings, but they can also be cyclised to from new 5-membered rings (e.g Scheme 24). [24]

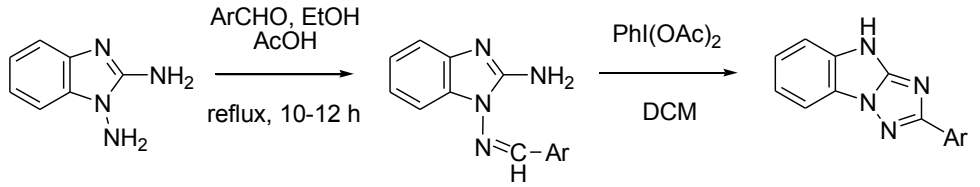

86 **87** **88**

a) Ar = 4-MeC_6H_4
b) Ar = 4-$MeOC_6H_4$
c) Ar = 4-ClC_6H_4
d) Ar = 4-BrC_6H_4

Scheme 24: Reaction scheme showing formation of 2-aryl-1,2,4-triazolo[1,5-*a*]benzimidazoles from 1,2-diaminobenzimidazole

Reaction of 1,2-diaminobenzimidazoles **86** with arylaldehydes in ethanol forms the 2-amino-1-(arylideneamino)benzimidazoles **87** in good yields of 76-81%. This reaction is regioselective at the 1-position, as the *N*-amino group is more nucleophilic than the 2-amino group. The next step involves the oxidation of the Schiff bases using a hypervalent iodine compound (diacetoxy)iodobenzene (DIB) at room temperature in DCM for 1 hour. This affords the 2-aryl-1,2,4-triazolo[1,5-*a*]benzimidazoles **88** in 48-57% yield after purification *via* column chromatography. Scheme 25 shows a plausible mechanism for the oxidation and subsequent cyclisation of the Schiff bases **87** to the triazolobenzimidazoles **88**.

Initially the DIB is involved in electrophilic attack of the C=N bond while intramolecular cyclisation of the 2-amino group happens simultaneously affording the cyclic adduct shown. This can then eliminate iodobenzene and acetic acid to produce the 2-aryl-1,2,4-triazolo[1,5-*a*]benzimidazoles **88**.

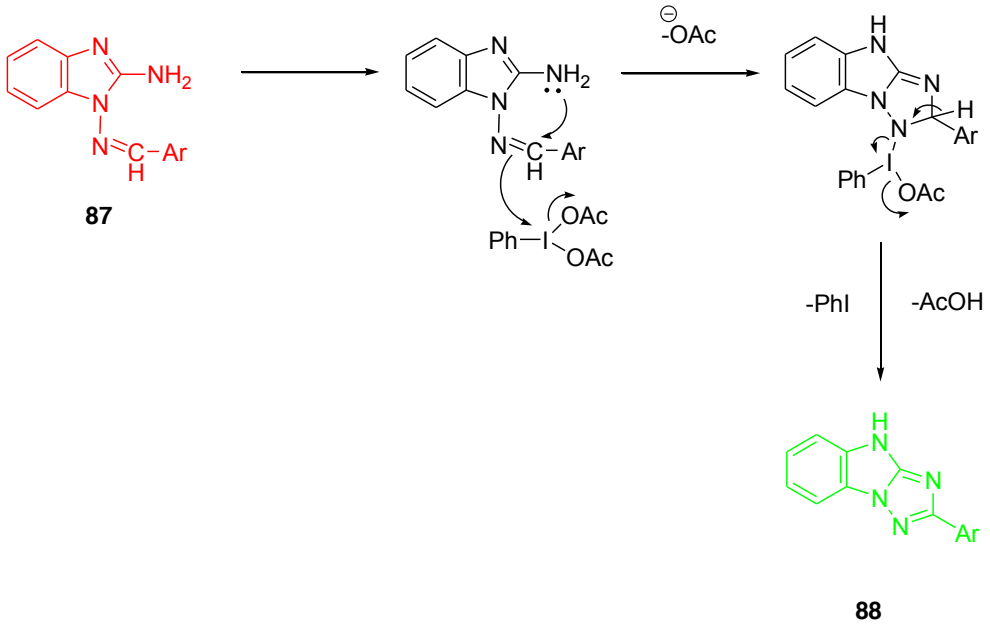

Scheme 25: Mechanism for formation of 2-aryl-1,2,4-triazolo[1,5-*a*]benzimidazoles

The reaction described above, as well as forming the desired triazolobenzimidazoles **88**, also produced an unexpected side-product, which upon analysis appeared to be the 3-amino-1,2,4-benzotriazine **90**. [24] Indeed, when 1,2-diaminobenzimidazole **86** itself was stirred with DIB in DCM at room temperature 3-amino-1,2,4-benzotriazine **90** (80% after chromatograhy) was the sole product from expansion of the imidazole ring. This ring expansion mechanism is thought to occur *via* a nitrene intermediate **89** which is generated by the attack of the *N*-amino group on the electron-deficient iodine. This produces the nitrene with the elimation of AcOH and iodobenzene, which subsequently inserts into the C-N bond expanding the ring and affording the benzotrazine **90**.

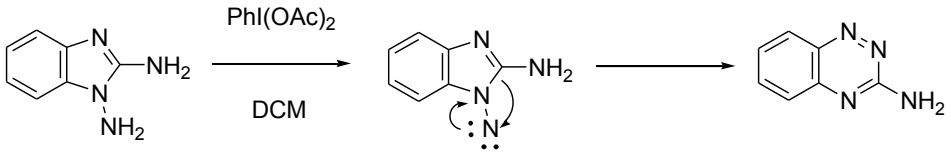

86 **89** **90**

Scheme 26: Ring expansion of 1,2-diaminobenzimidazole with DIB

Other diaminoheterocycles are also known to be very useful synthetic intermediates, for example 1,5-diaminopyrazole **92**. There is a problem encountered in their generation as *N*-amination of the 3-aminopyrazole **91** progresses with very little regioselectivity, resulting in a mixture of the desired 1,5-diaminopyrazole **92** and 1,3-diaminopyrazole **93** which are difficult to separate by chromatographic means. [25]

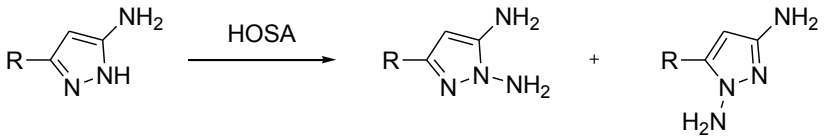

91 **92** **93**

a) R = H
b) R = Me
c) R = ^{t}Bu

a) R = H
b) R = Me
c) R = ^{t}Bu

a) R = H
b) R = Me
c) R = ^{t}Bu

Scheme 27: *N*-Amination of 3-aminopyrazole

Previous known reactions of **92** includes condensations with 1,2-dialdehydes, 1,2-diketones and 2-ketoaldehydes to form substituted derivatives of the pyrazolo[1,5-*b*]1,2,4-triazine ring system **94** [25], [26] However to explore the formation of new ring systems using 1,5-diaminopyrazole **95** a selective route to its formation was required.

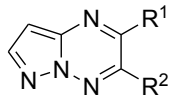

94

It was known that *N*-amination of the 3-aminopyrazole **91a** produced the diamino products **92a** and **93a** in approximately a 1:1 ratio. [25] 3-Amino-5-methylpyrazole **91b** under HOSA *N*-amination standard conditions gave **92b** and **93b** in a ratio of 60:40, a slight preference for the 1,5-diamino product. With the 3-amino-5-*tert*-butylpyrazole **91c** the diamino products **92c** and **93c** were obtained in yields of 57% and *ca* 3% respectively, with the remainder being unreacted starting material. It was clear that the *tert*-butyl group had effectively 'blocked' amination at the 1-position hence controlling the regiochemistry of the reaction. Using two equivalents of HOSA and then repeating the reaction on the recovered material with a further two equivalents of HOSA increased the yields of 3-*tert*-butyl-1,5-diaminopyrazole **92c**. [27] This repetition was also effective in the *N*-amination of the 4-chloro derivative **95** which produced the 1,5-diamino-3-*tert*-butyl-4-chloropyrazole **96** exclusively (Scheme 28). With the repetition of the *N*-amination reaction, yields of 60-70% were achieved for the products **92c** and **96**.

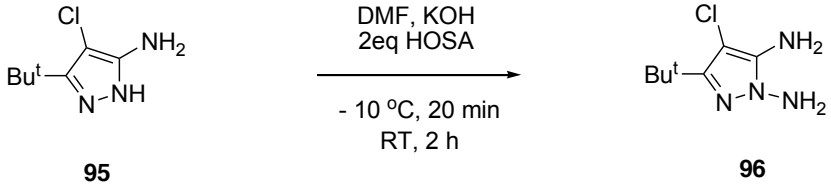

95 **96**

Reaction sequence applied twice

Scheme 28: Selective *N*-amination of 3-amino-5-*tert*-butyl-4-chloropyrazole using repeated HOSA method

Having achieved these two diaminopyrazoles, their reactivity was investigated with a range of electrophiles and compared alongside the chemistry of an aromatic diamine, *o*-phenylenediamine **97**. Initially the diaminopyrazole **92c** was reacted with an excess of DMF dimethyl acetal, which gave bis-amidine **98**. When the diaminopyrazole **92c** was then reacted with triethyl orthoformate, no products were detected. Under similar condition *o*-phenylenediamine **97** gives benzimidazole with both DMF dimethyl acetal and triethyl orthoformate, which goes to show that the reactivity of the diaminopyrazole **92c** is essentially different to the aromatic diamine. This may be because in the case of *o*-phenylenediamine the product is benzimidazole, a 6-5 fused ring system, whereas with diamine **92c** the cyclisation product would be a 5-5 fused ring system, which has additional ring strain. [27]

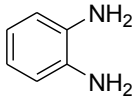

97

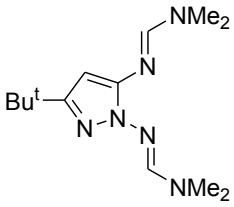

98

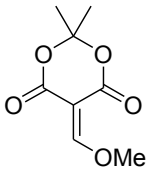

99

Reactions with other electrophiles tended to be selective, and reacted at only one of the amino groups, as was found with reaction of **92c** with methoxymethylene Meldrum's acid (MMMA) **99**. Analysis of the mono-substituted product showed that the MMMA had reacted with the *N*-amino group, however no cyclised product was apparent and the free amino group remained intact.

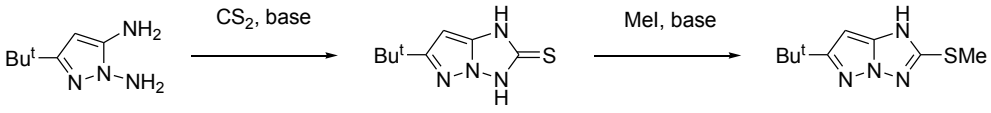

92c **100** **101**

Scheme 29: Formation of pyrazolo[1,5-*b*]1,2,4-triazole system

However, a cyclised product was achieved successfully when **92c** was reacted with carbon disulfide in the presence of base (Scheme 29). There has been previous work that sets some precedent for this reaction even in 5-5 fused ring systems. [28] On reaction with carbon disulfide, diamine **92c** forms the thione **100** which is alkylated *in situ* without work up using iodomethane to the pyrazolo[1,5-*b*]1,2,4-triazole system **101**. The pyrazolotriazole system is an important magenta coupler in colour photography [29] and the properties of **101** were subsequently investigated. [30]

Other cyclisations of the diaminopyrazole **95c** were also discovered. Reaction of the diaminopyrazole with acetylacetone in acetic acid at reflux presented the first example of the pyrazolo[1,5-*b*]1,2,4-triazepine system **102**. [27]

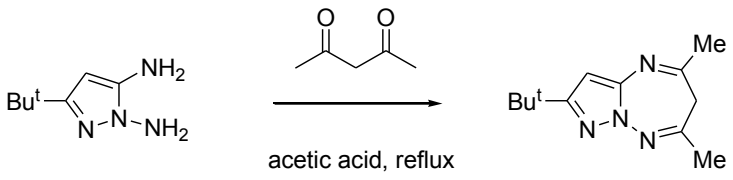

92c **102**

Scheme 30: Formation of the pyrazolo[1,5-*b*]1,2,4-triazepine system

β-Ketoesters have also been shown to undergo cyclisation reactions with the diaminopyrazoles **92c** and **95** under the same conditions (refluxing acetic acid, 1-1.5 h) to produce pyrazolo[1,5-*b*]1,2,4-triazepin-2-ones **103a-d**. The pyrazolotriazepinones **103a-c** were prepared from the appropriate ketoesters in yields ranging 42-55%, however when the diaminochloropyrazole **96** was used the yield was almost doubled, although the reason for this is uncertain.

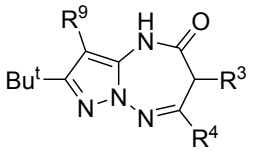

103

a) $R^3 = R^9 = H$, $R^4 = Me$
b) $R^3 = R^4 = Me$, $R^9 = H$
c) $R^3 = R^9 = H$, $R^4 = Pr^n$
d) $R^3 = H$, $R^4 = Me$, $R^9 = Cl$

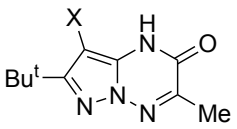

104

a) X = H
b) X = Cl

The diaminopyrazole **92c** and its chloro substituent analogue **96** were also treated with methyl pyruvate in acetic acid at reflux for 1.5 h, and from both reactions a single product was obtained. These products were found to be pyrazolo[1,5-*b*]1,2,4-triazin-2-ones **104a** and **b**, the product **104a** was obtained in a 32% yield and again the chloropyrazole produced a product yield of approximately double this. [27]

As has been shown in the previous example, *N*-amination reactions can be directed to certain positions by blocking off others with large, bulky adjacent groups. [27] However, in some cases the *N*-amination reaction can be naturally regioselective as non-equivalent nitrogen atoms in azoles and related compounds can have different reactivities. One example of this is shown in Scheme 31, which shows the reaction scheme for the *N*-amination of 6-amino-2-methylpyrimidin-4-one **105**. [31] The pyrimidinone **105** is aminated using MSH at room temperature in methanol and the sole product from the reaction is the *N*-aminopyrimidone **106** in a 50% yield. No evidence of the 1-amino isomer **107** was observed.

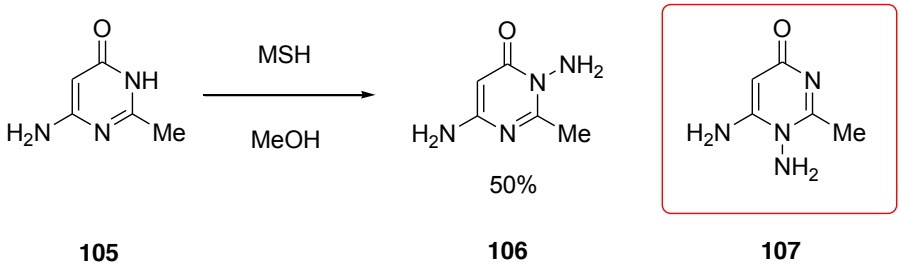

Scheme 31: *N*-amination of 6-amino-2-methyl-4-pyrimidone using MSH

To change the regioselectivity of the reaction in an attempt to synthesise the 1-aminopyrimidone **107**, the *N*-amination reaction was repeated, but using 3-amino-6-chloro-2-methylpyrimidine **108** (Scheme 32) with a view to replacing the chlorine after the amination.

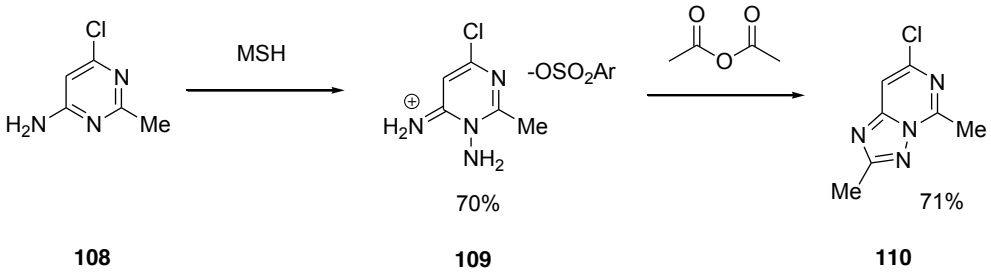

Scheme 32: Indirect route to 3-amino-6-chloro-2-methylpyrimidine and subsequent conversion to respective triazolopyrimidine

The 1-aminopyrimidine salt **109** was synthesised in a 70% yield by the *N*-amination of the chloropyrimidine **108** using MSH in chloroform at room temperature. The position of the amino group and hence the regioselectivity of the *N*-amination was determined by the conversion of the amination product **109** into the triazolopyrimidine **110**. Attempts were made to replace the chlorine by an oxygen

substituent; however this was unsuccessful as all conditions resulted in the destruction of the pyrimidine ring.

Because of the difficulty in replacing the chlorine in the reaction above, a different approach was required if the desired 1-aminopyrimidine **107** was to be successfully synthesised. 4-Amino-6-benzoyloxy-2-methylpyrimidine **111** was made from the reaction of pyrimidinone **105** with benzoyl chloride, and then subsequently *N*-aminated again using MSH to form the *N*-aminopyrimidine salt **112** as the only product in a 63% yield. Treatment of the salt **112** with ammonia/methanol solution successfully produced the *N*-aminopyrimidone isomer **107**. Again to confirm that the correct isomer had been achieved and because the differences in the ^{1}H and ^{13}C NMR spectra of pyrimidones **106** and **107** were not significant, a chemical demonstration of the position of the *N*-amino group was undertaken by reaction of the aminopyrimidinone **107** with acetic anhydride to form the triazolopyrimidine **113**.

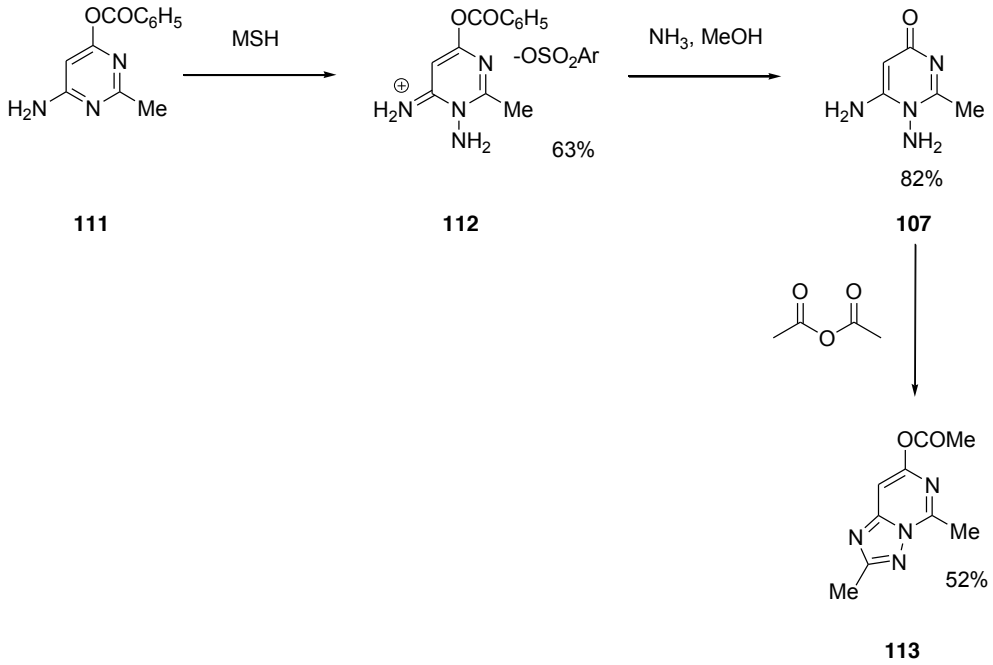

Scheme 33: Indirect route to desired 3-amino-2-methyl-4-pyrimidinone and subsequent conversion to respective triazolopyrimidinone

N-Amino groups can also be used as useful stepping-stones for conversion to other functional groups. The direct arylation of *N*-amino groups is much harder to achieve than the corresponding alkylation reaction, [6], [32] and the few examples that exist of this type of arylation involve the expected use of aryl halides activated by strong electron-withdrawing groups such as CN or NO_2. [33], [34] However it has been reported that arylamines can be *N*-arylated using arylboronic acids forming new heteroatom-carbon bonds, analogous to the way they are employed in the Suzuki reaction to form new carbon-carbon bonds. [35] It was then discovered that this method was directly applicable in the arylation of *N*-aminoazoles. [36]

Using this method, *N*-aminobenzimidazole **114** was successfully arylated to form 1-phenylaminobenzimidazole **115**, by reaction with phenylboronic acid in the presence of copper acetate and triethylamine (Scheme 34). The reaction was performed in dichloromethane at room temperature. This method was also successfully applied to produce the *N*-arylated products **116-118** from the corresponding *N*-aminoazoles in yields of 16-29%. These are low, but there is no other reported method for the preparation of *N*-(phenylamino)azoles.

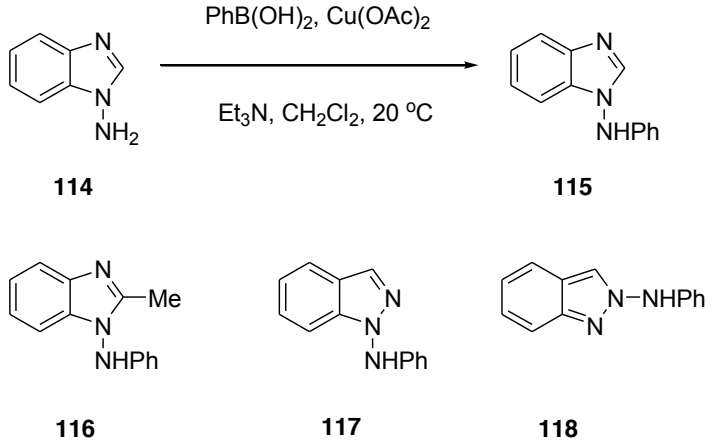

114 **115** **116** **117** **118**

Scheme 34: Arylation of *N*-aminoazoles using phenylboronic acid

N-Aminoheterocycles have also been used to study the structural and tautomeric properties of some Schiff bases. It has been shown that *N*-salicylidenearenamines (where salicylidene = (2-hydroxyphenyl)-methylene) demonstrate hydroxy/imino **119** to oxo/enamino **120** tautomerism due to proton transfer, and this is witnessed in both solution and solid state (Scheme 35). [37] [38]

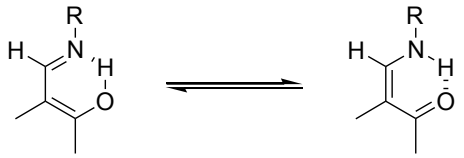

119 **120**

R = (2-hydroxyphenyl)-methylene

Scheme 35: Hydroxy/imino to oxo/enamino tautomerism

This tautomeric phenomenon has also been explored in the aromatic Schiff bases of *o*-hydroxybenzaldehydes, where it was found that the equilibrium usually favours tautomer **119**, but can be shifted towards conformation **120** when the polarity of the solvent used was increased or a stronger electron-withdrawing R group was used. [38], [39] Some studies have been conducted into the Schiff bases derived from 3-hydroxypyridine-4-carboxaldehyde **121** and *para*-substituted anilines in an attempt to model the hydrogen-bonded structure of the cofactor pyridoxal-5′-phosphate which is involved in many enzymatic transformations of amino acids. [40] This work was then extended to study the tautomers of the Schiff bases formed from **121** and the *N*-aminoazoles **122a-d** to then allow a comparison to be made between the two different kinds of substituents, aromatic *vs* heteroaromatic (Scheme 36). [41]

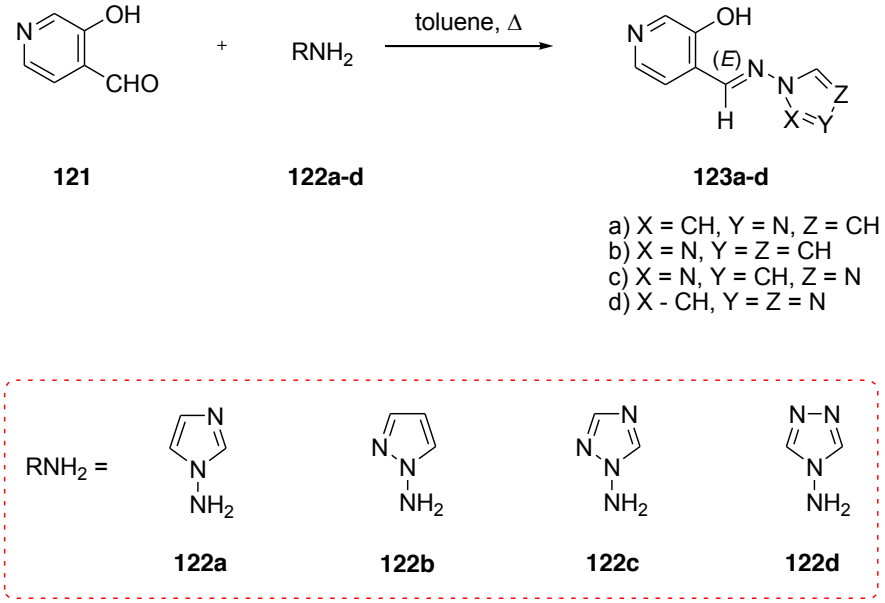

Scheme 36: Formation of Schiff bases from *N*-aminoazoles

The Schiff bases (or 4-[(1*H*-azol-1-ylimino)methyl] pyridin-3-ols) **123a-d** were prepared in yields of 85-90% from the condensation of 3-hydroxypyridine-4-carboxaldehyde **121** with the *N*-aminoazoles **122a-d** (Scheme 36). All of the Schiff bases **123a-d** can exsist as either (*E*)- or (*Z*)-isomers, however 2D-NOESY NMR showed that only the (*E*)-isomer was present in each case. DFT calculations on the **119/120** tautomerisation of the Schiff bases **123a-d** all showed that the **119** tautomer with the intramolecular bond was the most stable. Substantial ^{1}H-, ^{13}C-, and ^{15}N-NMR and X-ray crystallographic studies confirmed these calculations in all cases.

Maybe one of the most important functions of *N*-aminoheterocycles is that of intermediates in pharmaceutical synthesis; one example will be used to illustrate this point. There are two different types of α-adrenoceptors found in the body; α_1 and α_2. α_2-Adrenoceptors can be found in many different tissues in the body and mediate various functions in peripheral organs but are also highly prevalent in the central nervous system. α_2-Adrenoceptors agonists are an important type of pharmaceutical compounds because of their extensive breadth of uses in medicine. [(42), (43), (44)] Some

of their most common applications are as hypertensive drugs to treat high blood pressure, as muscle relaxants and to treat symptoms of attention deficiency and hyperactivity disorder (ADHD) and insomnia.

α-Adrenoceptors agonists often contain an imidazole/imidazoline ring moiety, and in recent years this in conjunction with an indazole ring has been found to have α-adrenoceptor agonist properties. The 4-substituted indazole derivative, indanidine **124** has been shown to have agonist activity selectively towards α_1-adrenoceptors [45] whereas the 6-substitued analogues of the form **125** were found to be selective agonists for α_2-adrenoceptors. [46] This led to an interest into the effect of relocation the aminoimidazoline group and hence compounds of type **126** were targeted for synthesis and investigation into their α-adrenoceptors selectivity and agonist properties. [47]

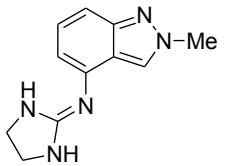

124

Indanidine

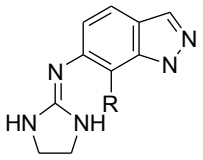

125

6-(imidazolidinimino)indazole

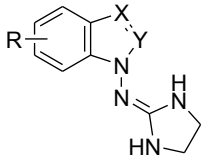

126

X, Y = CH or N

Marsanidine X = CH, Y = N, R = H

Compounds of the type **126** can be thought of as *N,N,N*-trisubstituted cyclic guanidines. Most methods in the literature for the synthesis of guanidine derivatives involve the reaction of an appropriate amine with the electrophilic precursors of a guanidine moiety. [48] Hence the 1-aminoindazole required was made *via* the *N*-amination of indazole using HOSA as shown in the reaction in Scheme 37. The 1-amino and 2-aminoindazoles were separated by column chromatography. [47]

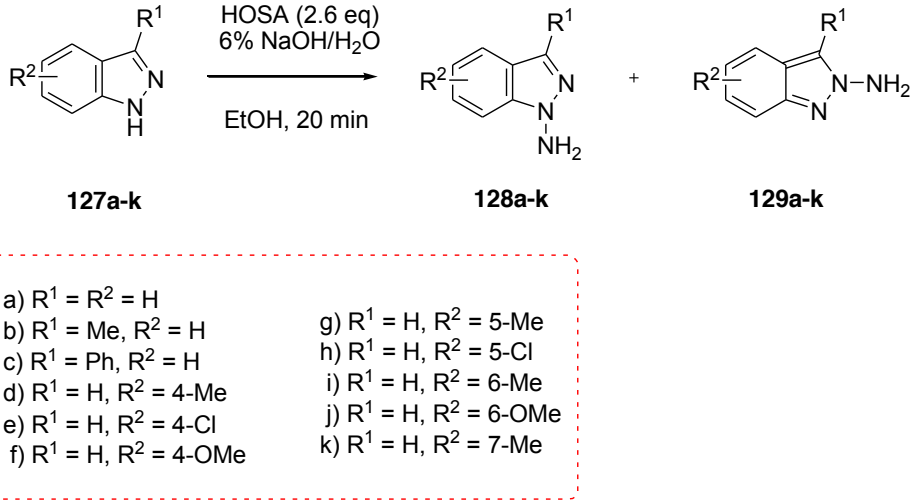

Scheme 37: *N*-Amination of substituted indazoles

N-Aminoazoles have been found to have poor nucleophilic reactivity under certain conditions [49] and indeed, reaction of the *N*-aminoindazoles with conventional guanylating agents was unsuccessful. However Kim's guanidine synthesis [50] which is illustrated in step a) of Scheme 38 and 39, involves reacting the *N*-aminoindazoles with preformed *N,N'*-bis-Boc-imidazolidine-2-thione [51] in the presence of $HgCl_2$ to produce bis-Boc-protected guanidines **130a-k** and **133a-k** (Scheme 38 and 39). After purification by chromatography on silica gel, the imidazolidines were deprotected to form the desired 1-[(imidazolidin-2-yl)imino]indazoles **131a-k** and 2-[(imidazolidin-2-yl)imino]indazoles **134a-k**. These were then also converted into the corresponding hydrochlorides **132a-k** and **135a-k** using a methanolic solution of HCl, for the purposes of SAR studies, as the hydrochloride salts are more water soluble and therefore more easily taken into cells.

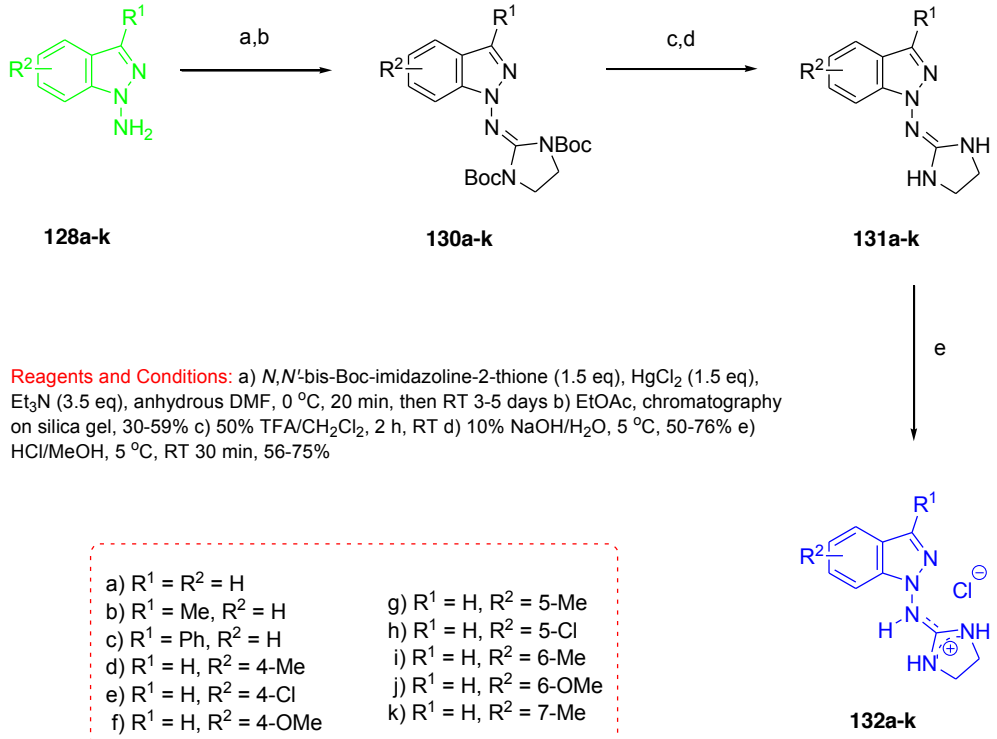

Scheme 38: Synthesis of 1-[(imidazolidin-2-yl)imino]indazoles

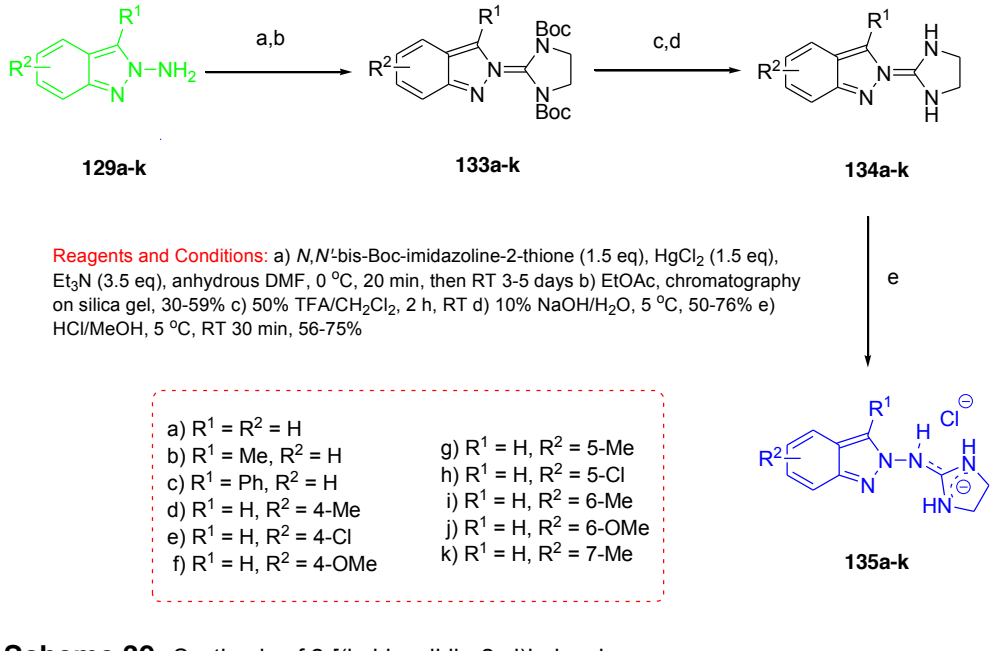

Scheme 39: Synthesis of 2-[(imidazolidin-2-yl)indazoles

All the compounds **132a-k** and **135a-k** were investigated *in vitro* for their binding affinities and selectivity towards α_2-adrenoceptors and the related imidazoline I_1 and imidazoline I_2 binding sites. All the compounds had very little or no affinity for I_2 receptors. The series **135a-k** showed very little affinity for any of the receptor types and further studies were abandoned. The SAR studies on compounds **132a-k** implied that their affinity for α_2-adrenoceptors was highly dependent on the nature and positions of the substituents. The unsubstitued 1-[(imidazolidin-2-yl)imino]indazole salt **132a** possessed significant activity towards α_2-adrenoceptors and very high selectivity *versus* imidazoline I_1 receptors. Placement of a methyl or phenyl group in the 3-position (**132b** and **c**) resulted in very low affinity for α_2-adrenoceptors, however repositioning the methyl group to position 4, 5 or 6 led to moderately active compounds (**132d**, **g** and **i**). The corresponding 4-chloro and 5-chloro substituted analogues **132e** and **h** were 2-3 times less active and **132f** which has an electron-donating OMe group at the 4-position was shown to be inactive towards α_2-adrenoceptors. Of all the methyl substituted compounds tested, the 7-methyl compound **132k** exhibited significant activity towards α_2-adrenoceptors and moderate activity towards imidazoline I_1 receptors, allowing it to be compared to clonidine-like "hybrid drugs" which work as agonists of both receptor types.

Following the *in vitro* tests outlined above, *in vivo* studies were carried out to determine the cardiovascular properties of **132a-k**. [47] The general trend observed was that most of the compounds showed a biphasic effect on blood pressure: momentary hypertension followed by a long-lasting hypotension effect. Conversely, no clear correlation was observed between the *in vivo* potencies and the *in vitro* affinities for α_2-adrenoceptors. For example, evaluation of the cardiovascular potency of **132a** demonstrated that this compound has a considerable effect on blood pressure at a dose of 0.1 mg/kg (ΔMAP [mean arterial blood pressure] = -30.9 mmHg) yet 4-Me and 6-Me substituted compounds **132d** & **i** (which showed less affinity for α_2-adrenoceptors) produced hypotensive results of a similar magnitude (ΔMAP = -29.0 mmHg and -23.4 mmHg respectively). On the contrary, the 5-Me substituted analogue **132g** which *in vitro* was slightly more active towards α_2-

adrenoceptors, exhibited a weak cardiovascular effect (ΔMAP = -4.9 mmHg). The most prominent discrepancy was observed for the 7-Me derivative **132k** which showed a similar affinity for α_2-adrenoceptors to the 5-Me derivative **132g** but which displayed a much greater hypotensive effect when administered at the same dose (ΔMAP = -43.5 mmHg). In summary, it was found that more pharmacokinetic studies are needed on structures of this type but that the 7-Me analogue **132k** was an effective hypotensive compound and could be a good potential lead structure for further development into a novel antihypertensive drug. [47] Further to this work, a patent has been obtained for the use of 1-[(imidazolidin-2-yl)imino)]indazoles as α2-adrenergic receptor agonists. [52]

1.5 Flash Vacuum Pyrolysis

Flash vacuum pyrolysis (FVP) is a technique which allows reactions to occur in the gas phase without any need for solvent and can be particularly useful for radical intramolecular transformations and for pericyclic reactions, often involving the generation of a ketene. Applications of both these processes are explained in this thesis.

FVP is a clean and straightforward technique and an example of 'green' chemistry method as no solvents are used. FVP involves the vacuum distillation of a substrate through a hot silica tube heated in a furnace. The substrate is heated in a borosilicate glass inlet tube by a small Kugelrohr oven until it volatilises through a silica furnace tube (30 × 2.5 cm) heated by a Carbolite electronically controlled laboratory tube furnace, where the reaction takes place. The resulting products are trapped in a borosilicate U-tube, which is cooled with liquid nitrogen, once they leave the furnace. When pyrolysis is complete, the coolant is removed from surrounding the U-tube and it is allowed to warm to room temperature under a nitrogen atmosphere.

The apparatus used for flash vacuum pyrolysis (FVP) is shown in Figure 3. [53] It is based on the design by W. D. Crow of the Australian National University. FVP experiments typically take place with furnace temperatures of 300-1000 ˚C with the whole apparatus evacuated to approximately 3.0×10^{-2} Torr. The average throughput rate for preparative purposes is approximately 1-2 grams of substrate per hour which implies that each substrate molecule spends only a fraction of a second in the furnace tube. "Small scale" pyrolyses involve approximately 20-50 mg of substrate, and in these cases the entire pyrolysate can be dissolved in a suitable solvent (usually $CDCl_3$) and the crude pyrolysis products examined directly by NMR spectroscopy.

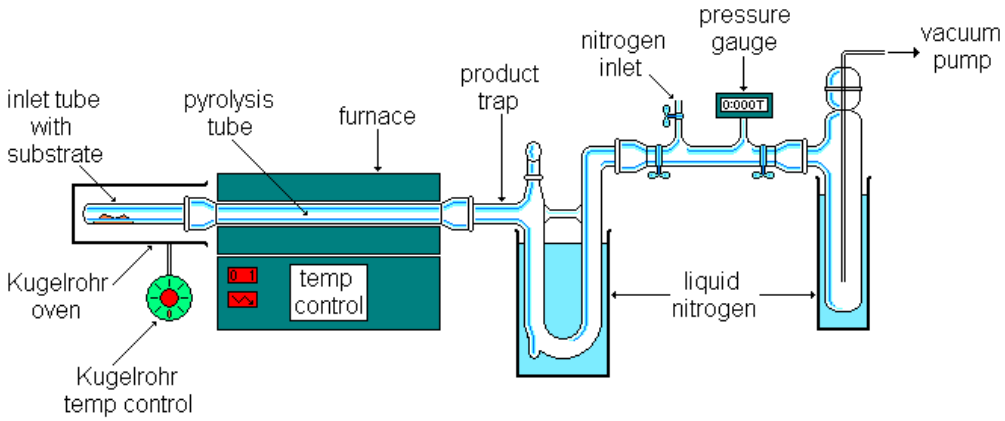

Figure 3: Schematic of flash vacuum pyrolysis equipment and set-up

A temperature profile experiment is used to identify the optimum pyrolysis temperature for substrates that produce more than one product or that degrade at certain furnace temperatures. This involves a series of small scale pyrolyses at varying furnace temperatures and analysing the whole of the pyrolysate produced to determine whether the ratio of products is temperature dependent, at what furnace temperature the products degrade or the optimum furnace temperature for a certain transformation. These temperature profiling experiments then allow the determined optimum temperature to be employed for preparative experiments.

1.6 References

1. Y. Shen and G. K. Friestad, *J. Org. Chem.*, 2002, 67, 6236.

2. H. Baldinger, E. M. Karitschka, J. Knoflach, *Synthesis*, 1982, 592.

3. M. Ikeda, J. Minamikawa and Y. Tamura, *Synthesis*, 1977, 1.

4. S. Fujii, K. Sumoto, M. Ikeda, J. Minamikawa, Y. Tamura, *J. Org. Chem.*, 1973, 38, 1239.

5. E. E. Glover and K. T. Rowbottom, *J. Chem. Soc., Perkin Trans. 1*, 1976, 367.

6. V. V. Kuz'menko and A. F. Pozharskii, *Adv. Heterocycl. Chem.*, 1992, 53, 85.

7. M. Hirobe, H. Koga and T. Okamoto, *Tetrahedron Lett.*, 1978, 15, 1291.

8. A. J. Boulton, *J. Chem. Soc., Perkin Trans. 1*, 1986, 1249.

9. B. M. Adger, S. Bradbury, M. Keating, C. W. Rees, R. C. Storr, M. T. Williams, *J. Chem. Soc., Perkin Trans. 1*, 1975, 31.

10. M. D. Badia, J. De Mendoza, T. Torres, *Monatsh. Chem.*, 1988, 119, 1041.

11. W. W. Doubleday, A. J. Dyckman, J. D. Godfrey, J. A. Grosso, J. Hynes, S. Kiau, K. Leftheris, *J. Org. Chem.*, 2004, 69, 1368.

12. A. Bhattacharya, J. A. Grosso, V. A. Palaniswamy, L. Parlanti, N. C. Patel, M. Peddicord, R. E. Plata, Q. Ye, *Tetrahedron Lett.*, 2006, 47, 5341.

13. D. C. Boyles, T. T. Curran, R. V. Parlett, *Organic Process Research and Development*, 2002, 6, 230.

14. J. Healy, A. Heim-Riether, *J. Org. Chem.*, 2005, 70, 7331.

15. V. V. Kuz'menko, O. V. Kryshtalyuk, A. F. Pozharskii, M. I. Rudnev, O. V. Vinogradova, *Chem. Heterocycl. Compd. (Engl Transl)*, 1994, 30, 1182.

16. O. V. Dyablo, M. G. Koroleva, A. F. Pozharskii, Z. A. Starikova, *Chem. Heterocycl. Compd. (Engl Transl)*, 2003, 39, 1161.

17. T. Itoh, M. Miyazaki, H. Maeta, Y. Matsuya, K. Nagata, A. Ohsawa, *Bioorg. Med. Chem.*, 2000, 8, 1983.

18. J. Balzarini, E. De Clercq, Z. Debyser, P. Herdewijn, Irene M. Lagoja, C. Pannecouque, A. Van Aerschot, M. Witvrouw, *J. Med. Chem.*, 2003, 46, 1546.

19. B. Rickborn, *1-Aminobenzotriazole,* John Wiley&Sons, Ltd., Chichester, UK, 2001, e-EROS Encyclopedia of Reagents for Organic Synthesis.

20. D. W. S. Latham, O. Meth-Cohn, H. Suschitzky, *J.C.S Chem. Comm.*, 1973, 41.

21. J. D. Loudon, G. Tennant, *Quart. Rev.*, 1964, 389.

22. J. P. Anselme, K. Sakai, *J. Org. Chem.*, 1972, 37, 2351.

23. L. N. Divaeva, A. S. Morkovnik, T. A. Kuz'menko, V. V. Kuz'menko, *Chem. Heterocycl. Compd. (Eng. Trans.)*, 2006, 42, 648.

24. A. Kumar, *Synthesis*, 2009, 10, 1663.

25. Y. Lin, M. Siegel, D. R. Sliskovic, *Synthesis*, 1986, 71.

26. D. R. Sliskovic, *J. Hetrocycl. Chem.*, 1989, 26, 1109.

27. A. J. Blake, D. Clarke, R. W. Mares, H. McNab, *Org. Biomol. Chem.*, 2003, 1, 4268.

28. K. Pilgram, G. E. Pollard, *J. Heterocycl. Chem.*, 1976, 13, 1225.

29. T. Kawagishi, N. Furutachi, *European Patent 119860.* 1985, *Chem. Abstr.*, 102, 36637b.

30. D. Clarke, R. W. Mares, H. McNab, *US Patent 5,723,623.* 1997, *Chem. Abstr.*, 127, 121724p.

31. M. B. Bodyagin, A. Y. Ivanov, P. S. Lobanov, A. A. Potelenin, J. G. Schantl, K. Wurst, *Chem. Heterocycl. Compd.*, 2003, 39, 195.

32. I. A. Filatova, V. V. Kuzmenko, A. F. Pozharskii, *Khim. Geterotsikl. Soedin.*, 1992, 1196.

33. R. A. Carboni, *US Patent No. 3,184,472.* 1965, *Chem. Abstr.*, 63, 4306.

34. Y. Isomura, E. Kawaminami, M. Kudoh, M. Okada, Y. Shimada, T. Yoden, *Chem. Pharm. Bull.*, 1997, **45**, 333.

35. D. M. T. Chan, K. L. Monaco, R. P. Wang, M. P. Winters, *Tetrahedron Lett.*, 1998, **39**, 2933.

36. O. V. Dyablo, M. G. Koroleva, A. F. Pozharskii, *Chem. Heterocycl. Comp.*, 2002, **38**, 620.

37. S. H. Alarcón, R. M. Claramunt, J. Elguero, A. C. Olivieri, D. Sanz, *J. Mol. Struct.*, 2004, **705**, 1.

38. P. E. Hansen, K. P. P. Nguyen, Q. T. That, *Magn. Reson. Chem.*, 2005, **43**, 302.

39. A. Filarowski, *Ber. Bunsenges. Phys. Chem.*, 1998, **102**, 393.

40. R. M. Claramunt, J. Elguero, A. Perona, D. Sanz, *Tetrahedron*, 2005, **61**, 145.

41. R. M. Claramunt, J. Elguero, A. Perona, D. Sanz, *Helv. Chim. Acta.*, 2006, **89**, 1290.

42. W. Koblinger, *Naunyn-Schmiedeberg's Arch. Pharmacol.*, 1986, **332**, 113.

43. P. A. Van Zweiten, *Am. J. Cardiol.*, 1988, **61**, D6.

44. W. Koblinger, L. Pichler, Centrally acting drugs, *Handbook of Experimental Pharmacology.* 1990, 227.

45. M. J. Mathy, M. J. M. C. Thoolen, P. B. M. W. M. Timmermans, P. A. van Zwieten, *Br. J. Pharmacol.*, 1984, **81**, 255.

46. J. J. Ares, S. E. Bogdan, T. L. Cupps, R. T. Henry, W. L. Seibel, R. J. Sheldon, 1998, *WO1998023609*

47. K. Boblewski, M. Gdaniec, A. L. Hudson, A. Kornicka, A. Lehmann, S. S. Miao, A. Rybczynska, F. Saczewski, *J. Med. Chem.*, 2008, **51**, 3599.

48. F. Saczewski, Functions containing an iminocarbonyl group. *Comprehensive Organic Functional Group Transformations*. 2005, 605.

49. J. Catalan, *J. Chem. Soc., Perkin Trans. 2*, 1993, 1687.

50. K. S. Kim, L. Quian, *Tetrahedron Lett.*, 1993, **34**, 7677.

51. A. Alsasua, *Bioorg. Med. Chem.*, 2000, 8, 1567.

52. F. Saczewski, June 2009, *WO 2009071906*.

53. R. Tyas, *FVP Apparatus,* 2006, University of Edinburgh, Edinburgh .

2. *N*-Amino heterocycles as azol-1-yl radical generators

2.1 Introduction

There is little published work available on azol-1-yl radicals, and that which exists seems to focus on the physical chemical and theoretical properties of pyrrol-1-yl radicals. [(1), (2), (3)] There is only one known published paper relating to its synthesis [(4)] and thus is an unexplored research area. Some undergraduate final year project work within the McNab group on azol-1-yl radical generation has been performed and it is from this that the work described here has been developed.

The azol-1-yl radicals can be generated by the flash vacuum pyrolysis (FVP) of the corresponding 1-amino (or 1-dimethylamino) azole which causes homolysis of a weak N-N bond which is built into the starting material. The only known reactions are of pyrrol-1-yl **2.1** and benzimidazol-1-yl **2.2** radicals (Figure 1); these radicals once generated usually react by cyclising with substituents which have been incorporated into the 2-position of the molecule.

2.1 **2.2**

Figure 1: Pyrrol-1-yl and benzimidazol-1-yl radicals

This area of interest stemmed from some early work done by Wright during a final year undergraduate research project into reactions of iminyl radicals (Scheme 1). [(5)] FVP of the oxime ether **2.3** resulted in the formation of two cyclised products; **2.4** with the methyl group *para* to the pyrrole nitrogen and **2.5** with the methyl group *meta* to the pyrrole nitrogen in a 1:1 ratio. When **2.3** is pyrolysed the iminyl radical **2.6** is generated by the homolysis of the weak N-O bond, and this radical then undergoes *ipso* attack to form the spirodienyl intermediate **2.7**. From this intermediate either bond A or B can migrate to an adjacent carbon to form the

cyclised product 2.4 or 2.5. The fact that these products are formed in an equal ratio suggests that both C-N bonds may have comparable migration abilities.

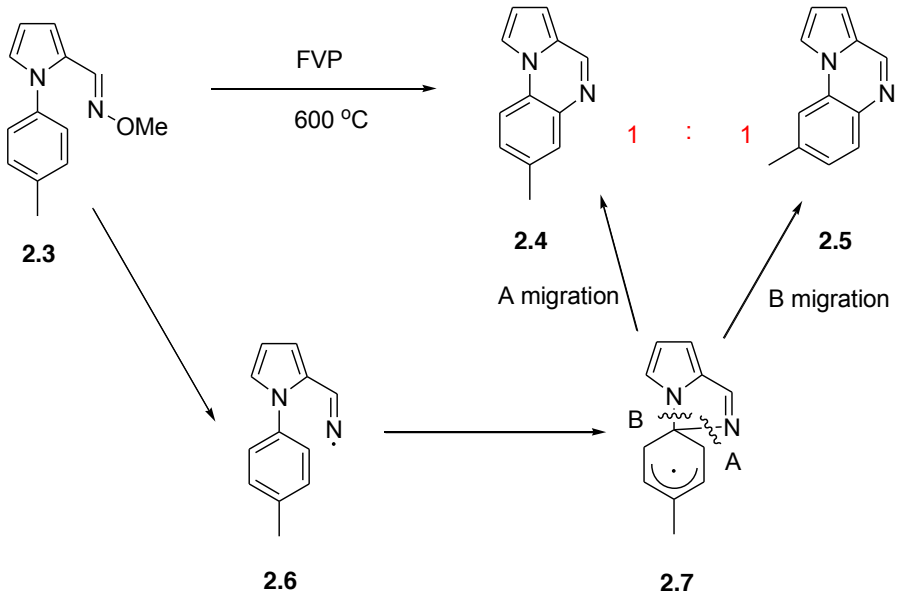

Scheme 1: Wright's work on iminyl radicals

The mechanism of this system was further investigated by changing the position of the radical centre to the pyrrole nitrogen (Scheme 2). Substrate 2.8 was designed so that the N-N bond of the 1-dimethylamino group would homolyse on FVP generating the desired pyrrol-1-yl radical 2.9, our first example of an azol-1-yl radical. This resulted in the same two cyclised products 2.4 and 2.5 as before, however in a 2:5 ratio respectively. As the spirodienyl intermediate might result in an equal ratio of products due to the two C-N bonds having comparable migration abilities, this result suggests that some direct cyclisation process competes, whatever the precursor.

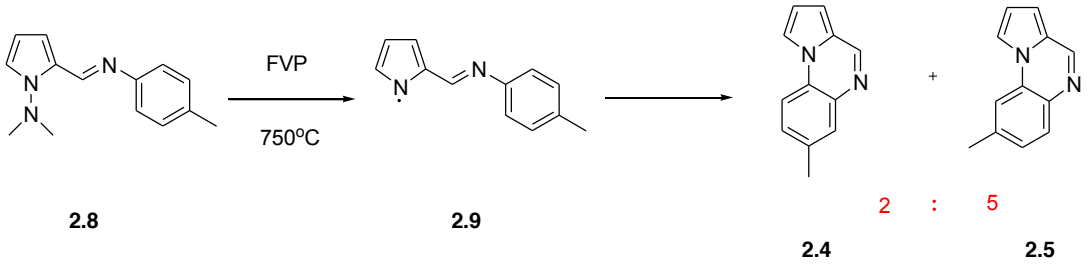

Scheme 2: Cyclisations of pyrrol-1-yl radicals

To explore this migration further, a similar substrate 2.10 was pyrolysed but lacking the imine nitrogen (Scheme 3). Again this generated a pyrrol-1-yl radical 2.11 which has the potential to undergo *ipso* attack (2.12) after thermal *E-Z* isomerisation of the alkene. The cyclisation occurred very cleanly and produced only one isomer; the *meta* product 2.13. This result suggests that either direct cyclisation occurs or that the C-N bond migration is preferred over C-C bond migration in the spirodienyl intermediate 2.12. The position of the methyl group was confirmed by NOESY spectroscopy.

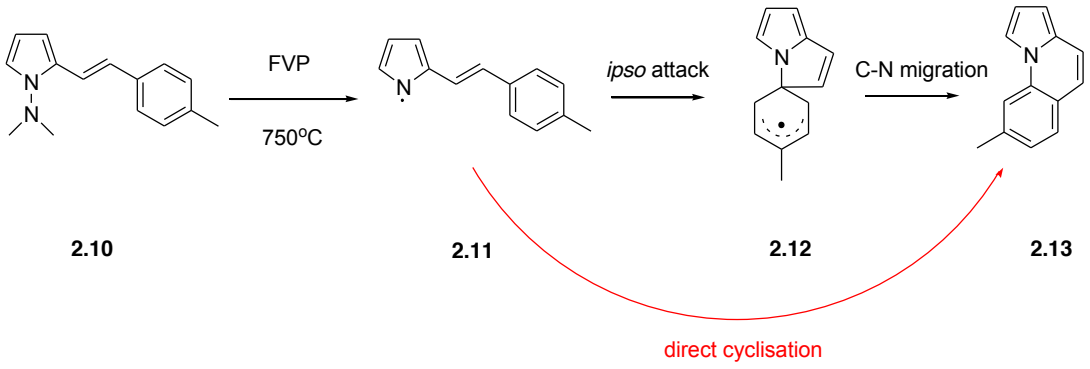

Scheme 3: Pyrrol-1-yl radical generation and subsequent cyclisation

This work has recently been re-visited by Ieva within the McNab group and DFT (density functional theory) calculations carried out on this transformation to produce

an energy surface. This is shown in Figure 2 and illustrates why only the product 2.13 is observed from the pyrolysis of 2.10.

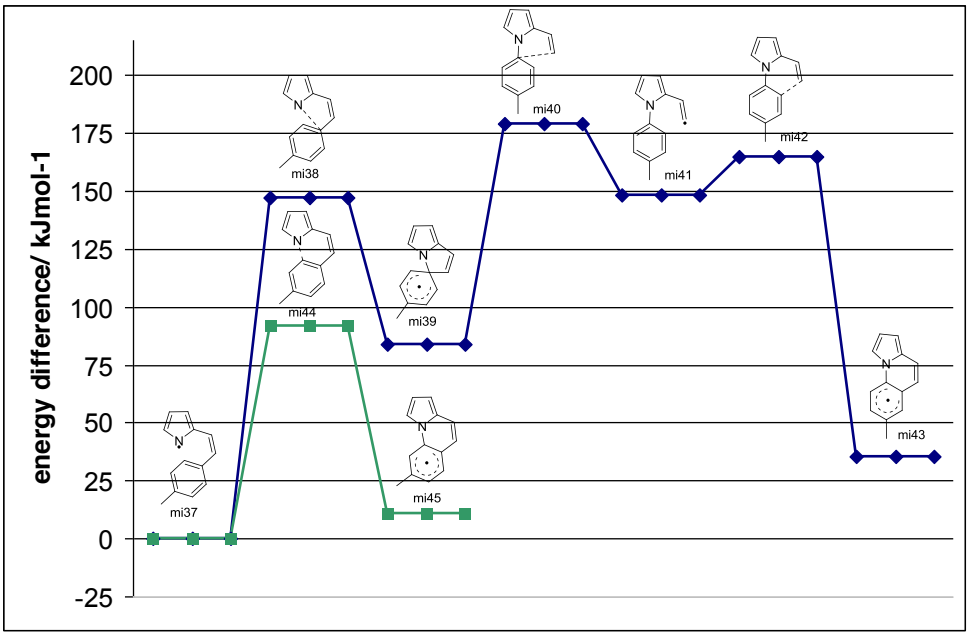

Figure 2: Ieva's recent DFT calculation work on the generation of pyrol-1-yl radicals – energy surface for cyclisation of **2.11**

The shape of the energy surface clearly shows that in this instance the formation of the spirodienyl radical is not likely to happen, as not only is the direct cyclisation product 2.13 significantly lower in energy than the other isomer, it also has a much smaller activation energy barrier.

This idea was then extended into the benzimidazole series by O'Neill [6] (Scheme 4). The benzimidazole was substituted at the 2-position with the same styryl type moiety as seen before with the pyrrole example. On FVP of substrate 2.14 the benzimidazol-1-yl radical 2.15 was generated and resulted in cyclised product 2.16 which was produced very cleanly and as a single product. Note that the pyrolysis temperature need in this case was higher than that before, as it was found that a higher temperature was needed in the *N*-amino case as opposed to the *N*-dimethylamino. Again the regiochemistry was confirmed by NOESY spectroscopy.

This agrees with the previous example, and gives two working azol-1-yl radical systems.

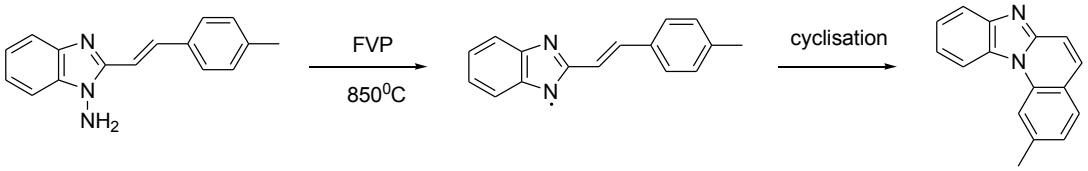

2.14 **2.15** **2.16**

Scheme 4: Benzimidazol-1-yl radical generation and subsequent cyclisation

The 1-amino-2-naphthylbenzimidazole 2.17, (Scheme 5) underwent FVP to generate the corresponding benzimidazol-1-yl radical 2.18 and subsequently produced the cyclised product 2.19. In this instance it is almost certain that the mechanism is a direct cyclisation as *ipso* attack would result in a 4-membered ring which is highly strained and therefore would be very unlikely to happen. This transformation demonstrates that 5-membered rings are formed just as readily as the previous 6-membered examples, and shows the potential for this area of chemistry, especially in creating fused heterocyclic ring systems which would be extremely difficult to synthesise *via* traditional methods.

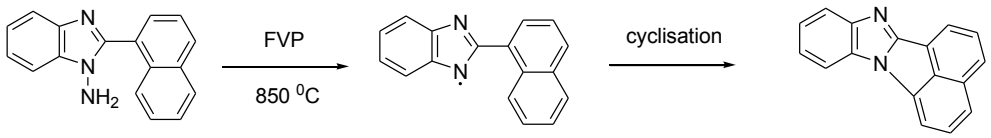

2.17 **2.18** **2.19**

Scheme 5: Cyclisation of benzimidazol-1-yl radical to form a new 5-membered ring

To investigate the generation and chemistry of the desired azol-1-yl radicals, the appropriate 1-amino-2-substituted azoles must first be synthesised. The initial focus was to be on benzimidazoles as the synthesis of 2-alkyl and aryl substituted benzimidazoles is well documented, and as discussed earlier, their *N*-amination has been successful with hydroxylamine-*O*-sulfonic acid, the most readily available and adaptable reagent for this transformation. Then the focus was intended to shift

towards 2-substituted imidazoles, whose *N*-amination is less well known.. However, since imidazol-1-yl radicals are unknown in the literature and imidazole-like systems are prevalent in research, their generation by flash vacuum pyrolysis reaction would be of interest.

2.2 Synthesis of 1-amino-2-alkylbenzimidazole precursors

Precursors of type shown were required:

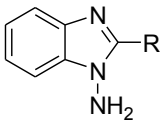

where R = alkyl

It was thought that with precursors of this nature during pyrolysis, the azol-1-yl radical would be formed and undergo some type of hydrogen transfer reaction with the alkyl group in the 2-position, which would complement the cyclisation reactions previously studied. Different sizes of alkyl chain would allow different sized transition states and thus longer groups could choose one of many different transition states, potentially producing a variety of products and allowing insight into the process.

2.2.1 Synthesis of 2-alkylbenzimidazoles

The starting point in the synthesis of suitable precursors for FVP was producing appropriately 2-substituted benzimidazoles. The most important synthetic method for their preparation is the condensation of *o*-diaminobenzenes with a suitable carbonyl species. [7] The general reaction is shown in Scheme 6.

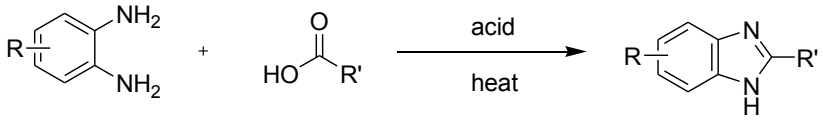

Scheme 6: Synthesis of 2-substituted benzimidazoles

The target 2-alkylbenzimidazole precursors 2.24 – 2.27 can be made from *o*-phenylenediamine 2.20 and the corresponding benzoic acids 2.21 (Scheme 7) and benzimidazole 2.23 is commercially available. Reactions of this type to produce 2-arylbenzimidazoles have been carried out in 4M hydrochloric acid,[8] but produce better yields when polyphosphoric acid (PPA) is used.[9] From earlier work carried out by O'Neill[6] (adapted from work by Hien[9]) to make 2-substituted benzimidazoles, the diamine and carboxylic acid must be heated in PPA to 180 °C for 2 hours with a subsequent aqueous work up. The PPA acts as a solvent and also the acid catalyst needed for the condensation reaction. This approach was applied successfully to the synthesis of the 2-alkylbenzimidazoles shown in Scheme 7. The general mechanism for the synthesis of benzimidazoles is shown in Scheme 8.

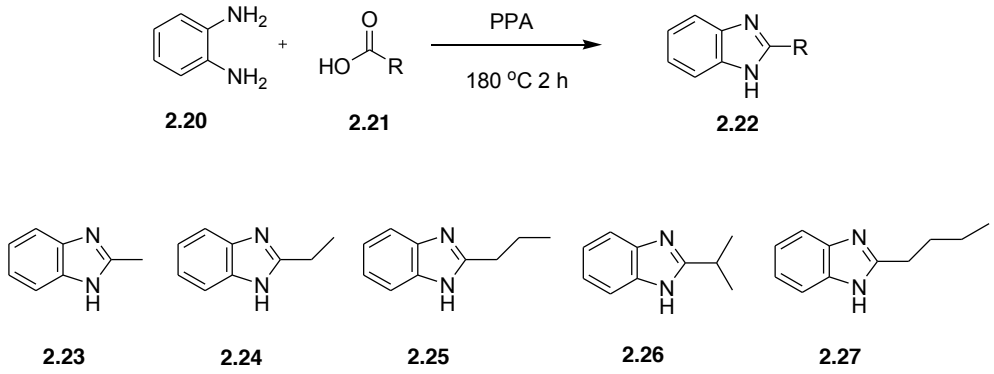

Scheme 7: Synthesis of 2-substituted benzimidazoles used and the 2-alkylbenzimidazoles made *via* this route

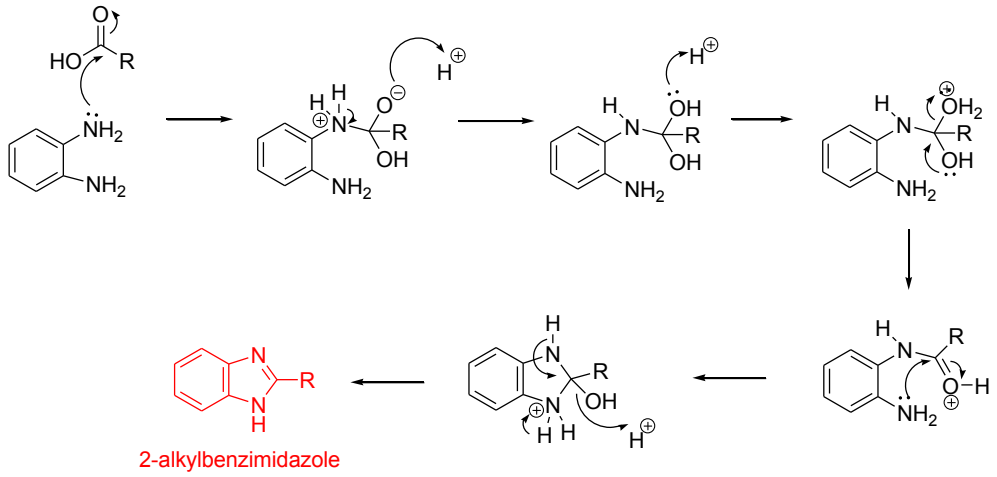

Scheme 8: Mechanism of 2-substituted benzimidazole formation

These target benzimidazoles were successfully synthesised in this way using the appropriate alkyl carboxylic acid in good yields (72 – 83%). The next step in the precursor synthesis was the *N*-amination of these benzimidazoles.

2.2.2 *N*-amination of 2-alkyl bezimidazoles

Various substituted benzimidazoles have been successfully *N*-aminated using hydroxylamine-*O*-sulfonic acid. Two main methods were found using HOSA as the aminating agent; the main difference between them was method 1 used DMSO as solvent [10] whereas the method 2 was carried out only in aqueous alkali. [10] Confirmation that the NH_2 group had successfully been added was easily established by the NH_2 signal at δ_H 4 – 5 ppm in the ^1H NMR spectrum. The general mechanism for *N*-amination using HOSA is shown in scheme 9. The benzimidazole nitrogen atom is deprotonated by the base, and then this attacks the electrophilic amine group of the hydroxylamine-*O*-sulfonic acid anion formed by the excess base in the reaction mixture. Sulfuric acid is produced in the process along with the desired *N*-amino compound.

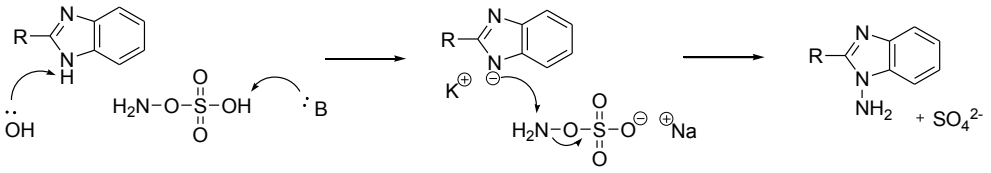

Scheme 9: Mechanism of *N*-amination of benzimidazoles using HOSA

Method 1 (Scheme 10) had been previously used by O'Neill to *N*-aminate 2-substituted benzimidazoles and hence was thought to be directly applicable in this instance. This method entailed dissolving the particular benzimidazole in DMSO, adding three equivalents of hydroxylamine-*O*-sulfonic acid, excess sodium hydroxide and heating to 60 °C for 1 hour then stirring at room temperature for 2 hours. Work up involved pouring the reaction mixture into iced water and filtering the resulting precipitate, then extracting the aqueous filtrate with ethyl acetate and repeating the entire *N*-amination process on the combined extracted solid and the precipitate. After this repetition and subsequent work up the reaction afforded the desired *N*-aminated benzimidazole.

Method 2 (Scheme 10) had been used successfully on 2-methylbenzimidazole [(10)] 2.23 previously and differed slightly from method 1 in that aqueous alkali was used as solvent. A solution of HOSA was neutralised with sodium hydrogen carbonate which was added instantly to a solution of the benzimidazole in aqueous alkali at 70 °C. The reaction was held at this temperature for 1 hour then allowed to cool to room temperature. At approximately 50 °C, a precipitate formed, this was filtered off and washed with water, to provide the *N*-aminated benzimidazole.

Method 1 was attempted on 2-methylbenzimidazole as this is a commercially available compound and its *N*-amination and product thereof was already known and characterised. However this method was shown to not go to completion, even after three repetitions. This was also the case when attempted with 2-ethylbenzimidazole 2.24, so it was concluded that method 1 was not suitable for 2-alkylbenzimidazoles

Method 2 was already cited as that used to aminate 2-methylbenzimidazole [10] **2.23** and was equally successful when carried out as a test reaction. 2-Ethylbenzimidazole was then subjected to this method. When heated in the aqueous alkali, the 2-ethylbenzimidazole was not completely soluble and the reaction did not go to completion. Hence DMSO was added dropwise to the benzimidazole/alkali solution at 70 °C, until a complete solution had been achieved. This proved to be effective and pure 1-amino-2-ethylbenzimidazole as obtained in a reasonable yield (53%).

Method 1

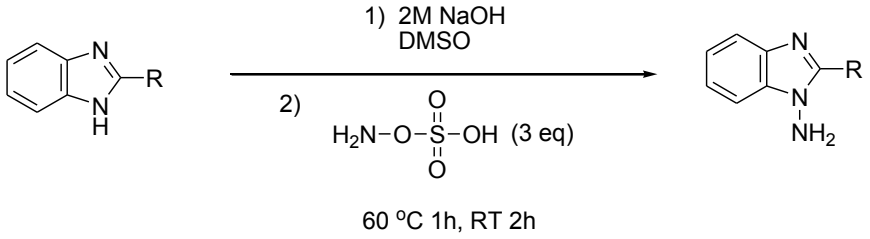

Method 2

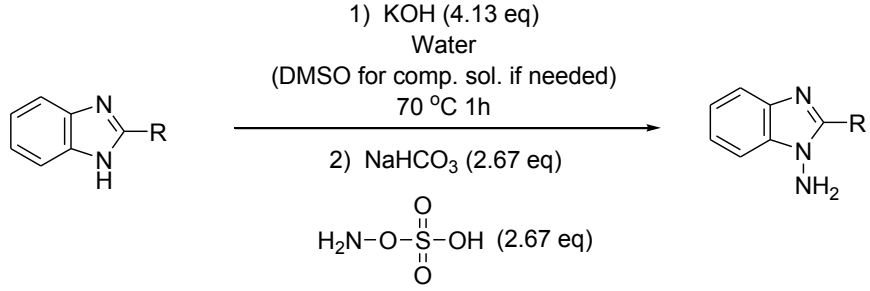

Scheme 10: Reaction conditions for *N*-amination of benzimidazoles for Methods 1 & 2

These two methods of *N*-amination were not successful when applied to the 2-alkylbenzimidazoles **2.25** – **2.27**; in all cases the reactions could not be taken to completion.

The focus was switched to 2-butylbenzimidazole **2.27**, as this would allow an insight into all possible hydrogen transfer transition states of the azol-1-yl radical formed

during pyrolysis and the subsequent carbon centred radicals that could be created (scheme 11).

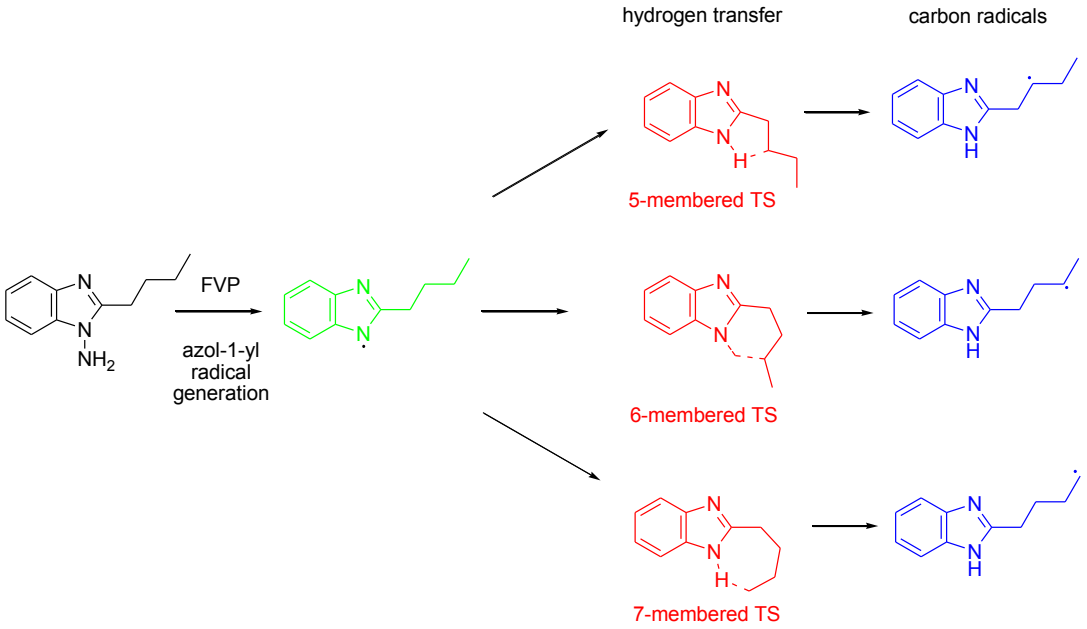

Scheme 11: Possible transition states from 2-butylbenzimidazol-1-yl radical

A third method was found in the literature which was developed for pyrazole [13], but as there was limited success with the two methods already applied in this work it was decided that a third may offer a chance for improvement. It was a simple variation on method 1. The benzimidazole was suspended in an aqueous solution of sodium hydroxide and heated to 55 °C, where ethanol was added dropwise until a complete solution was obtained. HOSA was added portionwise over 15 min with vigorous stirring to minimise foaming and after addition the reaction was heated to 60 °C for 1 h, then allowed to cool to room temperature and stirred overnight. Water was added and the aqueous solution extracted with dichloromethane. The organic extract was then dried and the solvent removed under reduced pressure. When applied to 2.27 it proved to be more successful, although the reaction still did not go to completion, a greater proportion of *N*-amino product to starting material was found, (*ca.* 70 : 30) compared with a 40 : 60 ration with two repetitions of method 2. It also transpired

that this was easier to separate from its starting material compared with 2.25 and 2.26, both of which were aminated to approximately a 50 : 50 ratio, and numerous attempts made to separate the products by chromatography were unsuccessful. However the *N*-amino-2-n-butylbenzimidazole 2.30 was much more soluble in hot hexane than the starting material, hence Soxhlet extraction using hexane provided an almost pure product. No purification method used would allow the complete removal of the small amount of starting material present but the mixture could be pyrolysed taking this fact into account.

To summarise, the *N*-amino-2-alkylbenzimidazoles that were successfully synthesised are shown in figure 3, *N*-amino-2-methylbenzimidazole 2.28, *N*-amino-2-ethylbenzimidazole 2.29 and *N*-amino-2-n-butylbenzimidazole 2.30.

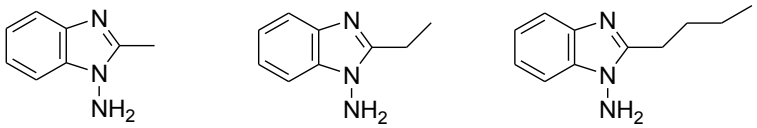

2.28 **2.29** **2.30**

Figure 3: *N*-Amino-2-alkylbenzimidazoles successfully obtained

2.3 Flash Vacuum pyrolysis of *N*-amino-2-alkylbenzimidazoles

2.3.1 Flash Vacuum pyrolysis of *N*-amino-2-methylbenzimidazole - Reaction of a radical with no obvious trapping group

As there are no easily available groups for the nitrogen radical generated to interact with, the result from the pyrolysis of 1-amino-2-methylbenzimidazole 2.28 was completely unpredictable. Precursors of type 2.28 are said to have no obvious 'trapping group' as H-transfer would involve a 4-membered transition state, which is very unlikely, and any cyclisation would form a 4-membered ring which is highly strained and has not been seen to occur in realated FVP processes. The pyrolysis temperature employed was 850 °C; small scale pyrolyses showed that starting material was present in the pyrolysate at lower furnace temperatures. Under these optimised FVP conditions pyrolysis of 2.28 produced a single product, which upon NMR analysis was found to be the original de-aminated benzimidazole 2.23 (97%). The ^{1}H NMR spectrum showed the disappearance of the NH_2 peak at δ_H 4.56 ppm and the emergence of the NH peak at δ_H 12.70 ppm and both ^{1}H and ^{13}C spectra matched the literature data. [11] The nitrogen radical had been generated and simply recombined with a hydrogen atom (Scheme 12).

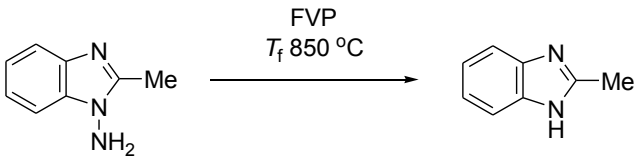

2.28 **2.23**

Scheme 12: Pyrolysis of 1-amino-2-methylbenzimidazole **2.28**

This behaviour has been commonly observed; there are many examples in FVP experiments where the leaving group, the weak bond built into the precursor having homolysed, leaves the parent radical behind, and if no obvious trapping group for the radical is present, it scavenges a hydrogen atom, most probably from the furnace tube

itself. The most recorded examples of this type of radical hydrogen scavenging are with phenoxyl radicals. When phenoxyl radicals of type 2.31 are generated by FVP, they scavenge a hydrogen atom to form phenol type compounds 2.32 (Scheme 13). A more specific example is the FVP of allyl *o*-benzylphenyl ether 2.33 which forms phenoxyl radical 2.34. [14] This was expected to cyclise to form xanthene 2.35, which indeed it does, but only in a 3% yield. The majority of the radical generated forms 2-benzylphenol 2.36 and 1-hydroxyfluorene 2.37, 2.36 is formed by the phenoxyl radical scavenging a hydrogen atom intermolecularly and 2.37 by intramolecular hydrogen transfer followed by cyclisation to form the 5-membered ring.

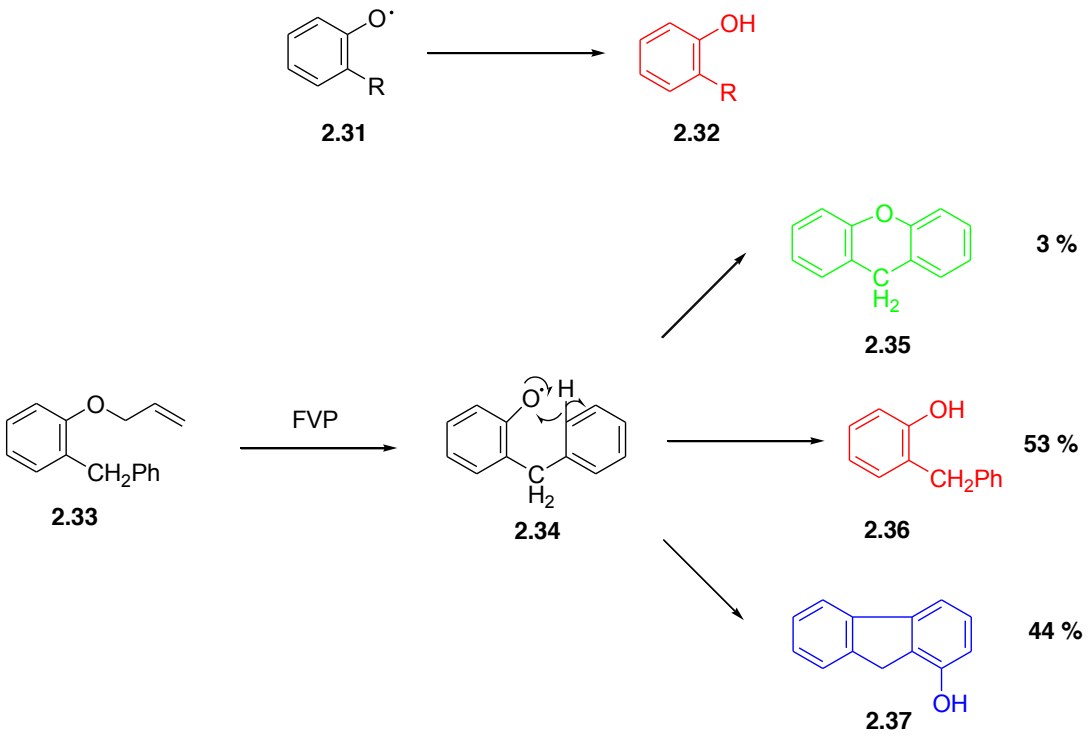

Scheme 13: Radical scavenging and transformations of phenoxyl radicals

2.3.2 Flash Vacuum pyrolysis of *N*-amino-2-ethylbenzimidazole

FVP of *N*-amino-2-ethylbenzimidazole 2.29 was expected to form an initial nitrogen based radical, then hydrogen transfer could occur *via* a 5-membered transition state with a terminal CH of the ethyl group at the 2-position. The optimum pyrolysis temperature was determined by a number of small scale pyrolyses, these revealed that a furnace temperature of 850 °C was optimal as lower temperatures showed unreacted starting material and higher showed signs of secondary decomposition. This along with the small scale pyrolyses carried out for the previous example suggest that a temperature of 850 °C is needed to homolyse the N-N bond of the *N*-amino group. On pyrolysis, *N*-amino-2-ethylbenimidazole was found to produce the 2-vinylbenzimidazole 2.38 shown in scheme 14.

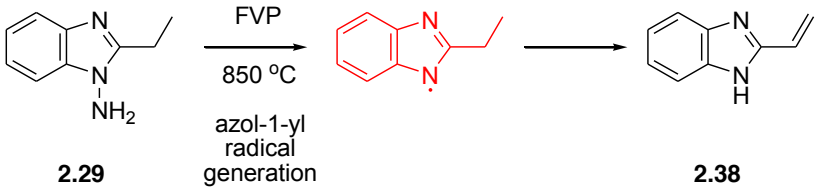

Scheme 14: Pyrolysis of 1-amino-2-ethylbenzimidazole **2.29**

The proposed mechanism for the formation of 2-vinylbenzimidazole 2.38 is shown in scheme 15. When the azol-1-yl radical is formed, it then undergoes hydrogen transfer *via* a 5-membered transition state with the terminal carbon of the ethyl group. This reacts further by loss of a hydrogen atom from the adjacent carbon, thus generating a new double bond and the 2-vinylbenzimidazole 2.38.

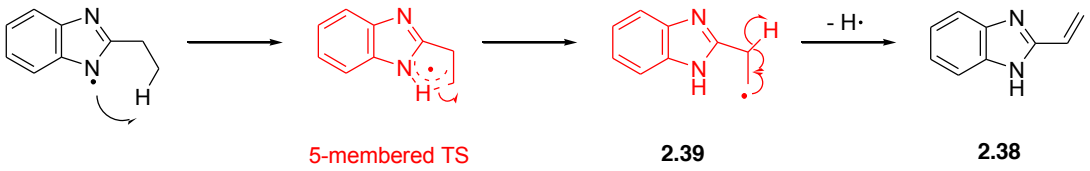

Scheme 15: Mechanism of formation for 2-vinylbenzimidazole **2.38**

2.3.3 Flash Vacuum pyrolysis of *N*-amino-2-*n*-butylbenzimidazole

The pyrolysis of *N*-amino-2-n-butylbenzimidazole 2.30 was greatly anticipated, as this one molecule had the capability of hydrogen transfer *via* three different possible transition states as discussed previously.

As FVP is a gaseous technique and involves no solvents or reagents, the radical or pericyclic intramolecular reactions that occur are ideal candidates for computer modelling using density functional theory (DFT) calculations. As these quantum mechanical calculations assume the molecule to be in a gaseous state, the ground state and transition state structures it produces have been found to correlate well with experimental data resulting from FVP experiments. [15] As there were multiple possible transition states possible for the pyrolysis of 2.30, DFT calculations were performed to see if any indication could be given of the preferred transition state, and thus any possible products. The energy profile figure 4 was produced from the DFT calculations performed.

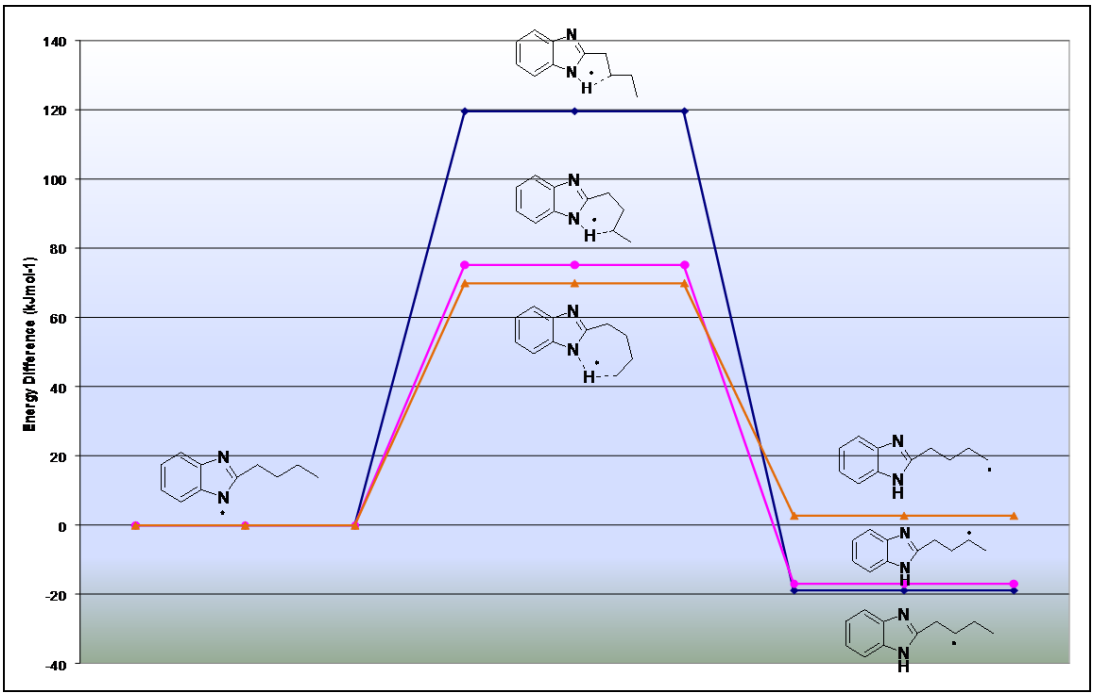

Figure 4: Energy profile showing possible transition states for 2-^{n}butylbenzimidazol-1-yl radical (calculated at B3LYP/cc-pVDZ)

The calculations showed a contrast between the transition state with the lowest energy *i.e* the fastest reaction, and the resulting radical of greatest thermodynamic stability. The terminal radical formed from a 7-membered transition state would be the highest of the three possible radicals in thermodynamic energy terms (in relation to the initial azol-1-yl radical formed) however the corresponding transition state showed the lowest activation energy barrier. The two possible secondary radicals that could be formed from either a 6- or 5-membered transition states are very close in thermodynamic energy value to each other, but their respective transition states differ by approximately 45 kJ mol^{-1}; the 6-membered transition state is the lower energy of the two, therefore the radical formed from a 6-membered transition state would likely be formed fastest.

The pyrolysis was carried out with a furnace temperature of 850 °C as had been previously established and the crude pyrolysate analysed by ^{1}H NMR spectroscopy. Unfortunately the pyrolysate showed that the major product was the de-aminated starting material, the benzimidazole 2.27, with many other peaks present to a much lesser extent. However this pyrolysis did confirm that there were no further possibilities in the area of *N*-amino-2-alkylbenzimidazoles. It is believed that the problem lies in the number of degrees of freedom available to the alkyl group. As the initial azol-1-yl radical formed has a very short lifetime, the hydrogen transfer must happen quickly in respect to the FVP timeframe. The fact that mostly de-aminated product is recovered tells us that the hydrogen scavenging properties shown by these radicals happens much faster, relatively, than the alkyl group attains a suitable geometry for hydrogen transfer. Thus a greater amount of rigidity must be introduced in the substituent at the 2-position of the benzimidazole to promote the desired hydrogen abstraction.

2.4 Synthesis of 1-amino-2-arylbenzimidazole precursors

In order to overcome the problems encountered with the *N*-amino-2-alkylbenzimidazoles, precursors of type **2.39** were designed, to introduce more rigidity into the precursors.

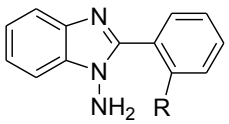

2.39

By altering the R group in the *ortho* position of the phenyl ring in relation to the benzimidazole, hydrogen transfer reactions with different sized transition states could be studied. Because the R group is held in a tighter configuration (so there are less degrees of freedom) due to the benzene ring, it was thought that the azol-1-yl radical formed upon FVP would be more likely to undergo a hydrogen transfer than to scavenge a hydrogen atom.

The target precursors were defined as 1-amino-2-(2-methylphenyl)-1*H*-imidazole **2.40**, 2-(2-methoxyphenyl)-1*H*-benzimidazole **2.41** and 2-(2-ethylphenyl)-1*H*-benzimidazole **2.42** (scheme 16), as these would allow possible well-defined transition states. Scheme 16 shows the target benzimidazoles **2.40-2.42** with the *ortho* R-groups rotated for clarity and also outlines the possible main products from hydrogen transfer reactions of the initial benzimidazol-1-yl radical formed *via* FVP.

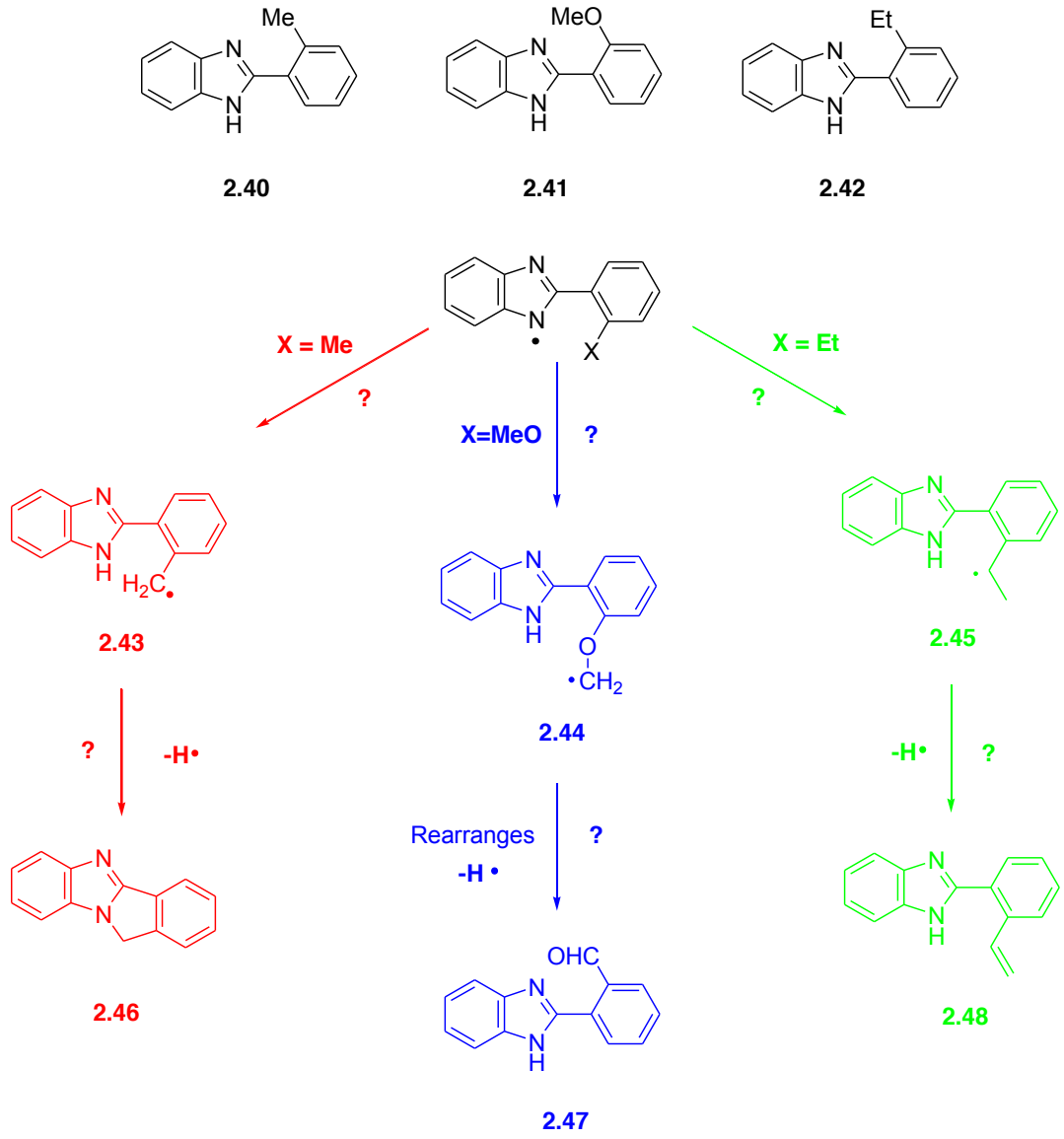

Scheme 16: Proposed pathways from pyrolysis of 1-amino-2-arylbenzimidazoles

The azol-1-yl radical formed from the pyrolysis of 2.40 could undergo hydrogen transfer with the *ortho* methyl group *via* a 6-membered transition state to create a CH_2 radical, which because of its proximity to the nitrogen atom and the knowledge that five-membered rings are readily formed in similar cases, could cyclise to form the product 11*H*-benzo[4,5]imidazo[1,2-*a*]isoindole 2.46. Pyrolysis of precursor 2.41

and subsequent hydrogen transfer *via* a 7-membered might produce an OCH_2 radical **2.44**. Such radicals are known from previous work to rearrange to an aldehyde,[16] so could produce the aromatic aldehyde **2.47**. Scheme 16 is intended to show possible results from pyrolyses; the 'best guess' based on previous knowledge and results of experimental work.

2.4.1 Synthesis of 2-arylbenzimidazoles

Synthesis of 2-arylbenzimidazoles had been successful using the polyphosphoric acid method as employed previously to make the 2-alkylbenzimidazoles. [6] Therefore this was the initial approach used for the target precursors **2.40**-**2.42**.

2-(2-Methylphenyl)-1*H*-benzimidazole **2.40** (70%), 2-(2-methoxyphenyl)-1*H*-benzimidazole **2.41** (57%) and 2-(2-ethylphenyl)-1*H*-benzimidazole **2.42** (65%) were successfully synthesised from *o*-toluic acid, *o*-anisic acid and 2-ethylbenzoic acid respectively, and *o*-phenylenediamine *via* the PPA method as previously discussed (scheme 17). No further purification was needed before further reaction in each case and all three products were characterised using ^{1}H and ^{13}C NMR spectroscopy. The successful formation of the benzimidazole ring was characterised by the appearance of the distinctive NH peak at ~13 ppm in the proton NMR spectrum. The 8 aromatic protons in each case were indistinguishable from each other and appeared as complex multiplets.

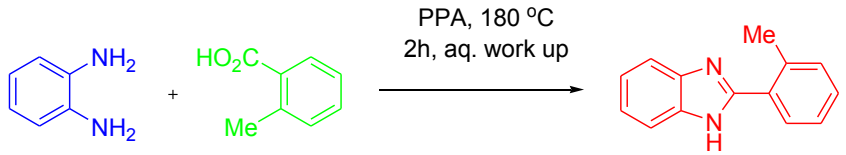

2.40

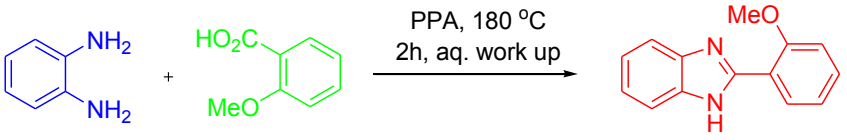

2.41

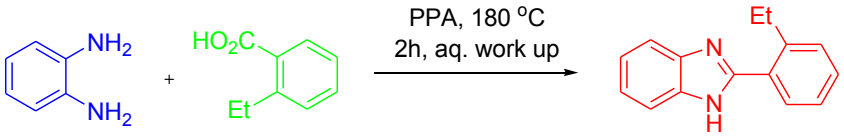

2.42

Scheme 17: Synthesis of desired 2-arylbenzimidazoles **2.40 – 2.42**

Upon analysis, the carbon NMR spectra in each case at first appeared to contain more signals than expected. Since the NH proton of the benzimidazoles can exchange between the two nitrogen atoms (Scheme 18), it was expected that the plane of symmetry caused by the exchange would render the carbon atoms on either side of this plane to be equivalent (2.49).

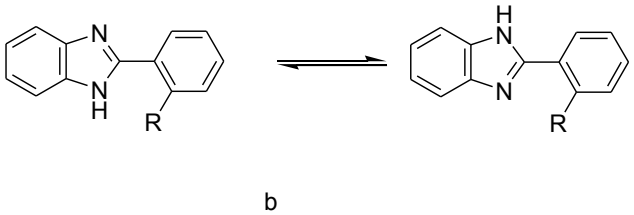

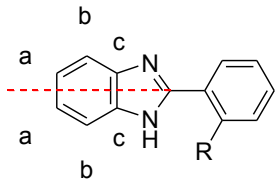

2.49

Scheme 18: Tautomers and equivalency expected in ^{13} NMR spectrum

One signal was expected for carbon atoms of type a, b and c, however this was not found to be the case. In all 13 signals were found, one for each carbon atom of the benzimidazole skeleton plus those according to the appropriate R group at the *ortho* position. This result shows that the proton exchange is slow on the NMR timescale, resulting in all carbon signals being different.

2-(2-Methylphenyl)-1*H*-benzimidazole **2.40** and 2-(2-methoxyphenyl)-1*H*-benzimidazole **2.41** have been previously synthesised by alternative methods [17], [18] but these were not applied in this case for several reasons.

2-(2-Methylphenyl)-1*H*-benzimidazole **2.40** was previously synthesised[17] in a 78% yield from 2-methyl-*N*-(2-nitrophenyl)benzamide **2.52** by refluxing in glacial acetic acid with iron powder (Scheme 19). However, although this yield is slightly better than the one reported here for the synthesis of **2.40**, it involves an extra step to make the benzamide **2.52**. This can be made in a 92% yield from 2-nitroaniline **2.50** and *o*-toluoyl chloride **2.51**, however the PPA method was preferred as it was a simple one step reaction in good yield from commercially available starting materials.

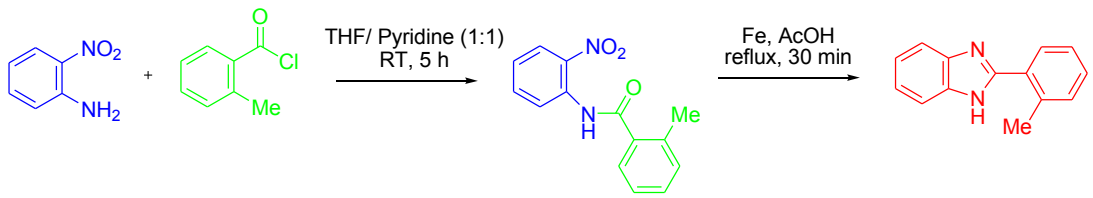

2.50 **2.51** **2.52** **2.40**

Scheme 19: Alternative synthetic route to 2-(2-methylphenyl)-1*H*-benzimidazole **2.40**

2-(2-Methoxyphenyl)-1*H*-benzimidazole **2.41** was previously synthesised[18] in a 63% yield from *N*-(2-methoxybenzylidene)-*o*-phenylenediamine **2.55** in dry pyridine under oxygen catalysed by copper(I) chloride (Scheme 20). Again this is a slightly better yield than that reported here, but again an extra step was required to

form the *N*-benzylidene-*o*-phenylenediamine 2.55, from *o*-phenylenediamine 2.53 and 2-methoxybenzaldehyde 2.54.

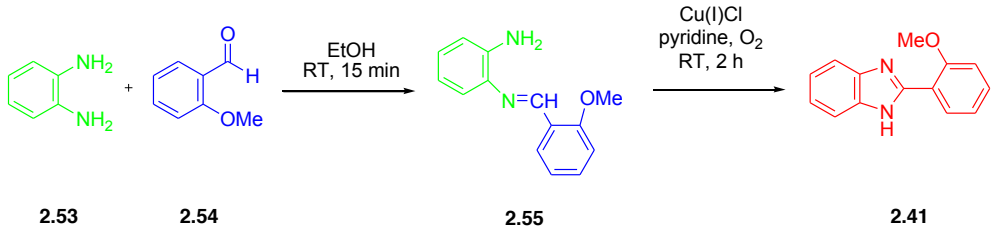

2.53 **2.54** **2.55** **2.41**

Scheme 20: Alternative synthetic route to 2-(2-methoxyphenyl)-1*H*-benzimidazole **2.41**

2.4.2 *N*-Amination of 2-arylbenzimidazoles

1-Amino-2-phenylbenzimidazole 2.57 (58%) was synthesised by *N*-amination *via* method 2 of the commercially available 2-phenylbenzimidazole 2.56 (scheme 21) as this method had been used previously on this structure in the literature [11]. The only change to the method was that a few drops of DMSO had to be added to the 2-phenylbenzimidazole to create a complete solution in aqueous alkali at 70 °C. Again the emergence of a peak at δ_H 4.86 ppm in the ^{1}H NMR confirmed the addition of the NH_2 group.

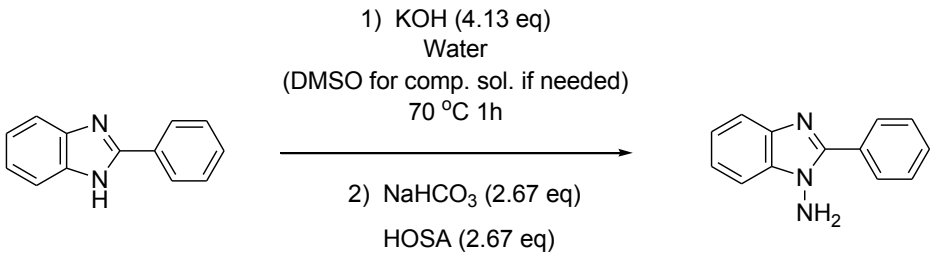

2.56 **2.57**

Scheme 21: *N*-Amination of 2-phenylbenzimidazole **2.56**

1-Amino-2-phenylbenzimidazole 2.57 was synthesised as the 2-arylbenzimidazole equivalent of the 1-amino-2-methylbenzimidazole discussed earlier, as an example of

a precursor with no obvious 'trapping group' for the azol-1-yl radical formed during pyrolysis.

Method 2 was applied to benzimidazoles 2.40, 2.41 and 2.42; however, each needed increasing amounts of DMSO to dissolve completely in the aqueous alkali. This affected the N-amination so that less aminated product was acheived with increasing addition of DMSO. Method 1 was then attempted and after two cycles of amination the corresponding 1-amino-2-arylbenzimidazoles 2.58, 2.59 and 2.60 were successfully obtained (figure 5).

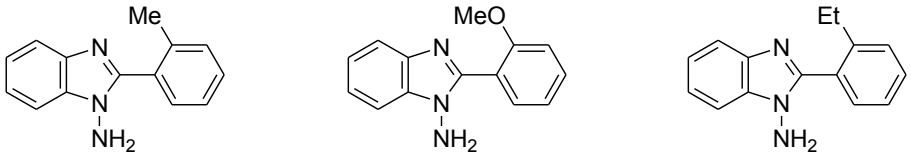

2.58 **2.59** **2.60**

Figure 5: Successfully aminated 2-arylbenzimidazoles achieved

There is some inconsistency in the literature regarding conditions required for *N*-amination using HOSA. Kuzmenko *et al*[11] state that amination with HOSA must be carried out in aqueous alkali; however, as method 1 demonstrates, amination is successful using DMSO as solvent. Method 1 does use a moderate amount of aqueous sodium hydroxide but it is not the main solvent. It could be that this amount is enough to allow the reaction to proceed, and the DMSO simply overcomes the solubility issues. This could also be the explanation behind the need to carry out the whole *N*-amination reaction twice to achieve full conversion to the *N*-amino benzimidazole.

2.5 Flash vacuum pyrolysis of *N*-amino-2-arylbenzimidazoles

2.5.1 Flash vacuum pyrolysis of 1-amino-2-phenylbenzimidazole - Reaction of a radical with no obvious trapping group

Again, as with the 1-amino-2-methylbenzimidazole **2.28**, there are no easily available groups for the nitrogen radical generated from the pyrolysis of 1-amino-2-phenylbenzimidazole **2.57** to interact with. This is another example of a precursor that is said to have no obvious 'trapping group' as H-abstraction would involve a 4-membered transition state. The pyrolysis temperature employed was 850 °C and again produced a single product, which upon NMR analysis was found to be the original de-aminated benzimidazole **2.56** (97%). The ^{1}H NMR spectrum showed the disappearance of the NH_2 peak at δ_H 4.86 ppm and the emergence of the NH peak at δ_H 12.12 ppm and both ^{1}H and ^{13}C spectra matched the literature data. The nitrogen radical had been generated and again simply recombined with a hydrogen atom (Scheme 22). This is another example of the radical hydrogen scavenging from the furnace tube.

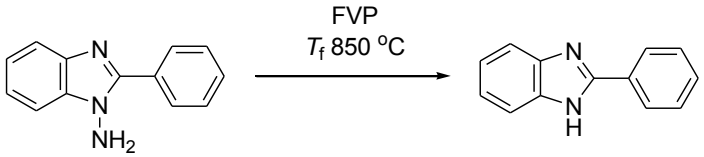

2.57 **2.56**

Scheme 22: Pyrolysis of *N*-amino-2-phenylbenzimidazole

2.5.2 Flash vacuum pyrolysis of 1-amino-2-(2-methylphenyl)-1*H*-benzimidazole

The same FVP conditions were applied to the pyrolysis of 1-amino-2-(2-methylphenyl)-1*H*-imidazole **2.58** as those used for the 1-amino-2-phenylbenzimidazole **2.57**. As this precursor contained a methyl trapping group on the 2-phenyl ring, it was thought that hydrogen transfer could occur more readily.

This would entail a 5-membered transition state and cyclisation could subsequently take place to produce a new 5-membered ring, which as discussed in the introductory section, has been previously reported. (6)

A preparative (~100 mg) FVP of 1-amino-2-(2-methylphenyl)-1*H*-benzimidazole **2.58** was carried out. TLC analysis of the crude pyrolysate showed three distinct products, which were consequently separated by dry-flash chromatography.

The first spot to be eluted was identified as the de-aminated precursor **2.40** (27%). ^{1}H NMR spectroscopy showed the re-appearance of the benzimidazole NH peak at δ_H 12.13 ppm and all other proton signals correlated well with the benzimidazole **2.40** data. This is proposed to be the result of hydrogen scavenging and would follow the results gathered for the FVP of precursors **2.28** and **2.57**, and suggests that although hydrogen transfer should be possible *via* a 5-membered transition state, the hydrogen scavenging will occur to some extent if this transfer happens quite slowly relative to the rate of collisions on the FVP timescale.

The second product was identified as the cyclised product 11*H*-benzo[4,5]imidazo[1,2-*a*]isoindole **2.61** (56%). The ^{1}H NMR spectrum displayed a distinctive CH_2 singlet at δ_H 4.96 ppm suggesting the formation of a new 5-membered ring. The other signals in the ^{1}H and ^{13}C NMR spectra matched the literature data well. (19) A proposed mechanism for this reaction is shown in Scheme 23. This mechanism would first involve hydrogen transfer from the 2-methylphenyl group *via* a 6-membered transition state **2.62** to the nitrogen radical centre, generating a CH_2 radical **2.63** which could then cyclise to create a new bond with the second nitrogen atom. The tertiary carbon radical **2.64** formed in the process can then regenerate a double bond by loss of a hydrogen atom forming the cyclised product **2.61**.

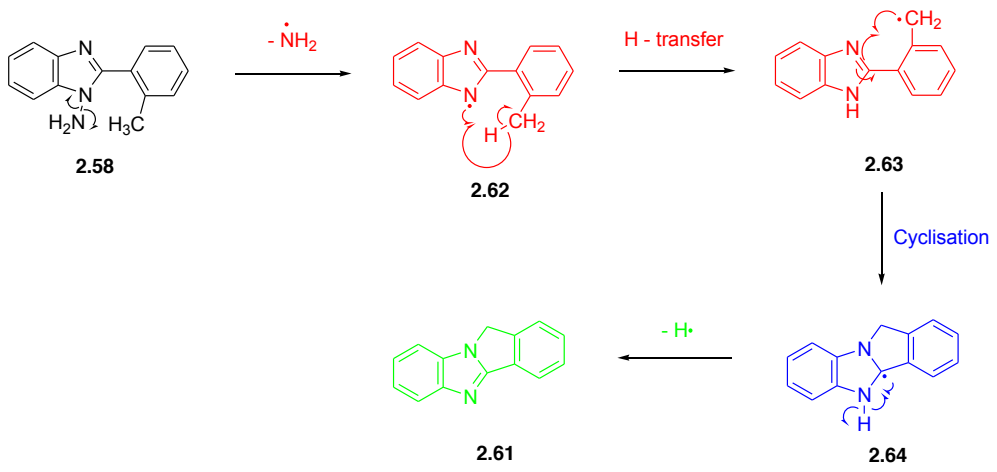

Scheme 23: Proposed mechanism for the formation of 11*H*-benzo[4,5]imidazo[1,2-*a*]isoindole **2.61**

The ^{1}H NMR spectrum of the third component, (17%), showed that it contained a methyl group, eight aromatic protons and a NH_2 group. The ^{13}C NMR spectrum confirmed eight aromatic CH groups and also five quarternary carbon atoms and a methyl group. The EI mass spectrum also illustrated that the unknown had the same molecular mass as the aminated precursor 2.58, confirming the survival of the NH_2 group. An HSQC experiment was used to associate the proton shifts to their corresponding carbon shifts, and the data derived from this is shown in Table 1.

Proton shift (ppm)	Associated carbon shift (ppm)
7.48-7.44 ppm (3H, m)	134.01 (CH), 132.97 (CH), 117.26 (CH)
7.39 (1H, m)	128.77 (CH)
7.33 (1H, d)	129.72 (CH)
7.16 (1H, t)	122.98 (CH)
7.01 (1H, t)	121.18 (CH)
6.76 (1H, d)	109.46 (CH)
2.11 (3H, s)	18.53 (CH_3)

Table 1: ^{1}H and ^{13}C NMR information for unknown product from pyrolysate

A 2D NOESY spectrum was also obtained which confirmed there were 2 different 4-spin systems present, however this information did not help in the diagnosis of how they were linked together. Using all of the data available two possible structures were suggested; indazole 2.65 and the benzimidazole derivative 2.66.

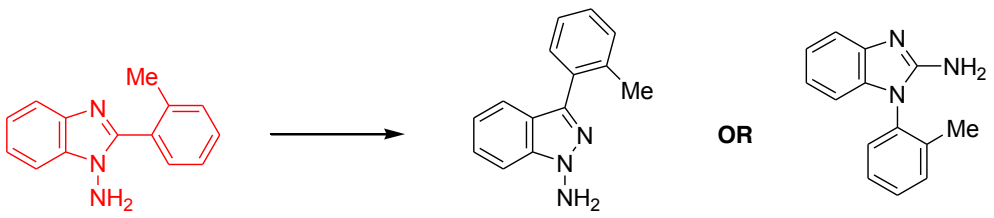

2.58 **2.65** **2.66**

The indazole 2.65 was proposed as homolysis of the C-N bond of the benzimidazole ring instead of the N-N bond and subsequent rearrangement and recombination could produce such a compound (Scheme 24). If the C-N bond homolysis was to occur forming radical 2.67 it could rearrange to radical 2.68, following the precedent known for the rearrangement of 2.69 to 2.70. If radical 2.68 was formed it could recombine to form indazole 2.65.

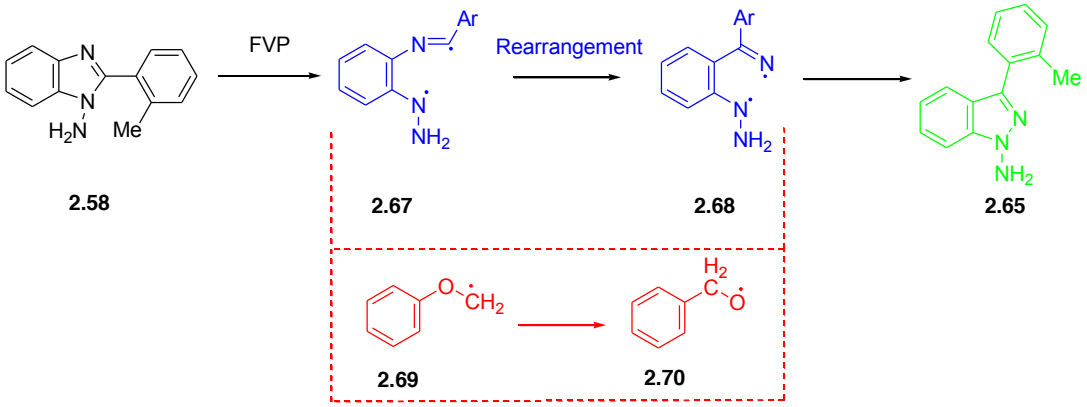

2.58 **2.67** **2.68** **2.65**

2.69 **2.70**

Scheme 24: Proposed route to indazole **2.65** and precedent for mechanism

Although 2.65 is unknown, comparisons with literature NMR data for 1-amino-3-(4-methoxyphenyl)indazole 2.71 [20] (table 2) do not suggest that this structure fits the unknown, as even the electron rich indazole 2.71 does not have aromatic peaks in its ^{1}H NMR spectrum that are as far below 7.00 ppm. The *N*-amino group however has an almost identical shift, perhaps confirming that this group is indeed present in the unknown compound.

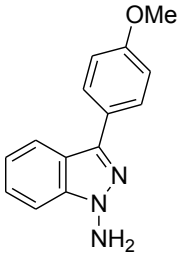

2.71

Indazole 2.68 δ_H (ppm)	**FVP unknown δ_H (ppm)**
8.00 – 6.95 (8H, m)	7.48-7.44 (3H, m)
4.91 (2H, NH_2, s)	7.39 (1H, m)
3.88 (3H, m)	7.33 (1H, d, ^3J 7.9)
	7.16 (1H, t, ^3J 7.8)
	7.01 (1H, t, ^3J 7.6)
	6.76 (1H, d, ^3J 7.7)
	4.93 (2H, br s)
	2.11 (3H, s)

Table 2: Comparison of unknown ^{1}H NMR shifts against those of indazole **2.71**

The benzimidazole-2-amine 2.66 is also unknown, so a comparison was made with 1-phenyl-2-aminobenzimidazole 2.72 (Table 3). This showed a much more positive correlation with regards to range of chemical shifts. [21] The aromatic protons seem to fit more into a similar range of shifts and the *N*-amino shift is almost identical. This evidence coupled with the mass spectrometry suggests that the benzimidazole-2-amine 2.66 is the most likely structure of the unknown compound

Benzimidazole 2.63 δ_H (ppm)	**FVP unknown δ_H (ppm)**
7.34 – 6.20 (9H, m)	7.48-7.44 (3H, m)
4.92 (2H, br s)	7.39 (1H, m)
	7.33 (1H, d, ^3J 7.9)
	7.16 (1H, t, ^3J 7.8)
	7.01 (1H, t, ^3J 7.6)
	6.76 (1H, d, ^3J 7.7)
	4.93 (2H, br s)
	2.11 (3H, s)

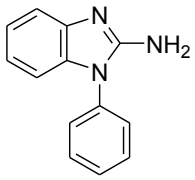

2.72

Table 3: Comparison of unknown ^{1}H NMR shifts against those of indazole **2.72**

If the unknown is indeed 1-(2-methylphenyl)-1*H*-benzo[*d*]imidazol-2-amine **2.66**, the 2-methylphenyl group and 1-amino group of the original precursor **2.58** appear to have 'swapped' positions to form **2.66**.

There are many examples of nitrogen to carbon migrations of substitutents in imidazoles, the most relevant of these in the context of this work is shown in scheme 25.

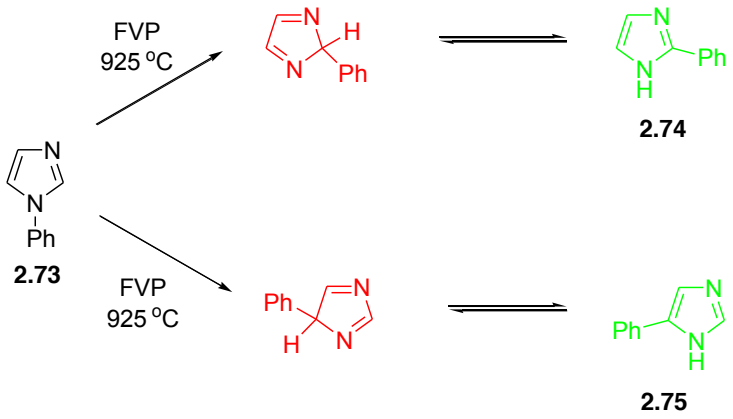

Scheme 25: Examples of nitrogen to carbom group migrations in FVP

Pyrolysis of 1-phenylimidazole **2.73** at 925 °C produces 2-phenylimidazole **2.74** and 4-phenylimidazole **2.75** in a 83:17 ratio respectively. [22] In addition to this, the hydrogen from the 2 or 4-position migrates to the nitrogen.

Conversely, when 2-phenylimidazole **2.74** was pyrolysed it did not produce 1 or 4-phenylimidazole, and pyrolysis of 4-phenylimidazole did not produce 1 or 2-phenylimidazole. This suggests that migration from a carbon atom to a nitrogen does not occur. However, although this example explains how the 1-amino group could migrate to the 2-position, it does not help in the explanation of how the 2-methylphenyl group migrates to the nitrogen at the 1-position.

The proposed mechanism for the formation of 1-(2-methylphenyl)-1*H*-benzo[*d*]imidazol-2-amine **2.66** is shown in Scheme 26, and involves a [1,5]-NH_2 shift, followed by a subsequent [1,5]-aryl shift.

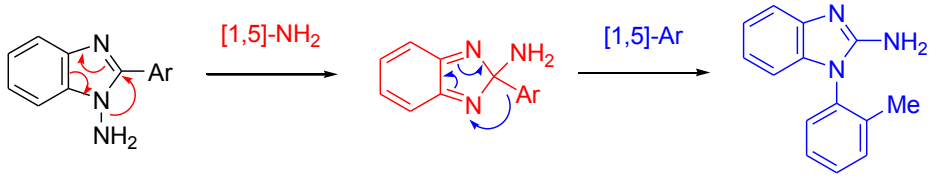

Where Ar = 2-MePh **2.63**

Scheme 26: Proposed mechanism for formation of 1-(2-methylphenyl)-1*H*-benzo[*d*]imidazol-2-amine **2.66**

Although a shift of this sort has not been reported before, a [1,5]-shift is an allowed transition, so it is very possible and the resulting product fits very well with the data collected.

2.5.3 Flash vacuum pyrolysis of 1-amino-2-(2-methoxyphenyl)-1*H*-benzimidazole

Identical FVP conditions were applied to the pyrolysis of 1-amino-2-(2-methoxyphenyl)-1*H*-benzimidazole 2.59. On analysis of the crude pyrolysate by ^{1}H NMR a very complex spectrum was obtained. There were no easily distinguishable peaks, and certainly none that would correspond to the proposed aldehyde product 2.47. TLC analysis showed a large number of spots and it was concluded that further separation and purification would be fruitless. However, of the three original 2-aryl substituted benzimidazole precursors proposed, this was perhaps the most least likely to yield useful results as the furnace temperature employed is close to the limit that can be tolerated by methoxy groups, which can suffer O-CH_3 cleavage to phenoxyl radicals. It would appear that this was indeed the case.

2.5.4 Flash vacuum pyrolysis of 1-amino-2-(2-ethylphenyl)-1*H*-benzimidazole

1-Amino-2-(2-ethylphenyl)-1*H*-benzimidazole **2.60** was subjected to the same FVP conditions as those above. Analysis of the crude pyrolysate by TLC showed five constituent products, which could be separated by dry flash chromatography using a gradient solvent system. All of components of the mixture have been separated and identified, as follows. All percentage yields quoted are relative estimates from the ^{1}H NMR spectrum of the crude pyrolysate (as separation of the components due to the small quantities involved is qualitative).

A pure sample of the first major product was proved by ^{1}H and ^{13}C NMR spectroscopy to be the de-aminated precursor **2.42** (~10%), which from the results of the previous FVP experiments was an expected product.

The next product was successfully identified as 5,6-dihydrobenzo[4,5]imidazo[2,1-*a*]isoquinoline **2.76** (~25%) by its ^{1}H and ^{13}C NMR spectra which agreed with literature data.[19] This is the major product of the pyrolysate by NMR determinations.

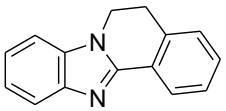

2.76

There are two possible mechanisms for the formation of 5,6-dihydrobenzo[4,5]imidazo[2,1-*a*]isoquinoline **2.76**.

Mechanism 1 (scheme 27) occurs *via* a primary CH_2 radical **2.79**, analogous to that seen previously in the formation of 11*H*-benzo[4,5]imidazo[1,2-*a*]isoindole **2.61**. The radical **2.79** could be formed from hydrogen transfer to the azol-1-yl radical **2.77** *via* a 7-membered transition state **2.78**. This radical **2.79** could then cyclise onto the

hydrogen free nitrogen atom of the benzimidazole forming the tertiary radical **2.80**, which can then eliminate a hydrogen radical to re-aromatise forming the 11*H*-benzo[4,5]imidazo[1,2-*a*]isoindole **2.61**.

Mechanism 1

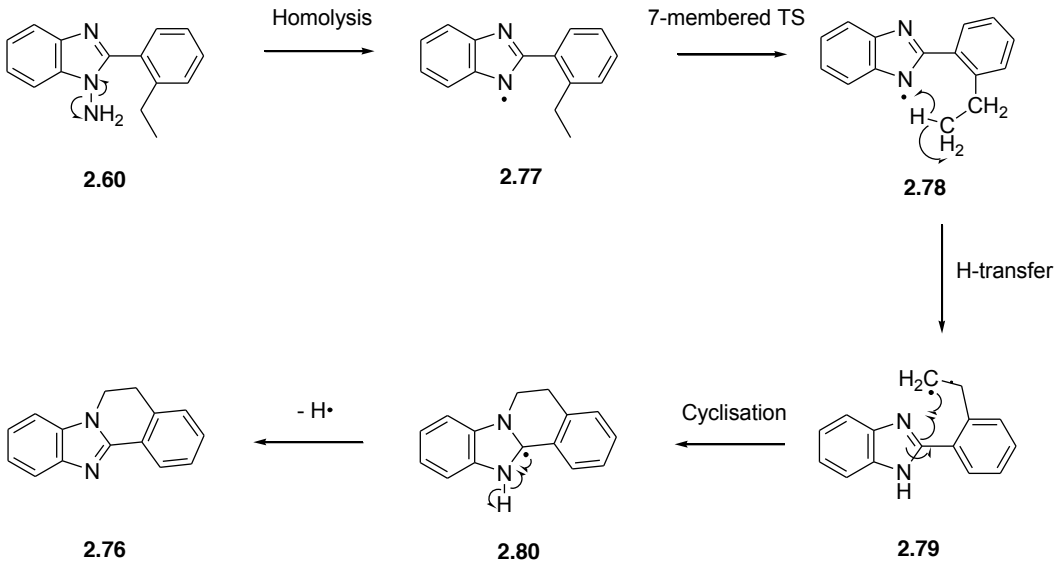

Scheme 27: Proposed mechanism 1 *via* primary CH_2 radical

Mechanism 2 (scheme 28) occurs *via* a secondary carbon radical **2.82** that then forms a terminal alkene **2.83** (analogous with the formation of 2-vinylbenzimidazole **2.38** from the pyrolysis of 1-amino-2-ethylbenzimidazole **2.29**) by the elimination of a hydrogen atom. It is possible for this terminal alkene to exist in equilibrium with the cyclised product **2.76**.

Mechanism 2

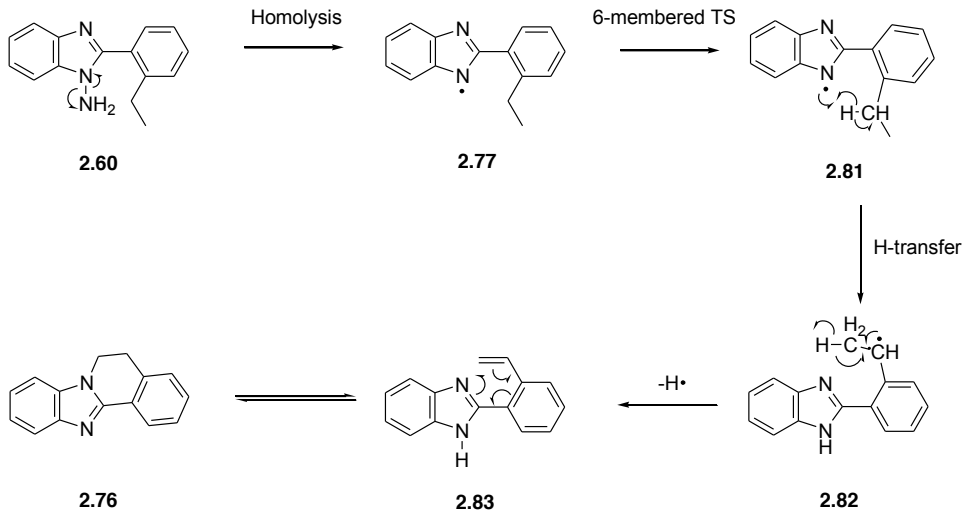

Scheme 28: Proposed mechanism 2 *via* secondary CH radical

Mechanism 2 is the most likely as it produces a secondary CH radical, which we know from DFT calculations on the 2-n-butylbenzimidazole is more thermodynamically stable than the corresponding primary CH radical. To gather more evidence for the proposal of mechanism 2, the equilibrium between the 2-styrylbenzimidazole and the cyclised product 2.76 was also modelled using DFT calculations and the result of this is shown in Figure 6. It can be seen that the energy surface shows this equilibrium to be very likely, there is a small energy barrier (*ca.* 59 kJ mol^{-1}) but the cyclised product is a more thermodynamically favoured product, it being approximately 70 kJ mol^{-1} lower in energy relative to the 2-styrylbenzimidazole.

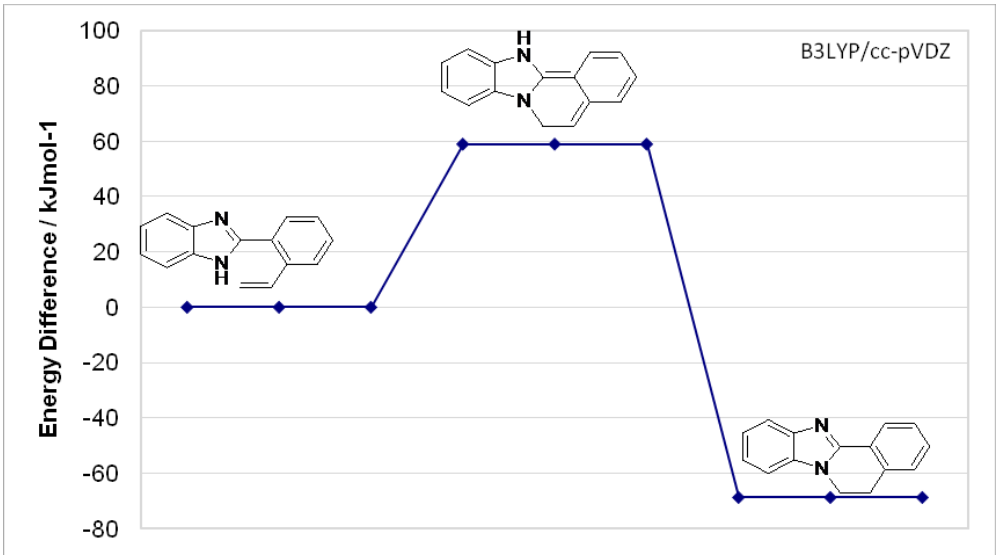

Figure 6: Equilibrium energy surface calculated using DFT

The third component to be isolated contained a distinctive doublet at 1.81 ppm in the ^{1}H NMR spectrum of the crude pyrolysate. As it has been shown than hydrogen transfer can occur readily *via* a 6-membered transition state 2.81, it is possible that a hydrogen could be transferred from the methylene carbon (scheme 29) to produce the secondary radical 2.84 which could cyclise onto the available nitrogen atom of the benzimidazole to form a new 5-membered ring, with loss of a hydrogen atom (2.85) in the process. This would result in the formation of product 2.86 whose methyl signal would be coupled with the proton attached to the same carbon, resulting in a clear doublet signal as is observed in this case.

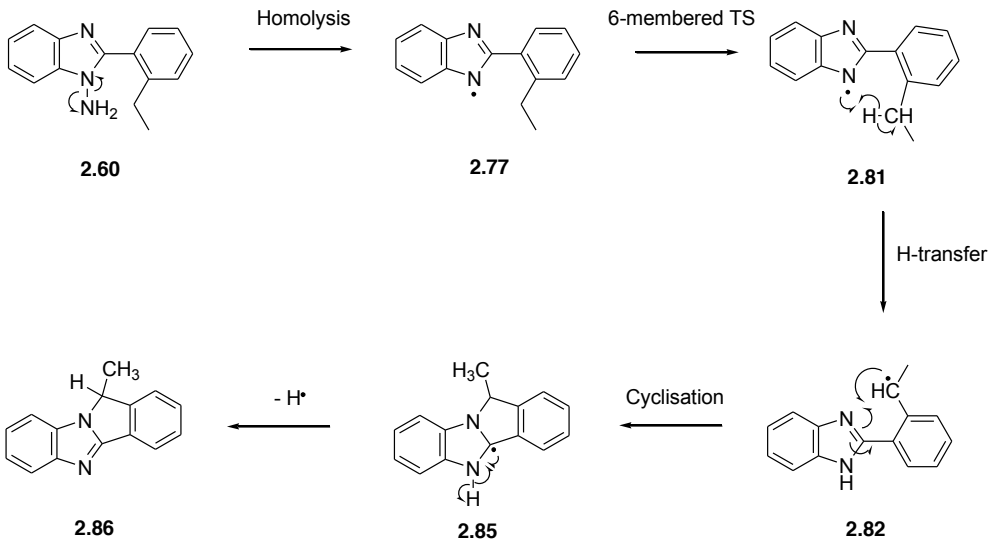

Scheme 29: Proposed mechanism for formation of **2.86**

Although 2.86 is not a known compound, pyrrolo[2,1-*a*]isoindole 2.87 is a good model for comparison. The ^{1}H NMR spectrum of 2.87 displays a mutually coupled doublet at δ_H 1.68 and quartet at δ_H 5.08, corresponding to the methyl group and adjacent proton. [23] These are similar to that seen in this instance where a doublet is apparent at δ_H 1.81 and a quartet at δ_H 5.32.

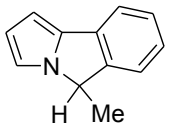

2.87

The fourth component may be a mixture of two different products. At δ_H 5.66 and 6.19 ppm there are distinctive styryl doublets but also at 3.06 and 3.24 ppm are two triplets that would suggest two CH_2 groups. The ratio of the styryl peaks to CH_2 was 1:2 and since these groups are likely to be derived from the ethyl substituent, there must be two different products or a dimeric species present. Further separation and purification allowed the analysis and confirmation that the majority product of this fraction is most probably the 2-styrylbenzimidazole 2.83, although some small

impurity peaks were always present and could not be removed. However, as an equilibrium between this species **2.83** and the cyclised product **2.76** has been proposed, this could explain why **2.83** could not be completely purified as any manipulation of the solid, by recrystallisation for example, may influence any equilibrium established at room temperature.

The most polar fraction was found to be 1-(2-ethylphenyl)-1*H*-benzo[*d*]imidazole-2-amine **2.88** (14%) and is analogous with the formation of 1-(2-methylphenyl)-1*H*-benzo[*d*]imidazol-2-amine **2.63**. This is very interesting, as it shows that the mechanism of formation is viable for both products and is another example of two subsequent 1,5-shifts. Comparison of the ^{1}H NMR spectra of the two 'swapped' products showed that similar aromatic peaks were evident between 7.00 and 6.70 ppm.

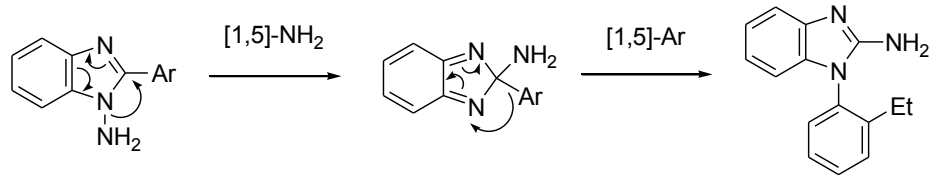

Where Ar = 2-EtPh **2.88**

Scheme 30: Proposed mechanism for two subsequent1,5-shifts for formation of 'swapped' products

The mechanism for the formation of **2.88** is again analogous with the 2-methylphenyl example **2.63**. The isolation of this product and in similar quantities to **2.63** suggests that this process is consistent with FVP of benzimidazoles of type **2.58** and **2.60** containing a 2-(2-alkylphenyl) group.

2.6 Extending to the Imidazole Ring System – Synthesis of 1-amino-2-arylimidazole precursors

Following on from the results of the 2-substituted benzimidazoles, an attempt was made to extend the work into the imidazole series, as imidazol-1-yl radicals have not been previously reported before in the literature. Imidazoles with the same *ortho*-substituted aryl groups at the 2-position as the previously described benzimidazoles were targeted as precursors (2.89-2.91), as the previous results were varied and would give a good set of comparable data. 2-Naphthylimidazole 2.92 was also investigated, as this could possibly form a new 5-membered ring, an analogous result to the 2-naphthylbenzimidazole case as discussed in the background section.

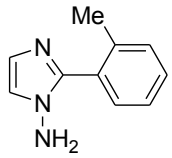

2.89

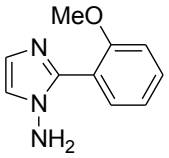

2.90

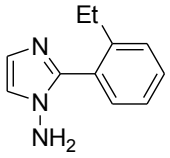

2.91

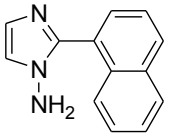

2.92

2.6.1 Synthesis of 2-arylimidazoles

There are two principle methods of synthesising 2-substituted imidazoles; direct C-2 arylation using palladium and copper catalysts, high temperatures and reaction times of up to 3 days, or dehydrogenation of the corresponding 2-substituted imidazoline. [24], [25] Direct arylation requires the appropriately halogenated aryl group as well as the catalysts and conditions mentioned. Due to the expensive reactants and conditions required, in this case it was decided that the corresponding 2-substituted imidazolines should first be made then dehydrogenated to generate the imidazole double bond. Their *N*-amination would then be attempted using the conditions developed previously using HOSA.

The synthesis of the desired imidazoles first required the synthesis of the corresponding 2-substituted imidazolines. These are simple to make from

ethylenediamine and the appropriate aldehyde using *N*-bromosuccinamide (NBS) as an oxidising agent. [26] The general mechanism for this reaction is shown in Scheme 31. The condensation reaction of the corresponding aldehyde with ethylenediamine forms the imine **2.93** which is in equilibrium with the cyclised product **2.94**. On addition of NBS, the cyclised product **2.94** is oxidised to the imidazoline salt **2.95**. As the cyclised product **2.94** is oxidised, the equilibrium position shifts until all the imine **2.93** has been consumed. The imidazoline salt produces the 2-substituted imidazoline **2.96** on alkaline work up.

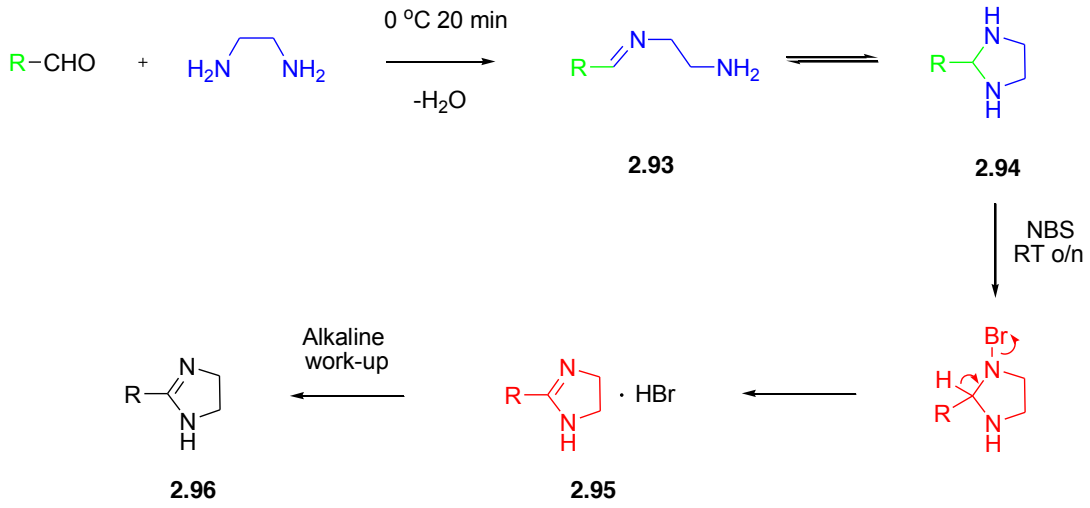

Scheme 31: Synthesis of 2-substituted imidazolines

This method is a mild and effective route to 2-substituted imidazolines and can be used for a range of aliphatic and aromatic aldehydes. Using this method, 2-(2-methylphenyl)-imidazoline **2.97**, 2-(2-methoxyphenyl)-imidazoline **2.98** and 2-naphthylimidazoline **2.99** were synthsised. The successful formation of the imidazolines was confirmed by the appearance of a distinctive 2 × CH_2 peak at δ_H ~ 4 – 3.5 in the ^{1}H NMR spectrum.

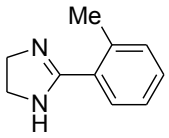

2.97

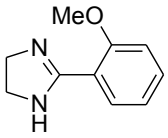

2.98

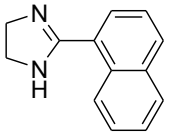

2.99

2.6.2 Dehydrogenation of Imidazolines

Dehydrogenations have been carried out previously within the McNab group using a tungsten trioxide catalyst plug inside the furnace tube of the FVP apparatus. [27] This is a simple and effective method, but one that relies on the volatilisation of the material to be dehydrogenated. This was attempted using the 2-naphthylimidazoline 2.99, however it was not volatile enough and the material in the inlet tube decomposed.

In the literature, dehydrogenations of imidazolines have been reported using potassium permanganate [28] and DMSO [29] but the reaction conditions in both instances are very harsh. However a recent paper reported successful dehydrogenation of imidazolines at room temperature using (diacetoxyiodo)benzene (DIB, 2.100) a hypervalent iodine complex. DIB had been compared against other known hypervalent iodine compounds [30] but these were found not to be as effective as the DIB. It is also effective for deydrogenations of 2-alkylimidazolines, though in lower yields. The mechanism of this dehydrogenation is shown in Scheme 32.

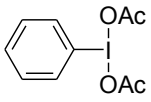

2.100

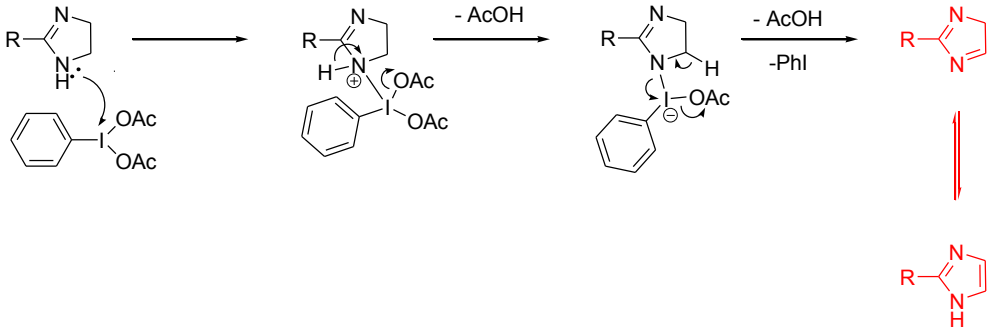

Scheme 32: Mechanism of imidazoline dehydrogenation using DIB

This method was applied to the 2-naphthylimidazoline initially, and produced the 2-naphthylimidazole in a 45% yield (Scheme 33).

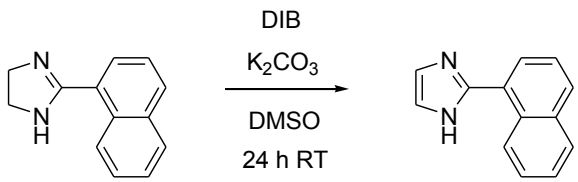

2.99 **2.101**

Scheme 33: Dehydrogenation of **2.99** using DIB

The successful dehydrogenation to 2-naphthylimidazole 2.101 was confirmed by ^{1}H and ^{13}C NMR spectroscopy. It was thought appropriate to take the 2-naphthylimidazole 2.101 through to the *N*-amination stage and apply/develop methods using HOSA before dehydrogenating the remaining imidazolines with DIB, as imidazoles are reactive and can decompose.

2.6.3 *N*-Amination of imidazoles

Although the literature suggested that the *N*-amination of imidazoles would not be effective using HOSA, all three previously developed methods were applied to the 2-naphthylimidazole **2.101**. Indeed none were effective, with none of the three yielding any of the desired *N*-aminated product. This along with the information from the literature seemed to prove that this method would not be efficient in *N*-aminating the imidazoles. However, information gleaned from a Japanese patent [31] suggested that amination may be more successful on the imidazoline species and that subsequent dehydrogenation of the *N*-aminated imidazolines would yield the required *N*-aminoimidazoles. This was attempted, again using all of the HOSA methods developed for the benzimidazoles. Again the ^{1}H NMR analysis of the product solid showed no signs of successful *N*-amination.

2.7 Conclusions

N-Amination of 2-alkylbenzimidazoles has been optimised and applied to produce *N*-aminobenzimidazoles **2.28-2.30** with varying 2-alkyl groups. The subsequent pyrolyses of these *N*-aminobenzimidazoles has shown that as the alkyl groups increase in length there becomes too many degrees of freedom for the radicals generated to be useful as regards hydrogen transfer. To introduce more rigidity into the precursors, *N*-amino-2-arylbenzimidazoles were explored and have been shown to undergo cyclisation and migration reactions. These migration reactions have resulted in the formation of new compounds 1-(2-methylphenyl)-1*H*-benzo[d]imidazol-2-amine **2.66** and 1-(2-ethylphenyl)-1*H*-benzo[d]imidazol-2-amine **2.88**, although further investigation into the mechanism of their formation is required.

2.8 References

1. S. M. Blinder, M. L. Peller, N. W. Lord, L. C. Aamodt, N. S. Ivanchukov, *J. Chem. Phys.*, 1962, **36**, 540.

2. D. A. Blank, S. W. North, Y. T. Lee, *Chem. Phys.*, 1994, **187**, 35.

3. V. M. Bierbaum, A. J. Gianola, R. L. Hoenigman, T. Ichino,S. Kato, W. C. Lineberger, *J. Phys. Chem A*, 2004, **108**, 10326.

4. R. J. Chriss, R. J. Gritter, *J. Org. Chem.*, 1964, **29**, 1163.

5. A. Wright, *Unpublished work*, 1998.

6. W. J. O' Neill, *Unpublished Work.* 2005.

7. J. B. Wright, *Chem. Rev.*, 1951, **48**, 397.

8. M. A. Phillips, *J. Chem. Soc.*, 1931, 1143.

9. R. J. Alheim, D. W. Hein, J. J. Leavitt, *J. Am. Chem. Soc.*, 1957, **79**, 427.

10. V. N. Komissarov, V. V. Kuz'menko, A. M. Simonov, *Chem. Heterocycl. Compd. (Engl Transl)*, 1980, **16**, 634.

11. V. V. Kuz'menko, O. V. Kryshtalyuk, A. F. Pozharskii, M. I. Rudnev, O. V. Vinogradova, *Chem. Heterocycl. Compd. (Engl Transl)*, 1994, **10**, 1182.

12. R. Tyas, *PhD Thesis.* The University of Edinburgh, 2001.

13. H. Rataj, Unpublished work, 1991.

14. E. Stevenson, *Unpublished Work.* 1998.

15. W. J. O'Neill, *PhD Thesis.*, The University of Edinburgh, 2009.

16. J. I. G. Cadogen, J. B. Husband, H. McNab, *J. Chem. Soc. Perkin Trans. II*, 1983, 697.

17. P. L. Boyer, W. W. Buckheit, S. H. Hughes, C. J. Michejda, M. L. Morningstar, T. Roth, *J. Med. Chem.*, 1997, **40**, 4199.

18. G. Speier, L. Parkanyi, *J. Org. Chem.*, 1986, **51**, 218.

19. S. M. Allin, W. R. Bowman, R. Karima, S. S. Rahman, *Tetrahedron*, 2006, **62**, 4306.

20. B. M. Adger, S. Bradbury, M. Keating, C. W. Rees, R. C. Storr, M. T. Williams, *J. Chem. Soc., Perkin Trans. 1*, 1975, 31.

21. F. D. Greene, C. J. Wilkerson, *J. Org. Chem.*, 1975, **40**, 3112.

22. E. Stevenson, *Unpublished Work.* 1998.

23. D. Reed, H. McNab, I. D. Tipping, R. G. Tyas, *Arkivoc*, 2007, *11*, 85.

24. J. L. Hughey, S. Knapp, H. Schugar, *Synthesis*, 1980, **6**, 489.

25. F. Bellina, C. Calandri, S. Cayteruccio, R. Rossi, *Tetrahedron*, 2007, **63**, 1970.

26. H. Fujioka, Y. Kita, O. Kubo, K. Murai, Y. Ohba, *Tetrahedron*, 2007, **63**, 638.

27. J. Campbell, G. McDougald, H. McNab, R. G. Tyas, L. V. C. Rees, *Synthesis*, 2007, 3179.

28. M. Abdollahi-Alibeik, I. Mohammadpoor-Baltork, M. A. Zolfigol, *Tetrahedron Lett.*, 2004, **45**, 8687.

29. M Anastassiadou, G. Baziard-Mouysset, M. Payard, M., *Synthesis*, 2000, 1814.

30. M. Ishihara, H. Togo, *Synlett.*, 2006, 227.

31. K. Hayashi, K. Hirano, Y. Ho, Y. Iwassawa, H. Kawamoto, S. Ozaki, *Japanese Patent*, WO 9854168.

3. *N*-Amino Heterocycles in the Synthesis of FVP Ketene Precursors

3.1 Introduction

For a considerable time now, the McNab group have developed and extended their research into the preparative applications of pyrolytic reactions of Meldrum's acid 3.1 (R = H) and its derivatives. Different applications and uses are continually evolving and indeed the work discussed within the main body of this chapter will take a reaction first discovered in the early 1990s and develop the principles for application in a different context.

Meldrum's acid 3.1 is known to decompose during flash vacuum pyrolysis (FVP) at furnace temperatures of >400 °C to produce acetone, carbon dioxide and a ketene, all of which are detectable within the pyrolysate obtained (Scheme 1). [(1)] As the decomposition products, along with the ketene, are carbon dioxide and acetone, they are very easy to remove from the pyrolysate; both co-products will evaporate once the condensed pyrolysate is brought back up to room temperature. This makes the pyrolysis of Meldrum's acid derivatives extremely attractive for the generation and study of ketenes that would be too reactive to investigate using solution phase chemistry.

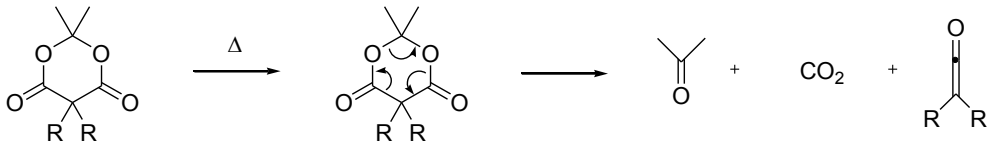

3.1

Scheme 1: Decomposition of Meldrum's acid under FVP conditions

One particularly useful Meldrum's acid derivative which is utilised extensively in FVP is methoxymethylene Meldrum's acid (MMMA) 3.2 (Scheme 2). In particular it is most often used in a condensation reaction with primary amines to form

Meldrum's acid derivatives of the type 3.3. This is a very clean, quick and straightforward condensation reaction, which very often results in the desired derivatives of type 3.3 precipitating out of solution, leaving most compounds clean enough to use directly, or requiring simple recrystallisation before pyrolysis. Yields are generally very good with a wide range of amines applicable.

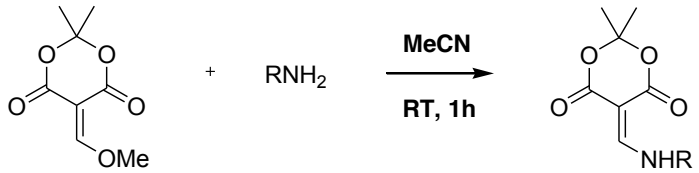

3.2 **3.3**

Scheme 2: Condensation reaction of methoxymethylene Meldrum's acid with amines

Under typical FVP conditions, derivatives of type 3.3 decompose, eliminating carbon dioxide and acetone, to generate a methyleneketene of type 3.4 as shown in Scheme 3. This methyleneketene then undergoes a [1,3]-hydrogen shift to produce the imidoylketene intermediate 3.5. This [1,3] shift is formally disallowed; however, it also involves orbitals that lie in the plane of the ketene hence it is a feasible shift. It is this highly reactive imidoylketene intermediate that can then undergo cyclisation or transfer reactions with the R group substituent, and the variation of this R group leads to a diverse collection of possible reactions and products. [(2), (3), (4)]

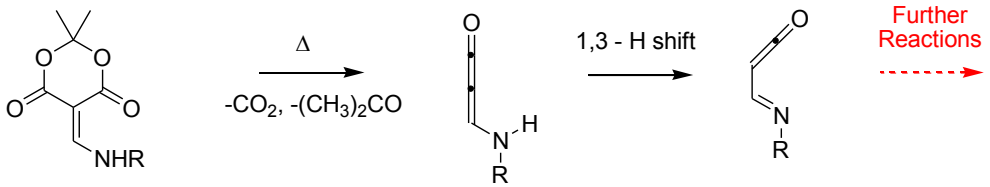

3.3 **3.4** **3.5**

Scheme 3: Formation of iminoketene intermediates from pyrolysis of derivatives **3.3**

Of particular interest to the work presented here is the reaction of methoxymethylene Meldrum's acid 3.2 with *N*-aminopyrazole 3.6 as illustrated in Scheme 4. This

reaction yields 5-(*N*-aminopyrazolyl)methylene-2,2-dimethyl-1,3-dioxane-4,6-dione 3.7.

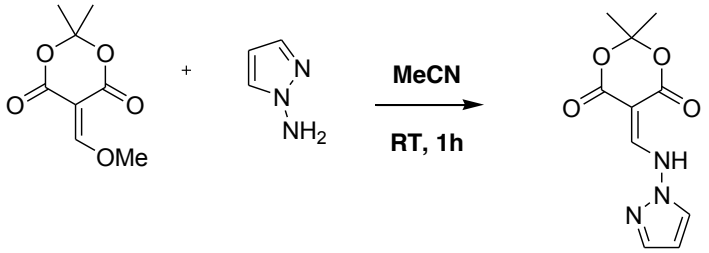

3.2 **3.6** **3.7**

Scheme 4: Synthesis of 5-(*N*-aminopyrazolyl)methylene-2,2-dimethyl-1,3-dioxane-4,6-dione

The 5-(*N*-aminopyrazolyl)methylene-2,2-dimethyl-1,3-dioxane-4,6-dione precursor 3.7 was subjected to FVP conditions over the furnace temperature range 450-700 °C, and it was found that two isomeric products were obtained from the pyrolysis (Scheme 5). [5] The proportion of each product obtained was dependent on the furnace temperature used. Pyrolysis of 3.7 produced the methyleneketene 3.8 which then undergoes the expected [1,3]-hydrogen shift to form the imidoylketene intermediate 3.9 whose reactive ketene moiety can then interact with the pyrazole ring. At furnace temperatures of 650-700 °C the major product was promptly identified as the pyrazolopyridazinone 3.10, as an analogous pyrolysis of the *N*-aminopyrrole derivative 3.12 generates the pyrrolopyridazinone 3.13 (Scheme 6). The major product at lower temperatures was discovered, by X-ray crystal determination, to be pyrazolo[1,2-*a*]1,2,3-triazinium-4-olate 3.11, the parent member of a novel class of heterocyclic mesomeric betaines. [5] The temperature dependence and relationship between these two products was confirmed when pyrolysis of the 'low temperature' betaine product 3.11 formed the 'high temperature' pyrazolopyridazinone product 3.10. The temperature profile data for this pyrolysis is illustrated in Figure 1.

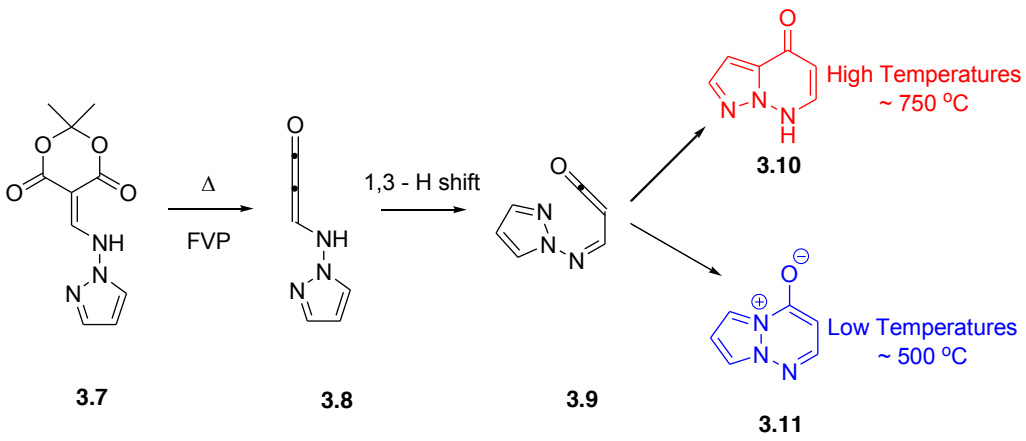

Scheme 5: Formation of pyrazolopyridazinone **3.10** and mesomeric betaine **3.11** from pyrolysis of 5-(*N*-aminopyrazolyl)methylene-2,2-dimethyl-1,3-dioxane-4,6-dione

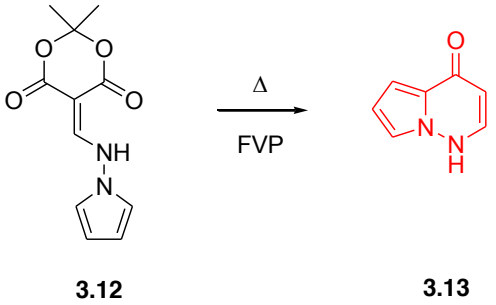

Scheme 6: Analogous formation of pyrrolopyridazinone from 5-(*N*-aminopyrrolyl)methylene-2,2-dimethyl-1,3-dioxane-4,6-dione

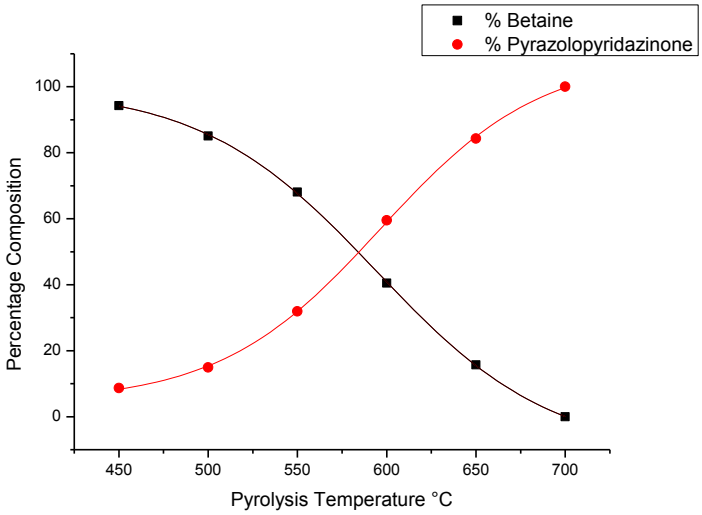

Figure 1: Temperature profile graph to show relationship between pyrazolopyridazinone **3.10** and mesomeric betaine **3.11**

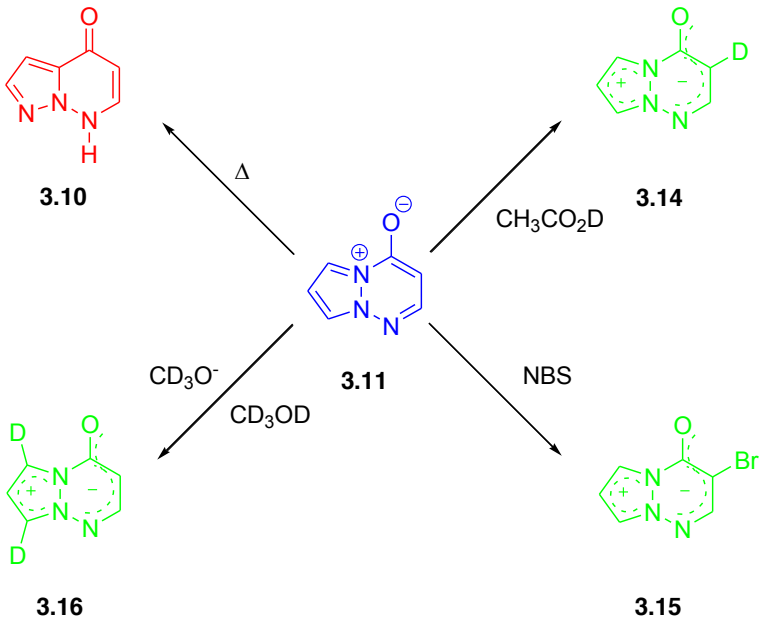

Scheme 7: Investigating the chemical properties of the mesomeric betaine **3.11**

An initial study of the chemical properties of the product 3.11 was undertaken, as this was a novel heterocyclic mesomeric betaine ring system. [5] A summary of those

are illustrated in Scheme 7. It proved to be relatively thermally stable as it was unaltered by sublimation at 100 °C or FVP using a furnace temperature of 500 °C, which we would expect as this is the optimum temperature for its formation as shown from the temperature profile graph Figure 3.1. It was however converted to the pyrazolopyridazinone 3.10 upon pyrolysis with a furnace temperature of 700 °C, again a result that was predicted from the temperature profile. This suggests that an equilibrium may be in force between the betaine 3.11 and the iminoketene intermediate 3.9 at higher furnace temperatures and hence that the iminoketene may be regenerated from the betaine to then undergo cyclisation onto the adjacent carbon to form the pyrazolopyridazinone 3.10. The six-membered ring of the betaine was expected to be electron-rich in nature and this was confirmed by reaction with deuteriated trifluoroacetic acid, which formed the compound 3.14 with the deterium replacing the hydrogen atom at the 3-position. This was also shown by reaction of the betaine with *N*-bromosuccinimide in chloroform, which resulted in the 3-bromo compound 3.15 in a yield of 94%. However, reaction of betaine 3.11 with methoxide ions did not give the expected product 3.18 (Scheme 8) but gave the di-deuterium exchange product 3.16 which is thought to occur *via* a ylide-like intermediate 3.17.

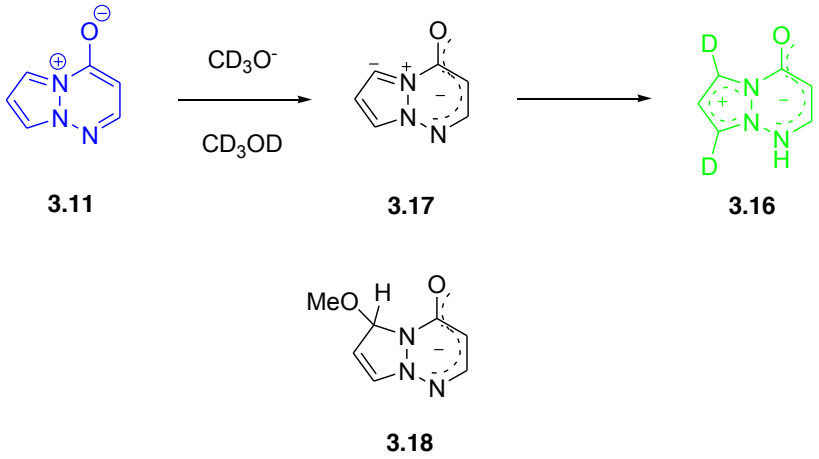

3.11 **3.17** **3.16**

3.18

Scheme 8: Reaction of mesomeric betaine **3.11** with methoxide ions in deuteriated methanol

The aim of the work described here was to take this parent reaction and extend the scope of it to produce a range of substituted betaines of the pyrazolotriaziniumolate

family and to take the experience from this and apply the same principles to other heterocyclic systems, using the knowledge previously gained from work on the *N*-amination of heterocycles. This in turn would hopefully yield a number of new heterocyclic mesomeric betaine systems for investigation into their chemical properties and applications.

3.2 Substituting the Pyrazolotriaziniumolate Around the Pyrazole Ring

The initial step thought appropriate to begin diversifying this new family of heterocyclic mesomeric betaines was substitution around the pyrazole ring, as this would entail making or using commercially available substituted pyrazoles and simply applying the optimised conditions for N-amination as found *via* the work carried out and discussed in Chapter 2.

3.2.1 Synthesis of Substituted Pyrazole FVP Precursors

There were four substituted pyrazoles identified as good starting points for this work, as illustrated in Scheme 9. 4-Methylpyrazole **3.19** and 3-methylpyrazole **3.20** are commercially available and would simply require N-amination, although the N-amination product of 3-methylpyrazole would require some separation as there are two possible isomers from this reaction. 3-*tert*-Butylpyrazole **3.21** was thought to be a good choice of substrate, as it was hoped that the large, bulky *tert*-butyl group would 'block' *N*-amination at the N2 atom producing only one isomer from the reaction, as this effect has been seen in other work carried out within the McNab group. [6] Finally the 4-phenylpyrazole **3.22** was a good aryl substituted option, as being substituted at the 4-position it was symmetrical thus cutting out the need for any separation.

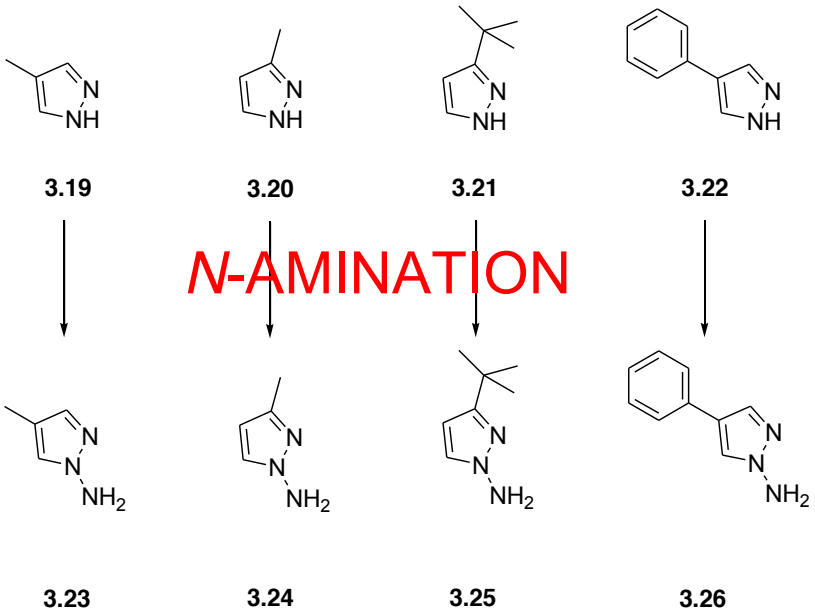

Scheme 9: Appropriate substituted pyrazoles for *N*-amination and subsequent reaction with MMMA

The original optimised conditions for N-amination were applied to both the 3-methyl and 4-methylpyrazoles 3.19 and 3.20, however neither of these reactions went to completion. All three general methods were applied yet on average went only to 40-50% completion. Attempts were made to separate the N-aminated product from the starting material, however these attempts were fruitless.

It was hoped that as the bulky *tert*-butyl group was present at the 3-position, that it may 'block' N-amination at the N2 atom producing only the 1-amino-3-*tert*-butyl product 3.22 (Scheme 10). On applying the optimised N-amination methods 1-3 it was apparent again that the reaction would not go to completion (even with multiple repetitions of the process) with the most successful reaction consuming 60% of the starting material. There were two products present in the reaction mixture along with unreacted starting material, these were the two possible isomers from N-amination, and although the 2-amino-3-*tert*-butylpyrazole 3.27 was present in the smaller amount (*ca.* 30% of total product present) this demonstrated that the *tert*-butyl group does not completely 'block' the 2-position. Again problems were encountered with

separating the starting material from the products and the products from each other; hence this substrate was not further investigated.

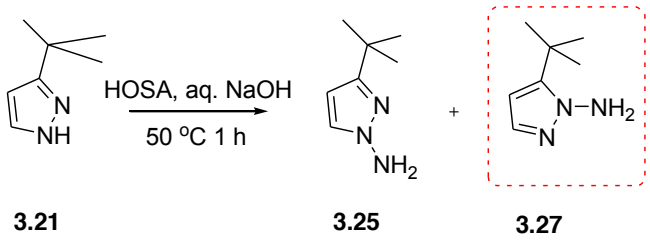

3.21 **3.25** **3.27**

Scheme 10: *N*-Amination of 3-*tert*-butylpyrazole

Similarly, 4-phenylpyrazole 3.22 is not widely available commercially, so it was synthesised *via* the reaction outlined in Scheme 11. [7] Phenylacetic acid 3.28 is added to the Vilsmeier Reagent at 0 °C and then heated at 70 °C overnight, before a basic work up which yields the phenyl acrolein 3.29. This is reacted with hydrazine monohydrate at room temperature overnight, and after recrystallisation from ethanol gives the pure 4-phenylpyrazole 3.22 in a 63% yield.

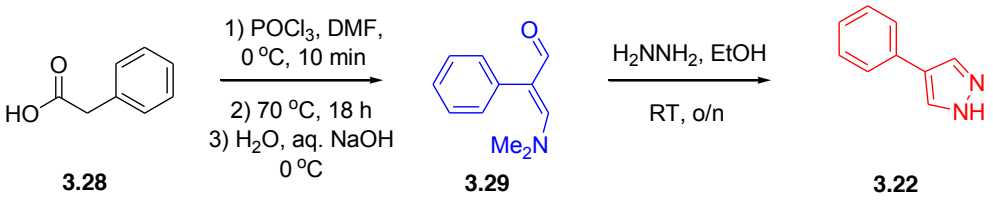

3.28 **3.29** **3.22**

Scheme 11: Synthesis of 4-phenylpyrazole **3.22**

The next step was the *N*-amination of the 4-phenylpyrazole and the reaction was incredibly successful (Scheme 12). This follows the pattern seen during the optimisation work of this reaction, as it was highlighted in Chapter 2 that aryl benzimidazoles were a lot more straightforward to *N*-aminate than the alkyl benzimidazoles, and it appears that this is also the case for pyrazoles.

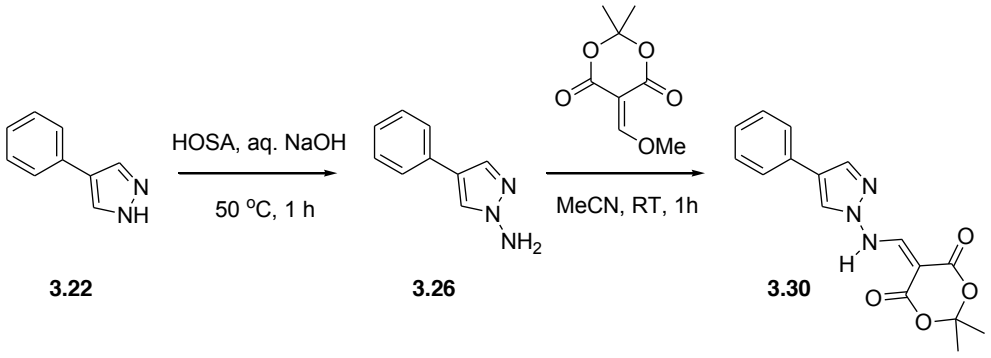

Scheme 12: *N*-amination of 4-phenylpyrazole and subsequent reaction with MMMA

To construct the appropriate pyrolysis precursor, the *N*-amino-4-phenylpyrazole 3.26 was then reacted with methoxymethylene Meldrum's acid (MMMA) under the usual conditions (Scheme 12). This was a quick and clean reaction, producing the desired Meldrum's derivative 3.30 in a 76% yield after recrystallisation from methanol.

3.2.2 Flash Vacuum Pyrolysis of Substituted Pyrazoles

The 4-phenylpyrazole precursor 3.30 was subjected to the same pyrolysis conditions as that for the parent pyrazole. A temperature profile experiment, consisting of small scale (~ 20 mg) pyrolyses at varying furnace temperatures, was carried out to determine if indeed the same temperature dependence could be observed, as with the parent example. The temperature profile graph resulting from these experiments is shown in Figure 2.

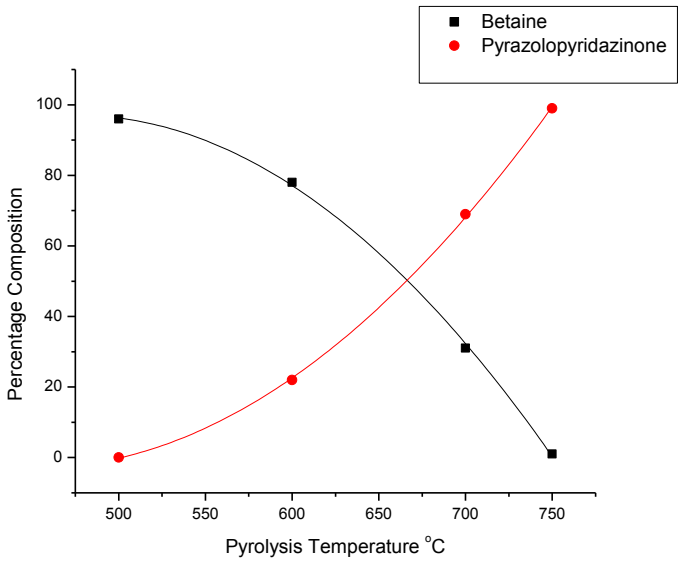

Figure 2: Temperature profile graph for FVP of 4-phenylpyrazole Meldrum's derivative **3.30**

Analysis of the pyrolysates, the data gathered from which was used to draw the graph Figure 2, showed that indeed the 4-phenyl substituted pyrazole followed the precedent set by the parent reaction. Once the methyleneketene 3.31 (Scheme 13) had been formed it could then undergo 1,3-hydrogen shift to form the imidoylketene 3.32. This then has the option of cyclising onto either the adjacent nitrogen atom, or the adjacent carbon atom. At lower furnace temperatures (*ca.* 500 °C) the imidoylketene cyclises onto the nitrogen atom at position 2 of the pyrazole, forming the substituted mesomeric betaine structure 3.33. At higher temperatures (*ca.* 700 °C) the imidoylketene cyclises onto the carbon atom at position 5 of the pyrazole, forming the substituted pyrazolopyridazinone 3.34. The mechanism of these cyclisations and the hypotheses behind the temperature dependence will be discussed later in this chapter. These are both previously unknown structures, and their synthesis *via* this method shows that, as long as the starting pyrazoles can be successfully *N*-aminated and purified prior to reaction with MMMA, that substitution around the pyrazole ring is tolerated and follows the precedent established by the parent reaction.

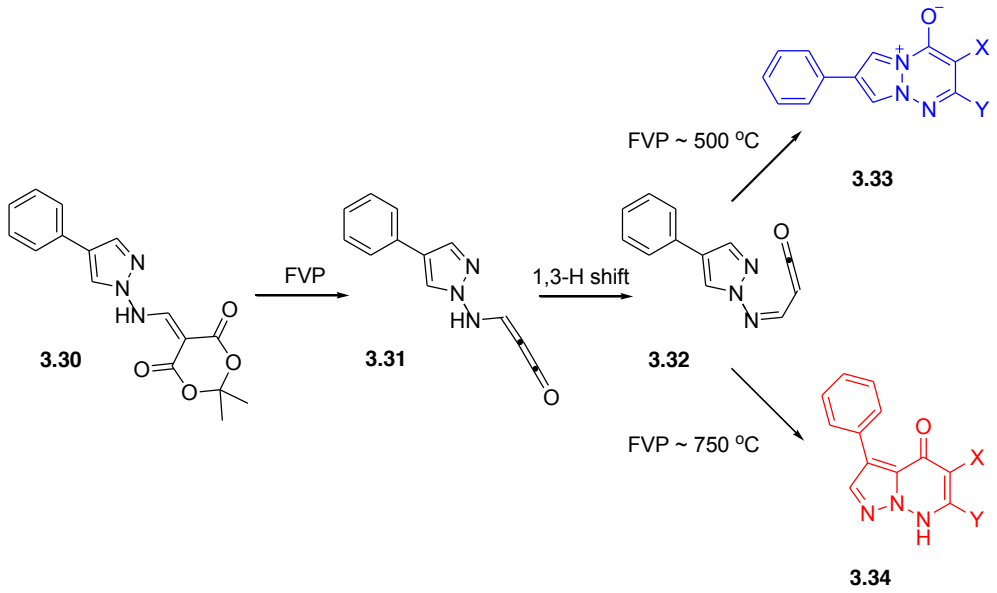

Scheme 13: FVP process for formation of phenyl substituted betaine **3.33** and substituted pyrazolopyridazinone **3.34**

3.3 Substituting Around the Pyridazinone Ring

Substituting the betaines and pyrazolopyridazinones around the pyridazinone or triazine rings requires the use of a different ketene generator, as it is not possible (or convenient) to substitute the methoxymethylene Meldrum's acid in the desired position/s to produce the appropriate substituted products. Methoxymethylene Meldrum's acid derivatives may be used to produce products substituted at the Y position (shown in Scheme 13) but not at the X position. It is known that acrylic esters can generate imidoylketenes when subjected to FVP, by eliminating methanol as illustrated in Scheme 14. This elimination is not limited to methanol though, and works equally well with the ethyl esters. These ketene generating groups are relatively easy to incorporate into the pyrazoles and hence form the starting point in producing precursors that will enable the generation of pyridazinone substituted betaines.

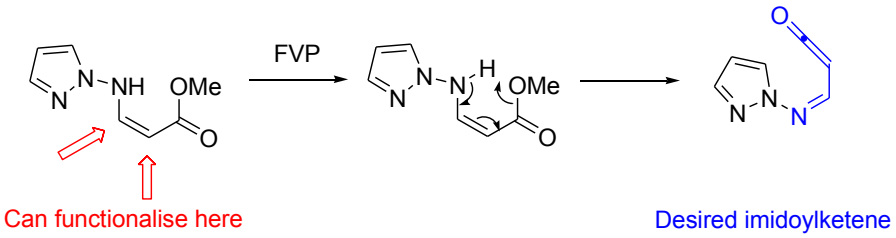

Scheme 14: Generation of imidoylketenes from acrylic esters

The starting point for all these derivatives will be *N*-aminopyrazole 3.6 (Scheme 15) as the pyrazole ring will be unchanged. Reaction of the *N*-aminopyrazole 3.6 with ethyl (ethoxymethylene)cyanoacetate will give the acrylic ester precursor 3.35a and reaction with diethyl ethoxymethylenemalonate will give the precursor 3.35b. It is hoped that these precursors will form the 3-substituted betaines 3.38a&b upon pyrolysis.

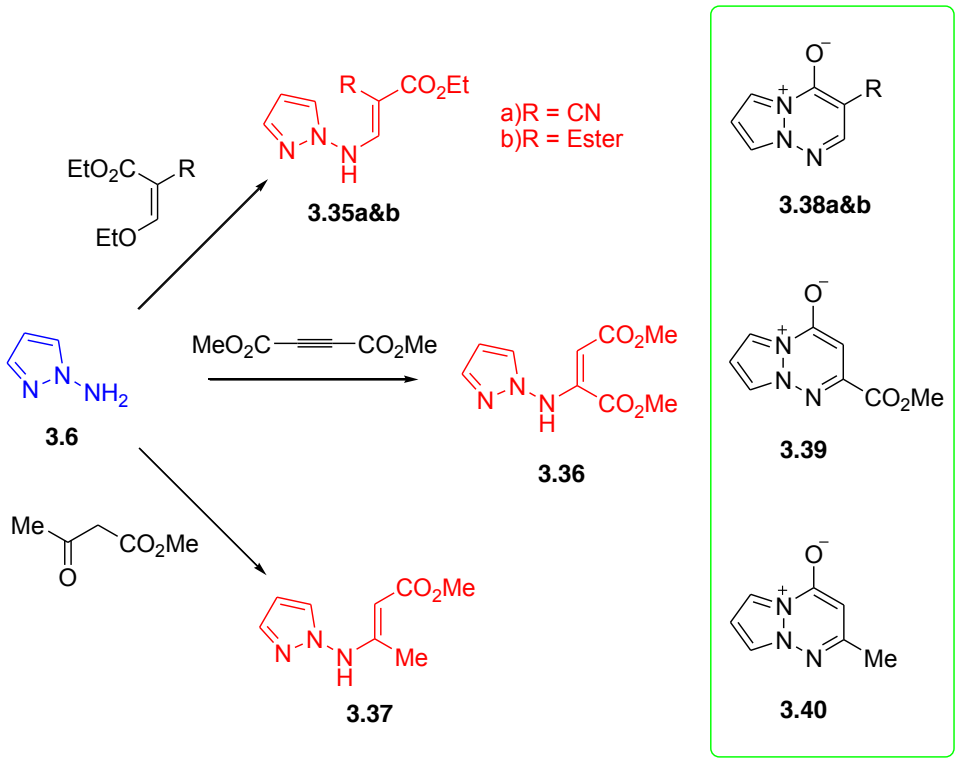

Scheme 15: Synthesis plan for appropriately substituted acrylic ester precursors

3.3.1 Synthesis of Acrylic Ester FVP Precursors

The precursors 3.35a and 3.35b were prepared by the condensation of *N*-aminopyrazole 3.6 with ethyl (ethoxymethylene)cyanoacetate and diethyl ethyoxymethylenemalonate respectively. These reactions were straightforward and carried out at room temperature in acetonitrile. In both cases the products precipitated and were recrystallised from ethanol. The yields reported are after recrystallisation.

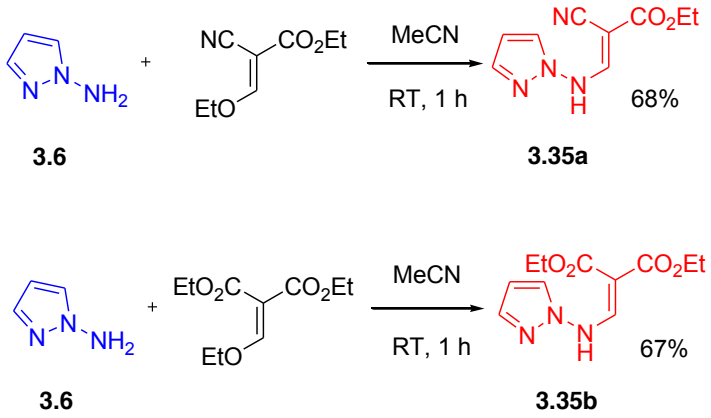

Scheme 16: Reaction schemes showing formation of acrylic ester precursors **3.35a** and **3.35b**

The proton NMR spectrum of the cyano acrylic ester 3.35a was initially very confusing at it showed more peaks than assignable to the structure. However this is due to 3.35a existing as two conformational isomers as illustrated in Scheme 17. There is restricted rotation around the C=C bond which means that 3.35a is found as a mixture of *E* and *Z* isomer resulting in extra ^{1}H NMR peaks. To confirm that this was indeed the case, some low temperature ^{1}H NMR experiments were carried out to see if the peaks coalesced into a single isomer. As the temperature decreased, peaks began to coalesce until only one set of signals was apparent; this confirmed that these were rotational isomers and not the presence of an unexpected side product.

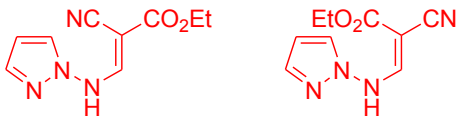

E isomer *Z* isomer

Scheme 17: Rotational isomers of **3.35a**

Other compounds with cyano acrylic ester type moieties are known to display rotational isomerism [8] so this was not wholly unexpected. It is suggested in the literature [8] that the most abundant isomer is the *Z* isomer, as its conformation would allow the formation of an intramolecular hydrogen bond between the NH and the ester carbonyl as shown in Scheme 18. This would also have a deshielding effect on the nitrogen proton, increasing the chemical shift. This is seen both in the literature [8] where the *Z* isomer NH proton is observed at δ_H 10.63 versus δ_H 8.27 for the *E* isomer, and in the example of 3.35a where the *Z* isomer NH proton is seen at δ_H 11.20 versus δ_H 10.38 in the *E* isomer

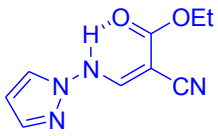

Z isomer

Scheme 18: Conformation of intramolecular hydrogen bond within the *Z* isomer

The dimethyl ester precursor 3.36 was synthesised from *N*-amino pyrazole 3.6 and dimethyl acetylenedicarboxylate in methanol at room temperature as shown in Scheme 19. After an hour the solvent was removed under reduced pressure to produce a thick oil.

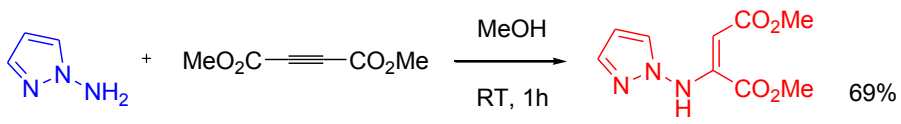

3.6 **3.36**

Scheme 19: Synthesis of dimethyl ester precursor **3.36**

The ^{1}H NMR spectrum of the product 3.36 was not what was expected; in fact the spectrum suggested that the product 3.36 was not what had been produced. A singlet at δ_H 4.40 which integrated to two protons was present and indicative of a CH_2 signal. This was confirmed by the ^{13}C NMR spectrum which showed a CH_2 signal at δ_C 35.81. This evidence suggested that the dimethyl ester precursor 3.36 in fact exists as the imine form [(dimethyl 2-(1H-pyrazol-1-ylimino)succinate)] 3.36b shown in scheme 20. This imine can exist in equilibrium with the enamine form, and as only the imine is observed, the equlibrium must lie strongly to the right.

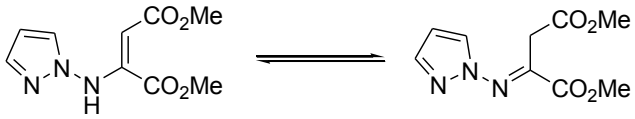

3.36 **3.36b**

Scheme 20: Suggested equilibrium

To back up this theory DFT calculations were carried out to determine the relative energies of these two tautomers in the gas phase. Results for the methyl analogue 3.37 were also calculated for comprison. The relative energies calculated are shown in Figure 3, and reveal that the imine tautomer 3.36b is indeed of a lower energy that the form of 3.36. The methyl derivative calculated for comparison is in fact the opposite; the imine form is found to be the higher energy form, and by approximately the same magnitude.

These calculations show that the imine form 3.36b is more thermodynamically stable than the corresponding enamine tautomer 3.36. this is surprising as the enamine

tautomer can form an internal hydrogen bond which could increase thermodynamic stability in this configuration.

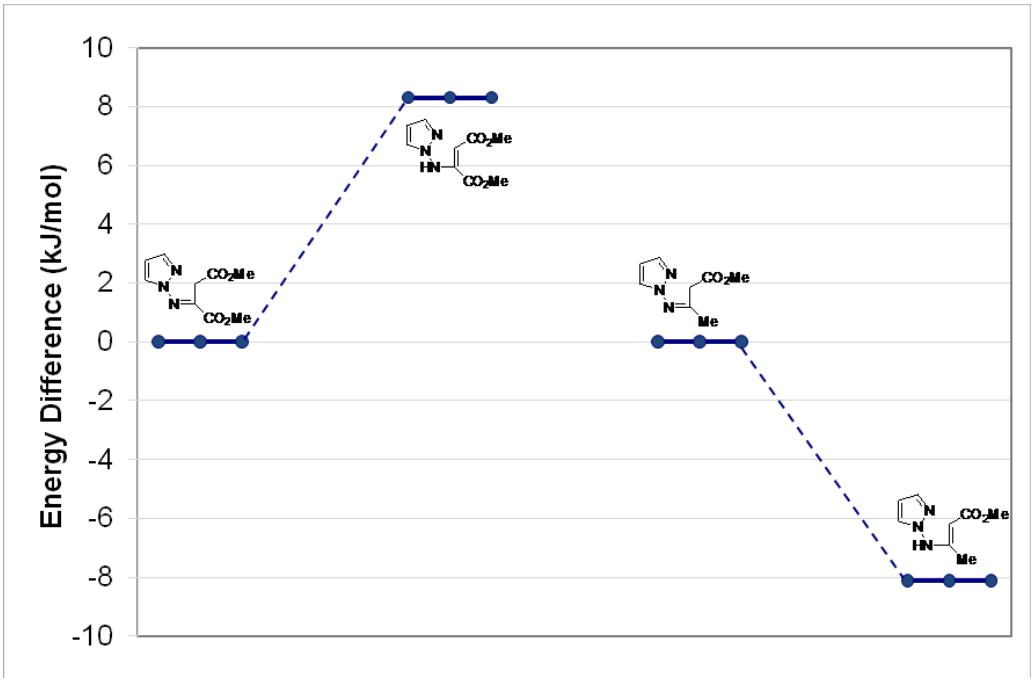

Figure 3: Relative energy differences in enamine vs imine tautomers

The methyl substituted presursor 3.37 was synthesised *via* the acid catalysed condensation of *N*-aminopyrazole 3.6 with methyl acetoacetate. The reaction was carried out in methanol under reflux for three hours and after removal of solvent under reduced pressure and recrystalisation from ethanol, 3-(pyrazol-1-ylamino)-but-2-enoic acid methyl ester 3.37 was obtained in a 63% yield (Scheme 21).

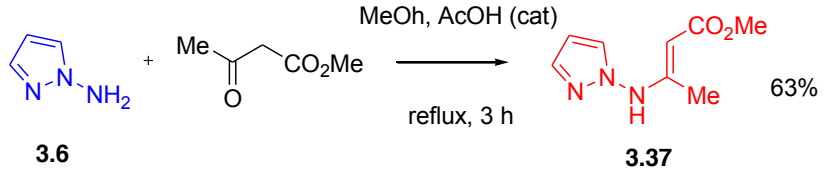

Scheme 21: Synthesis of 3-(pyrazol-1-ylamino)-but-2-enoic acid methyl ester **3.37**

The compound exists as the enamine tautomer and indeed this backs up the results from the DFT calculations. This implies that the greater thermodynamic stability of imine 3.36b compared to its enamine form may be attributed to the effect of the electron –withdrawing methyl ester group attached to the carbon adjacent to the amine nitrogen.

3.3.2 Flash Vacuum Pyrolysis of Acrylic Ester Precursors

Conditions for the pyrolyses were first established by using small scale experiments (*ca.* 20 mg) in which the entire contents of the trap were dissolved in a deuteriated solvent, usually DMSO as it was found that the pyrazolopyridazinones were insoluble in $CDCl_3$, and analysed at once by ^1H NMR spectroscopy. These small scales pyrolyses were then carried out at different furnace temperatures and the composition of the pyrolysate analysed and the results used to construct a temperature profile. This temperature profile allowed an optimum furnace temperature to then be selected for each product.

The temperature profile of the pyrolysis of 2-(cyano)-3-(pyrazol-1-ylamino)acrylic acid ethyl ester 3.35 is shown in Figure 4, and illustrates the relationship between the betaine 3.38a and its corresponding pyrazolopyridazinone 3.42. It can be seen that the betaine is initially the major product at lower furnace temperatures but that as the temperature increases so does the proportion of pyrazolopyridazinone. It is also worth noting that the starting material is still present in trace amounts until pyrolysis temperatures of 600 °C, due to a greater amount of energy needed to generate the ketene intermediate from the acrylic ester type precursor compared to the Meldrum's acid derivative precursor used in the parent reaction.

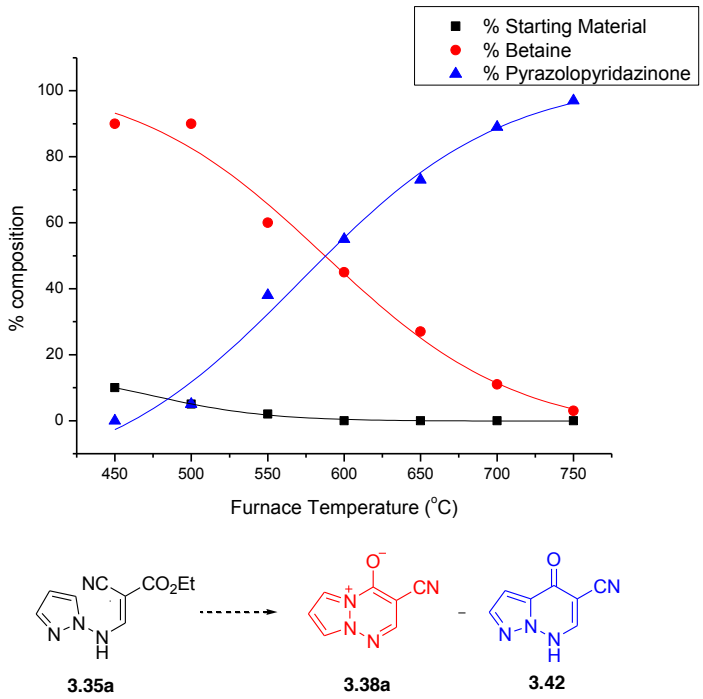

Figure 4: Temperature profile graph showing % composition of pyrolysate at varying furnace temperatures

Once the temperature profile was complete it was possible to choose suitable pyrolysis temperatures for preparative scale pyrolyses for both the cyano betaine **3.38a** and the cyano pyrazolopyridazinone **3.42** with both being formed from the imidoylketene intermediate **3.41** (Scheme 22). The optimum temperature found for the betaine **3.38a** was 500 °C as this produced the greatest proportion of betaine to pyrazolopyridazinone. The betaine was quite easily separated from the pyrazolopyridazinone as the difference in their solubility was so great; chloroform was gently distilled over the pyrolysate which dissolved the betaine, leaving the very insoluble pyrazolopyridazinone behind in the U-tube. This distillate was decanted off and the solvent removed to produce a clean sample of 3-cyanopyrazolotriazinium-4-olate **3.38a** for characterisation.

The optimum pyrolysis temperature for the preparation of the pyrazolopyridazinone **3.42** was found to be 750 °C, as this allowed maximum conversion and minimum

impurities. The pyrolysate was initially purified by the distillation of a small amount of chloroform to ensure any chloroform soluble impurities were removed if present, and then the pyrazolopyridazinone product was removed from the U-tube by partially dissolving in ethanol (it is only partially soluble) and scraping the remaining solid out. Again this produces a clean sample of 3-cyanopyrazolopyridazin-4-one 3.42 for analysis.

Both of these products were characterised by NMR and mass spectroscopy techniques. Cyano betaine 3.38a is an example of a 3-substituted pyrazolotriazinium-4-olate and was a good indication that further substituents could be incorporated into this novel betaine ring system.

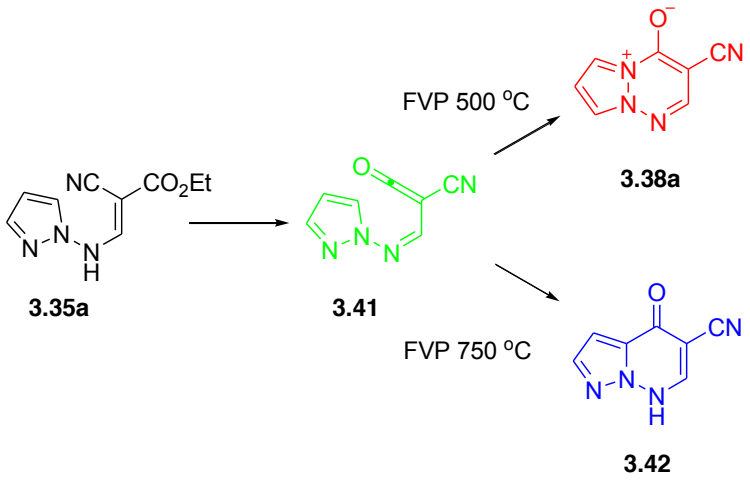

Scheme 22: Optimum pyrolysis conditions for preparation of betaine **3.38a** and pyrazolopyridazinone **3.42**

The diethyl ester precursor, 2-(pyrazol-1-ylaminomethylene)malonic acid 3.35b, was also subjected to the same small scale pyrolyses to determine the temperature profile and this is shown in Figure 5. It is clear on first inspection that the shape of this profile is different to the cyano example previously discussed. The proportion of starting material present in the pyrolysate is significantly greater at lower temperatures than was seen in the cyano example (Figure 3.3); the proportion of starting material at a furnace temperature of 450 °C is 10% for the cyano example

versus 80% for the diethyl ester precursor **3.35b**. This suggests that the generation of the ketene intermediate requires a significantly greater amount of energy in the diethyl ester case, hence its longevity in the temperature profile. This has a knock-on effect on the proportion of betaine **3.38b** produced as it is obviously dependent on the amount of ketene intermediate, and as the furnace temperature increases and the amount of ketene generate does also, the higher temperatures then begin to favour the production of the pyrazolopyridazinone **3.44**. It should be noted that this temperature profile ends with the furnace temperature of 650 °C, this is because after this significant decomposition of the ester group is observed, which in turn produces a pyrolysate comprising of many decomposition products.

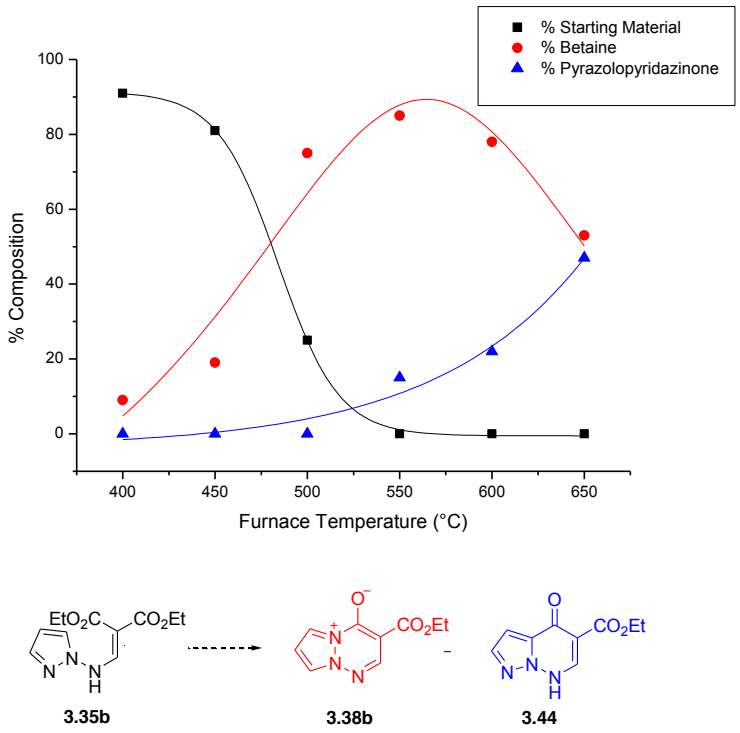

Figure 5: Temperature profile graph showing % composition of pyrolysate at varying furnace temperatures

By using the information from the temperature profile it was possible to choose suitable pyrolysis temperatures for preparative scale pyrolyses for both the betaine

3.38b and the pyrazolopyridazinone 3.44 (Scheme 23) with both being formed from the imidoylketene intermediate 3.43. The optimum furnace temperature chosen for the preparative pyrolysis of betaine 3.38b was determined to be 550 °C as this would allow the maximum proportion of betaine to be produced with minimum starting material and pyrazolopyridazinone impurities. The resulting pyrolysate was then purified using dry flash chromatography to yield a clean sample of 3-ethoxycarbonylpyrazolotriazinium-4-olate 3.38b for characterisation.

The optimum furnace temperature for the preparative scale pyrolysis of the pyrazolopyridazinone 3.44 was first taken to be 650 °C as this temperature produced the greatest proportion of 3.44 to betaine. However an attempt at this temperature, although producing the desired product and expected betaine also showed some decomposition products that were extremely difficult to remove. This also showed that the pyrazolopyridazinone 3.44 was slightly soluble in chloroform which did not allow the ease of separation seen in the previous example. To combat these issues the furnace temperature was reduced to 625 °C, which allowed a small amount of 3-ethoxycarbonylpyrazolopyridazin-4-one 3.44 to be obtained after purification of the pyrolysate by dry flash chromatography.

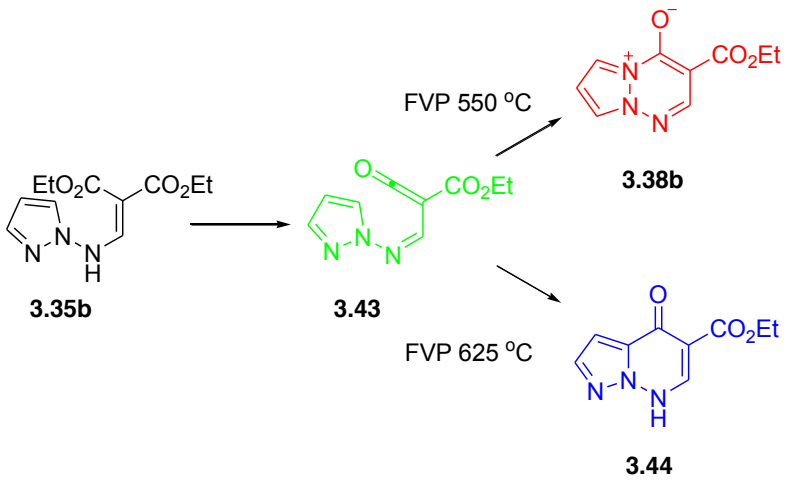

Scheme 23: Optimum pyrolysis conditions for preparation of betaine **3.38b** and pyrazolopyridazinone **3.44**

Because of the decomposition observed at higher furnace temperatures and its slight solubility in chloroform, it was difficult to obtain a significant sample of **3.44** for analysis and characterisation. But as isolation of the betaine **3.38b** was relatively easy to achieve in comparison it was thought that the temperature dependent relationship between the two products could be exploited, by subjecting the betaine **3.38b** to FVP to produce a significant quantity of the pyrazolopyridazinone **3.44**. This pyrolysis was undertaken using a furnace temperature of 600 °C, and analysis of the pyrolysate showed that the major product was not the pyrazolopyridazinone **3.44** but the corresponding acid, 3-carboxypyrazolopyridazin-4-one **3.45** as shown in Scheme 24. Pyrolytie *cis*-elimination reactions of ethyl esters are well known. [9] This would also explain the decomposition products seen, as a large broad peak in the NMR spectrum of the pyrolysate is now known to be attributable to the OH of the acid **3.45**.

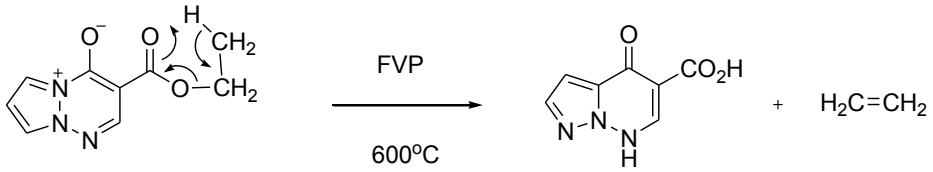

3.38b **3.45**

Scheme 24: Pyrolysis of betaine **3.38b** to form 3-carboxypyrazolopyridazin-4-one **3.45**

The imine precursor **3.36b** was unique to this work even before pyrolysis was attempted, as no previous examples exist of forming the required imidoylketene from an imine compound The imine precursor was subjected to the same small scale pyrolyses to determine the temperature profile and this is shown in Figure 6. It is clear on first inspection that the shape of this profile is different again to both the examples previously discussed. Even though it is substituted in a different position to the two previous examples, it does have certain similarities to the temperature profile of the diethyl ester precursor **3.35b** in that the starting material is detectable in trace amounts at a furnace temperature of 650 °C. This implies that, although this imine precursor follows the same reactions and pattern seen for the acrylic ester precursors,

it takes a significantly greater amount of energy and therefore a higher furnace temperature to generate the imidoylketene intermediate required. This is not unexpected as the imine would most likely first have to be converted to its enamine tautomer before the elimination of methanol and hence the generation of the imidoylketene could take place.

The magnitude of this extra energy required is significant; for illustration if we compare the starting material in the pyrolysate composition of the imine FVP versus the diethyl ester precursor FVP at 550 °C, we can see that there is approximately 40% starting material remaining in the imine pyrolysate compared to just about 2% in the diethyl ester case. This is a significant difference, and the imine needs a furnace temperature of 650 °C to achieve the same proportion.

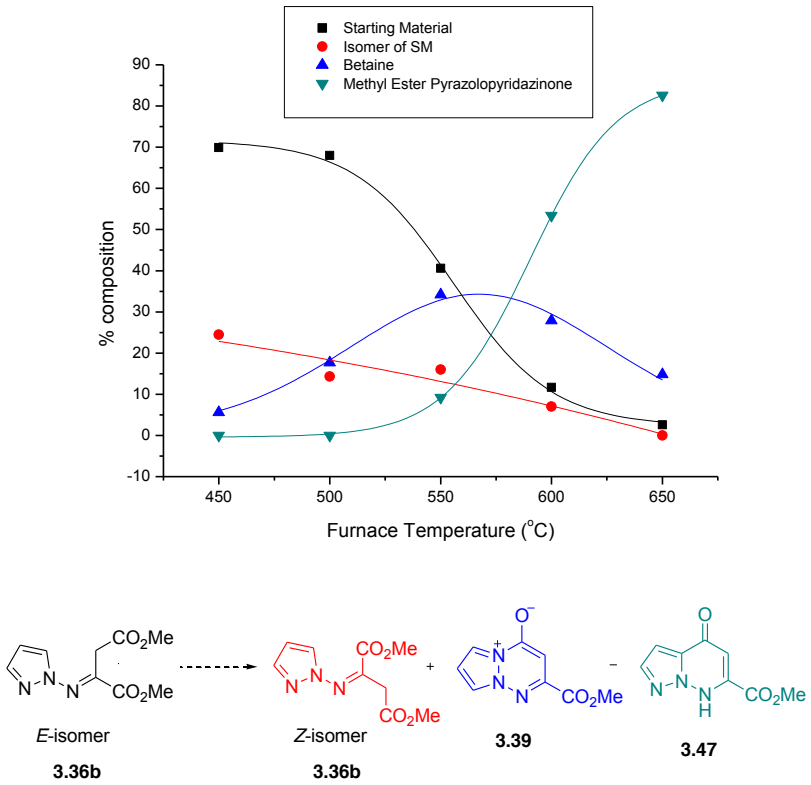

Figure 6: Temperature profile graph showing % composition of pyrolysate at varying furnace temperatures

By using the information from the temperature profile it was possible to choose suitable pyrolysis temperatures for preparative scale pyrolyses for both the betaine 3.39 and the pyrazolopyridazinone 3.47 (Scheme 25) with both being formed from the imidoylketene intermediate 3.46. The optimum furnace temperature chosen for the preparative pyrolysis of betaine 3.39 was determined to be 550 °C as this would allow the maximum proportion of betaine to be produced. After preparative pyrolysis and distillation of chloroform over the products, the residue remaining after removal of solvent was purified using dry flash chromatography to produce a sample of 2-methoxycarbonylprazolotriazinium-4-olate 3.39.

.

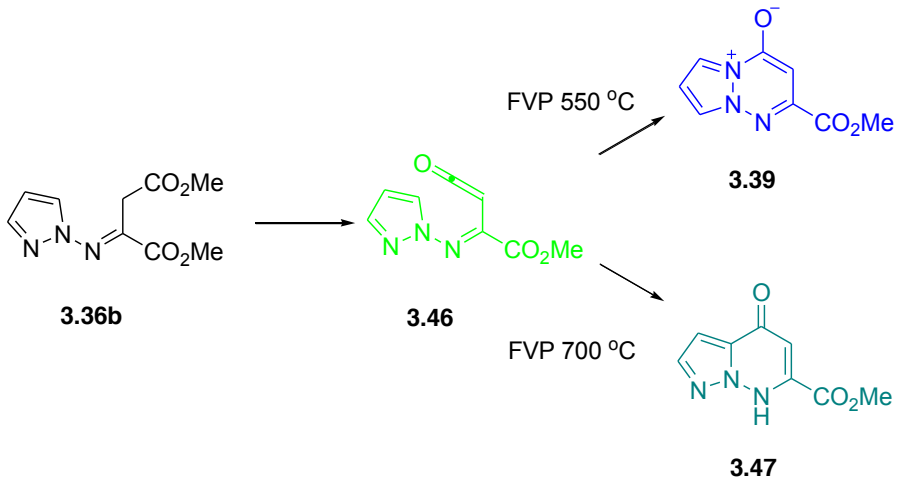

Scheme 25: Optimum pyrolysis conditions for preparation of betaine **3.39** and pyrazolopyridazinone **3.47**

The optimum furnace temperature for the preparative scale pyrolysis of the pyrazolopyridazinone 3.47 was decided to be 700 °C, as this would ensure all traces of starting material and betaine would be converted to the pyrazolopyridazinone, and there were no issues with possible decomposition, as the methyl ester is much more tolerant to high temperature FVP. The pyrolysate was then purified using dry flash chromatography to produce a pure sample of 2-ethylcarbonylpyrazolopyridazin-4-one 3.47 for analysis.

The final precursor of this type to be pyrolysed was the 3-(pyrazol-1-ylamino)-but-2-enoic acid methyl ester 3.37 and the resulting temperature profile is shown in Figure 7. The temperature profile graph illustrates the relationship between the betaine 3.40 and its corresponding pyrazolopyridazinone 3.49. It is apparent that there are some similarities to the previous imine example, in that the betaine again never predominates as the major product even at lower furnace temperatures and that the starting material is still present in the pyrolysate in significant amounts even after pyrolysis at 600 °C. This can again be attributed to the greater energy required to generate the imidoylketene intermediate, which appears to be a trend seen in these two precursors where a substituent is present on the carbon adjacent to the amine nitrogen.

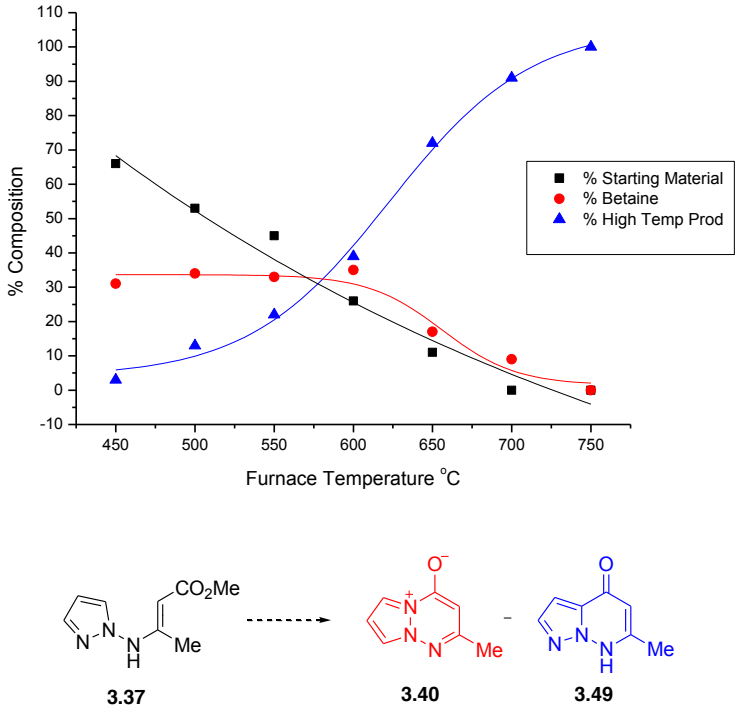

Figure 7: Temperature profile graph showing % composition of pyrolysate at varying furnace temperatures

By using the information from the temperature profile it was possible to choose suitable pyrolysis temperatures for preparative scale pyrolyses for both the betaine 3.40 and the pyrazolopyridazinone 3.49 (Scheme 26) with both being formed from the imidoylketene intermediate 3.48.

The optimum furnace temperature chosen for the preparative pyrolysis of betaine 3.39 was determined to be 600 °C as this would allow the maximum proportion of betaine to be produced with the minimum amount of starting material resent in the pyrolysate. It was found that the betaine was much harder to separate from residual starting material than from the pyrazolopyridazinone 3.49, and it proved to be impossible to achieve a pure sample of the 2-methylpyrazolotriazinium-4-olate 3.40.

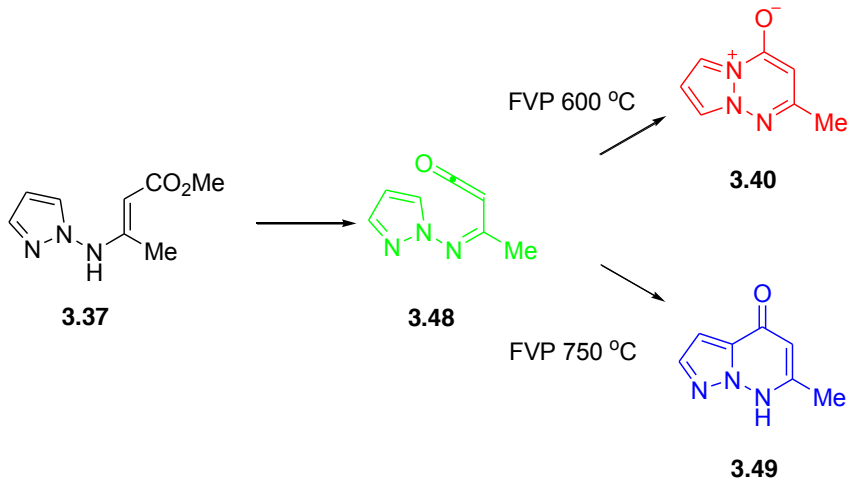

Scheme 26: Optimum pyrolysis conditions for preparation of betaine **3.40** and pyrazolopyridazinone **3.49**

The optimum furnace temperature for the preparative scale pyrolysis of the pyrazolopyridazinone 3.49 was decided to be 750 °C, as this would ensure the maximum conversion to the pyrazolopyridazinone, and again there were no issues with possible decomposition, as the methyl group is extremely tolerant of high temperature FVP. The pyrolysate was then purified using dry flash chromatography to produce a pure sample of 2-methylpyrazolopyridazin-4-one 3.49 for analysis.

3.3.3 DFT Calculations

DFT calculations were employed to model the energy surfaces for the cyclisations of the imidoylketenes to form the betaines and pyrazolopyridazinones. The calculations were performed at B3LYP/cc-pVDZ level and the energy surfaces obtained are discussed here.

The initial calculations were carried out on the parent system for the conversion of the ketene 3.9 to the betaine 3.10 and the pyrazolopyridazinone 3.11 as shown in Scheme 27.

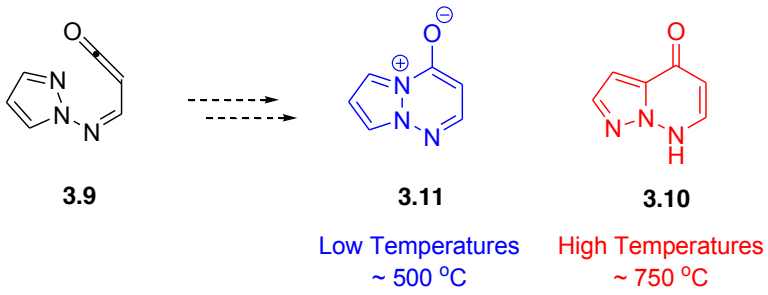

Scheme 27: Parent reaction – cyclisation of imidoylketene **3.9** to pyrazolopyridazinone **3.10** and betaine **3.11**

Pericyclic reactions can be defined as being concerted reactions that occur *via* cyclic transition states involving no distinct intermediates. All bond breaking and bond making take place simultaneously; pericyclic reactions are very different to stepwise reactions that involve intermediates. The formation of the betaine 3.11 is what can be referred to as a pseudopericyclic; that is that there is no 'mechanism' or intermediate for the betaine formation. This adheres to the definition of a pericyclic reaction; however there is no involvement of π electrons which is a prerequisite of pericyclic reactions such as electrocyclic ring closures and cycloaddition reactions. The psuedopericyclic nature of the betaine formation was confirmed by the reaction energy surface calculated, which is illustrated in Figure 8. Many possible

intermediates leading to the betaine were calculated, such as 3.50 where the ketene approaches the pyrazole nitrogen (Scheme 28), however the resulting structures were always the cyclised betaine 3.11. This shows that there is no energy barrier in place to the ketene to betaine cyclisation.

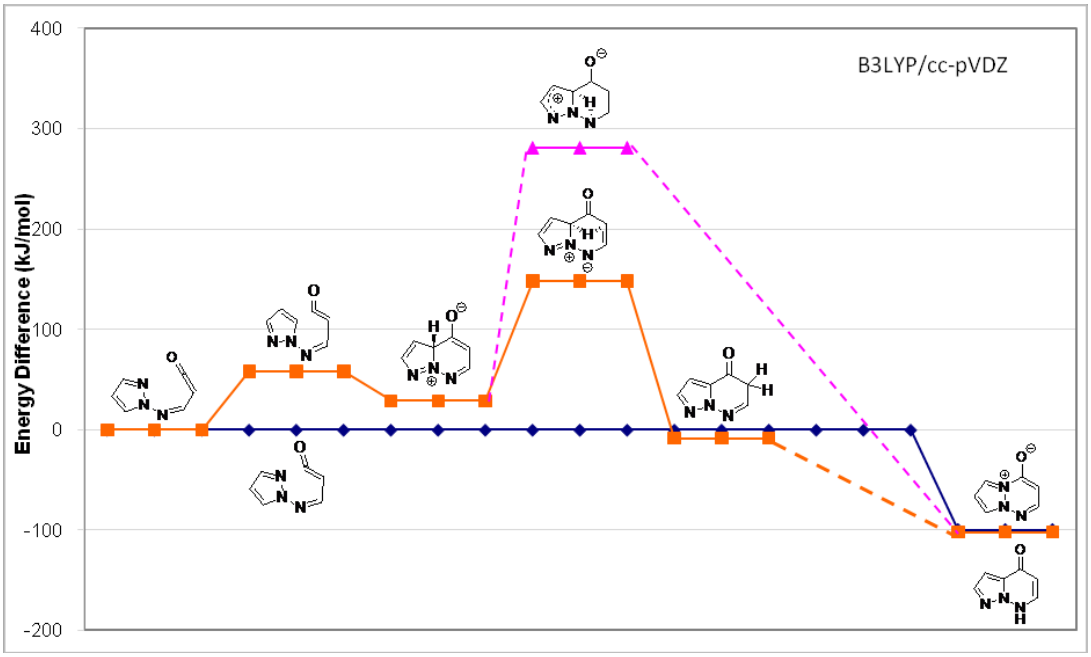

Figure 8: Energy surface calculated for formation of betaine **3.11** and pyrazolopyridazinone **3.10** from imidoylketene **3.9**

It was thought that there was a kinetic product versus thermodynamic product relationship between the betaine and pyrazolopyridazinone. This was because that as there was no activation barrier to the betaine formation it was the kinetic product and at higher furnace temperatures the imidoylketene could be regenerated from the betaine to then form the thermodynamically more stable pyrazolopyridazinone. DFT calculations have shown that the relative energy difference between the betaine and pyrazolopyridazinone is a mere 2.4 kJ mol^{-1}, therefore one can conclude that in this case it is not the stability of the final products that controls this reaction but the activation energy required to follow the reverse of the pyrazolopyridazinone pathway compared to the barrier-less collapse to form the betaine.

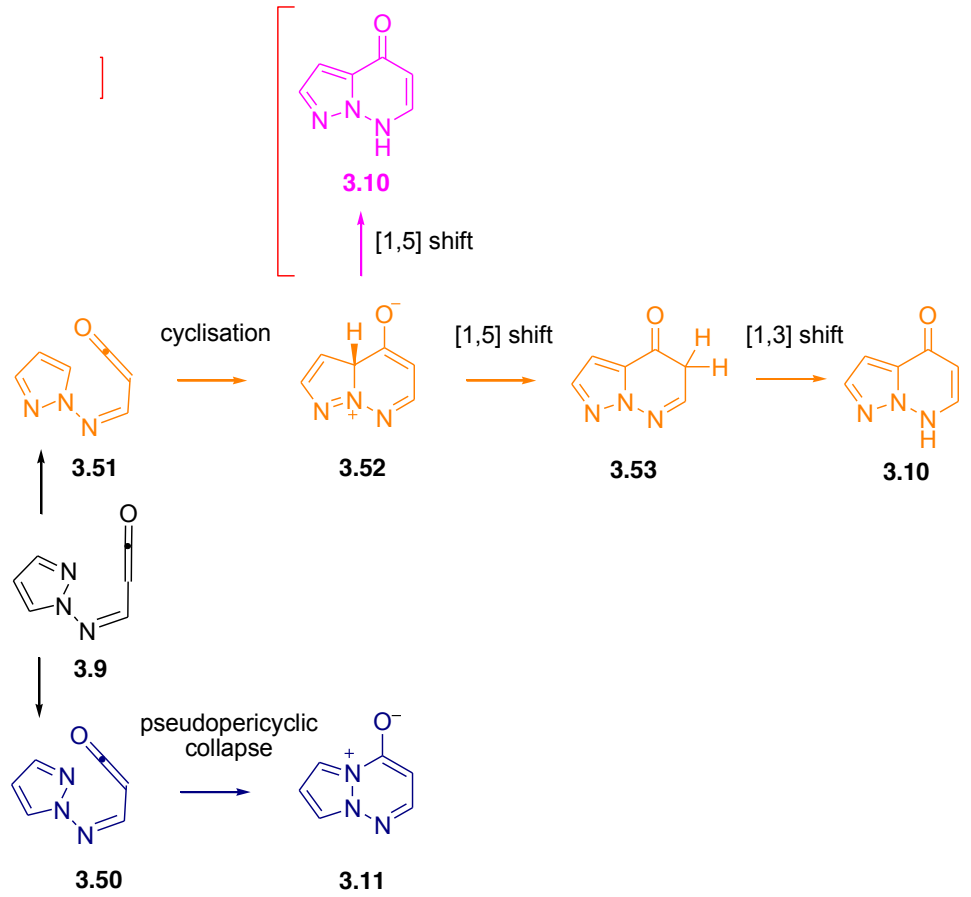

Scheme 28: Mechanisms for formation of betaine **3.11** and pyrazolopyridazinone **3.10** (colours correspond with energy surface Figure 3.8)

The formation of the pyrazolopyridazinone is *via* a completely different mechanism. Whereas at lower temperatures the betaine is predominately formed as there is no energy barrier to its formation (the blue surface, Figure 3.8), at higher furnace temperatures the system has sufficient energy to overcome the small barrier seen to form the cyclic intermediate 3.52 from the transition state 3.51. From here there were two possible routes to the pyrazolopyridazinone envisioned; either a direct [1,5] hydrogen shift to the pyidazinone nitrogen and re-aromatisation to 3.10 as shown by the pink surface of Figure 3.8 and in Scheme 28, or a [1,5] hydrogen shift in the opposite direction to form the second intermediate 3.53, followed by a subsequent

[1,3] hydrogen shift. The [1,3] shift is disallowed suprafacially and is not geometrically possible antarafacially by a intramolecular mechanism for this ring system. However it is known that disallowed shifts may occur *via* intermolecular mechanisms, for example as suggested by Wentrup [10] who proposes that this may happen after the condensation of product into the solid phase. These intermolecular mechanisms are not calculable by these DFT methods. The energy surfaces calculated have shown that the most likely is the orange pathway involving two subsequent hydrogen shifts, as the pink pathway has an activation energy that is approximately 130 kJ mol^{-1} greater.

DFT calculations were also used to map the energy surfaces of the cyclisations of ketenes 3.46 (from the imine precursor 3.36b) and 3.48 (from the methyl substituted precursor 3.37) as pyrolysis of these produced temperature profiles that showed the betaine was never the predominant product. Both were also substituted at the same position and it was hoped that DFT calculations may explain if this was a significant factor.

The energy surface calculated for the conversion of ketene 3.46 to the betaine 3.39 and pyrazolopyridazinone 3.47 is shown in Figure 9.

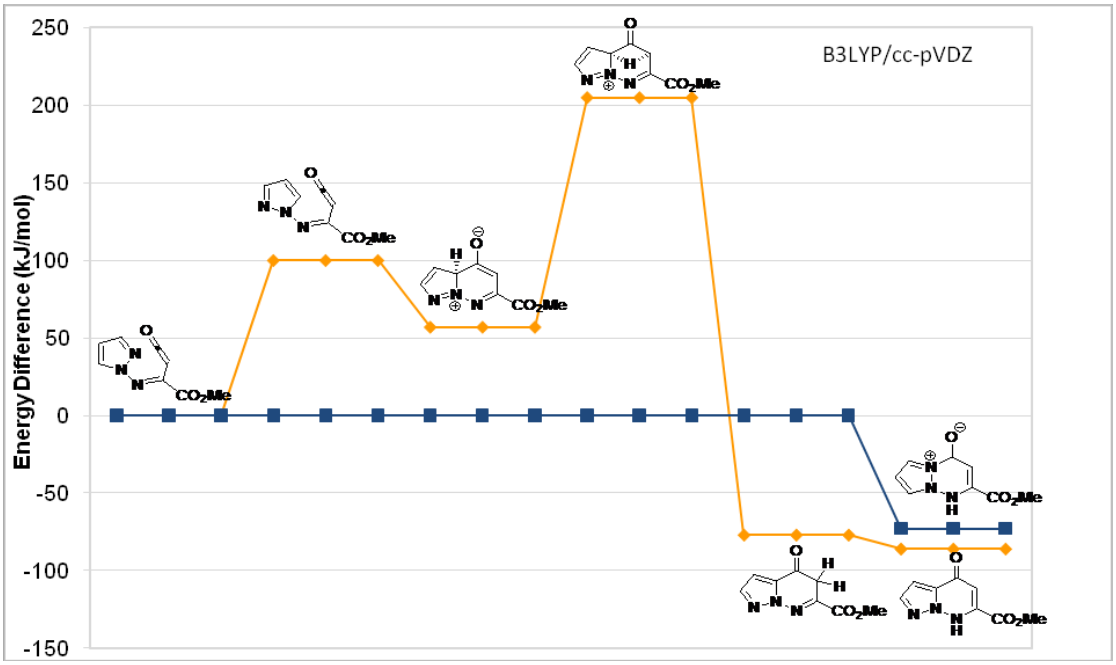

Figure 9: Energy surface calculated for formation of betaine **3.39** and pyrazolopyridazinone **3.47** from imidoylketene **3.46**

It is clear from Figure 3.9 that the same general shape as seen for the parent reaction is evident in the cyclisations of imidoylketene 3.46. The relative energy difference between the betaine and the pyrazolopyridazinone is greater in this example (13 kJ mol^{-1}), but this would not decrease the amount of betaine seen throughout the temperature profile, indeed the bigger gap would make the betaine a more definite kinetic product in relation to the pyrazolopyridazinone thus increasing its prevelence. The activation energies required for the formation of the intermediates 3.56 and 3.57 (Scheme 29) are both approximately 50 kJ mol^{-1} more than those of the parent reaction, which would suggest that greater temperatures would possibly need to be employed to afford conversion to 3.47 allowing betaine 3.39 to be present in pyrolysates from FVP at higher temperatures than expected. The converse was found, with the betaine never making up more than 35% of the pyrolysate. All this evidence suggests that the kinetic-thermodynamic relationship between the betaine and pyrazolopyridazinone is of no consequence in this case. A more plausible explanation of the results would be that it is the generation of the imidoylketene 3.46

which dictates the temperature profile, as it requires a much greater energy to be generated from the imine precursor, as is evident by its persistence in the pyrolysate even after FVP at 650 °C.

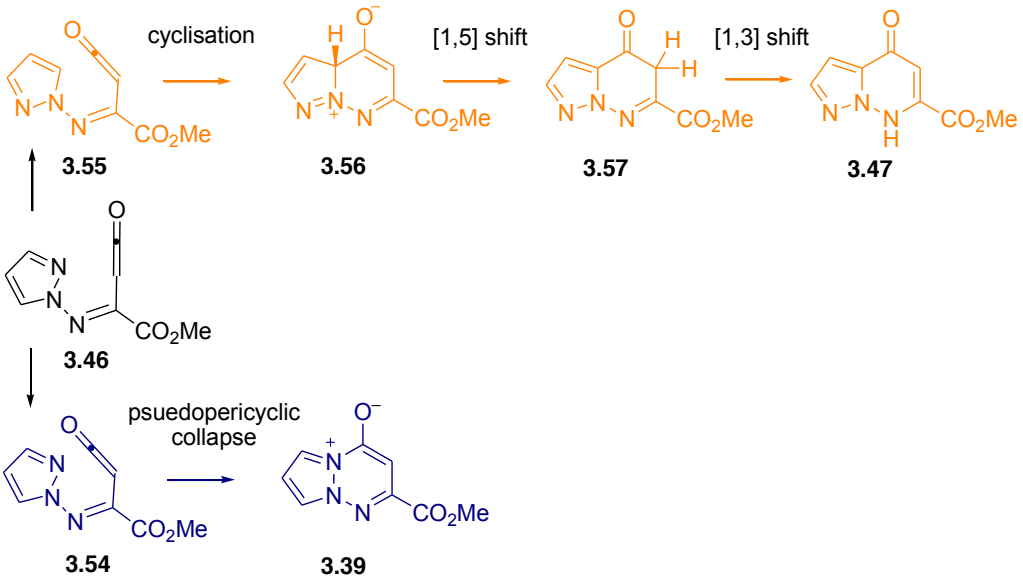

Scheme 29: Mechanisms for formation of betaine **3.39** and pyrazolopyridazinone **3.47** (colours correspond with energy surface Figure 3.9)

The energy surface calculated for the conversion of ketene 3.48 to the betaine 3.40 and pyrazolopyridazinone 3.49 is shown in Figure 10.

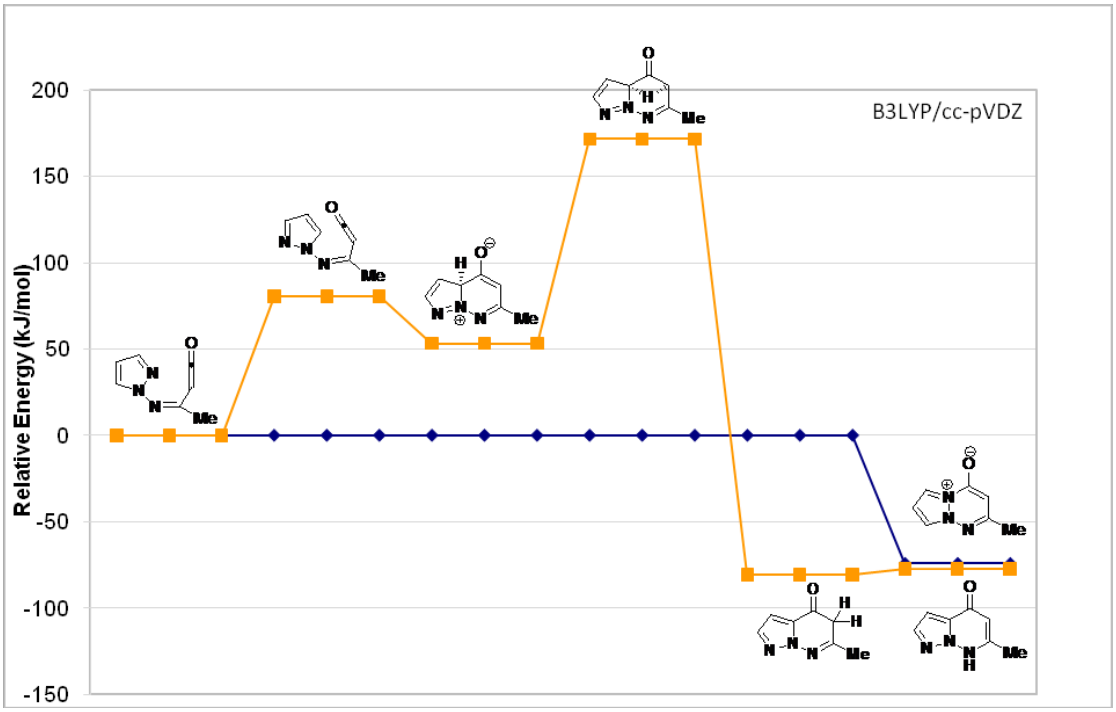

Figure 10: Energy surface calculated for formation of betaine **3.40** and pyrazolopyridazinone **3.49** from imidoylketene **3.48**

It can be seen from Figure 10 that the same general shape is again evident in the cyclisations of imidoylketene 3.48. The transition state 3.58 (Scheme 30) collapses to the betaine 3.40 with no energy barrier and the energy barriers to the formation of the intermediates 3.60 and 3.61 are of a similar magnitude to those in the parent energy profile The relative energy difference between the betaine and pyrazolopyridazinone is again very small (3 kJ mol^{-1}). This is another example of the energy surface obeying the general trend yet this not being reflected in the temperature profile produced. Again this is attributed to the greater temperatures required to generate the imidoylketene 3.48.

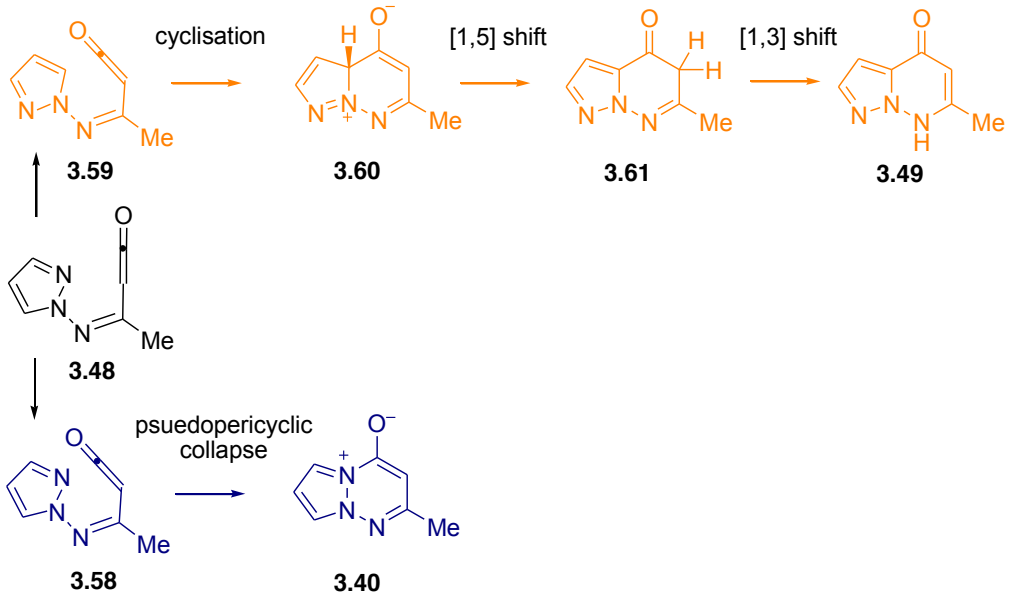

Scheme 30: Mechanisms for formation of betaine **3.40** and pyrazolopyridazinone **3.49** (colours correspond with energy surface Figure 3.10)

3.3.4 Conclusions

It has been shown that substitutions to the pyrazole ring do not alter the FVP temperature profile and that both the betaine and pyrazolopyridazinone products are achievable. It has also been shown that substituents may be incorporated around the pyridazinone ring by the use of acrylic ester type precursors which can generate the same imidoylketene as Meldrum's acid derivative precursors. This method has successfully been used to include substitutents at the 2- and 3- positions within the resulting betaine and pyrazolopyridazinone structures. Precursors used to incorporate substituents at the 2- position require a far greater pyrolysis temperature to generate the required imidoylketene than those acrylic ester precursors used to include substituents at the 3- position; however isolation of the corresponding betaine and pyrazolopyridazinone compounds are achievable.

3.4 Extending Investigations into Pyrazolylketene generation and Cyclisations

The following work was carried out by P. J. J. Thomson as part of his undergraduate final year research project under the supervision of Prof. H. McNab and myself. It is reported here with kind permission of P. J. J. Thomson.

3.4.1 Introduction

The previous work has shown that an imidolylketene substituent generated from either a Meldrum's acid derivative or an acrylic ester can cyclise at two positions on a pyrazole ring to give either a pyrazolotriazinium-4-olate (betaine) or a pyrazolopyridazinone, two new 5,6-fused heterocyclic ring systems. It was thought that this method could possibly be extended to introduce a third ring into the structure. The precedence for this comes from previous work [11] where ketenes of type 3.63 have been generated from the elimination of methanol from the FVP of anthranilic acid derivatives of the type 3.62 (Scheme 31) and cyclise to the acridone 3.64.

This provided the basis for the proposal that if a pyrazolylketene such as 3.65a (Scheme 31) could be generated, if it followed the model established previously in this chapter, there existed the potential to expand the system to three rings, resulting in the new betaine arrangement 3.66 and pyrazoloquinazolinone type structure 3.67.

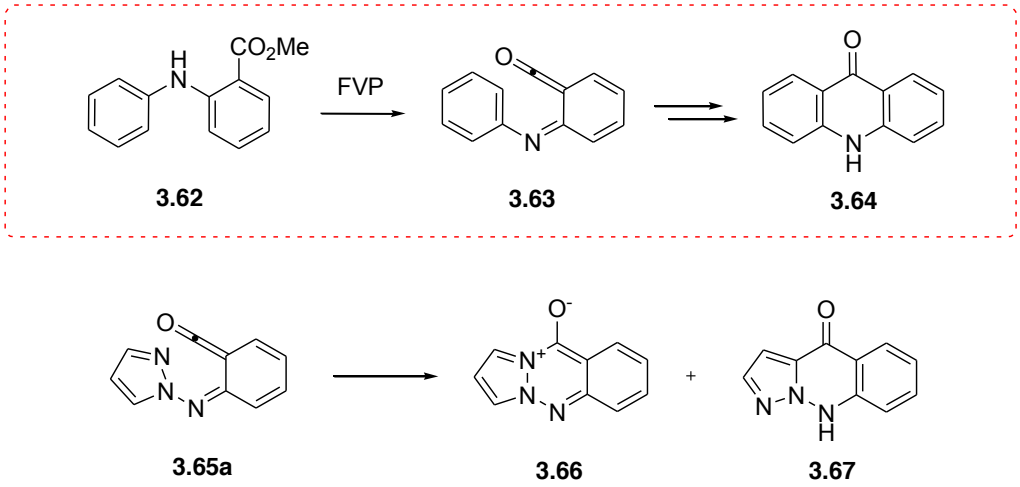

Scheme 31: Precedent for and demonstration of proposed pyrazolylketene system and resultant ring systems

A similar type of mechanism would take place for the pyrazolylketene cyclisations as was previously seen. The precursor 3.68 would eliminate methanol under FVP conditions to form the pyrazolylketene 3.65a which at lower furnace temperatures would collapse to the betaine structure 3.66 (Scheme 32). At higher furnace temperatures rotational isomerisation could occur to form the pyrazolylketene 3.65b which could cyclise and following subsequent hydrogen shifts, form the product 3.67.

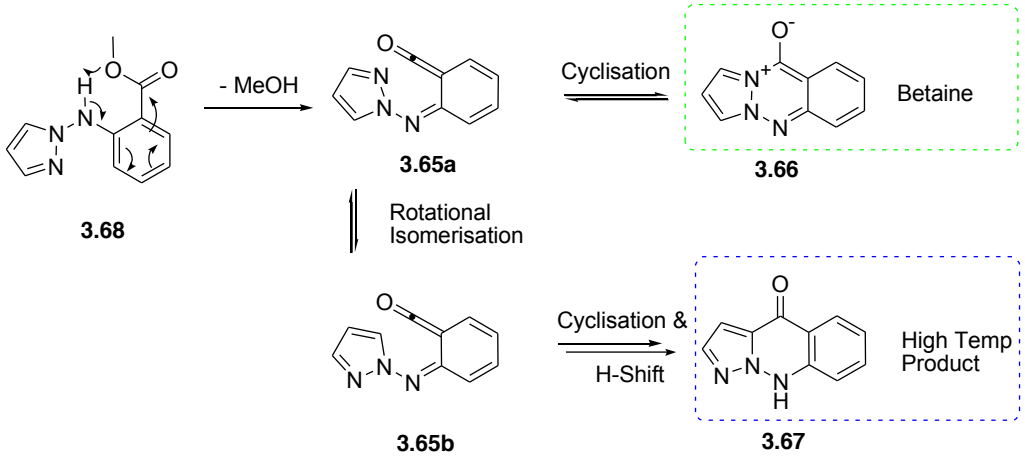

Scheme 32: Proposed mechanism for pyrazolylketene cyclisations and products

3.4.2 Synthesis of Precursors

Synthesis of the required precursor 3.68 was developed from test reactions using 4-amino-1,2,4-triazole as this is a commercially available reagent and would serve as a good model for the *N*-aminopyrazole without consuming large quantities of a regent which requires preparation. It was concluded that reaction of the *N*-amino heterocycle with 2-chlorobenzoic acid and subsequent esterification would be the most direct route to the desired precursors utilising the optimised *N*-amination of pyrazole. Initially there was no success with either nucleophilic aromatic substitution reactions or metal-mediated coupling reactions, however a successful coupling reaction was achieved using a method originally utilised for alkyl amines (Scheme 33). These conditions were developed by Wolf *et al*[12] using copper/copper oxide and successfully produced the acid 3.69. This was then esterified to the triazole precursor 3.70.

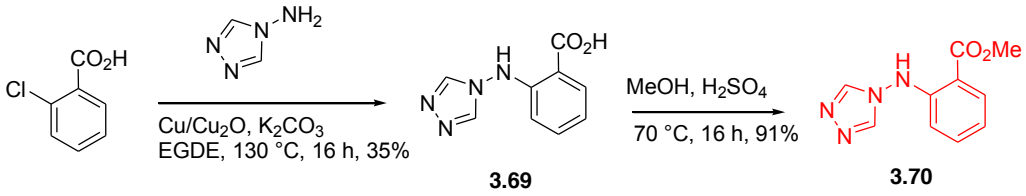

3.69 **3.70**

32% Overall Yield

Scheme 33: Coupling conditions to produce **3.69** and esterification to precursor **3.70**

This technique was then applied to the *N*-aminopyrazole, however attempts to isolate the coupled acid intermediate were unsuccessful. To remedy this the crude acid was esterified *in situ* and the resulting product purified using dry flash chromatography to yield the pyrazole precursor 3.68 (Scheme 34).

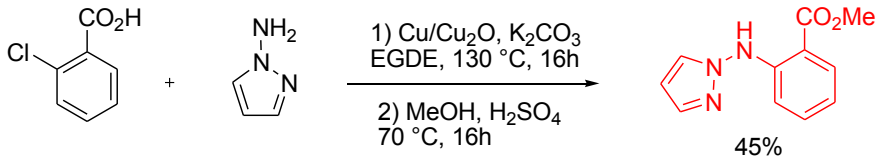

3.68

Scheme 34: Combined coupling and esterification conditions for synthesis of precursor **3.68**

3.4.3 Pyrolysis of Triazole Precursor

Compound 3.70 is a valid FVP precursor in its own right; therefore its pyrolysis was attempted. It was known that no betaine type structure would be possible, however its 'high temperature' product would be. After pyrolysis at 650 °C, and subsequent distillation of chloroform over the pyrolysate, the remaining solid was removed and discovered to be the expected cyclised product 3.71 (Scheme 35). The chloroform distillate revealed only starting material and substantial decomposition products upon analysis.

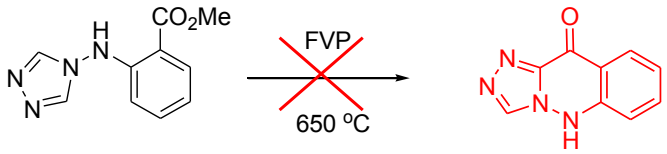

3.70 **3.71**

Scheme 35: Pyrolysis of triazole precursor **3.70**

During pyrolysis a significant pressure increase was noted; showing that a gas is produced which cannot be condensed by the liquid nitrogen trap. When examining the possible mechanism of the cyclisation (Scheme 36) a possible explanation was discovered to explain this observation. When the triazolylketene 3.72 cyclises onto the triazole carbon it forms the intermediate 3.73. This intermediate contains a N=N bond, which has been noted during previous work [13] of being capable of eliminating N_2 at furnace temperatures in excess of 650 °C and would hence explain the increase in pressure.

3.72 **3.73** **3.71**

Scheme 36: Mechanism for cyclisation of ketene **3.72**

3.4.4 Pyrolysis of Pyrazole Precursor

The pyrazole precursor 3.68 was subjected to small scale pyrolyses and the resulting temperature profile is shown in Figure 11. The temperature profile experiments revealed that there were two different products of the pyrolyses; the expected high temperature product 3.67 and an isomer whose structure was initially unknown. The temperature profile also shows that the starting material was the main product until pyrolysis temperatures of 700 °C. As previously discussed this is probably due to the

greater amount of energy required to generate the ketene 3.74 (Scheme 37) from the starting material. The effect is even more pronounced in this case as the generation of the ketene requires breaking the aromaticity of the benzene ring, which would require an even greater amount of energy than the acyclic cases discussed previously.

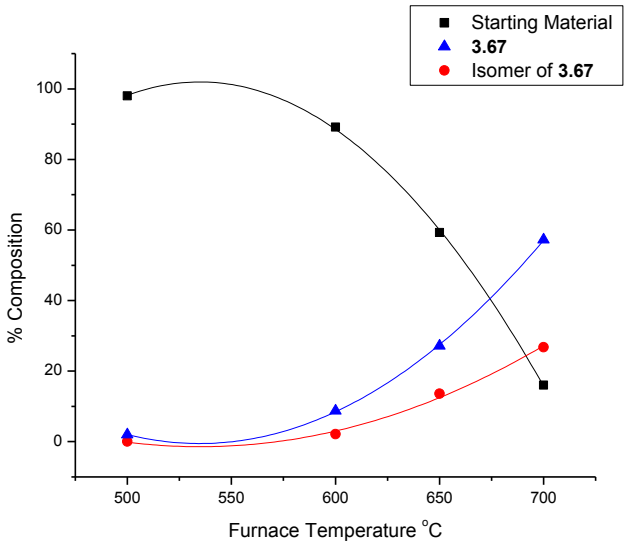

Figure 11: Temperature profile graph showing % composition of pyrolysate at varying furnace temperatures

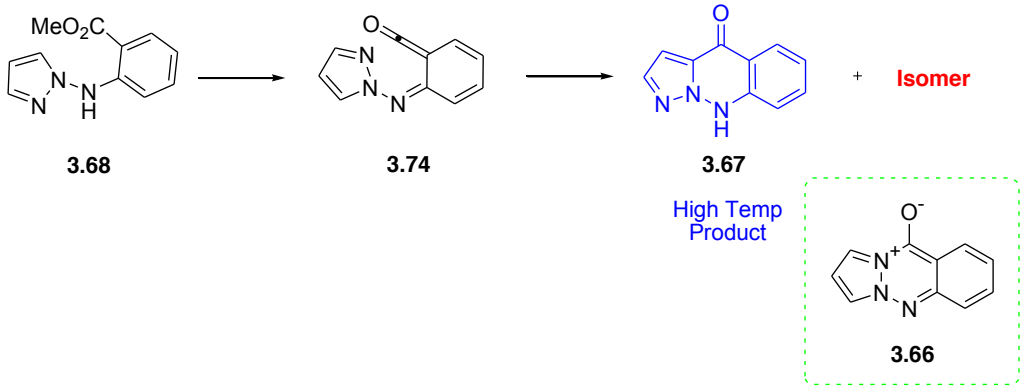

Scheme 37: Pyrolysis of pyrazole precursor **3.68**

To fully characterise the high temperature product 3.67 and to deduce the identity of the unknown isomer a preparative FVP at a furnace temperature of 700 °C was carried out. This temperature was chosen as it produced the greatest quantity of products to starting material according to the temperature profile. After FVP the pyrolysate was initially purified by distillation with chloroform; the remaining solid was found to be a 1:1 mixture of the product 3.67 and the unknown isomer. This mixture was purified by trituration with DCM to yield a pure sample of the unknown isomer. Analysis showed that this could not be the betaine, as this would require seven proton signals in its ^{1}H NMR spectrum, and this unknown isomer contained only six. The DCM mother liquor was purified by dry flash chromatography to obtain a pure sample of the product 3.67.

Both the expected product 3.67 and the isomer contained the same pattern of proton peaks in their ^{1}H NMR spectra (Figure 3.12); four related aromatic peaks and two distinctive pyrazole doublets where ^{3}J = 2 Hz. Scheme 38 outlines all possible isomers of this system containing the pyrazole moiety, and only two fit the proton patterns observed as shown in Figure 12; the expected product 3.67 and the isomer 3.75.

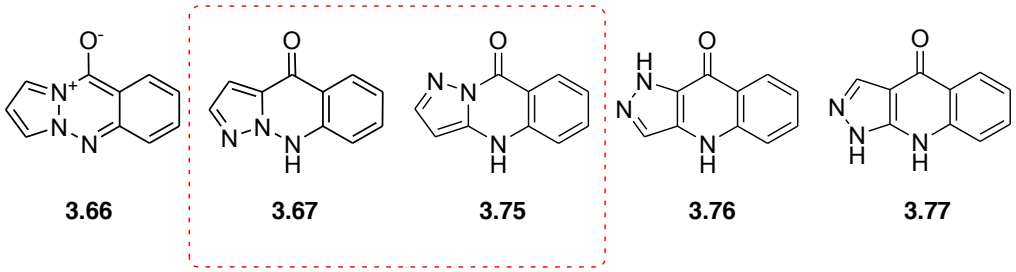

Scheme 38: Plausible isomers containing pyrazole ring

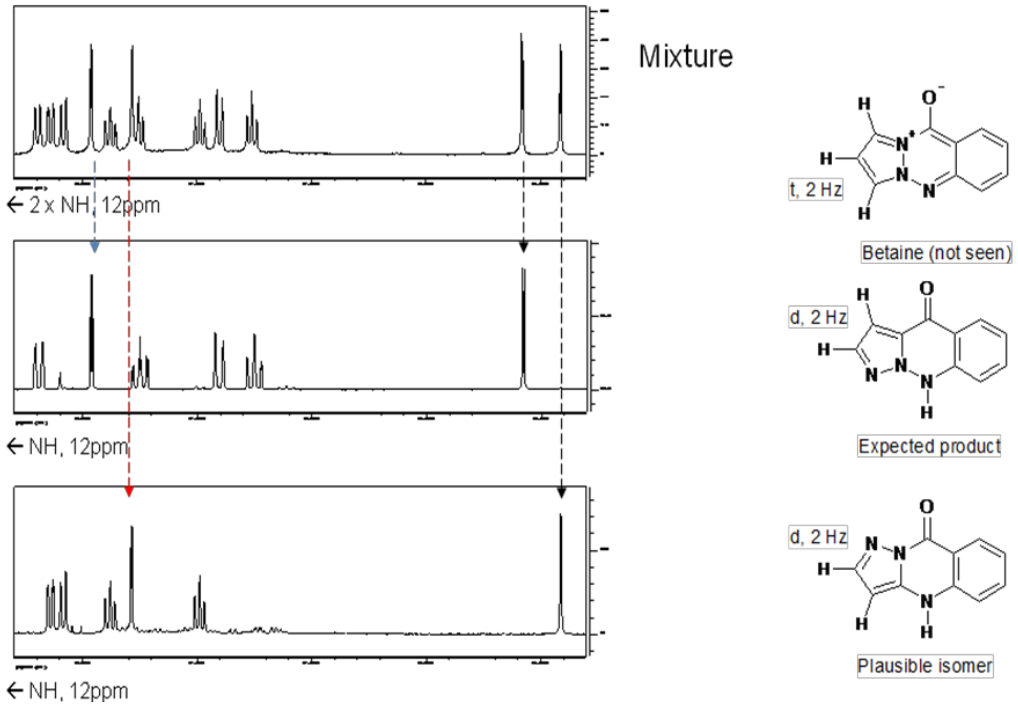

Figure 12: ^{1}H NMR spectrum of the mixture of products compared to the spectra of the product **3.67** and unknown respectively

To confirm that the isomer was in fact 3.75 an authentic sample was prepared. It can be found in the literature [14] however no NMR data has been reported. Isomer 3.75 was synthesised *via* the route shown in Scheme 39, and confirmed that it was formed in the pyrolysis of 3.68.

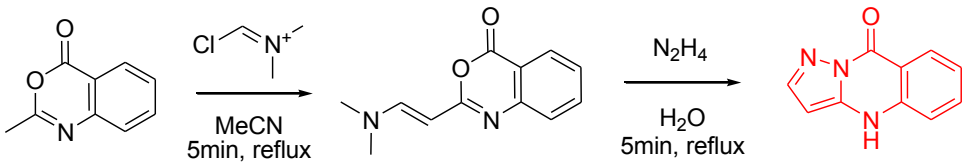

3.75

6% overall yield

Scheme 39: Synthesis of authentic sample of **3.75**

3.4.5 DFT Calculations and Possible Mechanisms

In the same way that DFT calculations were employed to map the energy surface for the parent reaction and some substituted examples, so they were used for this pyrazolylketene example too. The resulting energy surface is shown in Figure 13.

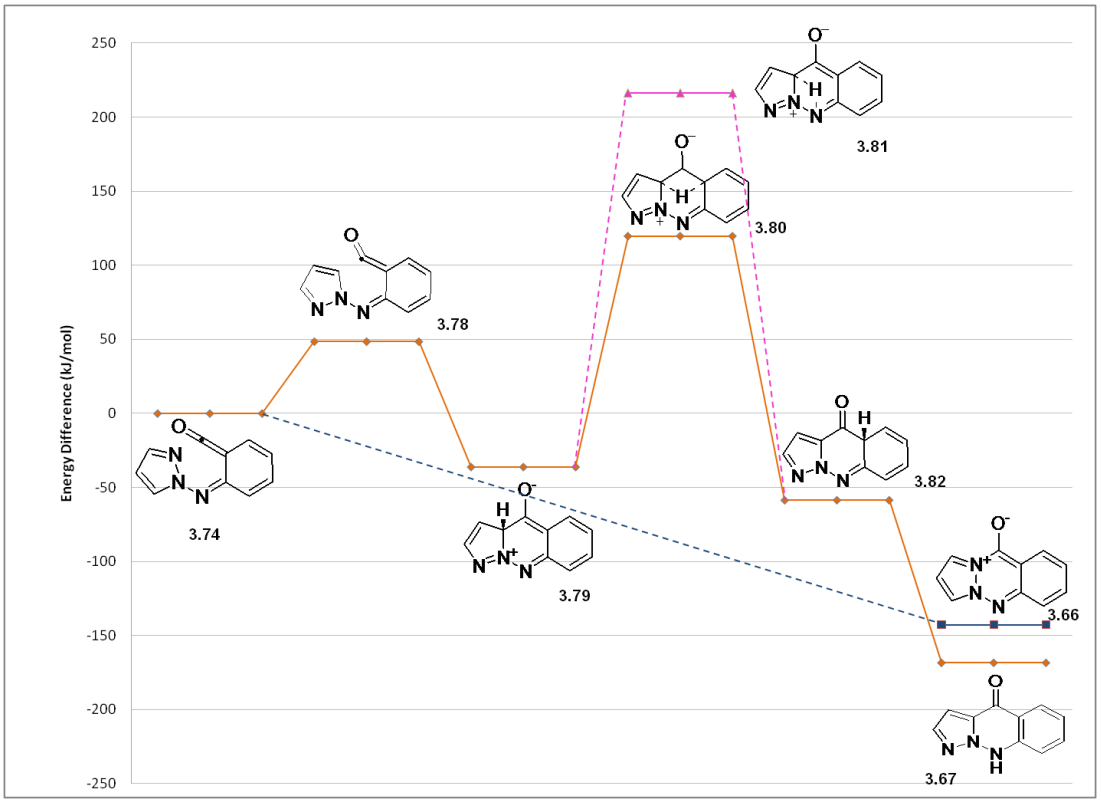

Figure 13: Energy surface from DFT calculations for collapse of ketene **3.74**

It can be seen that the general shape of the energy surface is consistent with the parent reaction without the extra ring and that its presence does not change the relative positions of any of the intermediates or transition states. The transition states 3.78 and 3.80 are of comparable value to the parent surface, and again the direct [1,5] H-shift transition state 3.81 is of a significantly higher energy. The same kinetic versus thermodynamic relationship between the betaine 3.66 and

pyrazoloquinazolinone 3.67 exists; however, as the generation of the ketene requires breaking the aromaticity of the ring, much higher furnace temperatures are required and hence the betaine is not observed. This mechanism does not explain the appearance of the isomeric product 3.75 so a different mechanism was required.

It has been proposed that the collapse of ketene 3.74 may in fact progress *via* the spirocyclic intermediate 3.83 (Scheme 40). The precedence for this is outlined in the red box of Scheme 40, the original work on the parent betaine system [5] proposed that there were two possible products from the collapse of the ketene; the betaine observed or the spirocyclic structure 3.84. This structure 3.84 in turn was believed to be possible as earlier work [15] on the thermolysis of 3.85 had shown that the intermediate 3.86 could be isolated before it went on to produce other products.

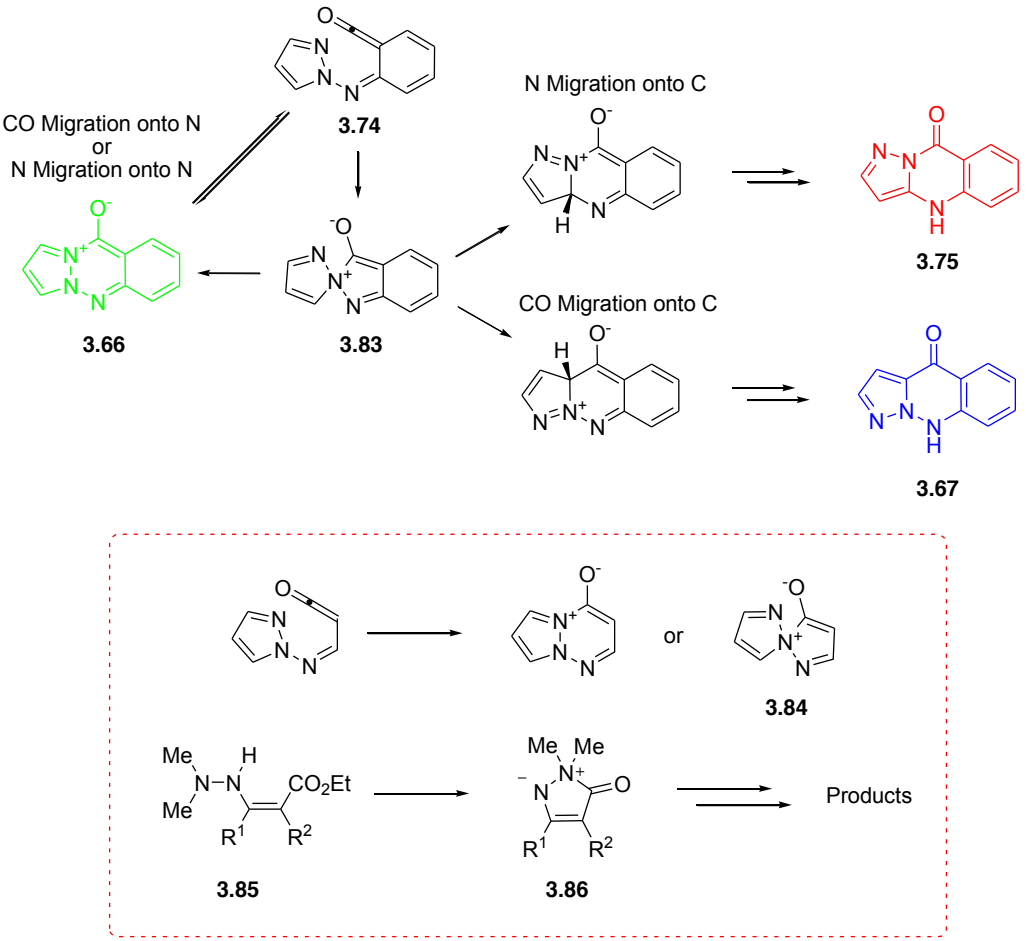

Scheme 40: New proposed mechanism and precedent from which it was developed

This spirocyclic intermediate could produce the betaine 3.66 by migration of the C=O or the amine nitrogen onto the pyrazole nitrogen, but as we have already established this betaine is then capable of regenerating the ketene 3.74 which can then go onto produce other more thermodynamically stable products. There has never been any evidence of the betaine in the pyrolysates but as previously mentioned this is most probably due to the furnace temperatures required to form the ketene 3.74 in the first place.

The spirocyclic intermediate 3.83 is also capable of undergoing two further transformations; migration of the C=O to the adjacent pyrazole carbon which after rearomatisation will result in the expected product 3.67, and migration of the amine nitrogen to the adjacent pyrazole carbon which again after rearomatisation will result in the unexpected product 3.75 we discovered in the pyrolysate. This mechanism therefore explains the products we observe from the pyrolyses; DFT modelling is currently in progress on this mechanism to discover if it is energetically sound.

3.4.6 Conclusions

Pyrolysis of the triazole precursor 3.70 has been shown to produce 5*H*-1,2,4-triazolo[4,3-*b*]cinnolin-10-one 3.71, which was initially thought to be unlikely due to elimination of N_2 in the pyrolysis intermediate. Pyrolysis of the pyrazole precursor 3.68 has been shown to produce two products; the expected product 3a,9-dihydro-1,9,9a-triazacyclopenta[*b*]naphthalen-4-one 3.67 and the isomeric pyrazolo[5,1-*b*]quinazolin-9(4*H*)-one 3.75. Mechanisms to explain the appearance of 3.75 have been suggested, but more work and DFT calculations are needed to confirm these.

3.5 Extending Investigations into the Indazole Ring System

The previous section described how the ring system was expanded to contain an extra ring on the ketene side, however some issues were encountered here as the ketene was only generated at high furnace temperatures due to it requiring the breaking of aromaticity in the benzene ring. However, it was thought that extending into the indazole ring system would be a much more straightforward approach, as *N*-aminoindazoles could be reacted with MMMA in an analogous way to *N*-aminopyrazole. An overview of the initial plan of the indazole work is shown in Scheme 41.

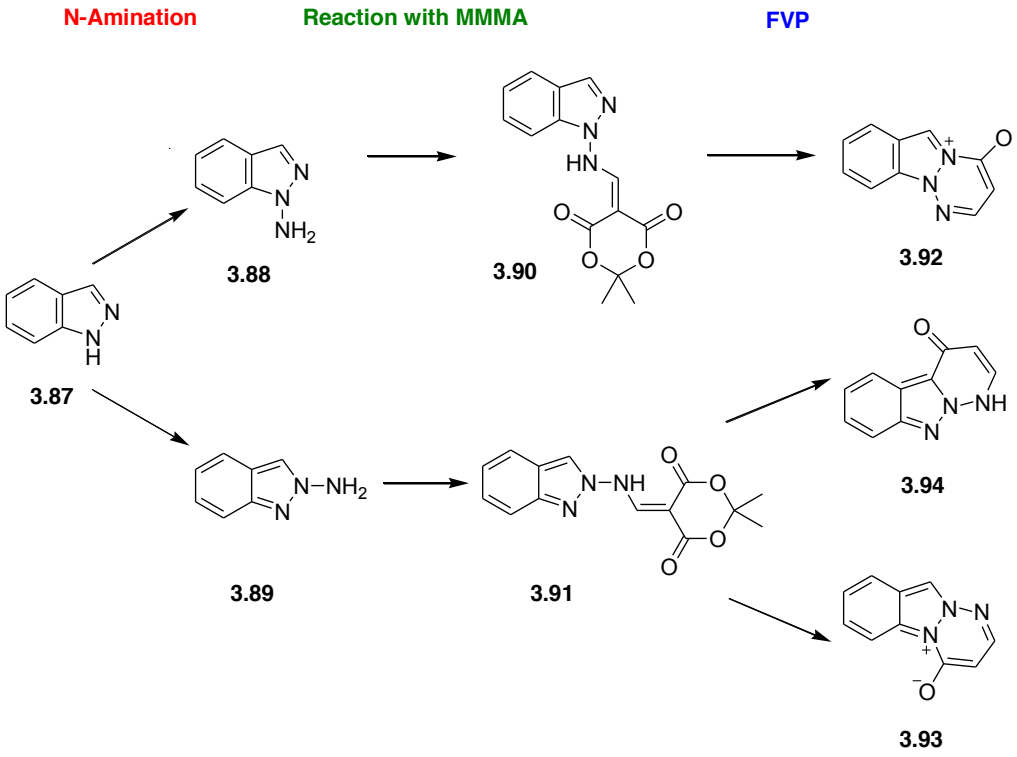

Scheme 41: Overview of initial plans to extend work into the indazole ring system

The primary target would be the known *N*-amination of indazole 3.87 followed by separation of the two resulting isomers, 1-aminoindazole 3.88 and 2-aminoindazole 3.89. Once separated, each would be reacted with MMMA to afford the 1- and 2-

substituted precursors 3.90 and 3.91 respectively. Pyrolysis of the 1-substituted precursor 3.90 at furnace temperatures of approximately 500 °C was hoped to give the betaine structure 3.92, a new heterocyclic mesomeric betaine system. Pyrolysis of the 2-substituted precursor 3.91 at similar furnace temperatures was expected to produce the betaine structure 3.93, again another new betaine ring system. Pyrolysis of the 2-substituted precursor at higher furnace temperatures is likely to provide the indazolopyridazinone 3.94.

3.5.1 Synthesis of Precursors

The first step in the precursor synthesis was the *N*-amination of the indazole 3.87. This method had already been reported in the literature [16] and was similar to the *N*-amination general method 3 used in the previous chapter (Scheme 42). The indazole was suspended in an aqueous solution of sodium hydroxide and heated to 55 °C, and then ethanol was added dropwise until a complete solution was achieved. The reaction solution was held at this temperature while the HOSA was added portionwsie with vigourous stirring over thirty minutes to minimise the amount of foaming then the solution stirred at room temperature for an hour before work up. The resulting solid was found to be the desired *N*-aminoindazole isomers in approximately a 1:1 ratio.

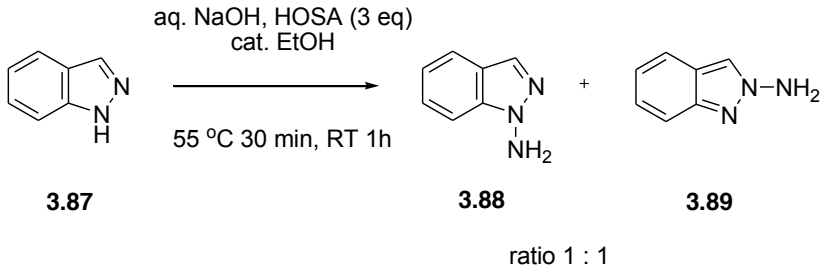

3.87 **3.88** **3.89**

ratio 1 : 1

Scheme 42: Reaction conditions for the *N*-amination of indazole **3.87**

The literature [16] indicates that separation of the isomers can be achieved by column chromatography, however when this was attempted following the conditions indicated neither isomer was separated from the mixture. It was discovered however that a single isomer could be attained *via* two subsequent recrystallisations from toluene. However the other isomer could not be recovered as a pure product; solid recovered from the recrystallisation liquor always contained the other isomer as well as other products and despite many attempts using different methods a satisfactorily pure sample was not obtained.

The pure isomer that was obtained was originally believed to be the 2-aminoindazole **3.89** from the spectral information compared with the original literature [16]. However, a crystal structure of this isomer was obtained (Figure 3.14) which clearly demonstrates that this is not the case.

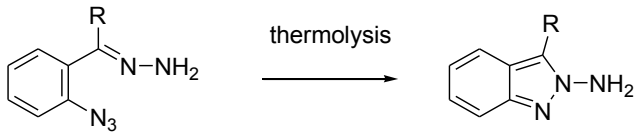

Scheme 43: Proposed route to authentic sample of 2-aminoindazole

On further investigation into the literature, a similar synthesis for 2-aminoindazole was found [17] by Anselme and Sakai, and is illustrated in Scheme 44, however only a melting point and CHN analysis data are given. Another reference [18] was found with a variation on this synthesis, but only quotes the reference to the Anselme and Sakai paper saying that the product was identical to that prepared *via* their route.

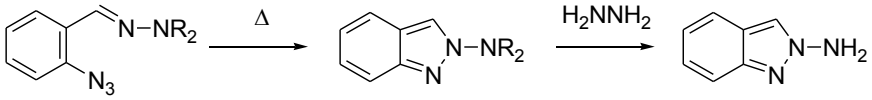

3.89

Scheme 44: Proposed synthesis of 2-aminoindazole by Anselme and Sakai

As good crystal data has been achieved which shows that the NMR data quoted in the original paper [16] has the isomers mis-assigned and no further NMR data is

available in the literature, the data set out in this work will be considered accurate. Therefore the pure isomer obtained is determined to be 1-aminoindazole **3.88**.

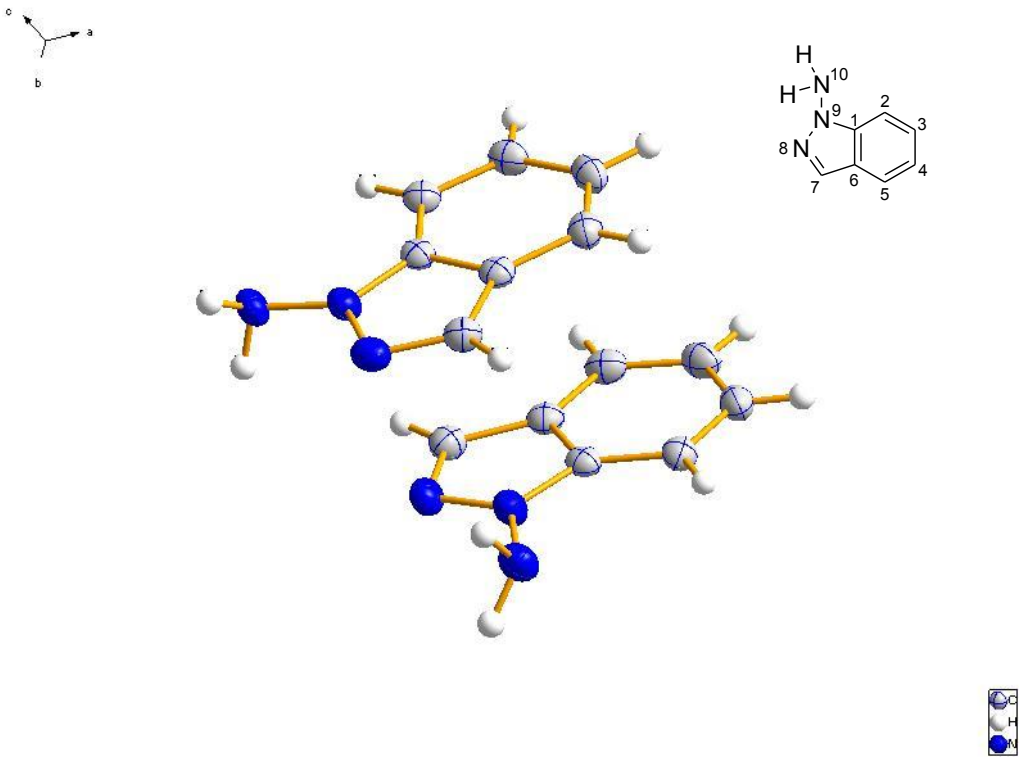

Atoms 1,2	d 1,2 [Å]	Atoms 1,2	d 1,2 [Å]
C1A—N9A	1.3611(19)	C1B—N9B	1.3573(18)
C1A—C2A	1.399(2)	C1B—C2B	1.401(2)
C1A—C6A	1.403(2)	C1B—C6B	1.407(2)
C2A—C3A	1.375(2)	C2B—C3B	1.373(2)
C2A—H2A	0.9500	C2B—H2B	0.9500
C3A—C4A	1.410(2)	C3B—C4B	1.413(2)
C3A—H3A	0.9500	C3B—H3B	0.9500
C4A—C5A	1.378(2)	C4B—C5B	1.370(2)
C4A—H4A	0.9500	C4B—H4B	0.9500
C5A—C6A	1.409(2)	C5B—C6B	1.408(2)
C5A—H5A	0.9500	C5B—H5B	0.9500
C6A—C7A	1.420(2)	C6B—C7B	1.419(2)
C7A—N8A	1.326(2)	C7B—N8B	1.332(2)
C7A—H7A	0.9500	C7B—H7B	0.9500
N8A—N9A	1.3656(18)	N8B—N9B	1.3595(18)
N9A—N10A	1.3926(18)	N9B—N10B	1.3959(18)
N10A—H10A	0.95(2)	N10B—H10C	0.918(19)
N10A—H10B	0.91(2)	N10B—H10D	0.91(2)

Figure 14: Crystal structure and bond length data for 1-aminoindazole **3.88**

This pure 1-aminoindazole was then reacted with methoxymethylene Medrum's acid (MMMA) under the standards conditions set out previously in this chapter (Scheme 45) to afford the 1-substituted FVP precursor 3.90.

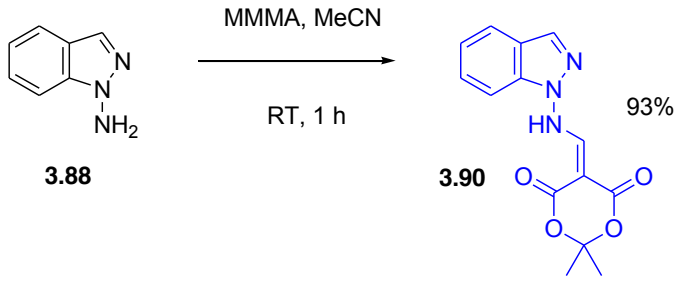

Scheme 45: Synthesis of 1-substituted indazole precursor **3.90**

As a pure sample of the 2-aminoindazole had not been obtained, the MMMA reaction was attempted on the 1:1 mixture of isomers initially produced from the *N*-amination of indazole (Scheme 46). It was hoped that by forming the MMMA derivatives that the two isomeric products would then be easier to separate. This was attempted, and after an hour at room temperature a precipitate had formed. This was filtered off and was shown by ^{1}H NMR spectroscopy to be the 2-substituted MMMA derivative 3.91. This was extremely fortuitous and resulted in a pure sample in sufficient quantity for pyrolysis.

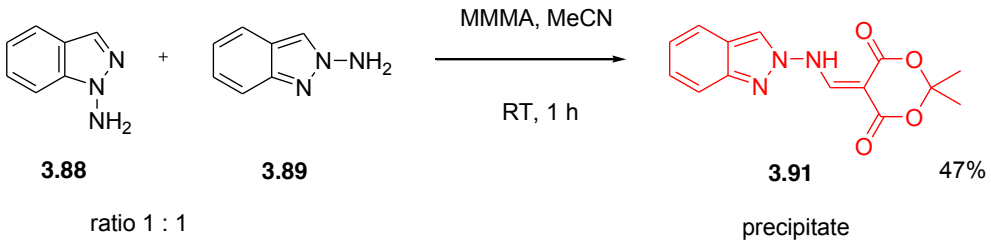

Scheme 46: Synthesis of 2-substituted MMA precursor **3.91**

To further prove the isomers had been assigned correctly, crystals were grown of 3.91, the resulting crystal structure is shown in Figure 15.

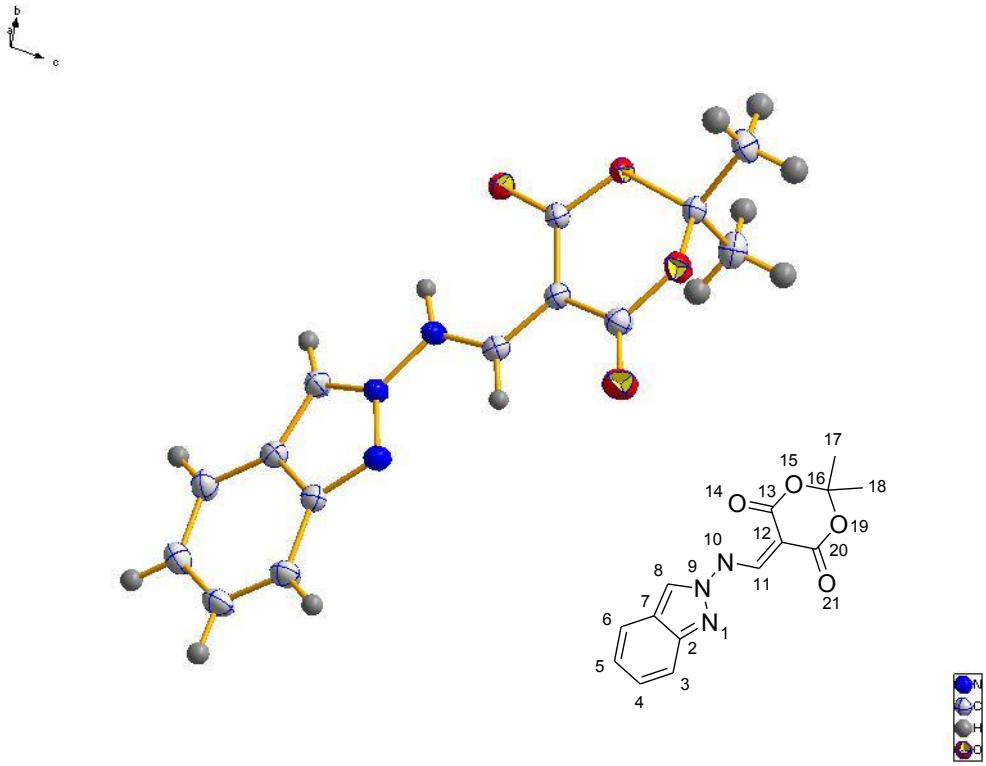

Atoms 1,2	d 1,2 [Å]	Atoms 1,2	d 1,2 [Å]
N1—N9	1.3441(14)	C11—C12	1.3786(16)
N1—C2	1.3562(15)	C11—H11	0.9500
C2—C3	1.4143(17)	C12—C13	1.4401(17)
C2—C7	1.4221(17)	C12—C20	1.4520(17)
C3—C4	1.3707(18)	C13—O14	1.2211(15)
C3—H3	0.9500	C13—O15	1.3508(14)
C4—C5	1.4209(19)	O15—C16	1.4494(14)
C4—H4	0.9500	C16—O19	1.4351(15)
C5—C6	1.3665(18)	C16—C17	1.5041(17)
C5—H5	0.9500	C16—C18	1.5095(17)
C6—C7	1.4152(17)	C17—H17A	0.9800
C6—H6	0.9500	C17—H17B	0.9800
C7—C8	1.3934(17)	C17—H17C	0.9800
C8—N9	1.3441(15)	C18—H18A	0.9800
C8—H8	0.9500	C18—H18B	0.9800
N9—N10	1.3885(13)	C18—H18C	0.9800
N10—C11	1.3165(16)	O19—C20	1.3685(15)
N10—H10	0.854(17)	C20—O21	1.2096(16)

Figure 15: Crystal structure and bond length data for 2-substituted precursor **3.91**

3.5.2 Flash Vacuum Pyrolysis of Indazole Precursors

The pyrolyses of the indazole precursors were not expected to produce temperature profiles significantly different to the parent reaction and 4-phenylpyrazole, as they all use the Medrum's acid moiety to generate the required imidoylketene during pyrolysis. Because of this, temperature profiles were not generated for the indazole precursors, instead the general temperatures already successfully employed were attempted on a small scale initially, and then on a preparative scale for product analysis and characterisation.

The pyrolysis of the 2-substituted precursor 3.91 (Scheme 47 appeared to be very messy, leaving a significant amount of residue in the inlet tube. During the pyrolysis the starting material turned from an off-white colour to yellow and finally to brown in the inlet. However a small ring of product formed in the inlet tube, and preliminary ^{1}H NMR spectrum showed promising results for the presence of the betaine.

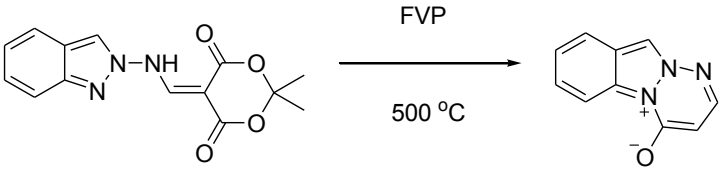

3.91 **3.93**

Scheme 47: Initial pyrolysis of 2-substituted precursor **3.91**

It appeared that the pyrolysis was not very efficient due to the volatility issues with the precursor, and that it was decomposing in the inlet tube. To remedy this, the pyrolysis was repeated, but using a diffusion pump instead if the usual oil pump, as it can achieve pressures of the order 2×10^{-7} Torr. By lowering the pyrolysis pressure, a lower inlet temperature is required, minimising decomposition in the inlet and allowing the pyrolysis to take place more effciently.

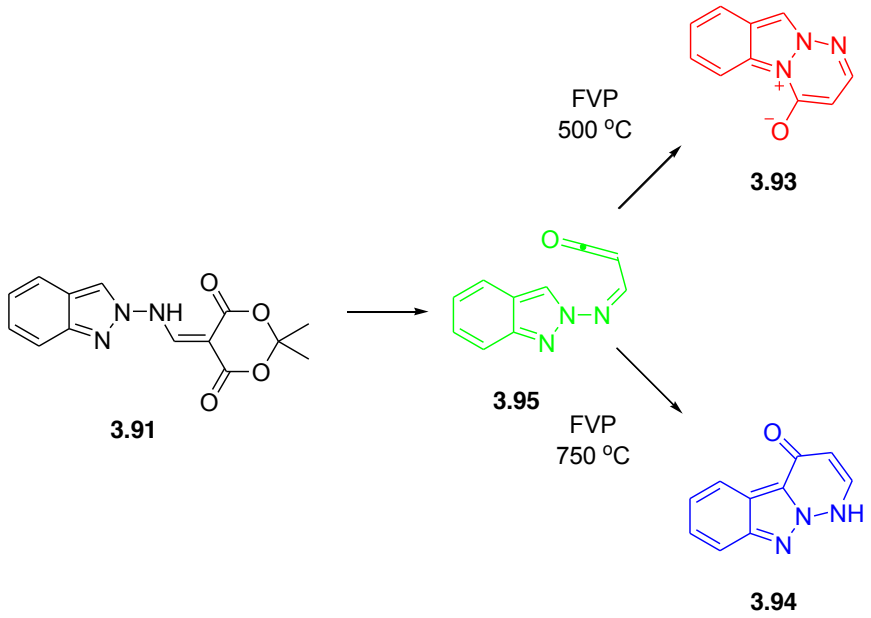

Scheme 48: Pyrolyses of 2-substituted precursor **3.91** to produce the betaine **3.93** and indazolopyridazinone **3.94**

The pyrolyses of precursor 3.91 are summarised in Scheme 48 above. With the use of the diffusion pump, the ketene 3.95 was generated, the betaine 3.93 was successfully obtained from FVP at 500 °C and the indazolopyridazinone 3.94 by FVP using a furnace temperature of 750 °C. These are two new ring systems whose syntheses have been possible by applying the basic principles established from earlier work to a new ring system. Although the extra ring decreases the volatility of the precursor, using a diffusion pump can remedy this and allow the pyrolyses to carry through to their desired conclusion.

A small scale pyrolysis was also undertaken for the 1-substituted precursor 3.90 (Scheme 49) to establish that the furnace temperature was correct. The diffusion pump was employed immediately due to its positive results on previous pyrolyses. Again the results were promising for the presence of the desired betaine 3.92.

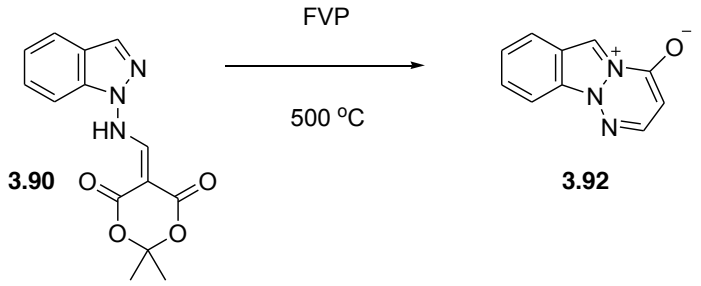

Scheme 49: Initial pyrolysis of 2-substituted precursor **3.90**

Once the conditions were established the betaine was prepared by FVP on a preparative scale for analysis and characterisation (Scheme 50). For completeness, the 1-substitued precursor 3.90 was also pyrolysed at 750 °C with a much unexpected outcome. The U-tube was cleaned by distillation of chloroform and it was expected that all the solid would be soluble, as the only expected product was the betaine and any decomposition products from it due to pyrolysis at a much higher furnace temperature. However, as has been repeatedly observed with other pyrolyses of this nature, an insoluble solid was left behind on the U-tube.

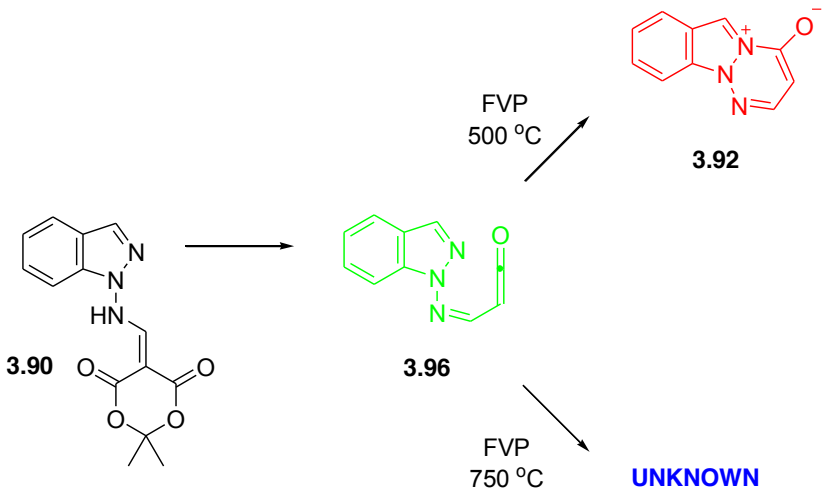

Scheme 50: Pyrolyses of 1-substituted precursor **3.90** to produce the betaine **3.93** and an unknown product

This unexpected solid was analysed by ^{1}H NMR spectroscopy and was found to be an aromatic compound with 6 protons. EI mass spectroscopy revealed it had the same molecular mass as the betaine and was therefore an isomer of it. Figure 16 shows the ^{1}H NMR spectrum along with a table of the chemical shifts and coupling constants.

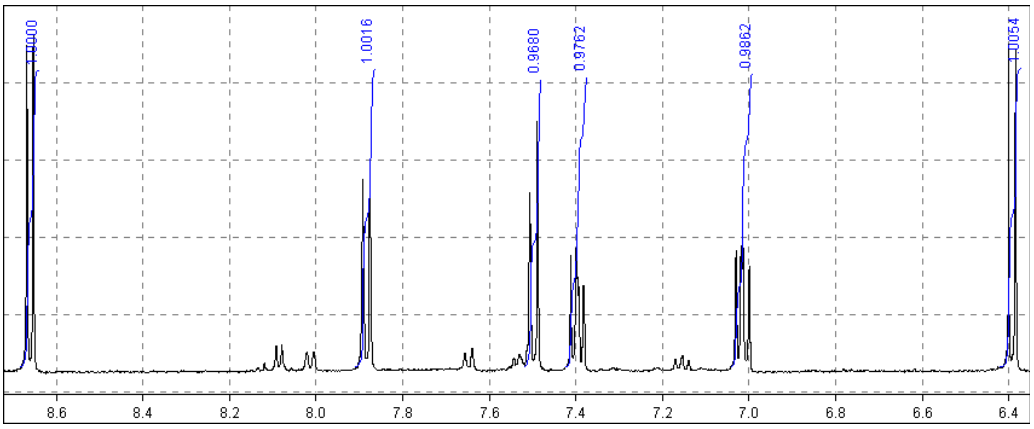

Chemical Shift	Peak	Coupling Constant	Chemical Shift	Peak	Coupling Constant
8.66	*d*	^{3}J 7.9	7.40	*t*	^{3}J *8.3*
7.88	*d*	^{3}J *8.5*	7.01	*t*	^{3}J *8.1*
7.48	*d*	^{3}J *8.8*	6.39	*d*	^{3}J *7.9*

Figure 16: ^{1}H NMR spectrum of unknown product

It is apparent that there are two distinct spin systems within the unknown, one 4-spin system which seems to be consistent with the aryl protons of the indazole backbone and one 2-spin system which matches the pyridazinone protons we have seen. This information allowed a shortlist of possible isomers to be drawn up and these are shown in Scheme 51.

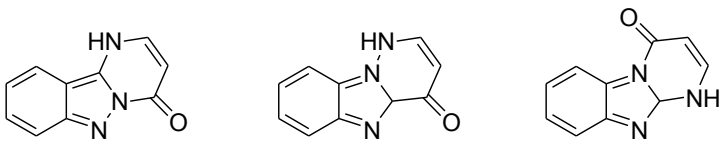

3.97 **3.98** **3.99**

Scheme 51: Plausible isomers for unknown product

Authentic samples of the indazolopyridazinone 3.97 and the benzimidazolopyridazinone 3.98 were prepared using the syntheses set out in Scheme 52. These employed the synthetic strategies already established in this work. 3-Aminoindazole was reacted with MMMA using the conventional conditions to afford the precursor 3.100. This underwent FVP using a furnace temperature of 600 °C to produce the indazolopyridazinone 3.97. Benzimidazole was *N*-aminated using the conditions established previously for indazole, and the resulting *N*-aminated product also reacted with MMMA to produce the precursor 3.101. This precursor was subjected to FVP using a furnace temperature of 700 °C which resulted in the benzimidazolopyridazinone 3.98.

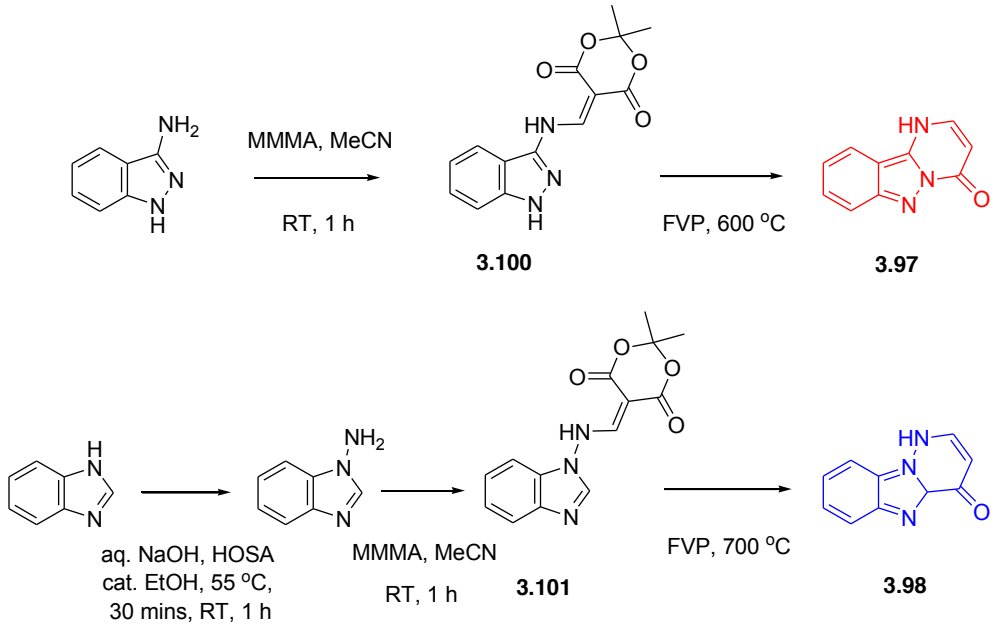

Scheme 52: Routes to authentic samples of indazolopyridazinone **3.97** and benzimidazolopyridazinone **3.98**

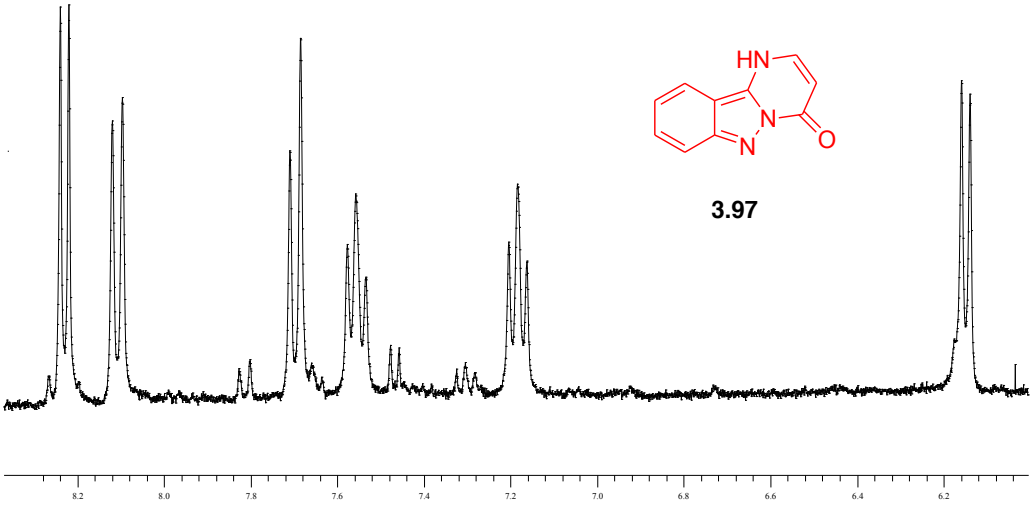

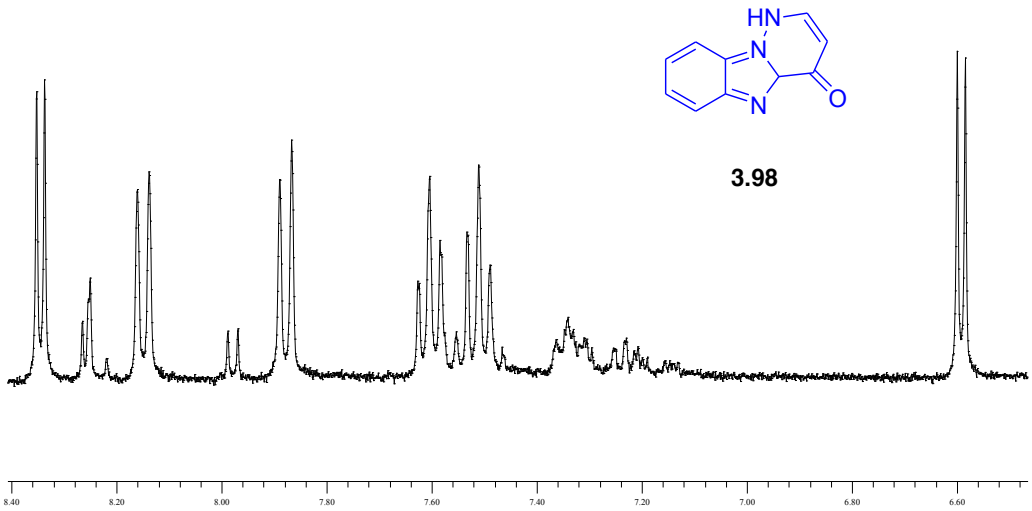

Unknown	3.97	3.98
8.66, d, ^{3}J7.9	8.23, d, ^{3}J7.2	8.34, d, ^{3}J5.2
7.88, d, ^{3}J8.5	8.11, d, ^{3}J8.3	8.15, d, ^{3}J7.9
7.48, d, ^{3}J8.8	7.80, d, ^{3}J8.9	7.88, d, ^{3}J8.1
7.40, t, ^{3}J8.3	7.56, t, ^{3}J7.8	7.60, t, ^{3}J7.6
7.01, t, ^{3}J8.1	7.18, t, ^{3}J7.7	7.51, t, ^{3}J7.9
6.39, d, ^{3}J7.9	6.15, d, ^{3}J7.1	6.59, d, ^{3}J5.6

Figure 3: Spectra of products **3.97** and **3.98**, and comparison of chemical shifts versus unknown product

Figure 17 shows the ^{1}H NMR data for the two isomers **3.97** and **3.98** compared against the data already established for the unknown. It is clear that neither of these are the unknown structure. The isomer **3.99** had previously synthesised, [19] a comparison with its data is seen in Figure 18. This shows that the unknown is not **3.99** either.

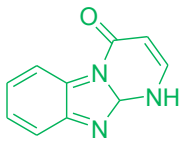

3.99

Unknown	3.99
8.66, d, ^{3}J 7.9	8.45, d, ^{3}J 8.0
7.88, d, ^{3}J 8.5	8.00, d, ^{3}J 7.1
7.48, d, ^{3}J 8.8	7.58, d, ^{3}J 8.0
7.40, t, ^{3}J 8.3	7.50, td, ^{3}J 7.1 ^{4}J 1,2
7.01, t, ^{3}J 8.1	7.34, td, ^{3}J 8.0 ^{4}J 1.2
6.39, d, ^{3}J 7.9	5.99, d, ^{3}J 6.9

Figure 18: Table comparing ^{1}H NMR shifts for **3.99** against those of the unknown

The same plausible mechanistic ideas were applied to the 1-substituted and 2-substituted imidazoles (Scheme 53). The top mechanism shows the outcomes from applying the spirocyclic intermediate to the 2-substituted imidazole. There are four possible products using this method; the expected betaine and imidazolopyridazinone products **3.93** and **3.94**, and also the isomeric betaine **3.92** and the imidazolopyridazione isomer **3.97**. The latter two products are not observed.

When this mechanism is applied to the 1-substituted imidazole there are also the same four possible products. Betaine 3.92 is the product observed at lower furnace temperature; however the unknown product has been shown to be none of the other three possible according to this mechanism.

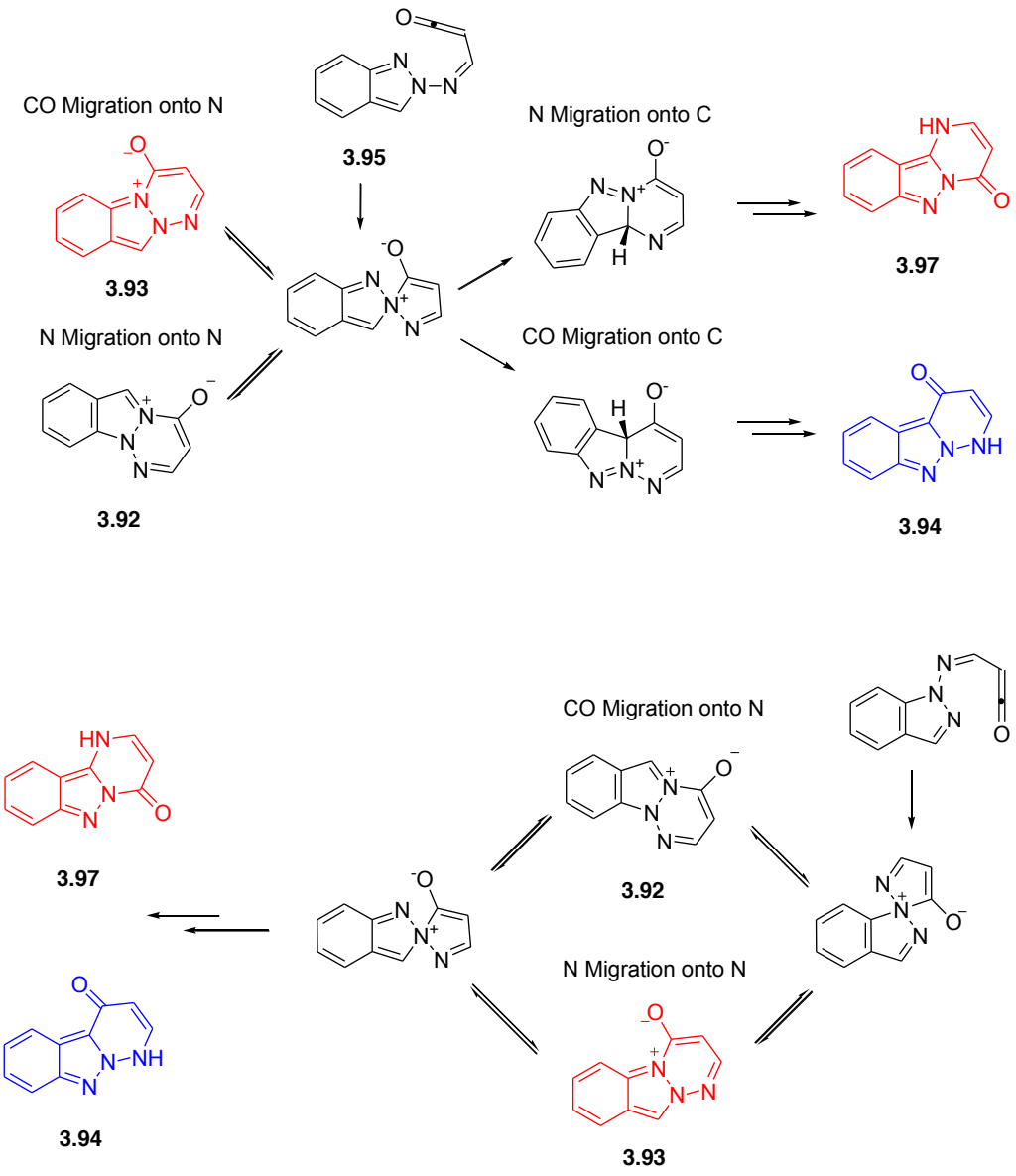

Scheme 53: Possible mechanisms *via* spirocyclic internediates for collapse of 2-imidazolylketene (top) and 1-imidazolylketene

3.5.3 Conclusions

Pyrolysis of the indazole precursor 3.91 has been shown to produce the betaine 3.93 and the indazolopyridazinone 3.94. Pyrolysis of the indazole precursor 3.90 has been shown to produce the betaine 3.92 and furnace temperatures of 500 °C. At higher furnace temperatures a yet unknown product is produced. Attempts have been made to identify this unknown by making authentic sample of three possible products, however none of these have proved to correlate to the unknown product. More work is needed to establish the identity of this unknown product, however this is out with the scope of this thesis. Mechanisms to explain these observations have been suggested, but more work and DFT calculations are needed to confirm these.

3.6 References

1. R. F. C. Brown, F. W. Eastwood, K. J. Harrington, *Aust. J. Chem.*, 1974, 27, 2373.
2. H. J. Gordon, J. C. Martin, H. McNab, *J. Chem. Soc., Perkin. Trans. 1*, 1984, 2129.
3. H. McNab, L. C. Monahan, *J. Chem. Soc., Perkin Trans. 1*, 1988, 863.
4. A. J. Blake, H. McNab, L. C. Monahan, *J. Chem. Soc., Perkin Trans. 1*, 1989, 425.
5. A. J. Blake, H. McNab, M. Morrow, H. Rataj, *J. Chem. Soc., Chem Commun.*, 1993, 840.
6. A. J. Blake, D. Clarke, R. W. Mares, H. McNab, *Org. Biomol. Chem.*, 2003, 1, 4268.
7. J. R. Gardinier, T. C. Grattan, D. L. Reger, M. D Smith, M. R. Smith, M. R., *New. J. Chem.*, 2003, 27, 1670.
8. H. Kelling, E. Knippel, M. Knipple, H. Kristen, M. Michalikh, *Tetrahedron*, 1977, 33, 231.
9. C. H.DePuy, R. W. King, *Chem. Rev.*, 1960, 60, 431.

10. L. George, K-P. Netsch, G. Pern, G. Kollenz, C. Wentrup, C., *Org. Biomol. Chem.*, 2006, 4, 558.

11. K.Werecka, K., *Undergraduate Report*, 2007.

12. S. Liu, J. Pestano, C. Wolf, *Synthesis*, 2007, 3519.

13. C. Thornley, *PhD thesis*, The 1993.

14. J.Bergnmn, C. Stalhandske, *Tetrahedron*, 1996, 52, 753.

15. X. Coqueret, F. Bourelle-Wargnier, J. Chuche, L. Toupet, *J. Chem. Soc., Chem. Commun.*, 1983, 1144.

16. B. M. Adger, S. Bradbury, M. Keating, C. W. Rees, R. C Storr, M. T. Williams, *J. Chem. Soc., Perkin Trans. 1*, 1975, 31.

17. J-P. Anselme, K. Sakai, *J. Org. Chem.*, 1972, 37, 2351.

18. M. Azadi Ardakani, R. K. Smalley, R. H. Smith, *J. Chem. Soc., Perkin Trans. 1*, 1983, 2501.

19. W. J. O'Neill, *PhD Thesis*, The University of Edinburgh, 2009.

4. Experimental Information

Instrumentation

Nuclear Magnetic Resonance (NMR) Spectroscopy

^{1}H and ^{13}C NMR spectra were recorded using Varian Gemini 200 (200 MHz), Bruker AC250 (250/63 MHz), WH360 (360/90 MHz) and AVA500 (500/125 MHz) spectrometers. All spectrometers were operated by the author with some assistance from Mr. J. R. A. Millar, Mr. J. Bella and Dr. M. Cremoux.

Chemical shifts are quoted in parts per million (ppm) relative to tetramethylsilane (δ = 0.0) and coupling constants (J) are given in Hz.

Mass Spectroscopy

Low resolution EI and high resolution EI/ESI were performed on a Thermomat 900XP spectrometer. Spectrometers were operated by Mr. A. T. Taylor and all spectra are assumed to be EI, unless otherwise stated.

Elemental Analysis

Elemental analyses were performed by Ms. Sylvia Wilson at the University of St. Andrews Elemental Analysis Service.

Chromatography

Thin-layer chromatography was carried out on pre-coated aluminium sheets (0.2 mm, silica gel, Merck, grade 60) impregnated with an ultra-violet indicator. Dry flash chromatography was carried out on silica gel (Merck, grade 60, 230-400 Mesh, 60 A). Crude material was pre-adsorbed onto silica and then loaded onto the column, and each solvent system was specifically optimised for each reaction system.

Melting Points

Melting points were recorded using Gallenkamp melting point apparatus. Samples of compounds were recrystallised from appropriate solvents as necessary.

X-Ray Diffraction

Crystal structures were obtained and solved by Prof. S. Parsons, Mr. R. D. L. Johnstone and Ms. A. Collins on Bruker Smart APEX CCD with a graphite monochromator.

Commerical Chemicals

All commercial starting materials were obtained from Sigma Aldrich, Acros or Lancaster.

Solvents

Solvents were generally obtained from Aldrich or Fisher, and were used without further purification.

N-Aminoheterocycles as radical FVP precursors

Benzimidazole Synthesis – General Method

The same general method was applied to the synthesis of all 2-substituted benzimidazoles. Polyphosphoric acid (PPA) was scooped into the reaction flask and warmed to approximately 80-90 °C. The warm PPA (*ca* 30 cm³) was poured into a mizture of *o*-phenylenediamine (2.16 g, 0.02 mol) and the corresponding *ortho*-substituted benzoic acid or alkyl carboxylic acid (0.02 mol) and stirred well to ensure the solid reagents were thoroughly mixed with the PPA. The reaction mixture was heated to 180 °C for 2 h allowed to cool to approximately 80 °C, and then poured as a thin stream into stirred cold water (*ca* 100 cm³). This solution was stirred at room temperature for 1 h, then neutralised by the addition of 35% ammonium hydroxide solution. The precipitate was filtered off and dissolved in a mixture of DCM and water (1:1, *ca* 200 cm³). The aqueous extract was extracted and separated twice with

DCM, the combined organic fractions were washed with aqueous sodium hydroxide solution (1M, *ca* 250 cm^3), dried ($MgSO_4$) and the solvent removed under reduced pressure.

The following benzimidazoles were made by this procedure.

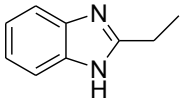

2-Ethyl-1*H*-benzimidazole 2.24 (83%), mp 171 – 172 °C [lit., [1] 172 -173 °C]; δ_H (360 MHz, DMSO-*d*$_6$) 12.16 (1H, s, NH), 7.52 (1H, d, ^3J 7.9), 7.41 (1H, d, ^3J 8.0), 7.13-7.09 (2H, m), 2.83 (2H, q, ^3J 7.6) and 1.33 (3H, t, ^3J 7.5) ; δ_C (90 MHz, DMSO-*d*$_6$) 157.62 (quat), 144.73 (quat), 135.78 (quat), 122.82 (CH), 122.21 (CH), 119.51 (CH), 112.12 (CH), 23.43 (CH_2) and 13.70 (CH_3) ; *m/z* 146 (M^+, 100%), 145 (49) and 131 (7)

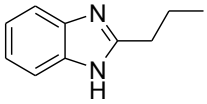

2-Propyl-1*H*-benzimidazole 2.25 (77%), mp 148 °C; (Found M^+ 160.0992, $C_{10}H_{12}N_2$ requires M 160.0995); δ_H (360 MHz, DMSO-*d*$_6$) 12.19 (1H, s, NH), 7.48 (2H, br d, ^3J 8.1), 7.14-7.09 (2H, m), 2.79 (2H, t, ^3J 6.8), 1.80 (2H, sextet, ^3J 6.7) and 0.96 (3H, t, ^3J 6.8); δ_C (90 MHz, DMSO-*d*$_6$) 156.46 (quat), 144.84 (quat), 135.73 (quat), 122.74 (CH), 122.25 (CH), 119.51 (CH), 112.11 (CH), 31.98 (CH_2), 22.45 (CH_2) and 15.18 (CH_3) ; *m/z* 160 (M^+, 68%), 145 (45), 132 (100) and 77 (10).

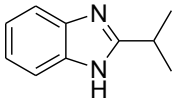

2-Isopropyl-1*H*-benzimidazole 2.26 (77%), mp 218 °C; (Found M^+ 160.0997, $C_{10}H_{12}N_2$ requires M 160.0995) δ_H (360 MHz, DMSO-*d*$_6$) 12.15 (1H, s, NH), 7.53 (1H, d, ^3J 7.9), 7.42 (1H, d, ^3J 7.9), 7.14-7.10 (2H, m), 3.15 (1H, septet, ^3J 6.9) and 1.38 (6H, d, ^3J 6.9); δ_C (90 MHz, DMSO-*d*$_6$) 161.30 (quat), 144.48 (quat), 135.79 (quat), 122.86 (CH), 122.21 (CH), 119.65 (CH), 112.20 (CH), 29.82 (CH) and 22.83 (2×CH_3) ; *m/z* 160 (M^+, 50%), 145 (100), 119 (7) and 92 (15).

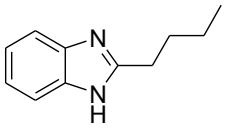

2-Butyl-1*H*-benzimidazole 2.27 (72%), mp 151 - 152 °C; (Found M^+ 174.2465, $C_{11}H_{14}N_2$ requires 174.2467); δ_H (250 MHz, $CDCl_3$) 10.40 (1H, br s), 7.59 (2H, m), 7.19 – 7.16 (2H, m), 2.84 (2H, t, ^3J 7.6), 1.77 (2H, quintet, ^3J 7.7), 1.35 (2H, sextet, ^3J 7.6) and 0.84 (3H, t, ^3J 7.4); δ_C (90 MHz, DMSO-*d*$_6$) 156.62 (quat), 144,63 (quat), 135.63 (quat), 122.44 (2 × CH), 119.31 (CH), 112.06 (CH), 31.17 (CH_2), 29.67 (CH_2), 23.27 (CH_2) and 15.12 (CH_3) ; *m/z* 174 (M^+, 100%), 159 (72) and 145 (50)

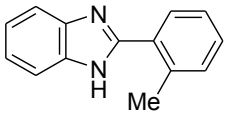

2-(2-Methylphenyl)-1*H*-benzimidazole 2.40, (70%), mp 214 °C [lit., [2] 215 °C], δ_H (360 MHz, DMSO-*d*$_6$) 12.63 (1H, s, NH), 7.75 (1H, d, ^3J 6.9), 7.69 (1H, d, ^3J 7.6), 7.53 (1H, d, ^3J 7.6), 7.34-7.41 (3H, m), 7.21 (2H, m) and 2.61 (3H, s); δ_C (90 MHz, DMSO-*d*$_6$) 153.42 (quat), 145.19 (quat), 138.49 (quat), 135.89 (quat), 132.74 (CH), 131.56 (quat), 130.92 (CH), 130.79 (CH), 127.44 (CH), 123.83 (CH), 122.87 (CH), 120.40 (CH), 112.73 (CH) and 22.53 (CH_3); *m/z* 208 (M^+, 100%), 207 (73), 180 (3), 137 (5), 123 (6), 103 (9), 81 (12) and 69 (23)

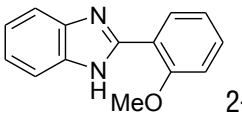

2-(2-Methoxyphenyl)-1*H*-benzimidazole 2.41, (57%), mp 158 °C [lit., [3] 155-158 °C], δ_H (360 MHz, DMSO-*d*$_6$) 12.16 (1H, s, NH), 8.35 (1H, m), 7.66 (2H, s), 7.51 (1H, m), 7.12-7.27 (4H, m) and 4.05 (3H, s); δ_C (90 MHz, DMSO-*d*$_6$) 158.25 (quat), 150.43 (quat), 144.22 (quat), 136.51 (quat), 132.74 (CH), 131.22 (CH), 123.54 (CH), 123.03 (CH), 122.36 (CH), 119.58 (quat), 113.58 (CH), 113.56 (CH) and 57.24 (CH_3); *m/z* 224 (M^+, 100%), 194 (45), 166 (100), 150 (25), 119 (21) and 69 (37)

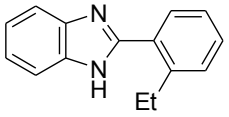

2-(2-Ethylphenyl)-1*H*-benzimidazole 2.42, (65%), mp 195 - 197 °C; Found δ_H (250 MHz, DMSO-*d*$_6$) 12.54 (1H, s, NH), 7.63 (2H, m), 7.32-7.49 (4H, m), 7.16 (2H, m), 2.95-3.04 (2H, q, ^3J 7.5) and 1.07 (3H, t, ^3J 7.5); δ_C (63 MHz, DMSO-*d*$_6$) 153.37 (quat), 145.22 (quat), 144.86 (quat), 135.87 (quat), 134.02 (quat), 131.21 (CH), 131.12 (CH), 131.03 (CH), 127.38 (CH), 123.76 (CH), 122.84 (CH), 120.40 (CH), 112.70 (CH), 27.66 (CH_2) and 17.16 (CH_3); *m/z* 222 (M^+, 100%), 221 (84), 207 (39) and 179 (24)

N-Amination of Benzimidazoles

General Method 1

The benzimidazole (9.6 mmol) was dissolved in DMSO (40 cm³) to which was added hydroxylamine-*O*-sulfonic acid (3 eq, 3.26 g) and sodium hydroxide solution (2M, 20 cm³). The mixture was heated to 60 °C for 1 h then stirred at room temperature for 2 h. The reaction mixture was then poured into ice water (*ca.* 100 cm³) and the resulting precipitate filtered off. The filtrate was extracted with ethyl acetate (3 × 30 cm³) and the organic combined layers back extracted with water (2 × 600 cm³) to remove residual DMSO. The filtered solid was combined with the organic layer (using more ethyl acetate if necessary) and washed with sodium hydroxide (1M, *ca* 300 cm³). The organic extract was then dried ($MgSO_4$) and the solvent removed under reduced pressure. The resulting solid was then subjected to the same reaction conditions, for a second time to yield the desired *N*-aminated product.

General Method 2

The benzimidazole (1.5 mmol) and potassium hydroxide (4.13 eq) were mixed in water (5 cm^3) and heated to 70 °C. At this temperature if a complete solution was not obtained, DMSO was added dropwise until it was achieved. A solution of hydroxylamine-*O*-sulfonic acid (2.67 eq) in water (1 cm^3) was neutralised with sodium hydrogen carbonate (2.67 eq). This solution was added to the benzimidazole solution at 70 °C and stirred at this temperature for 30 min. The heat was removed and the reaction mixture allowed to cool to room temperature. The resulting precipitate was filtered off and washed with water (5 cm^3), to give the *N*-aminated benzimidazole. If a precipitate was not apparent, the same amount of water as had made the KOH solution could be added again, the aqueous extracted with EtOAc, dried over $MgSO_4$ and solvent removed under reduced pressure to yield the *N*-aminated benzimidazole.

General Method 3

The benzimidazole (15 mmol) was suspended in an aqueous solution of sodium hydroxide (4 g in 50 cm^3 water) and heated to 55 ^oC. At this temperature ethanol was added dropwise until a complete solution was obtained. Hydroxylamine-*O*-sulfonic acid (3 eq) was added portionwise over 15 min with vigourous stirring to minimise foaming. After addition the reaction was heated to 60 ^oC for 1 h, then allowed to cool to room temperature and stirred overnight. Water (30 cm^3) was added and the aqueous solution extracted with dichloromethane (4 × 30 cm^3). The organic extract was then dried ($MgSO_4$) and the solvent removed under reduced pressure to yield the desired *N*-aminated product

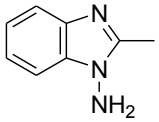

1-Amino-2-methyl-1*H*-benzimidazole **2.28** (method 2) (61%), mp 158 °C [lit., [4] 158-160 °C], δ_H (250 MHz, $CDCl_3$) 7.62 (1H, m), 7.16-7.25 (3H, m), 4.56 (2H, s, NH_2) and 2.56 (3H, s); δ_C 153.37 (quat), 140.83 (quat), 135.86 (quat), 122.56 (CH), 122.02 (CH), 119.57 (CH), 108.36 (CH) and 13.21 (CH_3).

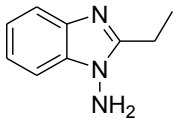

1-Amino-2-ethyl-1*H*-benzimidazole **2.29** (method 2) (53%), mp 116 – 117 °C, (Found M^+ 161.0948, $C_9H_{11}N_3$ requires *M* 161.0948); δ_H (250 MHz, DMSO-*d*$_6$) 7.73 – 7.67 (1H, m), 7.37 – 7.29 (1H, m), 7.26 – 7.23 (2H, m), 4.62 (2H, br s, NH_2), 3.01 (2H, q, ^3J 7.6) and 1.43 (3H, t, ^3J 7.6); δ_C (63 MHz, DMSO-*d*$_6$) 157.74 (quat), 140.64 (quat), 135.95 (quat), 122.71 (CH), 122.61 (CH), 119.76 (CH), 108.32 (CH), 20.42 (CH_2) and 12.18 (CH_3) ; *m/z* 161 (M^+, 100%), 145 (67), 77 (44) and 56 (43)

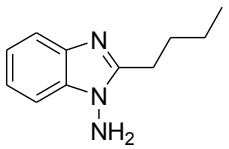

1-Amino-2-^{n}butyl-1*H*-benzimidazole **2.30** (method 3 and subsequent soxhlet extraction using hexane) (31%), mp 110 – 112 °C; (Found M^+ 189.1264, $C_{11}H_{15}N_3$ requires *M* 189.1261); δ_H (360 MHz, $CDCl_3$) 7.63 – 7.61 (1H, m), 7.28 – 7.26 (1H, m), 7.20 – 7.14 (2H, m), 4.53 (2H, br s, NH_2), 2.92 (2H, t, ^3J 7.7), 1.78 (2H, quintet, ^3J 7.8), 1.40 (2H, sextet, ^3J 7.7) and 0.91 (3H, t, ^3J 7.4); δ_C (90 MHz, $CDCl_3$) 155.00 (quat), 148.45 (quat), 135.34 (quat), 122.10 (CH), 119.17 (CH), 114.45 (CH), 107.84 (CH), 29.78 (CH_2), 26.13 (CH_2), 22.46 (CH_2) and 13.69 (CH_3); *m/z* 189 (M^+, 30%), 174 (25), 147 (100) and 132 (87)

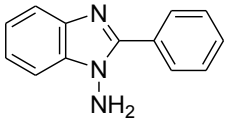

1-Amino-2-phenyl-1*H*-benzimidazole **2.57**, (method 2) (58%), mp 195 – 196 °C [lit., [5] 204 – 205 °C]; δ_H (250 MHz, $CDCl_3$) 8.24 – 8.03 (2H, m), 7.83 (1H, m), 7.59 – 7.29 (6H, m) and 4.86 (2H, s, NH_2); δ_C (63 MHz, $CDCl_3$) 156.70 (quat), 156.62 (quat), 141.82 (CH), 138.12 (CH), 130.30 (quat), 129.97 (2 × CH), 128.75 (CH), 127.04 (quat), 123.36 (2 × CH), 110.17 (CH) and 109.79 (CH).

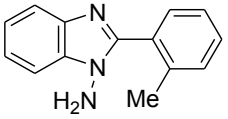

1-Amino-2-(2-methylphenyl)-1*H*-benzimidazole **2.58**, (method 1) (51%), mp 140 – 143 °C; (Found M^+ 223.1102, $C_{14}H_{13}N_3$ requires *M* 223.1104); δ_H (360 MHz, $CDCl_3$) 7.66 (1H, d, ^3J 8.2), 7.60 (1H, d, ^3J 8.2), 7.55 (1H, d, ^3J 8.2), 7.25-7.42 (5H, m), 5.99 (2H, s, NH) and 2.33 (3H, s); δ_C (90 MHz, $CDCl_3$) 154.45 (quat), 141.82 (quat), 139.29 (quat), 137.33 (quat), 132.35 (CH), 131.63 (quat), 131.49 (CH), 130.62 (CH), 126.59 (CH), 123.43 (CH), 123.11 (CH), 120.44 (CH), 111.73 (CH) and 21.41 (CH_3); *m/z* 223 (M^+, 96%), 208 (100), 207 (78), 206 (39) and 77 (32).

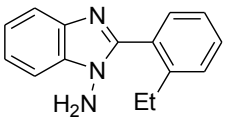

1-Amino-2-(2-ethylphenyl)-1*H*-benzimidazole **2.60**, (method 1) (43%), mp 109 - 111 °C; (Found M^+ 237.1261, $C_{15}H_{15}N_3$ requires *M* 237.1261); δ_H (360 MHz, $CDCl_3$) 7.79 (1H, dm, ^3J 8.0), 7.53-7.30 (7H, m), 4.62 (2H, s, NH), 2.66 (2H, q, ^3J 7.6) and 1.13 (3H, t, ^3J 7.6); δ_C (90 MHz, $CDCl_3$) 154.25 (quat), 145.34 (quat), 141.63 (quat), 136.24 (quat), 131.54 (CH), 131.25 (CH), 129.80 (CH), 129.69 (quat), 126.76 (CH), 124.04 (CH), 123.50 (CH), 121.14 (CH), 110.12 (CH), 27.37 (CH_2) and 16.31 (CH_3); *m/z* 237 (M^+, 100%), 222 (33), 219 (43), 206 (29) and 107 (66).

1-amino-2-(2-methoxyphenyl)-1*H*-benzimidazole **2.59**, (method 1) After the second amination reaction, the resulting dark yellow solid was purified by dry flash chromatography on SiO_2 using EtOAc : Hexane (80 : 20) as eluent to produce 1-amino-2-(2-methoxyphenyl)-1*H*-benzimidazole, (31%), mp 106 - 108 °C, δ_H (360MHz, $CDCl_3$) 7.76 (1H, dm, ^3J 7.9), 7.70 (1H, dd, ^3J 7.5, ^nJ 2.0), 7.58 (1H, dm, ^3J 7.8), 7.52 (1H, m), 7.35-7.25 (2H, m), 7.15 (1H, td, ^3J 7.8, ^nJ 1.0), 7.07 (1H, d, ^3J 8.1), 5.00 (2H, s, NH) and 3.89 (3H, s); δ_C (90MHz, $CDCl_3$) 158.05 (quat), 153.03 (quat), 141.81 (quat), 137.11 (quat), 133.75 (CH), 132.89 (CH), 123.92 (CH), 123.09 (CH), 122.70 (CH), 120.78 (CH), 120.17 (quat), 112.62 (CH), 110.81 (CH) and 57.19 (CH_3); *m/z* 239 (M^+, 100 %), 221 (50), 208 (27), 194 (46), 105 (33) and 77 (34).

Flash Vacuum Pyrolysis Experiments – Radical Precursors

Conditions for the pyrolyses were established in small scale experiments (*ca.* 20 mg) in which the entire contents of the trap were dissolved in a deuteriated solvent and analysed at once by ^{1}H NMR spectroscopy.

Once the conditions were established, preparative pyrolyses (>100 mg) were carried out if necessary. At the end of the pyrolysis, deuteriated solvent (usually $CDCl_3$) was distilled into the U-tube to dissolve the product(s), the NMR spectrum was monitored and then the solvent was removed under reduced pressure. The precursor, pyrolysis conditions [quantity of precursor, furnace temperature (T_f), inlet temperature (T_i), pressure range (P) and pyrolysis time (t)] and yields are given. In some cases, precursor was placed in a glass vial within the inlet tube and silica wool was inserted into the end of the vial to prevent the solid from being pulled into the furnace tube by the vacuum applied. The following flash vacuum pyrolysis experiments using radical generating precursors were undertaken:

FVP of 1-amino-2-methyl-1*H*-benzimidazole 2.28. (23.7 mg, T_f 850 °C, T_i 188 °C, P 2.8 – 3.4 × 10^{-2} Torr, t 12 min) gave 2-methyl-1*H*-benzimidazole, **2.23** (*ca.* 97%); δ_H (250 MHz, $CDCl_3$) 12.71 (1H, s, NH), 7.47 (2H, m), 7.12 (2H, m) and 2.53 (3H, s); δ_C 151.19 (quat), 138.93 (2 × quat), 120.96 (2 × CH), 114.40 (2 × CH) and 14.56 (CH_3). Data compatible with authentic sample.

FVP of 1-amino-2-ethyl-1*H*-benzimidazole 2.29. (25.4 mg, T_f 850 °C, T_i 193 °C, P 2.5 – 3.8 x 10^{-2} Torr, t 11 min) gave 2-vinyl-1*H*-benzimidazole, **2.38** (*ca.* 37%). Data compatible with authentic sample.

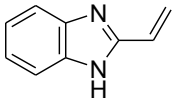

2-Vinyl-1*H*-benzimidazole **2.38** mp 152 – 153 °C [lit., [6] 149 - 153 °C]; δ_H (250 MHz, DMSO) 11.22 (1H, s, NH), 7.72 (2H, m), 7.37 (2H, m), 6.74 (1H, dd, ^3J 10.1, ^3J 18.2), 6.21 (1H, dd, ^2J 2.0, ^3J 18.1) and 5.76 (1H, dd, ^2J 2.1, ^3J 10.2); *m/z* 144 (M^+, 100%) and 118 (65). A ^{13}C NMR spectrum of suitable quality was not achieved.

FVP of 1-amino-2-phenyl-1*H*-benzimidazole 2.57. (27.1 mg, T_f 850 °C, T_i 188 °C, P 2.6 – 3.2 x 10^{-2} Torr, t 11 min) gave 2-phenyl-1*H*-benzimidazole, **2.56** (*ca.* 98%); δ_H (250 MHz, DMSO-d_6) 12.95 (1H, s, NH), 8.23 – 8.20 (2H, m), 7.71 – 7.47 (5H, m) and 7.30 – 7.23 (2H, m); δ_C 152.71 (quat), 145.28 (quat), 136.50 (quat), 131.65 (quat), 130.43 (2 × CH), 127.92 (2 × CH), 124.02 (CH), 123.16 (CH), 120.36 (CH), 118.54 (CH) and 112.81 (CH). Data compatible with literature data [7]

FVP of 1-amino-2-(2-methylphenyl)-1*H*-benzimidazole 2.58. FVP of **2.58** (106.1 mg, T_f 850 °C, T_i 175 °C, P 2.3 – 3.4 x 10^{-2} Torr, t 14 min) gave a pyrolysate which contained 2-(2-methylphenyl)-1*H*-benzimidazole **2.40** 11*H*-benzo[4,5]imidazo[1,2-*a*]isoindole **2.61** and 1-*o*-tolyl-1*H*-benzo[*d*]imidazol-2-amine **2.66** in a 3:2:7 ratio. These were separated by dry-flash chromatography on silica using a mixture of AcOEt and hexane, (80:20) as eluent. The following components were isolated in order of elution:

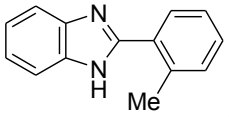

2-(2-methylphenyl)-1*H*-benzimidazole [(2)] **2.40** (27.2 mg, 27%) δ_H (360 MHz, DMSO-d_6) 12.13 (1H, s, NH), 7.79 (1H, d, ^3J 6.9), 7.68 (1H, d, ^3J 7.6), 7.51 (1H, d, ^3J 7.6), 7.32-7.40 (3H, m), 7.23 (2H, m) and 2.62 (3H, s); δ_C (90 MHz, DMSO-d_6) 153.42 (quat), 145.19 (quat), 138.49 (quat), 135.89 (quat), 132.74 (CH), 131.56 (quat), 130.92 (CH), 130.79 (CH), 127.44 (CH), 123.83 (CH), 122.87 (CH), 120.40 (CH), 112.73 (CH) and 22.53 (CH_3)

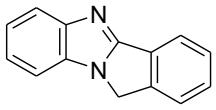

11*H*-benzo[4,5]imidazo[1,2-*a*]isoindole **2.61** (56.4 mg, 56%) mp 145 - 146 °C, [lit., [(8)] 144 - 149 °C] δ_H (360 MHz, $CDCl_3$) 8.01 (1H, m), 7.83 (1H, m), 7.55 - 7.39 (4H, m), 7.29 – 7.25 (2H, m) and 4.96 (2H, s); δ_C (90 MHz, $CDCl_3$) 158.28 (quat), 148.10 (quat), 143.31 (quat), 132.44 (quat), 129.61 (CH), 129.32 (quat), 128.53 (CH), 123.65 (CH), 122.50 (CH), 122.01 (CH), 121.81 (CH), 120.26 (CH), 109.17 (CH) and 47.01 (CH_2).

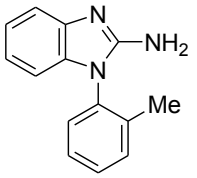

1-(2-methylphenyl)-1*H*-benzo[*d*]imidazol-2-amine **2.66** (17.1 mg, 17%) mp 162 - 164 °C, (Found M^+ 223.1101, $C_{14}H_{13}N_3$ requires *M* 223.1104); δ_H (360 MHz, $CDCl_3$) 7.48-7.44 (3H, m), 7.39 (1H, m), 7.33 (1H, d, ^3J 7.9), 7.16 (1H, t, ^3J 7.8), 7.01 (1H, t, ^3J 7.6), 6.76 (1H, d, ^3J 7.7), 4.93 (2H, br s) and 2.11 (3H, s); δ_C (90 MHz, $CDCl_3$) 154.18 (quat), 142.91 (quat), 138.32 (quat), 135.91 (quat), 134.01 (quat), 132.97 (CH), 130.97 (CH), 129.72 (CH), 128.77 (CH), 122.98 (CH), 121.18 (CH), 118.75 (CH), 109.46 (CH), 18.53 (CH_3); *m/z* 223 (M^+, 85%), 207 (71), 178 (100), 81 (21) and 69 (36).

FVP of 1-amino-2-(2-methoxyphenyl)-1*H*-benzimidazole 2.59 (23.2 mg, T_f 850 °C, T_i 170 °C, P 3.0 – 3.2 × 10^{-2} Torr, t 12 min) gave a complex mixture of products which are due to decomposition.

FVP of 1-amino-2-(2-ethylphenyl)-1*H*-benzimidazole 2.60. (118.8 mg, T_f 850 °C, T_i 164 °C, P 2.9 – 3.0 × 10^{-2} Torr, t 11 min) gave a pyrolysate which contained 2-(2-ethylphenyl)-1*H*-benzimidazole **2.42**, 5,6-dihydrobenzo[4,5]imidazo[2,1-*a*]isoquinoline **2.76**, 1-(2-ethylphenyl)-1*H*-benzo[*d*]imidazol-2-amine **2.88**, 2-styryl-1*H*-benzimidazole **2.83** and 11-methyl-11*H*-benzo[4,5]imidazo[2,1-*a*]isoindole **2.86**. These were separated by dry-flash chromatography on silica using a mixture of AcOEt and hexane, (gradiented from 30:70 to 60:40) as eluent. The following components were isolated in order of elution:

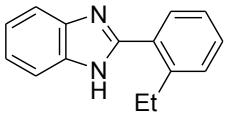

2-(2-Ethylphenyl)-1*H*-benzimidazole **2.42** δ_H (360 MHz, DMSO-d_6) 12.63 (1H, s, NH), 7.70 – 7.68 (2H, m), 7.52 – 7.37 (4H, m), 7.24 – 7.22 (2H, m), 3.05 (2H, q, ^3J 7.5) and 1.13 (3H, t, ^3J 7.5); δ_C (90 MHz, DMSO-d_6) 153.37 (quat), 145.22 (quat), 144.86 (quat), 135.87 (quat), 134.02 (quat), 131.21 (CH), 131.12 (CH), 131.03 (CH), 127.38 (CH), 123.76 (CH), 122.84 (CH), 120.40 (CH), 112.70 (CH), 27.66 (CH_2) and 17.16 (CH_3). Data compatible with authentic sample.

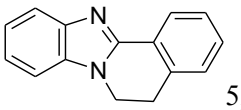

5,6-Dihydrobenzo[4,5]imidazo[2,1-*a*]isoquinoline **2.76** mp 126 – 128 °C [lit., [8] 125 - 130 °C] δ_H (360 MHz, $CDCl_3$) 8.28 (1H, m), 7.82 (1H, m), 7.39 – 7.28 (6H, m), 4.28 (2H, t, ^3J 6.9) and 3.24 (2H, t, ^3J 7.1); δ_C 150.14 (quat), 144.87 (quat), 135.66 (quat), 135.31 (quat), 131.21 (CH), 129.12 (CH), 128.77 (CH), 127.61 (quat), 126.65 (CH), 123.75 (CH), 123.54 (CH), 120.71 (CH), 110.11 (CH), 41.42 (CH_2), 29.25 (CH_2).

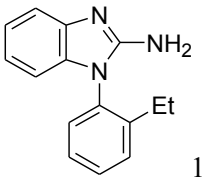

1-(2-ethylphenyl)-1*H*-benzo[*d*]imidazol-2-amine **2.88** mp 175 - 177 °C; (Found M^+ 237.1259, $C_{15}H_{15}N_3$ requires *M* 237.1261); δ_H (250 MHz, $CDCl_3$) 7.61 – 7.35 (6H, m), 7.14 (1H, t, ^3J 7.4), 6.81 (1H, d, ^3J 7.7), 3.56 (2H, br s), 2.42 (2H, q, ^3J 8.0) and 1.09 (3H, t, ^3J 7.6); δ_C (90 MHz, $CDCl_3$) 152.87 (quat), 142.95 (quat), 131.37 (CH), 130.63 (CH), 129.73 (quat), 128.57 (2 × CH), 128.18 (CH), 123.82 (quat), 122.54 (CH), 113.88 (CH), 113.63 (quat), 109.41 (CH), 23.81 (CH_2) and 14.27 (CH_3).

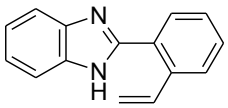

2-styryl-1*H*-benzimidazole **2.83** mp 177 – 179 °C; δ_H (250 MHz, $CDCl_3$) 7.92-7.86 (2H, m), 7.84-7.83 (1H, m), 7.79-7.74 (1H, m), 7.36-7.30 (2H, m), 7.26-7.19 (2H, m), 6.81 (1H, m), 6.20 (1H, m) and 5.61 (1H, m); δ_C (63 MHz, $CDCl_3$) 147.46 (quat), 129.47 (CH), 128.27 (CH), 126.94 (quat), 125.55 (CH), 123.58 (CH), 123.32 (quat), 123.27 (CH), 121.00 (CH), 120.28 (CH), 114.79 (quat), 117.00 (CH), 111.69 (CH), 109.77 (quat) and 105.90 (CH_2), *m/z*; 220 (M^+, 100%), 103 (64) and 118(57). As this compound could not be fully purified suitable elemental analysis data could not be achieved.

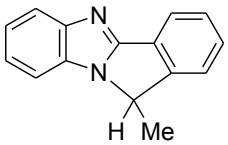

11-Methyl-11*H*-benzo[4,5]imidazo[2,1-*a*]isoindole **2.86** mp 202-204 °C; (Found M^+ 220.2749, $C_{15}H_{12}N_2$ requires *M* 220.2753) δ_H (250 MHz, $CDCl_3$) 8.28 (1H, m), 8.15-8.02 (2H, m), 7.77-7.70 (2H, m), 7.68-7.61 (1H, m), 7.58-7.49 (2H, m), 5.56 (1H, q, ^3J 6.8) and 2.06 (3H, d, ^3J 6.8); *m/z* 220.1 (M^+, 100%),

219.1 (64), 204.0 (41) and 194.1 (78). A ^{13}C NMR spectrum of a suitable quality was not achieved.

Imidazoline Synthesis – General Method

The same general method [9] was applied to the synthesis of all 2-substituted imidazolines. A solution of the appropriate aldehyde (0.043 mol) in dichloromethane (30 cm³) was added dropwise to a solution of ethylenediamine (1.05 eq) in dichloromethane (20 cm³). The reaction mixture was cooled to 0 °C and stirred at this temperature for 20 min. *N*-Bromosucinnimide (2.10 eq) was added very slowly to the solution at 0 °C as the addition is exothermic. The reaction mixture was stirred at room temperature for 24 h, then sodium hydroxide solution (2 M, approx 30 cm³) was added. The solution was extracted with dichloromethane (3 × 25 cm³), the combined organic extracts dried ($MgSO_4$) and solvent removed under reduced pressure. The resulting product was then recrystallised from toluene. The following imidazolines were made using this procedure:

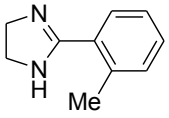

2-(2-Methylphenyl)-4,5-dihydro-1*H*-imidazole **2.97**, (58%), mp 89 °C, [lit., [9] 88 °C] δ_H (250 MHz, $CDCl_3$) 7.35 (1H, d, ^3J 7.1) 7.23-7.11 (3H, m), 5.39 (1H, br s), 3.67 (4H, s) and 2.38 (3H, s); δ_C 166.34 (quat), 137.30 (quat), 132.60 (quat), 131.34 (CH), 130.43 (CH), 128.82 (CH), 126.10 (CH), 49.90 (CH_2) and 20.78 (CH_3).

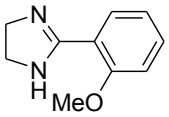

2-(2-Methoxyphenyl)-4,5-dihydro-1*H*-imidazole **2.98**, (55%), mp 72 °C, [lit., [10] 60 – 64 °C] δ_H (200 MHz, $CDCl_3$) 8.16 (1H, d, ^3J 7.6), 7.44 (1H, m) 7.13-6.97 (2H, m), 3.97 (3H, s) and 3.79 (4H, s); δ_C (63 MHz, $CDCl_3$) 132.13 (CH), 131.49 (CH), 121.49 (CH), 111.74 (CH), 62.37 (2 × CH_2) and 56.13 (CH_3).

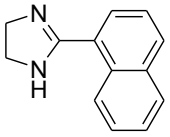

2-(1-Naphthyl)-4,5-dihydro-1*H*-imidazoline **2.99**, (61%), mp 132-133 °C, [lit., [11] 133.5 – 135.5 °C] δ_H 8.57 (1H, m), 7.83-8.63 (3H, m), 7.45-7.33 (3H, m) and 3.76 (4H, s); δ_C 165.38 (quat), 162.94 (quat), 134.08 (quat), 131.27 (quat), 130.78 (CH), 128.64 (CH), 127.16 (CH), 126.87 (CH), 126.52 (CH), 126.40 (CH), 125.58 (CH) and 62.85 (CH_2).

Dehydrogenation of Imidazolines

This general method was used to dehydrogenate 2-(1-naphthyl)imidazoline successfully. To a solution of 2-(1-naphthyl)imidazoline (3.18 g, 16.2 mmol) in dimethylsulfoxide (150 cm³) was added diacetoxyiodobenzene (1.1 eq, 5.75 g) and potassium carbonate (1.1 eq, 2.47 g). This solution was stirred under a nitrogen atmosphere at room temperature for 24 h, then sodium hydroxide solution (2 M, 40 cm³) and ethyl acetate (20 cm³) were added to the reaction mixture which was stirred for a further 10 min. The reaction was extracted with ethyl acetate (5 × 20 cm³) and the combined organic layers back extracted with water (2 × 500 cm³). The organic layer was then dried ($MgSO_4$) and the solvent removed under reduced pressure. The resulting solid was recrustallised from toluene.

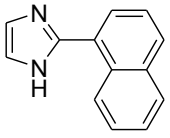

2-(1-Naphthyl)imidazole **2.101**, (45%), mp 195 – 197 °C, [lit., δ_H (250 MHz, DMSO-*d*$_6$) 12.54 (1H, br s, NH), 9.02 (1H, m), 8.30 (1H, s), 7.97 (2H, m), 7.78 (1H, dd, ^3J 7.2, ^nJ 1.1), 7.57 (2H, m), 7.33 (1H, br s) and 7.18 (1H, br s); δ_C (63 MHz, DMSO-*d*$_6$) 145.52 (quat), 133.77 (quat), 130.38 (quat), 129.06 (CH), 128.77 (CH), 128.31 (CH), 128.22 (quat), 126.69 (CH), 126.64 (CH), 126.27 (CH), 126.21 (CH), 125.40 (CH) and 117.61 (CH).

N-Amination of Imidazoles

N-amination method 1 was attempted on the 1-amino(2-naphthyl)imidazole and method 2 was attempted on 2-phenylimidazole, but neither were successful.

N-Amination of Imidazolines

Information gleaned from a Japanese patent proposes that the *N*-amination of imidazoles problem may be overcome by *N*-aminating the imidazoline before the dehydrogenation step. 2-(1-Naphthyl)-4,5-dihydro-1*H*-imidazoline 2.101 was subjected to the general *N*-amination general method 3 (which from experience is the most adaptable to various heterocycles). Although a peak appeared in the expected NH_2 region, it was very small, equating to approximately 5% of the material recovered after 2 subsequent amination reactions. This implied that the amination, although possible, was not a viable route to the desired imidazoles for practical reasons.

N-Amino Heterocycles in the Synthesis of Ketene Generating FVP Precursors

N-Amination of Pyrazole

The pyrazole (50 mmol) and sodium hydroxide (4.13 eq) were mixed in water (20 cm^3) and heated to 50 °C [12]. At this temperature a complete solution was obtained, to which hydroxylamine-*O*-sulfonic acid (3 eq) was added portionwise over 15 min with vigorous stirring to minimise foaming. After addition the reaction was heated to 60 °C for 1.5 h, then allowed to cool to room temperature and stirred for 1 h. The aqueous solution was extracted with dichloromethane (3 × 30 cm^3). The organic extract was washed with water (40 cm^3) then dried ($MgSO_4$) and the solvent removed under reduced pressure to yield the desired *N*-aminopyrazole **3.6** as a brown oil.

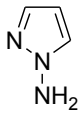

1-Aminopyrazole 3.6, (43%), bp 55 °C (2 Torr) [lit., [12] 80 °C (10 Torr)]; δ_H (250 MHz, $CDCl_3$) 7.25 (2 H, t, ^3J 3.1), 5.99 (1 H, t, ^3J 3.1) and 5.55 (2 H, br s); δ_C (63 MHz, $CDCl_3$) 138.21 (CH), 129.25 (CH) and 104.92 (CH).

Methoxymethylene Meldrum's acid 3.2

Meldrum's Acid (28.8 g, 120 mmol) and trimethyl orthoformate (140 cm^3) were heated to reflux for 3 h. The mixture was cooled to room temperature, then placed in the freezer overnight. The yellow-orange precipitate was filtered off and washed with light petroleum to give methoxymethylene Meldrum's acid **3.2** as a pale yellow solid (14.7 g, 40%).

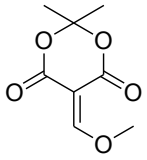

Methoxymethylene Meldrum's acid 3.2 mp 126 – 127 °C (lit., [13] 121 -122 °C), δ_H (250 MHz, $CDCl_3$) 8.10 (1H, s), 4.21 (3H, s) and 1.62 (6H, s); δ_C (63 MHz, $CDCl_3$) 175.04 (CH), 162.85 (quat), 158.33 (quat), 104.40 (quat), 96.42 (quat), 66.09 (CH_3) and 26.95 (2 × CH_3).

Reaction of *N*-aminopyrazole 3.6 with Methoxymethylene Meldrum's Acid 3.2

The *N*-aminopyrazole (5 mmol) was dissolved in acetonitrile (5 cm^3) and to this solution was added methoxymethylene Meldrum's acid (1 eq). The reaction solution was stirred at room temperature for 1 h and the solvent then removed under reduced pressure. The resulting solid was recrystallised from ethanol.

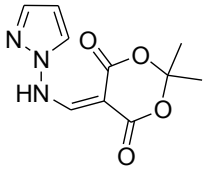

5-(*N*-aminopyrazolyl)methylene-2,2-dimethyl-1,3-dioxane-4,6-dione 3.7, (86%) mp 123-125 °C [lit., [12] 122-124 °C]; δ_H (250 MHz, $CDCl_3$) 11.53 (1H, br d, ^3J 9.0), 8.39 (1H, br d, ^3J 9.0), 7.55 (2H, m), 6.40 (1H, t, ^3J 2.3) and 1.75 (6H, s).

4-Phenylpyrazole 3.22

Phosphorous oxychloride (8.4 cm^3, 0.09 mol) was added to cold anhydrous DMF (8.5 cm^3) cooled with an ice bath and with vigourous stirring. This was left to stir with the ice bath in place for 10 min. A solution of phenylacetic acid (4.08 g, 0.03 mol) in anhydrous DMF (15 cm^3) was made, and added dropwise with care to the cooled phosphorous oxychloride solution. After addition the reaction mixture was heated to 70 °C for 18 h. The mixture was poured over crushed ice (~ 40 cm^3) in a large beaker and 30% (w/w) aq NaOH was added with stirring until the solution was

basic to pH paper, at this point a solid precipitated from the basic solution. This solid was filtered off and discarded, and the filtrate was extracted with DCM (3 × 30 cm^3). The combined organics were dried over $MgSO_4$ and the solvent removed under reduced pressure. The resulting residue is the phenylacrolein, which was dissolved in ethanol (35 cm^3), to which was added hydrazine monohydrate (3.75 g, 0.075 mol) and the reaction solution stirred at room temperature overnight. The solid phenylpyrazole product was filtered off and recrystallised from ethanol.

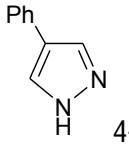

4-Phenylpyrazole 3.22, (62%) mp 226 – 228 °C [lit., [14] 228 °C]; δ_H (250 MHz, DMSO-*d*6); 12.95 (1H, br s), 8.06 (2H, br s), 7.61 (2H, m), 7.36 (2H, m) and 7.19 (1H, m); δ_C (63 MHz, DMSO-*d*6) 136.24 (quat), 132.88 (quat), 128.75 (2 × CH), 125.72 (CH), 125.33 (CH), 125.11 (2 × CH) and 121.11 (CH)

N-Amination of 4-phenylpyrazole

General method 3 had to be adapted for the *N*-amination of 4-phenylpyrazole. 4-Phenylpyrazole (0.151 g, 1.05 mmol) was suspended in aq. NaOH (0.150 g in 1.5 cm^3 water) and heated to 55 °C, and DMSO (0.68 cm^3) and IPA (0.68 cm^3) added to form a complete solution. To the reaction mixture was added hydroxylamine-*O*-sulfonic acid (0.4 g, 3.37 equiv) in small portions. After the addition, the heat was removed and the reaction stirred at RT for 1 h. The resulting white solid was filtered and subjected to the same reaction conditions for a second time. This solid was then recrystallised from ethanol and was identified as 1-amino-4-phenylpyrazole **3.26**.

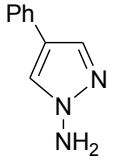

1-Amino-4-phenylpyrazole 3.26, (72%) mp 105 - 106 °C [lit. [15] 107 °C]; δ_H (360 MHz, DMSO-*d*6); 7.99 (1H, s), 7.73 (1H, s), 7.62-7.56 (2H, m), 7.38 – 7.32 (2H, m), 7.21 – 7.16 (1H, m) and 6.49 (2H, br s); δ_C (63 MHz, DMSO) 137.29

(quat), 131.33 (quat), 130.92 (CH), 128.75 (2 × CH), 125.39 (CH), 125.17 (2 × CH) and 121.45 (CH).

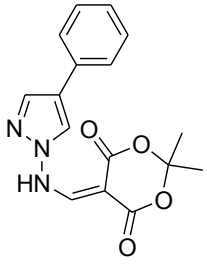

5-(4-Phenyl-*N*-aminopyrazolyl)methylene-2,2-dimethyl-1,3-dioxane-4,6-dione **3.30** was synthesised *via* the method used for condensation reaction of *N*-aminopyrazole with methoxymethylene Meldrum's acid and the product recrystallised from EtOH, (38%) mp 148 - 149 °C ; (Found M^+ 313.1058, $C_{16}H_{15}N_3O_4$ requires 313.1053) δ_H (360 MHz, $CDCl_3$); 11.53 (1H, br s), 8.40 (1H, s), 7.74 (2H, s), 7.41 (2H, d, ^3J 7.6), 7.34 (2H, t, ^3J 7.5), 7.25 (1H, t, ^3J 7.4) and 1.70 (6H); δ_C (90 MHz, $CDCl_3$) 164.70 (quat), 162.02 (quat), 157.22 (CH), 136.46 (CH), 130.53 (quat), 129.01 (2 × CH), 127.53 (CH), 125.72 (2 × CH), 124.59 (CH), 124.33 (quat), 105.72 (quat), 88.03 (quat) and 27.11 (2 × CH_3); δ_C (90 MHz, $CDCl_3$, dept 135) 157.22 (CH), 136.46 (CH), 129.01 (2 × CH), 127.53 (CH), 125.72 (2 × CH), 124.59 (CH) and 27.11 (2 × CH_3); *m/z* 313 (M^+, 5%), 255 (86), 211 (100), 159 (48) and 102 (21).

FVP Temperature Profile for 5-(4-phenyl-*N*-aminopyrazolyl)methylene-2,2-dimethyl-1,3-dioxane-4,6-dione 3.30

FVP at T_f 500 °C, (14.6 mg, T_i 198 - 200 °C, P 2.6 – 2.8 × 10^{-2} Torr, t 20 min) gave 6-phenylpyrazolotriazinium-4-olate **3.33** (*ca* 96%), and 5-(4-phenyl-*N*-aminopyrazolyl)methylene-2,2-dimethyl-1,3-dioxane-4,6-dione **3.30** starting material (*ca* 4%).

FVP at T_f 600 °C, (12.8 mg, T_i 197 - 199 °C, P 2.3 – 2.7 × 10^{-2} Torr, t 22 min) gave 6-phenylpyrazolotriazinium-4-olate **3.33** (*ca* 78%) and 5-phenylpyrazolopyridazin-4-one **3.34** (*ca* 22%).

FVP at T_f 700 °C, (14.1 mg, T_i 198 - 199 °C, P 2.7 – 3.4 × 10^{-2} Torr, t 21 min) gave 6-phenylpyrazolotriazinium-4-olate **3.33** (*ca* 31%) and 5-phenylpyrazolopyridazin-4-one **3.34** (*ca* 69%).

FVP at T_f 750 °C, (16.5 mg, T_i 194 - 196 °C, P 2.8 – 3.2 × 10^{-2} Torr, t 20 min) gave 5-phenylpyrazolopyridazin-4-one **3.34** (*ca* 99%).

FVP of dimethyl 5-(4-phenyl-*N*-aminopyrazolyl)methylene-2,2-dimethyl-1,3-dioxane-4,6-dione 3.30 (44.2 mg, T_f 500 °C, T_i 186 - 188 °C, P 2.5 – 2.7 × 10^{-7} Torr, t 35 min) gave 6-phenylpyrazolo[1,2–*a*]1,2,3-triazinium-4-olate **3.33** (*ca* 70%). Diffusion pump (Edwards Diffstak 63) was used to achieve a lower FVP pressure which allowed a lower inlet temperature to be used due to low precursor volitility. The pyrolysate was removed by distillation of $CHCl_3$ across the U-tube, and passed through a small silica plug to removed impurities. Solvent was removed under reduced pressure to yield 6-phenylpyrazolo[1,2–*a*]1,2,3-triazinium-4-olate.

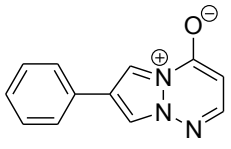

6-phenylpyrazolo[1,2–*a*]1,2,3-triazinium-4-olate 3.33, (46%) mp 195 - 197 °C ; (Found M^+ 211.0740, $C_{12}H_9N_3O$ requires M 211.0736); δ_H (360 MHz, $CDCl_3$) 8.61 (1H, s), 8.32 (1H, s), 7.81 (1H, d, ^3J 6.6), 7.62 (2H, d, ^3J 6.9), 7.51 (2H, ^3J 6.9), 7.45 (1H, ^3J 7.1) and 5.46 (1H, d, ^3J 6.6); δ_C (90 MHz, $CDCl_3$) 152.51 (quat), 148.29 (CH), 138.74 (quat), 134.43 (quat), 129.39 (2 × CH), 129.05 (CH), 128.80 (CH), 126.28 (2 ×CH), 120.22 (CH), and 113.80 (CH); dept 90 δ_C (90 MHz, $CDCl_3$) 148.29 (CH), 129.39 (2 ×CH), 129.05 (CH), 128.80 (CH), 126.28 (2 ×CH), 120.22 (CH), and 113.80 (CH); *m/z* 211 (M^+, 100%), 144 (95) and 89 (18).

FVP of dimethyl 5-(4-phenyl-*N*-aminopyrazolyl)methylene-2,2-dimethyl-1,3-dioxane-4,6-dione **3.30**, (32.0 mg, T_f 750 °C, T_i 180 - 183 °C, P 1.5 – 2.6 × 10^{-7} Torr, t 30 min) gave 5-phenylpyrazolopyridazin-4-one **3.34** (*ca* 54%), pyrolysate was purified by distillation of $CHCl_3$ across the U-tube to remove impurities, and the remaining solid purified by dry flash chromatography (ethyl acetate : hexane, 20 : 80). Solvent was removed under reduced pressure to yield 5-phenylpyrazolopyridazin-4-one.

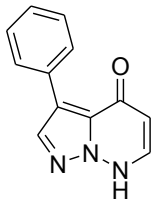

5-Phenylpyrazolopyridazin-4-one **3.34**, (32%) mp 231 – 234 °C; (Found M^+ 211.0738 $C_{12}H_9N_3O$ requires M 211.0736); δ_H (360 MHz, $CDCl_3$); 8.98 (1H, s), 8.11 (1H, br d, ^3J 5.0), 7.99 (1H, s), 7.62 – 7.57 (2H, m), 7.49 – 7.44 (2H, m), 7.40 – 7.38 (1H, m) and 6.50 (1H, br d, ^3J 5.0); δ_C (90 MHz, $CDCl_3$) 154.78 (quat), 142.56 (CH), 142.23 (CH), 134.55 (quat), 129.92 (CH), 129.85 (CH), 129.64 (2 × CH), 129.45 (2 × CH), 127.89 (quat) and 109.69 (quat); *m/z* 211 (M^+, 100%), 139 (43) and 89 (22).

Reaction of *N*-aminopyrazole to form acrylic ester type derivatives

The *N*-aminopyrazole (5 mmol) was dissolved in acetonitrile (5 cm^3) and to this solution was added the corresponding acrylic ester type reactant (1 eq). The reaction solution was stirred at room temperature for 1 h and the solvent then removed under reduced pressure. The resulting solid was recrystallised from ethanol.

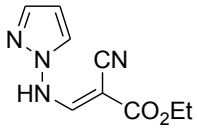

2-(Cyano)-3-(pyrazol-1-ylamino)acrylic acid ethyl ester 3.35a, (68%) from the reaction of *N*-aminopyrazole with ethyl (ethoxymethylene)cyano acetate. The ^{1}H NMR of 3.35a was extremely complicated, even after recrystallisation. This is due to the presence of two different rotomers and instances of these types of isomers, with the nitrile and ethyl ester groups either *E* or *Z* have been reported previously in the literature. [16] The following NMR data reported is that of the most prevalent isomer. mp 148 – 149 ^{o}C (Found M^{+} 206.0799, $C_9H_{10}N_4O_2$ requires *M* 206.0798); δ_H (250 MHz, $CDCl_3$) 9.36 (1H, m), 9.27 (1H, m), 8.70 (1H, s), 7.67 (1H, m), 4.38 (2H, q, ^{3}J 7.2) and 1.36 (3H, t, ^{3}J 7.0) NH signal not observed; δ_C (63 MHz, DMSO-*d*$_6$) 170.93 (quat), 153.83 (quat), 146.19 (CH), 136.92 (CH), 136.39 (CH), 127.31 (quat), 123.16 (CH), 61.57 (CH_2) and 14.84 (CH_3); *m/z* 206 (M^{+}, 100%), 160 (67), 122 (78), 113 (89), 84 (94), 68 (87) and 49 (94).

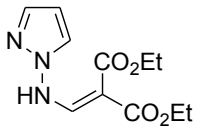

2-(Pyrazol-1-ylaminomethylene)malonic acid 3.35b, from the reaction of *N*-aminopyrazole with diethyl ethoxymethylenemalonate (67%) mp 94 – 96 ^{o}C; (Found M^{+} 253.1056, $C_{11}H_{15}N_3O_4$ requires *M* 253.1053); δ_H (250 MHz, $CDCl_3$) 11.09 (1H, NH, d, ^{3}J 10.8), 8.66 (1H, d, ^{3}J 10.8), 7.52 (2H, m), 6.36 (1H, m), 4.31-4.16 (4H, m, 2 × CH_2) and 1.39-1.21 (6H, m, 2 × CH_3) ; δ_C (60 MHz, DMSO) 168.41 (quat), 164.63 (quat), 157.06 (CH), 137.98 (CH), 129.12 (CH), 106.75 (CH), 95.53 (quat), 61.29 (CH_2), 60.77 (CH_2), 14.68 (CH_3) and 14.61 (CH_3); *m/z* 253 (M^{+}, 80%), 207 (100), 162 (61) and 135 (75).

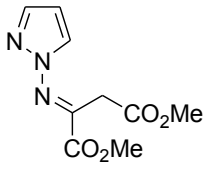

Dimethyl 2-(1H-pyrazol-1-ylimino)succinate 3.36b, from the reaction of *N*-aminopyrazole with dimethyl acetylenedicarboxylate (69%), bp 51 ^{o}C (2 Torr), (Found M^{+} 225.0743, $C_9H_{11}N_3O_4$ requires *M* 225.0744); δ_H (360 MHz,

$CDCl_3$) 6.96 (1H, d, ^3J 2.5), 6.74 (1H, d, ^3J 2.5), 5.52 (1H, t, ^3J 2.5), 3.50 (2H, s), 3.05 (3H, s) and 2.78 (3H, s) ; δ_C (90 MHz, $CDCl_3$) 168.88 (quat), 165.28 (quat), 143.20 (quat), 140.47 (CH), 133.46 (CH), 107.11 (CH), 53.21 (CH_2), 52.07 (CH_3) and 35.81 (CH_3) ; *m/z* 225 (M^+, 52%), 193 (100), 178 (40), 140 (28) and 108 (20).

3-(Pyrazol-1-ylamino)-but-2-enoic acid methyl ester

This precursor was prepared using the following method:

The *N*-aminopyrazole (3.6 mmol) and methyl acetoacetate (1 eq) were added to methanol (5 cm^3) to which was added a catalytic amount of glacial acetic acid (2 drops). The reaction solution was refluxed for 3 h after which time it was allowed to cool to room temperature and the solvent then removed under reduced pressure. The resulting solid was recrystallised from ethanol.

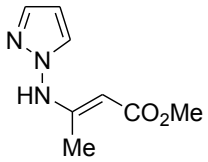

3-(Pyrazol-1-ylamino)-but-2-enoic acid methyl ester 3.37, from the reaction of *N*-aminopyrazole with methyl acetoacetate (63%), mp 78-80 °C (Found M^+ 181.0847, $C_8H_{11}N_3O_2$ requires *M* 181.0846); δ_H (250 MHz, $CDCl_3$) 10.64 (1H, s, NH), 7.46 (2H, dd, ^3J 7.7, ^4J 1.4), 6.27 (1H, t, ^3J 2.3) 4.86 (1H, s), 3.68 (3H, s) and 1.66 (3H, s) ; δ_C (63 MHz, $CDCl_3$) 170.11 (quat), 160.36 (quat), 138.73 (CH), 131.02 (CH), 105.66 (CH), 89.97 (CH), 51.23 (CH_3) and 17.59 (CH_3) ; *m/z* 181 (M^+, 100%), 149 (57), 121 (43), 108 (92) and 82 (59).

Flash Vacuum Pyrolysis Experiments – Ketene Precursors

Conditions for the pyrolyses were established in small scale experiments (*ca.* 20 mg) in which the entire contents of the trap were dissolved in a deuteriated solvent, usually DMSO-d_6 due to insolubility of pyrazolopyridazinones in $CDCl_3$, and analysed at once by ^{1}H NMR spectroscopy. These small scales pyrolyses were then

also carried out at varying furnace temperatures and the composition of the pyrolysate analysed, to construct a temperature profile. This temperature profile allowed an optimum furnace temperature to be selected for each product.

Once the conditions were established, preparative pyrolyses (>100 mg) were carried out if necessary. At the end of the pyrolysis, deuteriated solvent (usually $CDCl_3$) was distilled into the U-tube to dissolve the betaine product(s), the NMR spectrum was monitored and then the solvent was removed under reduced pressure. Any remaining solid in the U-tube that was not soluble in $CDCl_3$ was removed using ethanol/methanol, the solvent removed under reduced pressure, and a sample taken into DMSO-d_6 for NMR analysis. The precursor, pyrolysis conditions [quantity of precursor, furnace temperature (T_f), inlet temperature (T_i), pressure range (P) and pyrolysis time (t)] and yields are given. In some cases, the precursor was placed in a glass vial within the inlet tube and silica wool was inserted into the end of the vial to prevent the solid from being pulled into the furnace tube by the vacuum applied. The following flash vacuum pyrolysis experiments using ketene generating precursors were undertaken:

FVP of 5-(*N*-aminopyrazolyl)methylene-2,2-dimethyl-1,3-dioxane-4,6-dione **3.7** (148.5 mg, T_f 500 °C, T_i 145 °C, P 2.7 – 3.4 x 10^{-2} Torr, t 28 min) gave pyrazolo[1,2-*a*]1,2,3-triazinium-4-olate **3.11** (*ca* 93%).

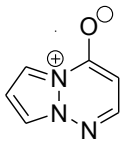

Pyrazolo[1,2-*a*]1,2,3-triazinium-4-olate **3.11**, mp 135 °C; [17] δ_H (250 MHz, $CDCl_3$) 8.39 (1H, m), 8.11 (1H, m), 7.80 (1H, d, ^3J 6.3), 6.91 (1H, t, ^3J 3.1) and 5.43 (1H, d, ^3J 6.3); δ_C (63 MHz, $CDCl_3$) 155.8 (quat), 149.53 (CH), 124.36 (CH), 118.23 (CH), 107.66 (CH) and 84.02 (CH).

FVP Temperature Profile for 2-(cyano)-3-(pyrazol-1-ylamino)acrylic acid ethyl ester 3.35a

FVP at T_f 400 °C, (19.3 mg, T_i 164 - 165 °C, P 3.1 – 3.3 × 10^{-2} Torr, t 14 min) gave 2-(cyano)-3-(pyrazol-1-ylamino)acrylic acid ethyl ester **3.35a** starting material exclusively.

FVP at T_f 450 °C, (19.9 mg, T_i 163 - 164 °C, P 3.1 – 3.3 × 10^{-2} Torr, t 12 min) gave 3-cyanopyrazolo[1,2-*a*]1,2,3-triazinium-4-olate (*ca* 95%) **3.38a** and 2-(cyano)-3-(pyrazol-1-ylamino)acrylic acid ethyl ester **3.35a** starting material (*ca* 5%).

FVP at T_f 500 °C, (19.6 mg, T_i 164 - 165 °C, P 2.2 – 32.5 × 10^{-2} Torr, t 14 min) gave 3-cyanopyrazolo[1,2-*a*]1,2,3-triazinium-4-olate **3.38a** (*ca* 96%), 2-(cyano)-3-(pyrazol-1-ylamino)acrylic acid ethyl ester **3.35a** starting material (*ca* 2%) and 3-cyanopyrazolopyridazin-4-one **3.42** (*ca* 2%).

FVP at T_f 550 °C, (20.6 mg, T_i 165 - 166 °C, P 2.6 – 2.9 × 10^{-2} Torr, t 12 min) gave 3-cyanopyrazolo[1,2-*a*]1,2,3-triazinium-4-olate **3.38a** (*ca* 61%), 3-cyanopyrazolopyridazin-4-one **3.42** (*ca* 38%) and 2-(cyano)-3-(pyrazol-1-ylamino)acrylic acid ethyl ester **3.35a** starting material (*ca* 1%).

FVP at T_f 600 °C, (19.2 mg, T_i 164 - 165 °C, P 2.1 – 3.2 × 10^{-2} Torr, t 12 min) gave 3-cyanopyrazolopyridazin-4-one **3.42** (*ca* 53%) and 3-cyanopyrazolo[1,2-*a*]1,2,3-triazinium-4-olate **3.38a** (*ca* 47%).

FVP at T_f 650 °C, (20.2 mg, T_i 166 - 167 °C, P 2.7 – 3.2 × 10^{-2} Torr, t 14 min) gave 3-cyanopyrazolopyridazin-4-one **3.42** (*ca* 77%) and 3-cyanopyrazolo[1,2-*a*]1,2,3-triazinium-4-olate **3.38a** (*ca* 23%).

FVP at T_f 700 °C, (20.3 mg, T_i 164 - 165 °C, P 2.7 – 3.1 × 10^{-2} Torr, t 12 min) gave 3-cyanopyrazolopyridazin-4-one **3.42** (*ca* 89%) and 3-cyanopyrazolo[1,2-*a*]1,2,3-triazinium-4-olate **3.38a** (*ca* 11%).

FVP at T_f 750 °C, (20.2 mg, T_i 165 - 166 °C, P 2.6 – 2.9 × 10^{-2} Torr, t 12 min) gave 3-cyanopyrazolopyridazin-4-one **3.42** (*ca* 99%).

FVP of 2-(cyano)-3-(pyrazol-1-ylamino)acrylic acid ethyl ester 3.35a (97.2 mg, T_f 500 °C, T_i 167-169 °C, P 1.6 – 1.7 × 10^{-2} Torr, t 12 min) gave 3-cyanopyrazolo[1,2-*a*]1,2,3-triazinium-4-olate **3.38a** (*ca* 90%).

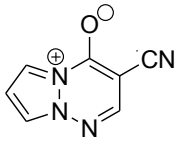

3-Cyanopyrazolo[1,2-*a*]1,2,3-triazinium-4-olate 3.38a, mp 172-174 °C, (Found M^+ 160.0378, $C_7H_4N_4O$ requires M 160.0380) δ_H (360 MHz, DMSO-d_6) 8.96 (1H, d, ^3J 3.4), 8.85 (1H, d, ^3J 3.4), 8.33 (1H, s) and 7.29 (1H, t, ^3J 3.4); δ_C (90 MHz, DMSO-d_6) 153.42 (quat), 150.14 (CH), 130.96 (CH), 123.96 (CH), 118.23 (quat), 109.85 (CH) and 70.77 (quat); *m/z* 160 (M^+, 100%), 132 (27), 129 (14) and 105 (14).

FVP of 2-(cyano)-3-(pyrazol-1-ylamino)acrylic acid ethyl ester 3.35a (102.4 mg, T_f 760 °C, T_i 165-167 °C, P 3.0 – 3.2 × 10^{-2} Torr, t 14 min) gave 3-cyanopyrazolopyridazin-4-one **3.42** (*ca* 72%).

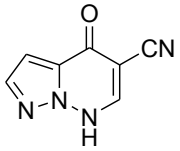

4-Oxo-4,7-dihydro-pyrazolo[1,5-*b*]pyridazine-5-carbonitrile 3.42, mp 203 - 205 °C; (Found M^+ 160.0378, $C_7H_4N_4O$ requires M 160.0380); δ_H (360 MHz, DMSO-d_6) 8.36 (1H, s), 7.96 (1H, d, ^3J 2.6) and 7.08 (1H, d, ^3J 2.6); δ_C (90 MHz, DMSO-d_6) 164.37 (quat), 145.08 (CH), 139.44 (CH), 131.06 (quat), 117.58 (quat), 100.77 (CH) and 84.92 (quat); *m/z* 160 (M^+, 58%), 147 (100) and 73 (75).

FVP Temperature Profile for 2-(pyrazol-1-ylaminomethylene)malonic acid diethyl ester 3.35b

FVP at T_f 400 °C, (21.5 mg, T_i 165 - 166 °C, P 2.1 – 2.3 × 10^{-2} Torr, t 9 min) gave 2-(pyrazol-1-ylaminomethylene)malonic acid diethyl ester **3.35b** starting material (*ca* 90%) and 3-ethoxycarbonylpyrazolo[1,2-a]1,2,3-triazinium-4-olate **3.38b** (*ca* 10%).

FVP at T_f 450 °C, (26.2 mg, T_i 163 - 164 °C, P 1.8 – 2.0 × 10^{-2} Torr, t 8 min) gave 2-(pyrazol-1-ylaminomethylene)malonic acid diethyl ester **3.35a** starting material (*ca* 81%) and 3-ethoxycarbonylpyrazolo[1,2-a]1,2,3-triazinium-4-olate **3.38b** (*ca* 19%).

FVP at T_f 500 °C, (20.3 mg, T_i 163 - 165 °C, P 1.7 – 2.0 × 10^{-2} Torr, t 8 min) gave 3-ethoxycarbonylpyrazolo[1,2-a]1,2,3-triazinium-4-olate **3.38b** (*ca* 76%) and 2-(pyrazol-1-ylaminomethylene)malonic acid diethyl ester **3.35b** starting material (*ca* 24%).

FVP at T_f 550 °C, (21.4 mg, T_i 164 - 166 °C, P 1.7 – 1.9 × 10^{-2} Torr, t 10 min) gave 3-ethoxycarbonylpyrazolo[1,2-a]1,2,3-triazinium-4-olate **3.38b** (*ca* 84%) and 4-oxo-4,7-dihydro-pyrazolo[1,5-b]pyridazine-5-carboxylic acid methyl ester **3.44** (*ca* 16%).

FVP at T_f 600 °C, (24.6 mg, T_i 163 - 165 °C, P 1.5 – 1.7 × 10^{-2} Torr, t 10 min) gave 3-ethoxycarbonylpyrazolo[1,2-a]1,2,3-triazinium-4-olate **3.38b** (*ca* 79%) and 4-oxo-4,7-dihydro-pyrazolo[1,5-b]pyridazine-5-carboxylic acid methyl ester **3.44** (*ca* 21%).

FVP at T_f 650 °C, (20.5 mg, T_i 166 - 167 °C, P 1.9 – 2.1 × 10^{-2} Torr, t 8 min) gave 3-ethoxycarbonylpyrazolo[1,2-a]1,2,3-triazinium-4-olate **3.38b** (*ca* 54%) and 4-oxo-4,7-dihydro-pyrazolo[1,5-b]pyridazine-5-carboxylic acid methyl ester **3.44** (*ca* 46%).

At furnace temperatures in excess of 650 °C pyrolysate showed a complex mixture of decomposition products which could not be separated for characterisation or quantification.

FVP of 2-(pyrazol-1-ylaminomethylene)malonic acid 3.35b (52.1 mg, T_f 575 °C, T_i 166 - 167 °C, P 2.2 – 2.6 × 10^{-2} Torr, t 15 min) gave 3-ethoxycarbonylpyrazolo[1,2-a]1,2,3-triazinium-4-olate **3.38b** (*ca* 85%). The pyrolysate was purified and the betaine separated using dry flash column chromatography (EtOAc : MeOH, 98 : 2).

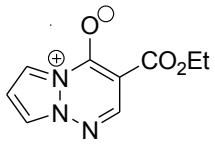

3-Ethoxycarbonylpyrazolo[1,2-*a*]1,2,3-triazinium-4-olate 3.38b, mp 161-163 °C; (Found M^+ 207.0636, $C_9H_9N_3O_3$ requires M 207.0638); δ_H (250 MHz, $CDCl_3$) 8.48 (1H, m), 8.41 (1H, s), 8.15 (1H, m), 6.91 (1H, t, ^3J 3.0), 4.28 (2H, q, ^3J 7.1) and 1.30 (3H, t, ^3J 7.1); δ_C (63 MHz, $CDCl_3$) 166.12 (quat), 162.22 (quat), 151.27 (CH), 127.43 (CH), 122.52 (CH), 108.33 (CH), 89.13 (quat), 61.64 (CH_2) and 15.51 (CH_3); *m/z* 207 (M^+, 82%), 179 (31), 162 (100), 135 (63) and 84 (45).

FVP of 2-(pyrazol-1-ylaminomethylene)malonic acid 3.35b (58.2 mg, T_f 625 °C, T_i 165 - 166 °C, P 2.6 – 2.9 × 10^{-2} Torr, t 14 min) gave 4-oxo-4,7-dihydro-pyrazolo[1,5-b]pyridazine-5-carboxylic acid methyl ester **3.44** (*ca* 46%). A pure sample was not obtained due to contamination with betaine and decomposition of product. The ^{1}H NMR spectrum quoted was established by comparison with related compounds. No other spectral information of sufficient quality was established.

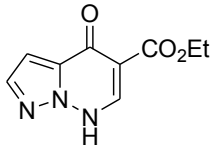

4-Oxo-4,7-dihydro-pyrazolo[1,5-b]pyridazine-5-carboxylic acid methyl ester **3.44** δ_H (250 MHz, $CDCl_3$) 8.53 (1H, s), 8.19 (1H, d, ^3J 2.7), 6.98 (1H, d, ^3J 2.7), 4.08 (2H, q, ^3J 7.1) and 1.23 (3H, t, ^3J 7.1).

FVP of 3-ethoxycarbonylpyrazolotriazinium-4-olate **3.38b** (194.1 mg, T_f 600 °C, T_i 106 - 108 °C, P 2.9 – 3.2 × 10^{-2} Torr, t 40 min) gave 4-oxo-4,7-dihydro-pyrazolo[1,5-b]pyridazine-5-carboxylic acid **3.45** (*ca* 41%).

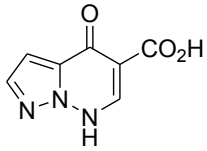

4-Oxo-4,7-dihydro-pyrazolo[1,5-b]pyridazine-5-carboxylic acid **3.45**, mp 194 - 196 °C; (Found M^+ 179.0333, $C_7H_5N_3O_3$ requires 179.0031); δ_H (250 MHz, DMSO-*d6*) 8.37 (1H, s), 7.88 (1H, d, ^3J 2.3) and 6.91 (1H, d, ^3J 2.3) OH and NH signals lost in water signal of DMSO-*d6* solvent; δ_C (90 MHz, DMSO-*d6*) 172.05 (quat), 165.43 (quat), 146.20 (CH), 140.73 (CH), 133.87 (quat), 102.36 (quat) and 101.51 (CH); *m/z*; 179 (M^+, 100%).

FVP Temperature Profile for dimethyl 2-(1H-pyrazol-1-ylimino)succinate **3.36b**

FVP at T_f 450 °C, (28.9 mg, T_i 119 - 124 °C, P 2.6 – 3.4 × 10^{-2} Torr, t 45 min) gave dimethyl 2-(1*H*-pyrazol-1-ylimino)succinate **3.36b** starting material (*ca* 69%), the *Z*-isomer of the starting material (*ca* 25%) and 2-methoxycarbonylpyrazolo[1,2-a]1,2,3-triazinium-4-olate **3.39** (*ca* 6%).

FVP at T_f 500 °C, (25.7 mg, T_i 118 - 124 °C, P 1.4 – 1.9 × 10^{-2} Torr, t 38 min) gave dimethyl 2-(1*H*-pyrazol-1-ylimino)succinate **3.36b** starting material (*ca* 67%), 2-

methoxycarbonylpyrazolo[1,2-a]1,2,3-triazinium-4-olate **3.39** (*ca* 18%) and the *Z*-isomer of the starting material (*ca* 15%).

FVP at T_f 550 °C, (30.1 mg, T_i 119 - 123 °C, P 3.1 – 4.1 × 10^{-2} Torr, t 45 min) gave dimethyl 2-(1*H*-pyrazol-1-ylimino)succinate **3.36b** starting material (*ca* 41%), 2-methoxycarbonylpyrazolo[1,2-a]1,2,3-triazinium-4-olate **3.39** (*ca* 36%), the *Z*-isomer of the starting material (*ca* 16%) and 4-oxo-4,7-dihydro-pyrazolo[1,5-b]pyridazine-6-carboxylic acid methyl ester **3.47** (*ca* 7%).

FVP at T_f 600 °C, (25.8 mg, T_i 120 - 124 °C, P 1.3 – 2.0 × 10^{-2} Torr, t 40 min) gave 4-oxo-4,7-dihydro-pyrazolo[1,5-b]pyridazine-6-carboxylic acid methyl ester **3.47** (*ca* 54%), 2-methoxycarbonylpyrazolo[1,2-a]1,2,3-triazinium-4-olate **3.39** (*ca* 28%), dimethyl 2-(1*H*-pyrazol-1-ylimino)succinate **3.36b** starting material (*ca* 10%) and the *Z*-isomer of the starting material (*ca* 8%).

FVP at T_f 650 °C, (32.3 mg, T_i 121 - 123 °C, P 3.2 – 4.0 × 10^{-2} Torr, t 45 min) gave 4-oxo-4,7-dihydro-pyrazolo[1,5-b]pyridazine-6-carboxylic acid methyl ester **3.47** (*ca* 80%), 2-methoxycarbonylpyrazolo[1,2-a]1,2,3-triazinium-4-olate **3.39** (*ca* 16%) and dimethyl 2-(1*H*-pyrazol-1-ylimino)succinate **3.36b** starting material (*ca* 4%).

FVP of dimethyl 2-(1H-pyrazol-1-ylimino)succinate 3.36b (134.1 mg, T_f 575 °C, T_i 120 - 123 °C, P 1.9 – 2.6 × 10^{-2} Torr, t 64 min) gave 2-methoxycarbonylpyrazolo[1,2-a]1,2,3-triazinium-4-olate **3.39** (*ca* 37%), pyrolysate was retrieved from the U-tube by distillation of $CHCl_3$, which was then removed under reduced pressure and the residue purified by dry flash chromatography (eluent EtOAc : Hexane, 20 : 80).

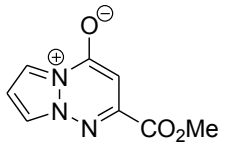

2-Methoxycarbonylpyrazolo[1,2-*a*]1,2,3-triazinium-4-olate 3.39, mp 147 - 149 °C; ($C_8H_7N_3O_3$ found M^+ 193.0593, requires M 193.0595); δ_H (250 MHz, $CDCl_3$) 8.97 (1H, m), 8.75 (1H, m), 7.36 (1H, t, ^3J 3.4), 5.81 (1H, s) and

3.93 (3H, s); δ_C (63 MHz, $CDCl_3$) 167.92 (quat), 159.85 (quat), 157.77 (CH), 124.42 (CH), 123.68 (CH), 110.64 (CH), 90.44 (quat) and 51.51 (CH_3); *m/z* 193 (M^+, 100%).

FVP of dimethyl 2-(1H-pyrazol-1-ylimino)succinate **3.36b**, (226.1 mg, T_f 700 °C, T_i 120 - 123 °C, P 2.2 – 3.0 × 10^{-2} Torr, t 84 min) gave 4-oxo-4,7-dihydro-pyrazolo[1,5-b]pyridazine-6-carboxylic acid methyl ester **3.47** (*ca* 49%). The pyrolysate was purified by distillation of $CHCl_3$ through the U-tube to removed all $CDCl_3$ soluble impurities, the remaining product scraped from the U-tube using EtOH to ensure all solid was harvested, which was then removed under reduced pressure and the residue purified by dry flash chromatography (eluent EtOAc : Hexane, 20 : 80).

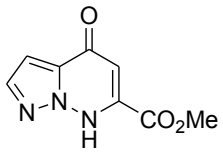

4-Oxo-4,7-dihydro-pyrazolo[1,5-b]pyridazine-6-carboxylic acid methyl ester **3.47**, mp 235 - 236 °C; (Found M^+ 193.0592, $C_8H_7N_3O_3$ requires *M* 193.0595); δ_H (250 MHz, DMSO – d_6) 12.72 (1H, br s), 8.20 (1H, d, ^3J 2.5), 7.01 (1H, s), 6.97 (1H, d, ^3J 2.5) and 3.99 (3H, s); δ_C (63 MHz, DMSO – d_6) 168.12 (quat), 157.56 (quat), 143.55 (quat), 140.89 (CH), 130.61 (quat), 97.34 (CH), 96.70 (CH) and 53.44 (CH_3); *m/z* 193 (M^+, 100%).

FVP Temperature Profile for 3-(pyrazol-1-ylamino)-but-2-enoic acid methyl ester 3.37

FVP at T_f 450 °C, (25.7 mg, T_i 143 - 146 °C, P 2.6 – 2.9 × 10^{-2} Torr, t 11 min) gave 3-(pyrazol-1-ylamino)-but-2-enoic acid methyl ester **3.37** starting material (*ca* 66%), 2-methylpyrazolo[1,2-a]1,2,3-triazinium-4-olate **3.40** (*ca* 31%) and 6-methyl-4-oxo-4,7-dihydro-pyrazolo[1,5-b]pyridazine **3.49** (*ca* 3%).

FVP at T_f 500 °C, (24.9 mg, T_i 142 - 146 °C, P 2.2 – 3.1 × 10^{-2} Torr, t 12 min) gave 3-(pyrazol-1-ylamino)-but-2-enoic acid methyl ester **3.37** starting material (*ca* 53%), 2-methylpyrazolo[1,2-a]1,2,3-triazinium-4-olate **3.40** (*ca* 34%) and 6-methyl-4-oxo-4,7-dihydro-pyrazolo[1,5-b]pyridazine **3.49** (*ca* 13%).

FVP at T_f 550 °C, (30.7 mg, T_i 143 - 147 °C, P 2.9 – 3.9 × 10^{-2} Torr, t 14 min) gave 3-(pyrazol-1-ylamino)-but-2-enoic acid methyl ester **3.37** starting material (*ca* 45%), 2-methylpyrazolo[1,2-a]1,2,3-triazinium-4-olate **3.40** (*ca* 33%) and 6-methyl-4-oxo-4,7-dihydro-pyrazolo[1,5-b]pyridazine **3.49** (*ca* 22%).

FVP at T_f 600 °C, (25.1 mg, T_i 143 - 146 °C, P 2.5 – 2.9 × 10^{-2} Torr, t 11 min) gave 3-(pyrazol-1-ylamino)-but-2-enoic acid methyl ester **3.37** starting material (*ca* 26%), 2-methylpyrazolo[1,2-a]1,2,3-triazinium-4-olate **3.40** (*ca* 35%) and 6-methyl-4-oxo-4,7-dihydro-pyrazolo[1,5-b]pyridazine **3.49** (*ca* 39%).

FVP at T_f 650 °C, (23.9 mg, T_i 142 - 144 °C, P 2.9 – 3.4 × 10^{-2} Torr, t 13 min) gave 3-(pyrazol-1-ylamino)-but-2-enoic acid methyl ester **3.37** starting material (*ca* 11%), 2-methylpyrazolo[1,2-a]1,2,3-triazinium-4-olate **3.40** (*ca* 17%) and 6-methyl-4-oxo-4,7-dihydro-pyrazolo[1,5-b]pyridazine **3.49** (*ca* 72%).

FVP at T_f 700 °C, (25.8 mg, T_i 141 - 144 °C, P 3.2 – 3.9 × 10^{-2} Torr, t 14 min) gave 2-methylpyrazolo[1,2-a]1,2,3-triazinium-4-olate **3.40** (*ca* 9%) and 6-methyl-4-oxo-4,7-dihydro-pyrazolo[1,5-b]pyridazine **3.49** (*ca* 91%).

FVP at T_f 750 °C, (25.7 mg, T_i 140 - 146 °C, P 2.6 – 3.6 × 10^{-2} Torr, t 11 min) gave 6-methyl-4-oxo-4,7-dihydro-pyrazolo[1,5-b]pyridazine **3.49** (*ca* 99%).

FVP of dimethyl 3-(pyrazol-1-ylamino)-but-2-enoic acid methyl ester 3.37 (163.1 mg, T_f 600 °C, T_i 136 - 140 °C, P 2.9 – 3.8 × 10^{-2} Torr, t 94 min) gave 2-methylpyrazolo[1,2-a]1,2,3-triazinium-4-olate **3.40** (*ca* 30%). The pyrolysate was retrieved from the U-tube by distillation of $CHCl_3$, which was then removed under reduced pressure and the residue purified by dry flash chromatography (eluent

EtOAc : Hexane, 20 : 80). However, chromatography could not remove all impurities present and so the betaine is chacterised by inference.

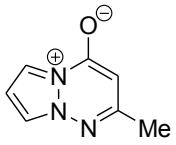

2-Methylpyrazolo[1,2-*a*]1,2,3-triazinium-4-olate **3.40**, mp 167 – 169 °C; (Found M^+ 149.0526, $C_7H_7N_3O$ requires *M* 149.0522); δ_H (360 MHz, DMSO – *d*$_6$) 8.32 (1H, m), 8.03 (1H, m), 6.86 (1H, t, ^3J 3.2), 5.35 (1H, s) and 2.29 (3H, s); δ_C (63 MHz, DMSO-*d*$_6$) 162.21 (quat), 154.22 (quat), 150.46 (CH), 121.44 (CH), 120.85 (CH), 111.44 (CH), and 21.77 (CH_3); *m/z*; 149 (M^+, 100%).

FVP of dimethyl 3-(pyrazol-1-ylamino)-but-2-enoic acid methyl ester **3.37** (84.6 mg, T_f 750 °C, T_i 138 - 141 °C, *P* 2.5 – 2.7 × 10^{-2} Torr, *t* 34 min) gave 6-methyl-4-oxo-4,7-dihydro-pyrazolo[1,5-b]pyridazine **3.49** (*ca* 30%). The pyrolysate was cleaned of impurities by distillation of $CHCl_3$ across the U-tube, and the product was then removed by dissolution into EtOH and the solvent was removed under reduced pressure.

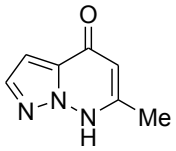

6-Methyl-4-oxo-4,7-dihydro-pyrazolo[1,5-b]pyridazine **3.49**, mp 222 - 223 °C; (Found M^+ 149.0523, $C_7H_7N_3O$ requires *M* 149.0522); δ_H (360 MHz, DMSO – *d*$_6$); 11.96 (1H, br s), 7.84 (1H, d, ^3J 2.5), 6.72 (1H, d, ^3J 2.5), 6.32 (1H, s) and 2.42 (3H, s); δ_C (90 MHz, DMSO – *d*$_6$) 157.16 (quat), 153.58 (quat), 138.64 (CH), 129.52 (quat), 99.94 (CH), 96.46 (CH) and 22.74 (CH_3); *m/z*; 149 (M^+, 100%).

Indazole ring systems

N-Amination of indazole

Indazole (17 mmol) was suspended in an aqueous solution of sodium hydroxide (4.0 g) in water (50 cm^3) water and heated to 55 ^oC. At this temperature ethanol was added dropwise until a complete solution was obtained. Hydroxylamine-*O*-sulfonic acid (3 eq) was added portionwise over 25 min with vigorous stirring to minimise foaming. After addition the reaction was allowed to cool to room temperature and stirred for 1 h. Water (30 cm^3) was added and the aqueous solution extracted with dichloromethane (4 × 30 cm^3). The organic extract was then dried ($MgSO_4$) and the solvent removed under reduced pressure to yield the two *N*-aminoindazole isomers in approximately 1:1 ratio. The 1-aminoindazole could be obtained as a pure isomer by recrystallisation of the mixture twice from toluene. 2-Aminoindazole is characterised by inference as subsequent recrystallisations could not remove all traces of the 1-aminoindazole. Original ^1H NMR spectroscopy data from Adger *et al*[18] assigns the indazole singlet signals as δ_H 8.05 for 1-aminoindazole and δ_H 7.75 for 2-aminoindazole, with an aromatic multiplet integrating to four protons at δ_H 7.95 – 6.85 and δ_H 7.75 – 6.75 respectively. This would suggest that the isomer with the highest δ_H value would be expected to be the 1-aminoindazole. This was the authors original assignment, however X-ray crystal data has found this is not the case.

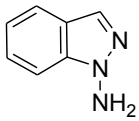

1-Aminoindazole **3.88**, (46%) mp 98 - 101 °C ; δ_H (360 MHz, $CDCl_3$); 7.87 (1H, s), 7.67 (1H, m), 7.59 (1H, m), 7.40 (1H, m), 7.14 (1H, m) and 5.28 (2H, br s); δ_C (90 MHz, $CDCl_3$) 143.33 (quat), 126.13 (CH), 121.23 (quat), 120.88 (CH), 120.11 (CH), 119.93 (CH) and 117.44 (CH); *m/z* 133 (M^+, 71%) and 118 (100).

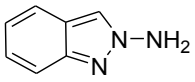

2-Aminoindazole **3.89**, (53%); δ_H (360 MHz, $CDCl_3$); 7.94 (1H, s), 7.64 (2H, m), 7.31 (1H, t, ^3J 7.9), 7.10 (1H, m) and 5.79 (2H, br s); δ_C (90 MHz, $CDCl_3$) 145.91 (quat), 125.17 (CH), 120.83 (quat), 120.06 (CH), 119.98 (CH), 119.88 (CH) and 116.74 (CH); *m/z* 133 (M^+, 66%) and 118 (100).

Reaction of *N*-aminoindazoles with methoxymethylene Meldrum's acid

1-Aminoindazole derivative

As the 1-aminoindazole was successfully obtained as a single pure isomer, this was reacted with MMMA by the same method as the previous *N*-amino heterocycles. However when the 1:1 mixture of 1- and 2-aminoindazoles was reacted with MMMA under the same conditions, a precipitate was quickly observed from the reaction mixture. On filtration and NMR analysis it was found to be the methylene Meldrum's acid derivative of the 2-aminoindazole, so that in two different ways both methylene Meldrum's acid derivatives could be obtained as pure isomers.

The 1-aminoindazole (5 mmol) was dissolved in acetonitrile (5 cm^3) and to this solution was added methoxymethylene Meldrum's acid (1 eq). The reaction solution was stirred at room temperature for 1 h and the solvent then removed under reduced pressure. The resulting solid was recrystallised from ethanol to give 5-(1-aminoindazol-1-yl)methylene-2,2-dimethyl-1,3-dioxane-4,6-dione **3.90** (71%).

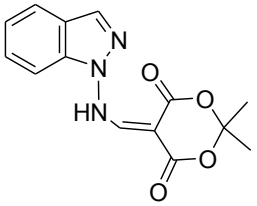

5-(1-Aminoindazol-1-yl)methylene-2,2-dimethyl-1,3-dioxane-4,6-dione **3.90** (71%) mp 153 - 154 °C; (Found M^+ 287.0904, $C_{14}H_{13}N_3O_4$ requires *M* 287.0905) ; δ_H (360 MHz, $CDCl_3$) 11.43 (1H, s, NH), 8.51 (1H, s), 8.10 (1H, s), 7.83 (1H, d, ^3J 8.0), 7.58 (1H, t, ^3J 8.0), 7.50 (1H, d, ^3J 8.0), 7.36 (1H, t, ^3J

8.0), 1.84 (6H, s); δ_C (90 MHz, $CDCl_3$) 170.26 (quat), 169.92 (quat), 159.41 (CH), 146.77 (quat), 134.34 (CH), 128.59 (CH), 122.92 (CH), 121.76 (quat), 121.57 (CH), 116.80 (quat), 109.53 (quat), 108.30 (CH), 27.21 (2 × CH_3), *m/z* 287 (M^+, 17%), 229 (87), 131 (50) and 42 (100)

2-Aminoindazole derivative

A 1:1 mixture of 1- and 2-aminoindazoles (5 mmol) was dissolved in acetonitrile (5 cm^3) and to this solution was added methoxymethylene Meldrum's acid (1 eq). The reaction solution was stirred at room temperature for 1h to ensure complete reaction, but a precipitate was quickly observed from the reaction mixture. The precipitate was removed from the reaction mixture by vacuum filtration and the solid recrystallised from ethanol to give 5-(2-aminoindazol-2-yl)methylene-2,2-dimethyl-1,3-dioxane-4,6-dione **3.91** (42%).

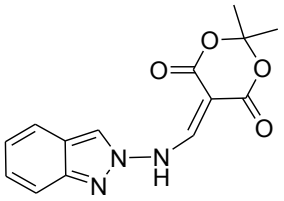

5-(2-Aminoindazol-2-yl)methylene-2,2-dimethyl-1,3-dioxane-4,6-dione 3.91 (42%) mp 166 - 167 °C; (Found M^+ 287.0902, $C_{14}H_{13}N_3O_4$ requires *M* 287.0905) ; δ_H (360 MHz, $CDCl_3$) 12.11 (1H, s, NH), 8.70 (1H, s), 8.12 (1H, s), 7.72 – 7.67 (2H, m), 7.41 (1H, m), 7.21 (1H, m), 1.79 (6H, s); δ_C (90 MHz, $CDCl_3$) 184.64 (quat), 171.145 (quat), 169.65 (quat), 159.06 (CH), 155.14 (CH), 142.65 (CH), 142.53 (CH), 140.17 (quat), 135.35 (quat), 134.24 (quat), 119.64 (CH), 117.22 (CH) and 26.79 (2 × CH_3), *m/z* 287 (M^+, 23%), 229 (81), 131 (60) and 42 (100).

FVP of 5-(2-aminoindazol-2-yl)methylene-2,2-dimethyl-1,3-dioxane-4,6-dione 3.91

FVP of 5-(2-aminoindazol-2-yl)methylene-2,2-dimethyl-1,3-dioxane-4,6-dione 3.91, (26.2 mg, T_f 500 °C, T_i 178 - 180 °C, P 2.8 – 4.5 × 10^{-7} Torr, t 30 min) gave indazolo[1,2-*a*]1,2,3-triazinium-4-olate 3.93 (*ca* 64%). The pyrolysate was removed from U-tube by distillation of $CHCl_3$, and the solvent removed under reduced pressure. The remaining solid was purified by dry flash chromatography (ethyl acetate : hexane, 40 : 60). Solvent was removed under reduced pressure to yield indazolo[1,2-*a*]1,2,3-triazinium-4-olate (32%) 3.93.

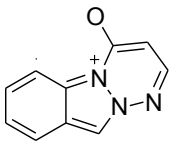

Indazolo[1,2-*a*]1,2,3-triazinium-4-olate 3.93, (32%) mp 192 - 194 °C; (Found M^+ 185.0584, $C_{10}H_7N_3O$ requires *M* 185.0584) ; δ_H (360 MHz, $CDCl_3$) 8.87 (1H, d, ^3J 7.0), 8.48 (1H, s), 7.87 – 7.84 (2H, m), 7.66 (1H, t, ^3J 7.1), 7.58 (1H, t , ^3J 7.1), 5.57 (1H, d, ^3J 6.7); δ_C (90 MHz, $CDCl_3$) 162.64 (quat), 152.12 (CH), 133.42 (quat), 130.22 (CH), 128.77 (CH), 121.62 (quat), 121.54 (CH), 119.03 (CH), 117.74 (CH), and 88.79(CH); *m/z* 185.0 (M^+, 100%), 157.0 (16), 118.0 (36) and 103.0 (17).

FVP of 5-(2-aminoindazolyl)methylene-2,2-dimethyl-1,3-dioxane-4,6-dione 3.91 (21.6 mg, T_f 750 °C, T_i 174 - 175 °C, P 2.8 – 3.6 × 10^{-7} Torr, t 30 min) gave pyridazino[1,6-*b*]indazol-4(1*H*)-one 3.94 (*ca* 71%). The pyrolysate was purified by distillation of $CHCl_3$ through the U-tube, and the remaining solid scraped from the U-tube with the aid of ethanol. Solvent was removed under reduced pressure to yield pyridazino[1,6-*b*]indazol-4(1*H*)-one (44%) 3.94.

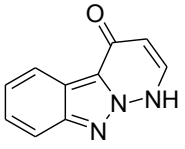

Pyridazino[1,6-*b*]indazol-4(1*H*)-one **3.94**, (44%) mp 223 - 225 °C; (Found M^+ 185.0583, $C_{10}H_7N_3O$ requires *M* 185.0584); δ_H (360 MHz, DMSO-d_6) 10.26 (1H, br s, NH), 8.50 (1H, d, ^3J 5.8), 8.22 (1H, d, ^3J 8.0), 7.86 (1H, d, ^3J 8.0), 7.59 (1H, t, ^3J 8.0), 7.34 (1H, t , ^3J 8.0) and 6.75 (1H, d, ^3J 5.8); δ_C (90 MHz, DMSO-d_6) 158.57 (quat), 146.47 (CH), 145.43 (quat), 127.67 (CH), 122.74 (quat), 121.50 (CH), 121.37 (CH), 115.91 (CH), 113.84 (quat) and 98.33 (CH); *m/z* 185 (M^+, 76%), 149 (18), 84 (100), 78 (26) and 66 (100).

FVP of 5-(1-aminoindazolyl)methylene-2,2-dimethyl-1,3-dioxane-4,6-dione 3.90

FVP of 5-(1-aminoindazolyl)methylene-2,2-dimethyl-1,3-dioxane-4,6-dione **3.90**, (21.2 mg, T_f 500 °C, T_i 184 - 186 °C, *P* 1.4 – 2.1 × 10^{-7} Torr, *t* 33 min) gave indazolo[1,2-*a*]1,2,3-triazinium-6-olate **3.92** (*ca* 51%). The pyrolysate was removed from U-tube by distillation of $CHCl_3$, and the solvent removed under reduced pressure. The remaining solid was purified by dry flash chromatography (ethyl acetate : hexane, 10 : 90). Solvent was removed under reduced pressure to yield indazolo[1,2-*a*]1,2,3-triazinium-6-olate (32%) **3.92**.

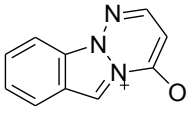

[1,2,3]triazino[2,1-*a*]indazol-5-ylium-4-olate **3.92**, (32%) mp 162 - 164 °C; (Found M^+ 185.0584, $C_{10}H_7N_3O$ requires 185.0584) ; δ_H (360 MHz, $CDCl_3$) 8.86 (1H, s), 8.17 (1H, d, ^3J 7.9), 7.99 – 7.95 (2H, m), 7.71 (1H, t, ^3J 7.8), 7.56 (1H, t , ^3J 7.8) and 5.60 (1H, d, ^3J 6.3); δ_C (90 MHz, $CDCl_3$) 166.57 (quat), 165.08 (CH), 145.66 (CH), 139.17 (quat), 138.76 (quat), 133.96 (CH), 129.42 (CH), 121.33 (CH), 112.55 (CH) and 107.21 (CH); *m/z* 185 (M^+, 100%), 157 (22), 118 (28) and 103 (36).

Exploratory work towards confirmation of unknown product

3-Aminoindazole derivative

3-Aminoindazole (0.83 mmol) was dissolved in aceonitrile (12 cm^3), to which was added MMMA (1 eq) and the reaction mixture stirred at room temperature for 1 h. After this time the solvent was removed under reduced pressure and the resulting orange solid recrystallised from ethanol to yield 5-(3-aminoindazol-3-yl)methylene-2,2-dimethyl-1,3-dioxane-4,6-dione (74%) **3.100**.

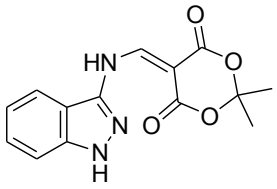

5-(3-Aminoindazol-3-yl)methylene-2,2-dimethyl-1,3-dioxane-4,6-dione **3.100**, (74%) mp 172 - 173 °C; (Found M^+ 287.0901, $C_{14}H_{13}N_3O_4$ requires *M* 287.0904); δ_H (360 MHz, $CDCl_3$) 13.12 (1H, s, NH), 11.59 (1H, br d, ^3J 6.6), 8.80 (1H, br d, ^3J 6.9), 7.91 (1H, d, ^3J 8.2), 7.56 (1H, d, ^3J 8.4), 7.46 (1H, t, ^3J 7.8), 7.22 (1H, t, ^3J 7.8) and 1.73 (6H, s); δ_C (90 MHz, $CDCl_3$) 163.60 (quat), 162.72 (quat), 152.95 (CH), 141.32 (quat), 140.45 (quat), 127.27 (CH), 120.76 (CH), 119.30 (CH), 113.30 (quat), 110.56 (CH), 104.27 (quat), 87.23 (quat) and 26.48 (2 × CH_3), *m/z* 287 (M^+, 14%), 211 (100), and 44 (100).

FVP of 5-(3-aminoindazol-3-yl)methylene-2,2-dimethyl-1,3-dioxane-4,6-dione **3.100**, (28.8 mg, T_f 600 °C, T_i 203 - 205 °C, *P* 3.2 – 3.8 × 10^{-7} Torr, *t* 26 min) gave 1*H*,4*H*,6*H*,10b*H*-pyrimido[1,2-*b*]indazol-4-one **3.97** (*ca* 89%). The pyrolysate was purified by distillation of $CHCl_3$ through the U-tube, and the remaining solid product scraped from the U-tube with the aid of ethanol. Solvent was removed under reduced pressure to yield 1*H*,4*H*,6*H*,10b*H*-pyrimido[1,2-b]indazol-4-one (56%) **3.97**.

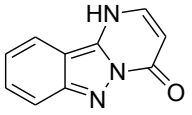

Pyrimido[1,2-b]indazol-4(1H)-one **3.97**, (56%) mp 223 - 225 °C; (Found M^+ 185.0582, $C_{10}H_7N_3O$ requires *M* 185.0584); δ_H (360 MHz, DMSO-d_6) 8.18 (1H, d, ^3J 7.0), 8.06 (1H, d, ^3J 8.0), 7.65 (1H, d, ^3J 8.0), 7.51 (1H, t, ^3J 8.0), 7.14 (1H, t , ^3J 8.0) and 6.10 (1H, d, ^3J 7.0); δ_C (90 MHz, DMSO-d_6) 188.69 (quat), 159.53 (quat), 156.59 (CH), 130.15 (CH), 130.02 (CH), 129.97 (CH), 126.80 (quat), 120.96 (CH), 120.29 (CH) and 105.06 (quat); *m/z* 185 (M^+, 100%), 157 (25), 147 (22), 84 (99) and 66 (93).

N-Aminobenzimidazole

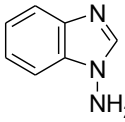

N-Aminobenzimidazole, synthesised *via* *N*-amination general method 3 of benzimidazole, (56%) mp 152 - 153 °C [lit. 150 - 152 °C]; [19] δ_H (360 MHz, DMSO-d_6) 8.11 (1H, s), 7.63 (1H, d, ^3J 7.9), 7.55 (1H, d, ^3J 7.9), 7.29 (1H, t, ^3J 7.2), 7.20 (1H, t , ^3J 7.2) and 6.17 (2H, br s); δ_C (90 MHz, DMSO-d_6) 145.12 (quat), 141.91 (quat), 135.21 (quat), 122.97 (CH), 121.85 (CH), 119.99 (CH) and 110.67 (CH).

1-Aminobenzimidazole derivative

1-Aminobenzimidazole (1.14 mmol) was dissolved in aceonitrile (20 cm^3), to which was added MMMA (1 eq) and the reaction mixture stirred at room temperature for 1 h. After this time the solvent was removed under reduced pressure and the resulting orange solid recrystallised from ethanol to yield 5-(1-aminobenzimidazol-1-yl)methylene-2,2-dimethyl-1,3-dioxane-4,6-dione (56%) **3.101**.

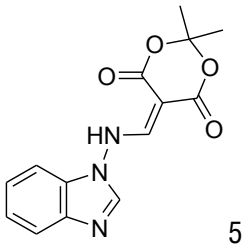

5-(1-Aminobenzimidazol-1-yl)methylene-2,2-dimethyl-1,3-dioxane-4,6-dione **3.101**, (74%) mp 184 - 185 °C; (Found M^+ 287.0902, $C_{14}H_{13}N_3O_4$ requires *M* 287.0904); δ_H (360 MHz, $CDCl_3$) 10.92 (1H, s), 8.37 (1H, s), 8.06 (1H, s), 7.80 (1H, m), 7.45 – 7.36 (3H, m) and 1.80 (6H, s); δ_C (90 MHz, $CDCl_3$) 167.47 (quat), 164.83 (quat), 158.93 (CH), 140.82 (quat), 140.73 (CH), 132.66 (quat), 125.07 (CH), 124.03 (CH), 121.23 (CH), 108.33 (CH), 105.90 (quat), 88.76 (quat) and 27.22 (2 × CH_3), *m/z* 287 (M^+, 64%), 211 (100), and 43 (94).

FVP of 5-(1-aminobenzimidazol-1-yl)methylene-2,2-dimethyl-1,3-dioxane-4,6-dione **3.101**, (20.1 mg, T_f 600 °C, T_i 172 - 175 °C, *P* 1.8 – 2.3 × 10^{-7} Torr, *t* 40 min) gave pyridazino[1,6-*b*]benzimidazol-4(1*H*)-one **3.98** (*ca* 89%). The pyrolysate was purified by distillation of $CHCl_3$ through the U-tube, and the remaining solid product scraped from the U-tube with the aid of ethanol. Solvent was removed under reduced pressure to yield pyridazino[1,6-*b*]benzimidazol-4(1*H*)-one (66%) **3.98**.

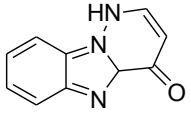

Pyridazino[1,6-*b*]benzimidazol-4(1*H*)-one **3.98**, (66%) mp 206 - 207 °C; (Found M^+ 185.0586, $C_{10}H_7N_3O$ requires *M* 185.0584) ; δ_H (360 MHz, DMSO-d_6) 9.58 (1H, br s, NH), 8.34 (1H, d, ^3J 5.5), 8.15 (1H, d, ^3J 8.0), 7.87 (1H, d, ^3J 8.0), 7.60 (1H, t d, ^3J 7.2, ^4J 1.2), 7.51 (1H, t d, ^3J 7.2, ^4J 1.2) and 6.58 (1H, d, ^3J 5.5); δ_C (90 MHz, DMSO-d_6) 159.69 (quat), 156.12 (quat), 145.32 (CH), 138.66 (quat), 130.52 (quat), 126.61 (CH), 123.25 (CH), 118.73 (CH), 112.65 (CH) and 103.63 (CH); *m/z* 185 (M^+, 100%), 157 (18), 84 (99) and 66 (93).

References

1. D. L. W. Burford, Y-P. Ho, F. D. Popp, B. C. Uff, *J. Heterocycl. Chem.*, 1987, 1349.

2. P. L. Boyer, R. W. Buckheit, Jr., S. H. Hughes, C. J. Michejda, M. L. Morningstar, T. Roth, *J. Med. Chem.*, 1997, 40, 4199.

3. G. Speier, L. Parkanyi, *J. Org. Chem.*, 1986, 51, 218.

4. V. V. Kuz'menko, V. N. Komissarov, A. M. Simonov, *Chem. Heterocycl. Compd. (Engl Transl)*, 1980, 16, 634.

5. R. A. Abramovitch, K. Schofield, K., *J. Chem. Soc.*, 1955, 2326.

6. J. W. Hubbard, A. M. Piegols, B. C. G. Soederberg, *Tetrahedron*, 2007, 63, 7077.

7. E. H. Jeoung, C. K. Lee, I-S. H. Lee, *J. Heterocyl. Chem.*, 1996, 33, 1711.

8. S. M. Allin, W. R. Bowman, R. Karima, S. S. Rahman, *Tetrahedron*, 2006, 62, 4306.

9. H. Fujioka, Y. Kita, O. Kubo, K. Murai, Y. Ohba, *Tetrahedron*, 2007, 63, 638.

10. K. Handlíř, V. Lišková, M. Ludwig, P. Pařík, S. Šenauerová, *J. Heterocycl. Chem.*, 2006, 43, 835.

11. M. Harfenist, *J. Med. Chem.*, 1978, 21, 405.

12. H. Rataj, *Unpublished Work.* 1992.

13. W. J. O' Neill, *PhD Thesis*, The University of Edinburgh, 2009.

14. I. M. Aldre, E. W. Parham, *J. Org. Chem.*, 1960, 25, 1259.

15. K. Angermund, M. Clausen, H. Neunhoeffer, C. Krueger, H. Ohl, H. D. Voetter, *Liebigs Ann. Chem.*, 1985, 1732.

16. F. Bures, J. Kulháneka, O. Pytela, T. Szotkowskia, Z. Trávnísek, *J. Hetercycl. Chem.,* 2006, 43, 1583

17. A. J. Blake, H. McNab, M. Morrow, H. Rataj, *J. Chem. Soc., Chem. Commun.*, 1993, 840.

18. B. M. Adger, S. Bradbury, M. Keating, C. W. Rees, R. C. Storr, M. T. Williams, *J. Chem. Soc., Perkin Trans. 1*, 1975, 31.

19. H. Nakajima, *J. Org. Chem.*, 1978, 43, 2693.

Appendix – Computational data for Energy Surface Figure 8, Chapter 3

Computational Studies

Computational studies were performed using the Gaussian03 program from Gaussian Inc., on the 'Hare' cluster managed by Dr. P. Richardson of the EaStCHEM research computing facility. Inputs were created using Planaria software's ArgusLab program and modified as necessary. DFT calculations were typically performed at B3LYP/cc-pVDZ level. Energies are quoted in Hartrees (Ha). Transition states are optimised to a first order state (one negative frequency). All the data obtained from the calculations are contained on a DVD attached to this thesis. The following is an example of the data obtained and shows all optimised structures used to construct Figure 8 from Chapter 3 reproduced below for ease.

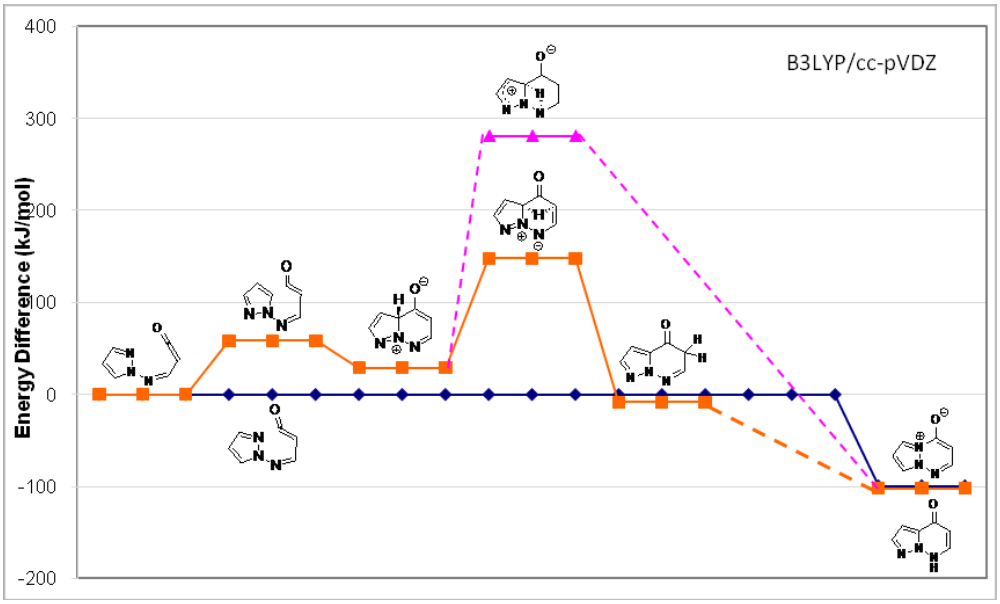

Figure 8 from Chapter 3: Energy surface calculated for formation of betaine **3.11** and pyrazolopyridazinone **3.10** from imidoylketene **3.9**

ER128aa

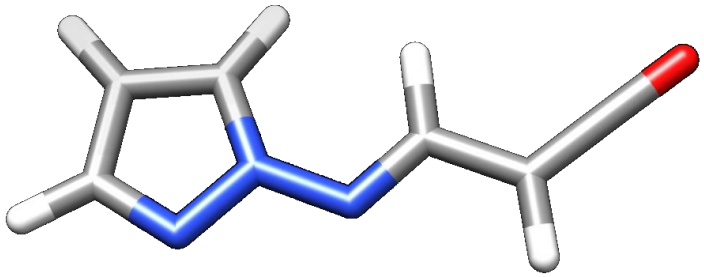

Energy of Optimised structure = -471.0553761 Ha

Cartesian Co-ordinates

0 1

C	3.337860	-0.279988	-0.110964
C	2.983999	1.089458	0.004514
C	1.607402	1.085725	0.102251
N	1.222055	-0.233418	0.039861
N	2.272194	-1.073656	-0.082425
N	-0.015140	-0.820374	0.101309
C	-1.050523	-0.062640	-0.005220
C	-2.367887	-0.660700	0.085317
C	-3.493243	0.042022	-0.021375
O	-4.483012	0.648364	-0.108523
H	4.328920	-0.719198	-0.207954
H	3.638496	1.956562	0.028011
H	0.899878	1.897792	0.231930
H	-0.999451	1.024259	-0.166317
H	-2.463173	-1.737464	0.244155

ER128HTTS1NoEigen

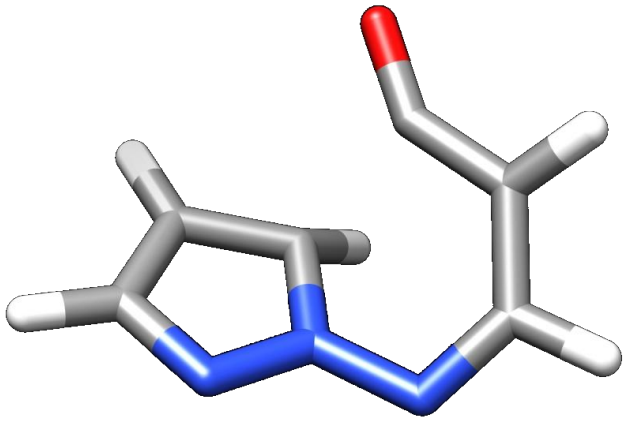

Energy of Optimised structure = -471.0443724 Ha

Artesian Co-ordinates

0 1

N	1.787636	-0.882542	-0.471883
C	2.340254	0.362541	-0.373685
C	1.526307	1.234736	0.325859
C	0.370986	0.473109	0.670637
N	0.654911	-0.812949	0.177984
N	-0.193184	-1.888209	0.201369
C	-1.447465	-1.538041	0.019985
C	-2.019439	-0.261975	-0.218873
C	-1.357541	0.950617	-0.134050
O	-1.490843	2.125823	-0.231875
H	3.306838	0.543545	-0.838102
H	1.700976	2.279953	0.565266
H	-0.138287	0.531841	1.635919
H	-2.129430	-2.394317	0.011488
H	-3.037508	-0.207626	-0.611105

Calculated negative frequency = -379.6199 cm^{-1}

ER128h

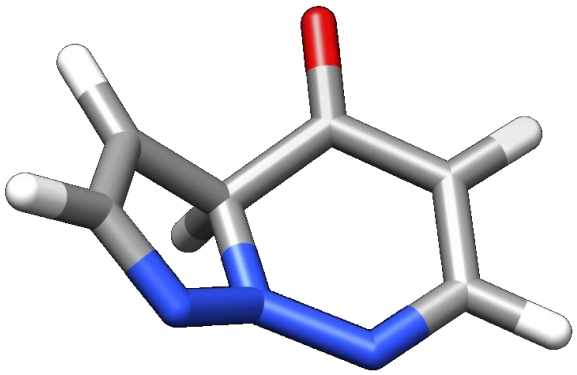

Energy = -471.0443724 Ha

Cartesian Co-ordinates

0	1		
C	2.310191	0.098747	-0.412103
C	1.549092	1.100774	0.038607
C	0.320548	0.507690	0.661019
N	0.539399	-0.898548	0.373459
N	1.751357	-1.053299	-0.238372
C	-0.963967	0.958584	0.031093
C	-1.997390	-0.058183	-0.249372
C	-1.704465	-1.367973	-0.147844
N	-0.495049	-1.778007	0.125222
O	-1.196500	2.182736	-0.168721
H	3.280514	0.224320	-0.887406
H	1.814052	2.155601	0.003607
H	-3.000897	0.252849	-0.535981
H	-2.481776	-2.104212	-0.342323
H	0.306101	0.680692	1.761307

ER128k

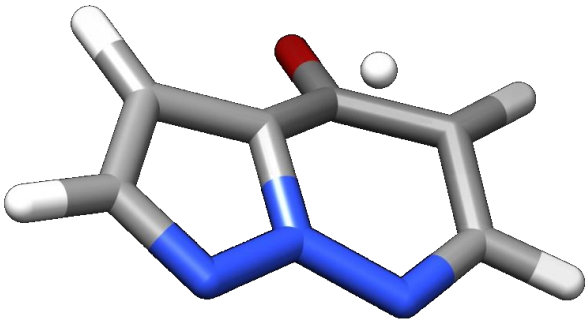

Energy = -470.9990078 Ha

Cartesian Co-ordinates

0 1

C	-1.376284	1.352849	0.257880
C	-2.412339	0.450139	0.037428
N	-1.987612	-0.816420	-0.186832
N	-0.668162	-0.749367	-0.116413
C	-0.198985	0.575117	0.194885
C	1.254906	0.879038	-0.117671
C	1.943862	-0.345005	0.348607
C	1.364920	-1.614466	0.047794
N	0.092670	-1.842745	-0.215353
O	1.712812	1.958321	-0.409678
H	-1.428534	2.424379	0.422149
H	-3.483165	0.644752	0.023088
H	0.687544	0.147928	1.239880
H	1.988589	-2.511767	0.063156
H	3.018328	-0.298165	0.545803

Calculated negative frequency = -1590.3152 cm^{-1}

ER128i

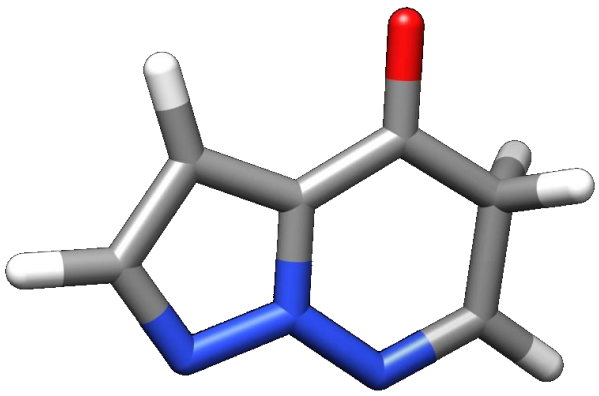

Energy = -471.0585644 Ha

Cartesian Co-ordinates

0 1

C	1.464090	1.224000	0.000378
C	2.475216	0.266292	-0.000117
N	1.937770	-0.989126	-0.000327
N	0.627594	-0.823651	0.000141
C	0.304935	0.479160	0.000569
C	-1.024814	0.882085	0.000303
C	-2.072277	-0.105679	0.000404
C	-1.612310	-1.474986	-0.000173
N	-0.275718	-1.795989	-0.000314
O	-1.322276	2.129267	-0.000750
H	1.568512	2.304035	0.000432
H	3.540358	0.471310	-0.000086
H	-2.709583	0.050982	-0.899811
H	-2.348343	-2.273487	-0.000395
H	-2.709297	0.049144	0.901178

ER128b

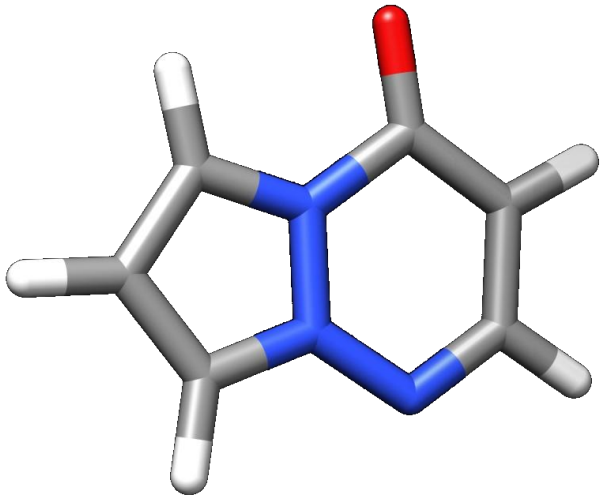

Energy = -471.0933206 Ha

Cartesian Co-ordinates

0 1

C	1.306852	1.283802	-0.000070
C	2.427585	0.461806	0.000187
C	1.961695	-0.857906	-0.000155
N	0.609031	-0.824978	-0.000021
N	0.207469	0.487485	-0.000057
C	-1.210687	0.893449	-0.000139
C	-2.050160	-0.247477	0.000058
C	-1.514073	-1.536225	0.000055
N	-0.229334	-1.885064	-0.000047
O	-1.429246	2.092516	0.000114
H	1.175147	2.360292	-0.000122
H	3.466099	0.777421	0.000358
H	2.467792	-1.817229	-0.000260
H	-3.126793	-0.088399	0.000219
H	-2.185710	-2.399006	0.000147

ER128c

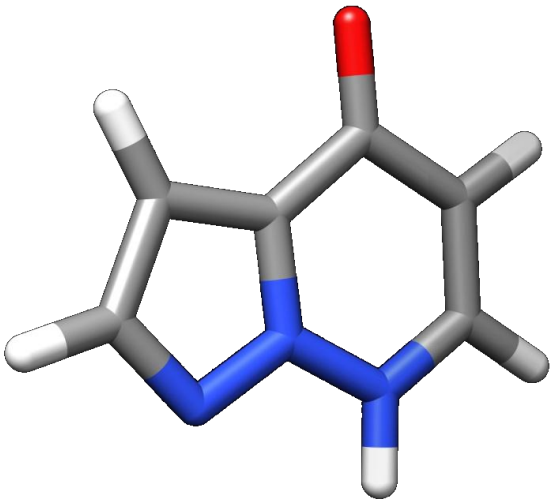

Energy = -471.094227 Ha

Cartesian Co-ordinates

0 1

C	-1.408709	1.363156	-0.000063
C	-2.444748	0.415961	0.000052
N	-1.983364	-0.853326	0.000117
N	-0.662174	-0.695012	0.000062
C	-0.232184	0.609932	-0.000080
C	1.212182	0.915644	-0.000198
C	2.054072	-0.283602	-0.000022
C	1.520552	-1.539347	0.000110
N	0.178283	-1.765681	0.000135
O	1.634446	2.068324	-0.000174
H	-1.469922	2.446254	-0.000141
H	-3.519994	0.580004	0.000090
H	3.135125	-0.150020	-0.000014
H	2.123975	-2.447695	0.000213
H	-0.280958	-2.667465	0.000255

ER128HTTS2B3LYPccpVDZ (1,6-Hshift TS)

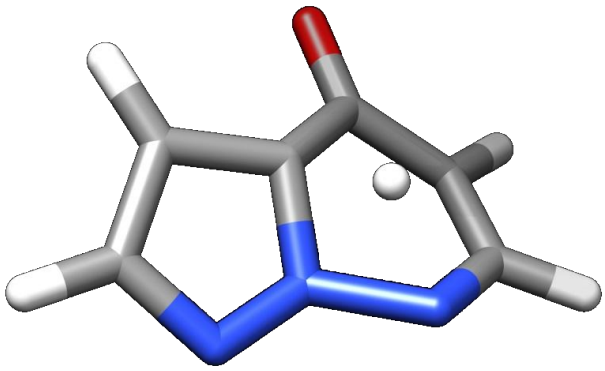

Energy = -470.9483897 Ha

Cartesian Co-ordinates

0 1

C	-2.413923	0.337081	-0.180408
C	-1.468452	1.222710	0.310899
C	-0.244766	0.482851	0.354963
N	-0.626236	-0.773940	-0.155619
N	-1.879106	-0.922033	-0.381222
C	1.167617	0.932183	-0.060046
C	2.009614	-0.217521	-0.315889
C	1.556961	-1.472277	0.019896
N	0.263622	-1.804247	0.381074
O	1.462535	2.117107	-0.078783
H	-3.464996	0.501348	-0.405215
H	-1.591272	2.278552	0.536365
H	3.051211	-0.042519	-0.584691
H	2.251240	-2.309938	0.140729
H	0.103273	-0.572923	1.256953

Calculated negative frequency = -2013.9564 cm^{-1}